Spring 2011

Photopolymerizations of multicomponent epoxide and acrylate/epoxide hybrid systems for controlled kinetics and enhanced material properties

Ho Seop Eom
University of Iowa

PHOTOPOLYMERIZATIONS OF MULTICOMPONENT EPOXIDE AND ACRYLATE/EPOXIDE HYBRID SYSTEMS FOR CONTROLLED KINETICS AND ENHANCED MATERIAL PROPERTIES

by

Ho Seop Eom

An Abstract

Of a thesis submitted in partial fulfillment
of the requirements for the Doctor of
Philosophy degree in Chemical and Biochemical Engineering
in the Graduate College of
The University of Iowa

May 2011

Thesis Supervisors: Professor Alec B. Scranton and
Associate Professor Julie L.P. Jessop

ABSTRACT

Cationic photopolymerization of multifunctional epoxides is very useful for efficient cure at room temperature and has been widely used in coatings and adhesives. Despite excellent properties of the final cured polymers, cationic photopolymerizations of epoxides have seen limited application due to slow reactions (relative to acrylates) and brittleness associated with a highly crosslinked, rigid network. To address these issues, two reaction systems were studied in this thesis: photoinitiated cationic copolymerizations of a cycloaliphatic diepoxide with epoxidized elastomers and acrylate/epoxide hybrid photopolymerizations. Oligomer/monomer structures, viscosity, compositions, and photoinitiator system were hypothesized to play important roles in controlling photopolymerizations of the epoxide-based mixtures. A fundamental understanding of the interplay between these variables for the chosen systems will provide comprehensive guidelines for the future development of photopolymerization systems comparable to the epoxide-based mixtures in this research.

For diepoxide/oligomer mixtures, the observed overall enhancement in polymerization rate and ultimate conversion of the cycloaliphatic diepoxide was attributed to the activated monomer mechanism associated with hydroxyl terminal groups in the epoxidized oligomers. This enhancement increased with increasing oligomer content. The mixture viscosity influenced the initial reactivity of the diepoxide for oligomer content above 50 wt.%. Real-time consumption of internal epoxides in the oligomers was successfully determined using Raman spectroscopy. Initial reactivity and ultimate conversion of the internal epoxides decreased with increasing the diepoxide content. This trend was more pronounced for the oligomer containing low internal epoxide content. These results indicate that the reactivity of the hydroxyl groups is higher toward cationic active centers of the diepoxide than those of the internal epoxides in the oligomers. These conclusions are consistent with physical property results. The enhanced

fracture toughness and impact resistance were attributed to multimodal network chain-length distribution of copolymers containing the oligomer content between 70% and 80%.

For acrylate/epoxide hybrid mixtures, diacrylate oligomers significantly suppressed reactivities of cycloaliphatic mono/diepoxides, which was attributed to high mixture viscosity and highly crosslinked acrylate network. In this case, the dual photoinitiator system did not favor the epoxide reaction. Depending on the monovinyl acrylate secondary functionalities, enhanced reactivity and ultimate conversion of the diepoxide were attributed to a combined effect of a reduced viscosity and the radical-promoted cationic polymerization associated with the dual photoinitiator. The retarded and inhibited diepoxide reactivities with ether and urethane secondary groups were attributed to solvation and nucleophilicity/basicity effects, respectively. The influence of the diepoxide on the acrylate reactivity was attributed to dilution and polarity effects. In this case, high concentration of the free-radical photoinitiator is required for the dual photoinitiator system. Physical properties of hybrid polymers also varied with acrylate structures and monomer composition. Dynamic modulation methods were proposed to enhance the diepoxide reactivity and final properties in the presence of urethane acrylates.

Abstract Approved: _____
Thesis Supervisor

_____
Title and Department

_____
Date

_____
Thesis Supervisor

_____
Title and Department

_____
Date

PHOTOPOLYMERIZATIONS OF MULTICOMPONENT EPOXIDE AND ACRYLATE/EPOXIDE HYBRID SYSTEMS FOR CONTROLLED KINETICS AND ENHANCED MATERIAL PROPERTIES

by

Ho Seop Eom

A thesis submitted in partial fulfillment
of the requirements for the Doctor of
Philosophy degree in Chemical and Biochemical Engineering
in the Graduate College of
The University of Iowa

May 2011

Thesis Supervisors: Professor Alec B. Scranton and
Associate Professor Julie L.P. Jessop

Graduate College
The University of Iowa
Iowa City, Iowa

CERTIFICATE OF APPROVAL

_____

PH.D. THESIS

_____

This is to certify that the Ph.D. thesis of

Ho Seop Eom

has been approved by the Examining Committee
for the thesis requirement for the Doctor of Philosophy
degree in Chemical and Biochemical Engineering at the May 2011 graduation.

Thesis Committee: _____
Alec B. Scranton, Thesis Supervisor

_____
Julie L.P. Jessop, Thesis Supervisor

_____
C. Allan Guymon

_____
Joon B. Park

_____
Chris N. Coretsopoulos

To my dearest family and parents, providing unconditional support and unchanging love

ACKNOWLEDGEMENTS

First of all, I feel really thankful for this moment finalizing my Ph.D. thesis. To me, life at Iowa was full of unknown news because there was a big transition in my major from the Biomedical Engineering to the Chemical Engineering. When I switched my major, it was a big decision and full of challenges because at that time my research interests were all about biomaterials. Although I was not sure about the destination of my Ph.D. journey at my gloomy days, I found new hopes and opportunities in photopolymerization when I met Professor Alec Scranton and Professor Julie Jessop, both my current academic advisors. Of course, it was not easy to change my research interests in the beginning. However, with endless patience and encouragements Professor Scranton and Professor Jessop have offered special opportunities for me to explore different photopolymerization systems and contribute to such an exciting and cutting-edge field of research through NSF and I/UCRC projects. The researches on several topics allowed me to get feedbacks and learn flexible-thinking skills from several companies such as 3M, DSM, Henkel, National Starch, and Cytec through Industry/University Cooperative Research Center program. From the bottom of my heart I really thank Professor Scranton and Professor Jessop for always inspiring me with motivational comments throughout the years. When I look back on my Ph.D. journey, I have earned more than Ph.D. degree from their true leadership as mentors and friends. I was able to successfully travel this far because of their cooperative direction and found a fantastic position in Micron Technology in Boise, Idaho.

I would like to say a special thanks to Professor Jun Park and Tae Hong Lim in Biomedical Engineering Department for being mentors to me over the years. Especially, I am very glad having Professor Jun Park in my research committee. I am the last student receiving Ph.D. by him because he retired after having my individual Ph.D. defense with him. Before switching my major, he was my hero and now he becomes my life mentor.

His devotion in research and teaching will affect me throughout my life. In addition, I would like to thank Professor Coretsopoulos and Professor Allan Guymon for their supports and help. I will never forget the laughing sound of Professor Coretsopoulos as well as nice conversations with him as a friend.

There are many other people without whom I have not successfully finished my Ph.D. program in the Chemical and Biochemical Engineering Department. I would like to thank Linda and Natalie for their professional assistance keeping me on track. I also thank former (Leroy, Josh, Beth, Cindy, Dongkwan, Peter, Chris, Yuan, and so forth) and current graduate students in our department who went through all difficulties together. Friends! Our devotion to making a small step in all fields of engineering was never worthless. Specially, I would like to give special thank Br. Soonki to help me decide my career path between academia and industry.

Under the direction of my advisors, I was given many opportunities in mentoring undergraduate students including Na Yeon Kang, Collette Black, James Kim, Sasha Abdalla and cooperating with other graduate students. Such opportunities have profited all of us: one of the students became a winner of the best poster award among undergraduate students in a conference; research articles have been published.

I would like to give all the credits that I have earned during my whole Ph.D. journey to my family. I really want to see my parents who have provided unconditional support for a long time. My daughter and son motivate me to live my life as best as I can every day. Finally, I give super special thanks to my loving wife, for sacrificing her career as a teacher to support me, for understanding me more than anyone in any occasions, for showing me unchanging love and trust with a sweet smile. Above all, I really thank my Lord and God, Jesus for his exceeding mercy and love upon me and my family. “O give thanks unto the LORD; for he is good: because his mercy endureth for ever” (Psalms 118:1). Praise the LORD!!

TABLE OF CONTENTS

LIST OF TABLES

LIST OF FIGURES

CHAPTER 1
INTRODUCTION AND BACKGROUND

Introduction

Advantages of Photopolymerizations

Photopolymerization technology is an efficient way to convert monomers to polymers due to the use of radiation energy instead of heat. Energy requirement to initiate the photopolymerization is approximately 60% less than heat energy required for conventional thermal polymerizations. The radiation primarily used in industry is ultraviolet (200-380nm) and visible (380-740nm) light. This efficient curing method have led to the rapid growth of coating and adhesive markets for decades and has begun to find new applications in optical fiber communication, holographic data storage/recordings, coating of 3-dimensional objects through stereolithography, food packaging, and biomedical/aerospace materials.[1-8] In addition, a distinguishing feature of using a light source is that it enables the spatial and temporal control of the initiation and propagation reactions during the photocuring process by directing light onto a location of interest in a system along with the on/off modulation of a light source. This is not attainable by thermal curing methods.[1, 2] The mono/polychromatic radiations directly routed onto reactive molecules promote immediate initiation and propagation in the order of seconds to a few minutes which result in much faster curing rates compared to thermal curing systems.[1-3] The photopolymerizations can be achieved at ambient or physiological temperature (37℃) allowing superficial formation of polymers.[5-7] Along with these attributes, eco-friendly process without solvents has facilitated in-situ fabrication of polymers which is very useful in a variety of biomedical applications.[1, 5-7] Furthermore, coating or adhesive resins are readily cured on a substrates that are sensitive to heat or solvents.[2, 8-10]

Cationic and Free-Radical Photopolymerizations

Free-radical and cationic photopolymerization systems are mostly prevalent in industrial applications. Their distinct reactions are facilitated by radical and cationic species, respectively. Accordingly, specific photoinitiators have been developed for the two distinct photopolymerizations. Typical monomers for the free-racial and cationic photopolymerizations are (meth)acrylates and epoxides, respectively. Radicals generated from the photodecomposition of photoinitiators rapidly promote initiation and propagation of (meth)acrylate free-radical polymerizations via a chain reaction. The propagation of active radical species generally stops due to radical-radical coupling termination when lights are shut off.[1, 3, 11, 12] On the other hand, cationic photopolymerizations of epoxides are initiated by protonic acids generated from cationic photoinitiators. Unlike radical-radical coupling termination, cationic polymerizations tend to exhibit non-terminating characteristics because cationic species is not coupled to terminate growing polymer chains even if light is eliminated.[3, 11-15]

However, each photopolymerization system has a critical issue to be addressed. For (meth)acrylate free-radical photopolymerizations, oxygen is continuously diffused from atmosphere. The oxygen in triplet energy state then quenches or deactivates triplet state photoinitiators/photosensitizers under an illuminating condition. Moreover, the oxygen also consumes initiating or growing radicals by forming stable peroxide intermediates due to its biradical nature. [12, 16-18] Subsequently, the oxygen inhibition introduces a long induction period in which free-radical polymerization is delayed until the oxygen dissolved in the reaction systems is consumed to a certain degree. The oxygen inhibition at air/coating interface cause a reduction in kinetic chain length and conversion, thereby leading to the formation of a tacky surface of films and poor physical properties of final products.[11, 12, 19-22] In industry, this problem has been treated by nitrogen purging[23]. However, other basic approaches including high PI concentration, high light intensity, and physical oxygen barriers (e.g. waxing or shield film) are practically

avoided [20, 21, 24] since these methods highly increase manufacturing cost and do meet several requirements for specific applications (e.g. dental/biomaterials).[5-7, 25]

Unlike the free radical photopolymerization, epoxide cationic photopolymerizations are sensitive to nucleophiles such as moisture, alcohols, and other basic compounds (e.g. amine) in the reaction system.[1, 26-33] For instance, water molecules affect the photoinitiation efficiency of cationic PIs via hydrolysis of cations and anions when cationic photoinitiators are exposed to highly humidity for a long time.[34] Furthermore, in the presence of water or different types of alcohols, the chemical interaction between hydroxyl groups with cationic active centers can alter the propagation mechanism.[35-42] Consequently, the physical and mechanical properties of final polymers cured by cationic photopolymerizations can be controlled as a function of those nucleophile concentrations or molecular structures of alcohols.

Importance of Modification of Neat Epoxide Photopolymerization Systems

Epoxides are a common denominator for two different reaction systems investigated in this research. In general, multifunctional epoxides are very versatile compounds that have been widely used for traditional applications such as adhesives, coatings, and electronics due to their excellent adhesion, relatively low shrinkage, and good solvent and corrosion resistance. With the advent of cationic photoinitiators, the photopolymerization technology allows conventional epoxides to find new markets and extend their possible applications in new cutting-edge areas such as stereolithography, automotive topcoats, dental/biomedical materials, and so forth. Despite a successful combination of photochemistry with the epoxide curing, problems associated with sluggish polymerizations (relative to acrylates) and the brittleness of the final cure polymer must be addressed. Thus, enhancement in the kinetics of cationic photopolymerization is important for room temperature process. In addition, enhanced flexibility or toughness is generally required to prevent catastrophic fracture failure and

poor impact resistance for a variety of applications. A number of investigations have been conducted to enhance photopolymerization kinetics of neat epoxide systems and properties of final cured polymers. However, the majority of the studies were based on amine-based thermal curing. In spite of recent studies on photopolymerizations of epoxide-based mixtures, there is still a lack of a comprehensive understanding of the relationship between reaction formulation and polymerization kinetics and ultimate polymer properties. Therefore, a fundamental understanding of interplay between the variables associated with several epoxide-based photopolymerization systems can provide comprehensive guidelines for the future development of multicomponent reaction formulations comparable to the epoxide-based mixtures in this research.

Background

Photoinitiation and Cationic photoinitiators

The development of cationic photoinitiators was challenging back in 1970's. In 1972, the invention of cationic photoinitiators by researchers at the GE Corporate Research and Development Center opened new potential of cationically polymerizable monomers such as a variety of vinyl ethers and epoxides to many applications in a practical view. The new products based on these cationic photopolymerizations have been successfully marketed.[43]

Various cationic photoinitiators (PIs) have been developed: onium salts (diazonium-type salts diaryiodonium-type salts and triphenylsulfonium-type salts and pyridinium-type salts), [44-46] and organometallic salts (iron-aren complex-type salts). In the past, aryldiazoium salts were typically used for cationic photopolymerizations. However, the aryldiazoium salts exhibited two major problems such as poor stability for long storage and the release of by-product (N_2 gas) of photolysis that cause premature gelation of resin mixture under dark conditions and poor film formation during

photopolymerization occurs, respectively. Other types of cationic photoinitiators aforementioned have been widely used in practical applications instead[44, 47].

The main characteristics of cationic PIs are attributed to the structures of the cation and anion parts.[43, 48] The chemical structure of the cation component is so important, because it is responsible for the light absorption characteristics and photosensitivity. This results in the different molar absorption coefficient and quantum yield based on its structure[49]. The degree of photosensitization of a cationic PI in the presence of a photosensitizer (PS) is also intimately related to the cation structure. In addition, the thermal stability and solubility of a cationic PI, a key issue in the early stage of development of PIs, could be overcome by introducing aryl groups with a long alkyl chain into the cation part.

On the other hand, the inherent peculiarity and stability of the anion component significantly affect the kinetics of cationic polymerization, i.e. propagation and termination, or livingness of cationic active centers, by controlling the acidic strength of the protonic (brønsted) acids produced during the photolysis of cationic PIs. The typical anions used for cationic PIs are BF_4^-, PF_6^-, AsF_6^-, and SbF_6^- in the order of their low nucleophilicity: their weak nucleophilicities are critical for controlled/living polymerizations. These anions are known as non-nucleophilic anions, because they do not form covalent bonds between active centers and counter anions.[44, 50, 51] It is known that the degree of separation of ion pairs between cationic active centers and its counter anions increases as the nucleophilicity of the anion decrease but this increases leads to less stability of the anions.[44, 48] Though arsenic and antimony-containing onium salts in use have the highest polymerization rate and initiation efficiency, the toxic nature of these heavy metals is undesirable. This led to the discovery of a new anion, tetrakis pentafluorophenyl borate, which does not contain a heavy metal but is as effective as SbF_6^- and reduces the potential risk in long term usage of the heavy metal halides as an anion. Another anion group involves the noncomplex anions, such as

ClO_4^-, $CFSO_3^-$, and $CH_3SO_3^-$, that use two electrons from the oxygen atom to form a sigma bond with an active center; this causes the reversible formation of a covalent bond between a cationic center and a noncomplex anion.[52]

(A) Diaryliodonium salts

Initiation: (1) $Ar_2I^+MtX_n^- \xrightarrow{hv} [Ar_2I^+MtX_n^-]^* \longrightarrow \begin{bmatrix} ArI^{+\cdot}MtX_n^- + Ar\cdot \\ ArI + Ar^+MtX_n^- \end{bmatrix}$

(2) $ArI^{+\cdot}MtX_n^- \xrightarrow{R-H} ArI^+H\ MtX_n^- + R\cdot$

(3) $ArI^+H\ MtX_n^- \longrightarrow ArI + H^+MtX_n^-$

Propagation: (4) $H^+MtX_n^- + M \longrightarrow HM^+\ MtX_n^-$

(B) Triphenylsulfonium salts

Initiation: (5) $Ar_3S^+MtX_n^- \xrightarrow{hv} [Ar_3S^+MtX_n^-]^* \longrightarrow \begin{bmatrix} Ar_2S^{+\cdot}MtX_n^- + Ar\cdot \\ Ar_2S + Ar^+\ MtX_n^- \end{bmatrix}$

(6) $Ar_2S^{+\cdot}MtX_n^- \xrightarrow{R-H} Ar_2S^+H\ \ MtX_n^- + R\cdot$

(7) $Ar_2S^+H\ \ MtX_n^- \longrightarrow Ar_2S + H^+MtX_n^-$

Propagation: (8) $H^+\ MtX_n^- + M \longrightarrow HM^+\ MtX_n^-$

Figure 1.1 The Type-I photoinitiation mechanism of onium salt photoinitiators upon illumination during the cationic photopolymerization. The photolysis process is same for both diaryliodonium-type salts (A) and the triphenylsulfonium-type salts (B). A star-shaped mark indicates the exited energy stages of the photoinitiator upon illumination.

In general, the photoinitiation mechanism in cationic photopolymerizations using onium salts, such as diaryliodonium salt and triarylsulfonium salt, can be depicted as (1)-(4) and (5)-(8) in Figure 1.1. Upon illumination, the onium salt PIs in a reaction mixture become electronically excited by the absorption of photons with the corresponding wavelength of 200 to 300 nm, typically, in the UVA/B region. Excited singlet/triplet state

PIs then undergo the photolysis via either of hemolytic and heterolytic decompositions of the carbon and iodine/sulfur bond. This leads to concurrent formation of an aryl iodine radical cation, aryl radical, and aryl cation species. The aryl radical cation is the most reactive fragment so that the highly reactive radical cation will abstract a hydrogen atom from any hydrogen donor, i.e. monomers, solvents, or impurities. Thus, the hydrogen abstraction of an aryl iodine radical cation subsequently generates an aryl iodine cation and a radical species; the generated aryl iodine cation releases a proton that initiates cationic polymerization.

The whole initiation process of the triphenylsulfonium salt PI in Figure 1.1B is the same as the diaryliodonium salt PI. Despite the superiority of onium salt photoinitiators, the light absorption characteristic and photosensitivity of those PIs only available for the short wavelength photons that limit their applications to UV-induced cationic polymerizations, resulting in high energy consumption relative to near UV/visible light source. For instance, visible laser curing approaches favor various applications such as three-dimensional microfabrication, optical data storage, photoresist, and printing inks, and microencapsulation, controlled release, and heavily pigmented resin systems.

To achieve visible light-induced cationic photopolymerizations, photosensitizers (PS) such as perylene[49], anthracene[53], thioxanthone[54], and carbazole[55, 56] have been used with onium salts to allow the initiating wavelength to be shifted from the deep UV region of the spectrum to the near UV/Visible region.[53, 57, 58] It has been reported that the use of a photosensitizer such as thioxanthone with iodonium salts increases the rate of polymerization and final conversion as the concentration of the photosensitizer increases due to the reduced activation energy of the photosensitized epoxide systems.[59]

In Figure 1.2, the main mechanism of photosensitization of onium salts is the electron transfer between a PS and an onium salt in the exciplex that occurs after a PS is

first raised to an electrically exited state by the absorption of the light and subsequent energy transfer from the exited PS (singlet/triplet state) to onium salts takes place as described as (1)-(2). Thus, this energy transfer produces a diaryl iodine free radical by reducing onium salts to an unstable aryl iodine radical which is rapidly decomposed to a neutral aryl iodine and an aryl radical (3). Finally, a PS radical cation is simultaneously formed and initiates the cationic polymerization (4).

Initiation: (1) $PS + Ar_2I^+MtX_n^- \xrightarrow{hv} PS^* + Ar_2I^+MtX_n^- \longrightarrow [PS \cdots Ar_2I^+MtX_n^-]^*$

(2) $[PS \cdots Ar_2I^+MtX_n^-]^* \longrightarrow Ar_2I^{\cdot} + PS^{+\cdot}\ MtX_n^-$

(3) $Ar_2I^{\cdot} \longrightarrow ArI + Ar\cdot$

Propagation: (4) $PS^{+\cdot}\ MtX_n^- + (m+1)M \longrightarrow PS^{+\cdot}(M)_mM^+\ MtX_n^-$

Figure 1.2 The Type-II photoinitiation mechanism of triphenylsulfonium salt photoinitiators upon illumination during the cationic photopolymerization. A star-shaped mark indicates the exited energy stages of the exciplex formed between a photosensitizer and a photoinitiator upon illumination.

Thermodynamic feasibility of a photo-induced electron transfer between the electron donor (PS) and the electron acceptor (PI) can be predicted by the Rhem–Weller equation (eq. 1.1) which concerns the excited state energy of PS and redox potentials of the excited PS and PI.[1, 29, 30, 60, 61]

$$\Delta G_{ET} = F\left[E_{OX}\left(\frac{D}{D^{+\cdot}}\right) - E_{RED}\left(\frac{A}{A^{-\cdot}}\right)\right] - E^* \qquad (eq.\ 1.1)$$

Where ΔG_{ET} stands for the thermodynamic driving force for electron transfer. A negative value of Gibbs free energy change indicates that the electron transfer is thermodynamically feasible. F is Faradays constant. $E_{OX}(D/D^{+\cdot})$ is the oxidation potential of the electron donor and $E_{RED}(A/A^{-\cdot})$ is the reduction potential for the

electron acceptor. E* is the excited state energy of the electron acceptor. With the Rhem–Weller equation, the free energy change can be estimated for a given PI and PS if their redox potentials are known as well as the excited state energy of the PI. Therefore, it gives general criteria for the selection of a pair of PS and PI for the effective photoinitiation from the thermodynamic point of view. Another mean of broadening spectra response is to use a free-radical photoiniator with an onium salt. This two component photoinitiator system is known as a dual photoinitiator system which will be discussed later.

Epoxide Monomers

Conventional cationically polymerizable monomers that are widely used for photopolymerizations in many applications would be epoxides, vinyl ethers, propenyl ethers, siloxanes, and oxetanes (Figure 1.3). Carbon-carbon double bond with an electron donating substituent, e.g. an alkoxy, phenyl, vinyl, or 1,1-dialkyl group of vinyl/propenyl ethers, explains their polymerizability via cationic mechanism.[62] On the other hand, cyclic ethers like oxiranes and oxetanes have a 3-or 4-membered ring structure, which is highly strained due large distortion of their bond angles. Oxiranes and oxetanes also have a heteroatom in the ring that makes them thermodynamically and kinetically favorable for the electrophilic and nucleophilic attack by super acids and monomers in the initiation and the propagation, respectively.[62]

Other interesting cyclic ethers are cycloaliphatic epoxides containing oxirane rings attached to their cyclic structures (Figure 1.3). A general synthesis of this type epoxide involves the oxidation of cycloolefins with unsaturated substituents.[63] This structure causes a higher strained oxirane ring resulting in higher reactivity compared to the ordinary oxirane ring. For example, the cationic ring opening polymerization of mono-functional cyclohexene oxide extremely increases because of its additional ring

strains, i.e. no induction period is introduced and polymerization rate is higher than common glycidyl ethers.[64, 65]

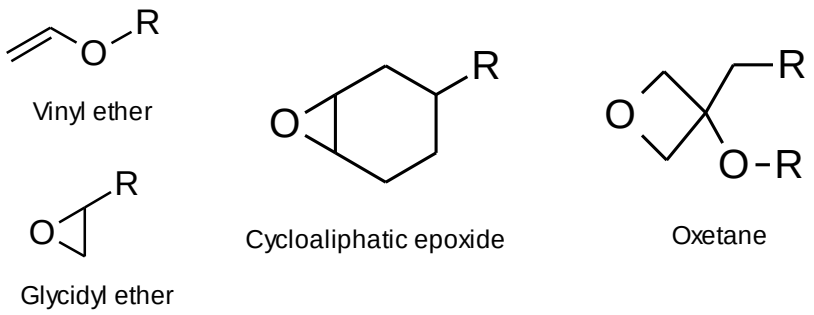

Figure 1.3 General structures of cationically polymerizable monomers

In this study, cycloaliphatic epoxides were used as a main epoxide component for the reaction formulation because the epoxide monomers have been well characterized and widely used in a variety of applications such as adhesives, coatings, printing inks, stereolithography, and composites.[64, 66-68]

Generally, reactivities of cationically polymerizable cyclic ethers are lower than those of acrylates that undergo free-radical polymerizations, but insensitive to oxygen inhibition because of positive nature of cationic active centers (no radical coupling with oxygen molecules). The relatively low reactivity of the cyclic ethers may arise from the nature of cationic PIs and from the interaction of cationic active centers with their counter anions during the propagation.[69, 70] The inherently slow kinetics of cationic polymerizations can affect its practical utility when a short irradiation time or low temperature processing is required for certain applications.

To address this issue, intensive investigations have been performed to ascertain the relationship between structure and kinetics for various epoxide monomers. Crivello *et al.* classified three different types of epoxide monomers, namely class I, II, and III,

according to their kinetic behaviors during propagation, i.e. an induction time and the rate of polymerization, and their structures.[64, 65] A typical monomer that belong to class I is monofunctional cycloaliphatic epoxides (e.g. cyclohexene oxide) without electron withdrawing side-groups. Compared to class II and III type epoxides, class I type epoxides exhibit a high polymerization rate, high ultimate conversion, and no introduction of an induction period.

In contrast, class II type epoxides such as neopentyl glycol diglycidyl ether generally exhibit a long induction, followed by a rapid, exothermic propagation behavior. The long induction period of such an epoxide was attributed to the interaction of a neighboring oxygen atom adjacent to the oxirane ring with the secondary oxonium ions. This interaction allows the secondary oxonium ions are stabilized by hydrogen bonding to form a tentative tautomeric structure.

Class III type epoxides such as phenyl glycidyl ether exhibit no extensive induction period but relatively slow cationic polymerizations between class I and II type monomers. However, it was also noticed by Crivello *et al.* that this classification might be ambiguous to some degree, because the propagation of some alkyl monoglycidyl ethers with a long additional ether side group may be substantially delayed by the formation of highly stabilized conformational structure via hydrogen bonding between a protonic acid and ether groups on the backbone or the side group.[65]

Propagation of Cationic Photopolymerizations

Generally known propagation mechanism of cationic photopolymerization is briefly expressed in the following scheme: $\mathrm{HM^+\ MtX_n^-} + m\mathrm{M} \longrightarrow \mathrm{H(M)_mM^+\ MtX_n^-}$. This simple propagation can be explained by the nucleophilic attack of monomers on the electron deficient α-carbon of the secondary oxonium ions which is formed by the protonation of monomers after the photoinitiation. This SN_2 reaction results in the ring opening polymerization of epoxides, followed by the formation of the propagating

tertiary oxonium ions such that epoxide polymer chains are growing. This ordinary propagation reaction is known as the active chain end mechanism (ACE) as shown in Figure 1.4.

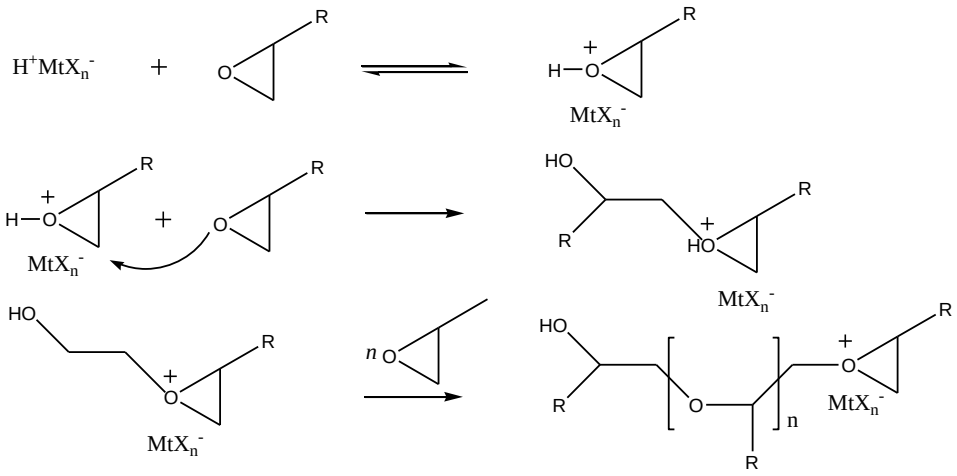

Figure 1.4 General propagation of cationic active centers via active chain end mechanism during the photoinitiated cationic polymerization.

However, this propagation mechanism in cationic photopolymerizations of cyclic ethers might be more complicated when nucleophiles such as water and alcohols are present in the polymerization system. It the presence of these nucleophiles, another propagation mechanism, known as activated monomer (AM) mechanism begins to compete with the ACE mechanism. The AM mechanism was originally termed and developed by Szwarc for N-carboxy-aminoacid anhydride (NCA) polymerization system[71]. Later in the middle of 1980s Kubisa and Penczek utilized the AM mechanism for the cationic polymerization of heterocyclic ethers in the presence of hydroxyl group-containing compounds.[72, 73] In the AM mechanism during cationic polymerizations of epoxides a nucleophilic hydroxyl group attacks a protonated oxonium ion. Consequently, one hydroxyl end group is generated in a growing chain, and a new

initiating proton is released and protonate an unreacted epoxide as shown in Figure 1.5. Therefore, the propagation of a polymer chain proceeds via a chain transfer reaction in which the generated hydroxyl end groups in the growing chains continuously protonated epoxide monomers. Further details of the AM mechanism will be more discussed in other sections.

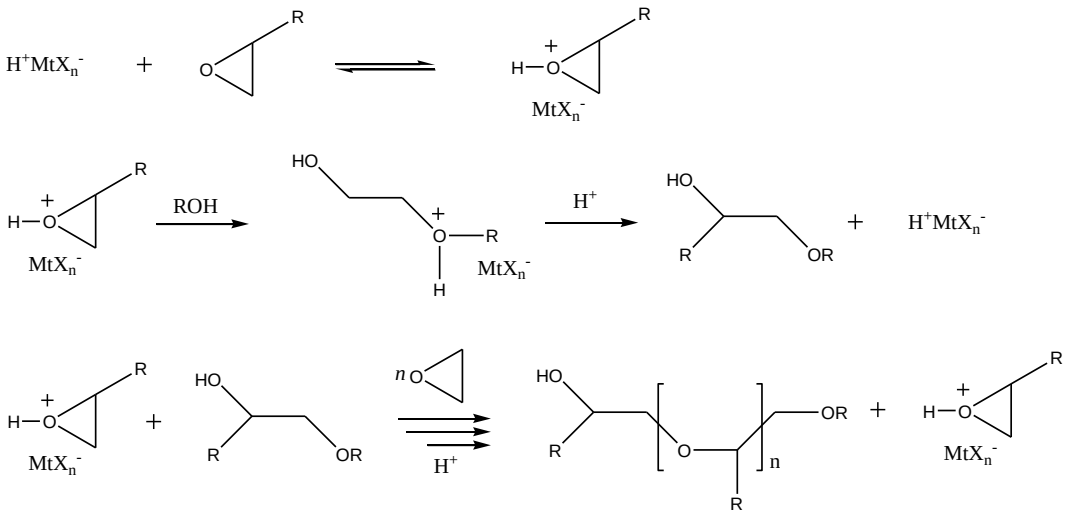

Figure 1.5 Chain-transfer associated propagation of cationic active centers via activated monomer mechanism in the presence of alcohols during the photoinitiated cationic polymerization.

The Role of Water in Propagation

In the late 1940's cationic polymerizations of thoroughly dried isobutene in the presence of Lewis acids such as BF_3 and $TiCl_4$ were immediately promoted when a trace of water was introduced.[74, 75] Since then, there had been lots of debates that resulted in several theories on the role water. It was proposed that such Lewis acids forms an initiator-coinitiator complex with proton donors such as water when low or moderate polarity solvents are used for cationic polymerizations of some vinyl monomers. This

was supported by proportional increase in the initiation rate and carbocation concentration with the increase of water concentration.[76, 77] However, in the middle of 1960s, it was discovered that in the case of water-$AlCl_3$ in methylene chloride, water rather reduced both polymerization rate and degree of conversion during the cationic polymerization of isobutene.[78] Also, the higher concentration ratio of water to tin-chloride beyond a critical point resulted in lower rates of the cationic polymerization in carbon tetrachloride.[62] The latter phenomenon was rationalized by the higher basicity of water toward carbocation ions or oxonium ions than that of the carbon-carbon double bond in the vinyl monomers. This indicates that water in cationic polymerizations compete with monomers to react with cationic active centers.

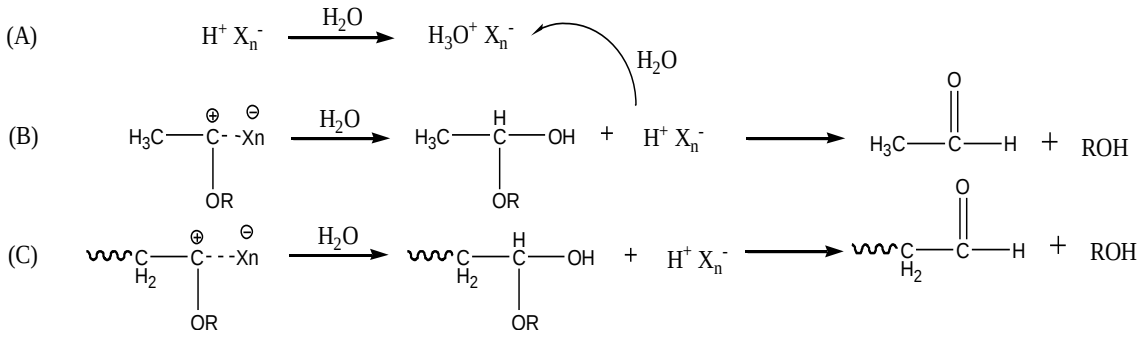

Figure 1.6 The effect of water on the cationic polymerization of vinyl ether as an inhibitor or a retarder: the formation of hydronium ions (A), acetaldehyde (B), and aldehyde (C). This drawing was modified from the reference.[40]

Similar to conventional cationic polymerization based on Lewis acids, the role of water in the cationic photopolymerizations was recently investigated to ascertain the effect of moisture on the kinetics and physical property for cationic photopolymerizations of vinyl ethers and epoxides. Lin *et al.* compared the kinetic behavior of vinyl ethers without hydroxyl groups (VEs) to hydroxyl group-incorporated vinyl ethers (VE-OHs) in

order to speculate the effect of water on both VE systems.[40] In their study, the concentrations of the monomers and water were simultaneously monitored using Real-time NIR spectroscopy and it was revealed that an induction period was observed for both VE and VE-OH systems in the absence of water. In the presence of water, a proportional increase in the induction period was observed with the increase of the water concentration for the VEs, whereas only a proportional decrease of polymerization rate was observed with an increase in water concentration for the VE-OHs. The further increased induction period of the VEs was attributed to two factors: (1) a decrease in proton concentration at an early stage via the solvation of protons by water to form hydronium ions (Figure 1.6) and (2) the hydrolysis of propagating carbocations which causes the formation of acetaldehyde or aldehyde (Figure 1.6B and 1.6C). These two factors are basically caused by the higher basicity of water toward the propagating carbocations than vinyl ether carbon-carbon double bonds. Interestingly, this implication is consistent with previous findings obtained from the cationic polymerizations of vinyl monomers in the presence of some Lewis acid-water initiator systems.

Finally, the difference in the kinetic behavior between VEs and VE-OHs after their induction periods was attributed to discrepancy in their molecular structures which allows for distinct propagation mechanisms. Especially, for the VE-OHs, a step-growth polyaddition via AM mechanism was proposed: a high nucleophilic hydroxyl group attacks a propagating carbocation to form polymer chains of an acetal structure and regenerate a proton. Therefore, it was concluded that water acts as a terminating agent/retarder and a chain transfer agent that promote the AM mechanism during the propagation. However, it was not clear whether the regenerated proton is transferred to water to reform hydronium ions. [42]

However, it was not clear whether sensitivity of cationic active centers to the water may differ depending on epoxide monomer types. Hartwig *et al.* clarified this ambiguity of the role of water in cationic photopolymerizations. [42] They considered the

energetic differences in the reactions between the oxonium ions and water and in the subsequent proton transfer reactions. By a molecular modeling approach, the ΔE was calculated for three different reactions: -91 $kJmol^{-1}$ and -131 $kJmol^{-1}$for addition of the water molecule to the respective propagating oxonium ions of cycloaliphatic epoxide and glycidyl ether; 182 $kJmol^{-1}$ and 192 $kJmol^{-1}$ for the proton transfer from the two respective intermediates, formed from the first reaction step, to the water; -147 $kJmol^{-1}$ and -136 $kJmol^{-1}$ for proton transfer from the two restive intermediates to counter anions.[42] Therefore, the release of the proton from the intermediates formed between water and cationic active centers is more retarded for glycidyl ether. In addition, transfer of the released proton to another water molecule in proximity is not energetically favored. Consequently, the released proton is captured by anions in proximity and lead to subsequent cationic polymerizations. Therefore, it is understood that the role of water could act as a retarder or an accelerator (chain transfer agent) depending on molecular structures of epoxide or vinyl ether monomers.

Acceleration of Cationic Photopolymerizations

In general, most of cyclic ethers classified as class II and III type epoxides undergo slow or moderate cationic photopolymerizations. Although class I type monomers like cyclohexene oxide undergo fast cationic polymerizations, much more attention for a wide range of photocuring applications has been made to cycloaliphatic di-epoxides (CDEs) due to their better physical and mechanical properties of CDEs than those of mono-functional ones. CDEs were synthesized and employed for the outdoor electric insulation as a UV resistant plastic around 1960s. However, many of CDEs that have nucleophilic groups such as carboxylate groups that typically undergo very slow cationic polymerizations and reach low conversions.[63, 79] For example, widely used di-functional cycloaliphatic epoxides (EEC) with ester groups in the middle have been known to undergo very slow cationic polymerizations and reach low conversions without

any accelerating agent because of the intramolecular interruption of the ester group via its nucleophilic attack on either of the alkylated active centers that are propagating in equilibrium with the formation of dioxacarbenium ions. The overall interaction between the nucleophilic ester carbonyl with growing cationic active center are illustrated in Figure 1.7.[79] Although high light intensity, high concentration of photoinitiators, or high temperature may be applied to accelerate the polymerization kinetics of multifunctional cycloaliphatic diepoxides, these conventional approaches increase the manufacturing cost. For room temperature cure, the sluggish kinetic behavior of the cycloaliphatic epoxides must be addressed.

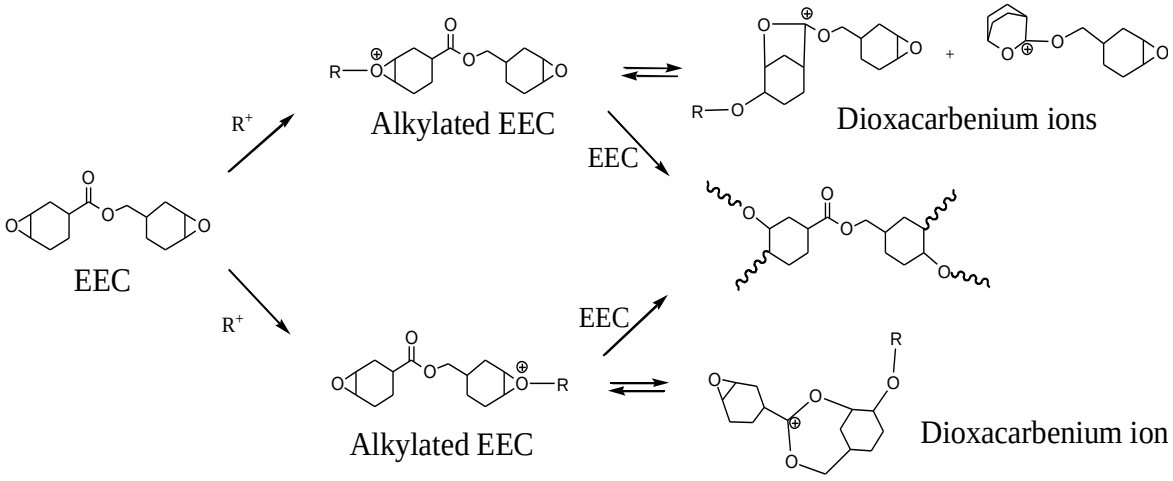

Figure 1.7 The formation of less reactive intermediates than growing oxonium ions during the propagation of EEC cationic photopolymerization.

Many efforts have been made to accelerate the rate of the cationic photopolymerizations. The strategies for enhancing cationic photopolymerizations can be classified into three different approaches. The first operative method is to increase the reactivity of epoxides by incorporating effective functional groups that are capable of inducing radical-promoted cationic polymerizations. According to Crivello *et al.*[80], the

requirements for higher reactivity can be redescribed. First, a functional group attached to an epoxide should bear labile hydrogen that is readily abstractable. Second, the redox reaction between a cationic PI and the free radical formed by the hydrogen abstraction should be thermodynamically feasible. Finally, the carbocations generated by the oxidation of the free radical by a photoinitiator should be stable and reactive enough to initiate cationic photopolymerizations. Thus, various functional groups that meet those requirements have been incorporated into epoxide monomers: enol ether groups (1-propenyl ether[81, 82], 1-butenyl ether[83], allyl ether[82], and benzyl ether[84, 85]) and acetal groups[84] (methyl acetal, allyl acetal, propargyl acetal, and benzyl acetal).

Epoxides with these functional groups can be further tuned for better reactivity.[85] The key advantages of this approach are that the concentration of cationic active species further increases with the generation of new carbocations on the functional group via a subsequent process as described above. In addition, the carbocations may serve as a branching point that leads to the formation of a crosslinked network structure. Some functionalized epoxide monomers are PEC, BEC, and XE as shown in Figure 1.8.

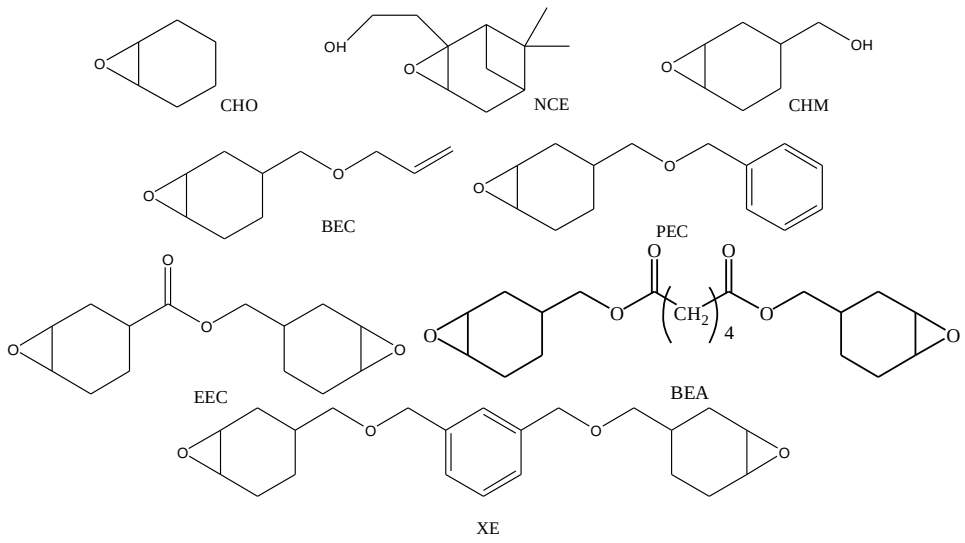

Figure 1.8 The structures of various cycloaliphatic epoxy monomers.

The second method is to take advantage of the AM mechanism by introducing hydroxyl groups to the polymerization systems. There are two means to separately introduce additional hydroxyl groups into cationic photopolymerization systems. One is simply to introduce alcohols into the formulation for epoxides. The other is to chemically incorporate hydroxyl moiety into epoxide monomers. It has been reported that alcohols induce faster cationic polymerizations as compared to no alcohol-containing systems. The enhanced rate of the cationic polymerization was attributed to the higher nucleophilicity of hydroxyl groups toward protonated epoxide monomers than that of (cycloaliphatic) oxirane rings. [86] Thus, the propagation of cationic active centers in the presence of alcohol proceeds by two distinguishing propagation mechanisms (ACE and AM). Kubisa and Penczek confirmed that the propagation rate constant of the AM mechanism is higher than that of the ACE mechanisms, i.e. $k_{p,AM} \geq 5\ k_{p,ACE}$ in the cationic polymerization of epichlorohydrin in the presence of a Lewis acid or a protonic acid.[86] Since the AM mechanism was based on a chain transfer reaction associated with the hydroxyl groups, the propagating active centers appeared to be limitedly growing until they reached a molecular weight threshold during the course of the reaction in the given conditions.[52, 73, 86-92] The high concentration ratio of hydroxyl groups to epoxides is very critical for the AM mechanism to prevail over the ACE mechanism.[89]

For this method, alcohol structure is one of the key factors affecting the kinetics of cationic photopolymerizations. Sangermano *et al.* studied the effects of primary, secondary, and tertiary alcohols on the kinetics of divinyl ethers.[28] The tertiary alcohols with higher nucleophilicity proved to be the most effective in increasing the polymerization rate and degree of conversion. It was also observed that the maximum rate of polymerization, $R_{p,\,max,}$ decreased as the concentration increased up to alcohol of 5 wt.%; after 5 wt.% of alcohol, $R_{p,max}$ increased. In addition, Olsson *et al.* assessed the effect of temperature on the cationic photopolymerization of a *di*-functional epoxide, EEC, in the presence of 1,6-hexanediol.[37] They found that polymerization rate and

final conversion monotonically increased with increasing the alcohol concentration at 60ºC. This result was not found at room temperature, because of the formation of non-reactive crystalline phase of linear, flexible hexandiols below their melting point. Furthermore, Crivello *et al.* investigated the effect of various benzyl alcohol derivatives, that bear a labile hydrogen, on the kinetics of epoxidized natural oils and other epoxides in the presence of cationic PIs at room temperature.[35, 36] The accelerated cationic photopolymerizations with benzyl alcohols are caused by a combined effect by the AM mechanism, radical-promoted cationic polymerizations, and hydrogen abstraction due to benzyl hydrogen. The key advantages of this method are that the kinetics of cationic photopolymerizations can be controlled by the ratio of the concentration of alcohols to epoxides, and that the physical and mechanical properties of final products can be tuned by selecting appropriate alcohols and epoxides according to their molecular weights, functionality, and the feed ratio.

Another method of utilizing the AM mechanism is to introduce hydroxyl moiety into epoxide monomers. This method was found to be a very effective way to significantly enhance cationic photopolymerization. Epoxides that bear hydroxyl groups (epoxide-OH) undergo a faster cationic photopolymerization via the AM mechanism[93]. Epoxide-OH monomers, also known as monofers according to the definition by Goethals, function as both monomers and chain transfer agents. With monofers, the controlling of the ratio of hydroxyl groups to epoxide functional groups is not unless additional alcohols are deliberately added to the polymerization system. However, the comparison of the monofers with other epoxides bearing a labile hydrogen only showed that the monofers are more effective in enhancing kinetics and degree of conversion.[93]

Finally, the acceleration of cationic photopolymerizations can be also achieved by copolymerizations of two different cationically polymerizable monomers. A range of pairs of epoxides and enol ethers that have been investigated are listed here[94-96]: n-butyl glycidyl ether (BGE), phenyl glycidyl ether (PGE), p-cresyl glycidyl ether (CGE),

1,2-epoxydodecane (V12), or EEC with n-butyl vinyl ether (BVE), EEC with tetraethyleneglycol divinyl ether (DVE-4) 1,4-cyclohexanedimethanol divinyl ether (CHM-DVE) or triethyleneglycol divinyl ether (TEGDVE), and 6-methyl-3,4-epoxycyclohexylmethyl propyl ether with 3,4-cyclohexenylmethyl 1-propenyl ether. The acceleration of the rate of polymerization and the increased conversion were observed for epoxides in agreement with the increase of the amount of VE monomers whereas the induction time and the rate of polymerization rate for VE cationic photopolymerization is reduced in the presence of epoxides. The enhanced kinetic behaviors in epoxide-vinyl ether photopolymerizations were attributed to a diluent effect of less viscous vinyl ether monomers associated with a plasticization of the resin matrix. Unfortunately, it is, however, still controversial about whether the copolymerizations between epoxides and enol ethers took place during the photopolymerization.[82, 94, 96, 97] Oxetane monomers were also found to act as a reactive diluent like enol ether monomers that effectively increases epoxide reactivity.[98]

Termination of Cationic Photopolymerization

In general, the characteristics of growing chain end groups in cationic polymerizations can be categorized into two broad viewpoints, a non-living end and a living end characteristic[62, 69, 70]. In the case of cyclic ethers, secondary and tertiary oxonium ions, formed by the protonation of monomers or the attack by unreacted monomers, are also relatively stable like carbocations from vinyl monomers. Although it has been known that the most of cyclic ethers such as epoxides undergoes cationic living polymerizations, a chain transfer to a polymer is a commonly thought to occur most frequently in moderately polar solvents. This irreversible, chain terminating mode may occur in an inter- or intra-molecular manner. For example, the cationic ring-opening polymerization of tetrahydrofuran (THF) proceeds with Lewis or protonic acids in a living manner. However, back-biting or transesterification reactions allow the

propagating cationic active centers to be terminated by the formation of cyclic oligomers or short linear oligomers, as shown in Figure 1.9.[91] The former reaction serves as a termination mode while the latter one is recognized as a chain transfer reaction; this indicates both reactions may lead to the broad distribution of polymer molecular weight, e.g. closed to about 2.

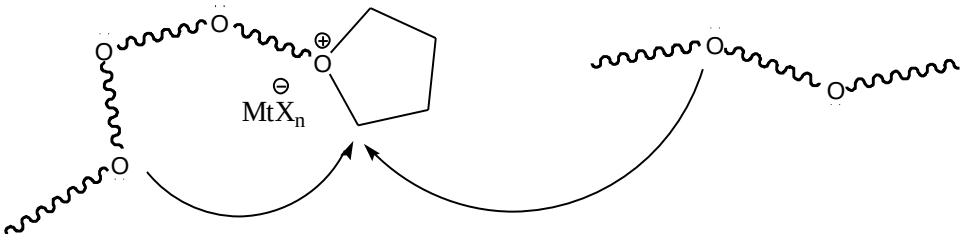

Figure 1.9 An example of two types of termination modes by back-biting associated with the highly nucleophilic ether oxygen in a growing polymer chain on the oxonium ion (cyclization as an intramolecular reaction) and by the attack by the foreign ether oxygen on the oxonium ion (transesterification as an intermolecular reaction).

The back-biting reaction is more pronounced in cationic polymerizations of cyclic ethers with lower membered ring structures. The relative reactivity of cyclic ethers toward oxonium ions in order of the nucleophilicity from lowest to highest is oxirane, oxetane, and tetrahydrofuran during propagation. In other words, the possibility of cyclization of a growing polymer chain is reduced in this same order. In spite of the possibility of various termination modes, a steady state assumption which is applied for free-radical polymerizations is not valid for cationic polymerizations, because the rate of polymerization rapidly increases towards a non-steady state between the initiation and the termination (R_i » R_t). Also, the bimolecular termination of cationic active species is not observed as it is in free-radical polymerizations, because there is an electrostatic repulsion between the positively charged active centers.

Living Characteristic of Cationic Photopolymerization

Controlled/living cationic polymerizations can be achieved under certain conditions on several factors such as the initiator system, the existence of the equilibrium state between active species and inactive dormant species, the rapidness of initiation, monomer type, solvent, and temperature [62, 69, 70]. Three mechanisms including pseudo-cationic (or electrophilic), quasi-living, and ideal-living propagations were proposed to explain the livingness of cationic polymerizations in a controlled way as shown in Figure 1.10.

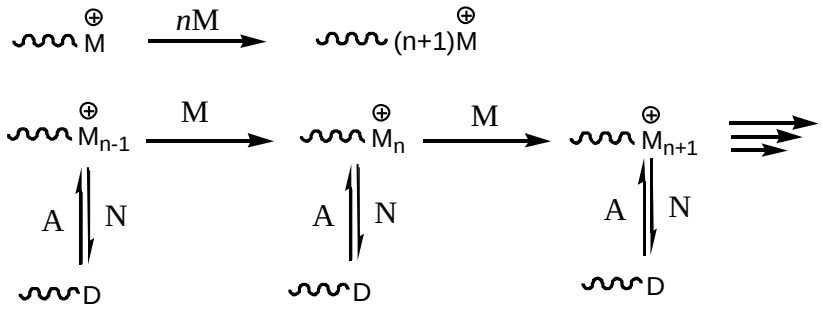

Figure 1.10 Ideal living mechanism (A) and Quasi-living mechanism (B). Counter anions are omitted. N indicates nucleophiles that can deactivate cationic active centers to form inactive dormant species, D. Dormant species should be reactivated by activators, A. The equilibrium between an active state and a dormant state can be also controlled by counter anions or in aid of an additive with weak basicity. This figure was modified from the reference.[69]

In general, it is most realistic that cationic living polymerizations proceed with the quasi-living mechanism in which the propagation of cationic active centers proceeds in equilibrium with inactive dormant state via the reversible interchange between active and inactive state. Thus, the factors needed to achieve living polymerizations should be adjusted appropriately. First, the nucleophilicity of counter anions in the initiator system, which is considered most important, should be low enough not to permanently form an

irreversible covalent bond with cationic active species but high enough to stabilize cationic active centers during the propagation. Second, the reversible interchange between active and inactive dormant species should be faster than the addition of monomers to the growing polymer chain when the equilibrium state between active species and inactive dormant species exists. In addition, the initiation rate should be much greater than the propagation rate (R_i » R_p). Finally, no irreversible chain transfer reactions and early termination of propagating cationic species should be observed. Thus, a diverse array of investigations led to the overall consensus that living/controlled cationic polymerizations can be effectively achieved via two ways: controlling the degree of stabilization of propagating active centers and maintaining the concentration of cationic active species at low level relative to the inactive dormant species. The second method can be achieved by shifting the equilibrium more toward the inactive dormant state which may be also controlled by reaction temperature or solvent polarity.

Concerning the photopolymerization, photoinitiated cationic ring-opening polymerizations (ROP) is practically performed in a bulk condition rather than in solution. PIs are added in the form of a salt containing relatively non-nucleophilic counter anions such as BF_4^-, PF_6^-, AsF_6^-, SbF_6^-, and $(C_6F_5)B^-$. In general, the photoinitiation takes place very rapidly over the propagation (R_i » R_p). The resulting product of the photolysis of PIs is strong protonic acids, $H^+MtX_n^-$. The initiation of cationic polymerizations then takes place in a quantitative way by protonating unreacted monomers. After initiating ring-opening reaction of epoxides, propagating oxonium ions are weakly stabilized by non-nucleophilic counter anions in spatial coordination with the cationic active species. Thus, it is deduced that the photoinitiated cationic ring-opening polymerizations will exhibit quasi-living characteristics, which have been also confirmed by recent studies. Vishal *et al.* determined the active center life time during the dark photopolymerization of phenyl glycidyl ether in which the light source was removed after a short illumination time. Two aryliodonium salt photoinitiators (IHA and IPB) were examined for the same

monomer system to compare the effect of different counter anions in size and nucleophilicity on the active center life time. The active center life time was longer for IPB with bulkier counter anions than that of IHA, in other words, lower nucleophilic counter anions provided more pronounced living characteristics for photoinitiated cationic ROPs. They also found that the effective propagation rate constant increased with lower concentration of PIs used after a threshold conversion at which propagating active species is shifted from ion pairs toward separated ions. Beth *et al.* showed that the long active center life time of cationic active centers such as oxonium ions enabled the curing of thick polymer systems using the shadow curing technique by which the unilluminated monomer region of a thick system begins to be polymerized by the migration of active centers out of the illuminated region.

Cationic Copolymerizations

The cationic copolymerizations of oxiranes such as propylene oxide(PO) and epichlorohydrin (ECH) with alcohols have been reported in a solvent such as methyl dichloride in the presence of a Lewis acid/protonic acid, e.g. $BF_3 \cdot OEt_2$ or $HBF_4 \cdot OEt_2$. When ECH was copolymerized with alcohols, the propagation rate constants ($k_{p,\,AM}$) of the AM mechanism was ~5 times higher than $k_{p,\,ACE}$ of the ACE mechanism,.[99]. It was also found that the concentration ratio of oxirane rings to the concentration of hydroxyl groups controls the contribution of AM mechanism to propagation such that the ratio of [oxirane rings] to [OH] needs to be maintained below 1 [100].

Using a similar method, telechelic oligodions with the functionality of 2 was prepared via a cationic copolymerization of ECH and ethylene glycol. This reaction resulted in the reduction of cyclic formation of the growing chains, and controlled/narrow distributed molecular weight macromers. The same technique was also used to polymerize PO and ECH in the presence of hydroxyl ethylacrylate or hydroxyl methyl methacrylate (Figure 1.11) and produced PO and ECH pre-copolymers with a acrylate

functional group such that either of pre-copolymers could be used for a radical copolymerization with styrene monomers.[88] In these studies, hydroxyl groups served as an initiator, while a protonic acid generated by the interaction between a Lewis acid and PO/ECH behaves as a catalyst, because it is regenerated throughout the AM mechanism. However, the molecular weight of the resulting copolymer was limited.

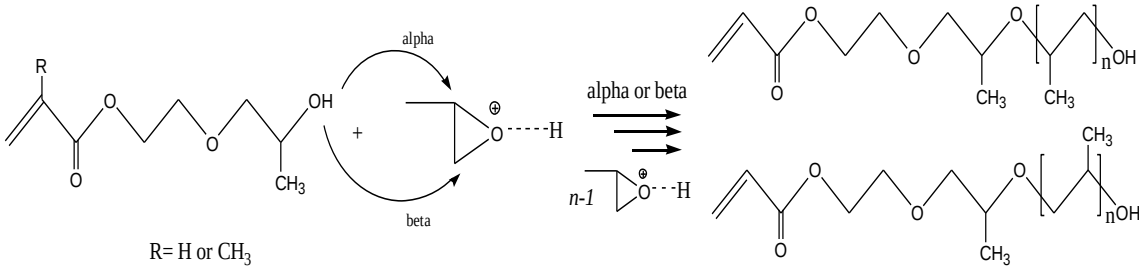

Figure 1.11 Copolymerization of propylene oxide and hydroxyl containing compounds via active chain end mechanism. This figure was modified from the reference [88]

Guo *et al.* performed cationic photo-co-polymerizations using the redox reaction between radical species and cationic initiators such as diphenyliodonium hexafluorophosphate.[101] It resulted in the transformation of propagating free-radical active centers of p-methoxystyrene into cationic active centers. Subsequent reactions of the styrene cationic active centers with cyclohexene oxide led to the formation of AB type-block. The underlying mechanism of this approach is a radical promoted cationic polymerization for which a radical initiator and a cationic initiator are co-used. The oxidation of the cationic initiator by radical species relies on the stabilizing ability of the substituent on the radicals. This is confirmed by two different model radical initiators of which one contains an electron-containing group and the other an electron-withdrawing group.

Cationically polymerized copolymers with a photosensitive pendant group were prepared using $BF_3 \cdot OEt_2$ as an initiator in the toluene solution at the low temperature of ~60 to ~65ºC. A 2-(4Nitrophenoxy) ethyl vinyl ether and 2-(4-Nitrop-1-naphtyloxy) ethyl vinyl ether were used as photosensitive pendant groups bearing monomers for cationic copolymerizations with 2-vinyloxy-ethyl cinnamate. The pendant cinnamate moiety has its acrylate double bond undergoing free-radical polymerization by self-sensitizing which is induced by the photosensitive pendant groups of the former two monomers.[102] The similar studies to this cationic copolymerization system have been performed to study of the synthesis and the characterization of photocrosslinkable non-linear optical (NLO) materials.[103] The preparation of a mixture of two copolymers having two different mesogenic properties, resulting in phase separation due to immiscibility, was attempted by the cationic copolymerization of two constitutional ethoxy vinyl ether isomers with two different pendant groups using $BF_3 \cdot OEt_2$ in methylene chloride.[104] Cationic copolymerizations are also performed to impart flexibility to rigid materials such as styrene.

Physical Properties of Cured Epoxides

One of typical cationically polymerizable monomers is bisphenol A glycidyl ether (DGEBA). Cured DGEBA polymers usually possess highly crosslinked network structures and offer good tensile, shear strength, and chemical and heat resistance associated with its backbone structure as shown in the Figure 1.12. However, the highly crosslinked, rigid structure of cured epoxides, like DGEBA, can impart high glass transition temperature and Young's modulus and can lead to undesirable brittleness. This brittleness can result in catastrophic fracture failure and poor impact resistance under high-rate loading conditions, high speed impact, etc. [66]. In addition, the low degree of elongation and shear displacement of unmodified epoxide thermosets limits their utility in certain applications such as joint adhesive due to low peel strength, especially when

they are used below their glass transition temperature. Furthermore, high viscosity of DGEBA-type epoxides makes their handling difficult during the process and occasionally leads to undesirable mechanical performance due to poor mixing with other components. These issues are commonly faced with all different types of epoxides made from chemical derivatives of bisphenol A.

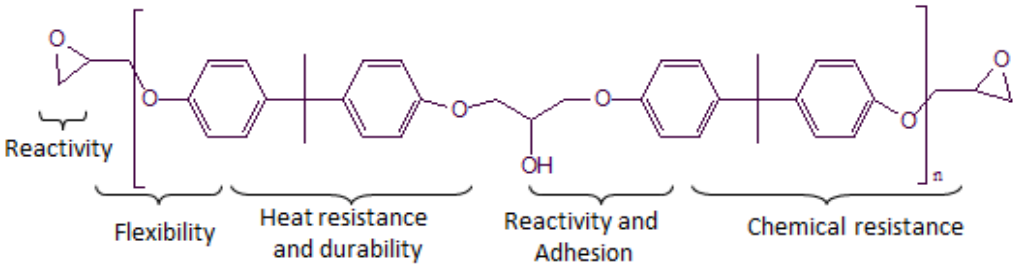

Figure 1.12 Structure-property relationship of a conventional epoxide, Bisphenol-A-glycidyl ether.

To overcome these issues, flexibility and/or toughness are necessarily imparted to a brittle network structure. The flexibility is a degree of elongation. Introduction of the flexibility into a brittle epoxide matrix generally causes a reduction in tensile strength and modulus, and lowers the glass transition temperature via decreasing the crosslink density of the epoxide network structure[66, 68]. Toughness is related to how a polymer matrix efficiently absorb and dissipate internal stress concentrated near crack tip under an external force to delay crack propagation before reaching mechanical failure [68, 105]. Thus, the enhancement in toughness results in high elongation and high tensile strength as well as moderate glass transition temperature. Consequently, toughness is considered more critical in avoiding structural frailty and improving performance adaptability in various conditions.

Toughening Mechanisms

Improving toughness of a brittle material generally involve distribution of internal stress generated by the force exerted to a material in the given time in order to delay a failure point. There are several well-known toughening mechanisms as shown in Figure 1.13: crack pinning and broadening (crack blunting), crack path deflection, shear band formation, and crazing or microcracking for stress relaxation. [106-109] In the crack pinning and broadening mechanism, a crack tip is throttled and broadened through interacting with a secondary phase. This second phase is usually a rigid material that is impenetrable enough to dissipate the internal stress applied to the crack tip.

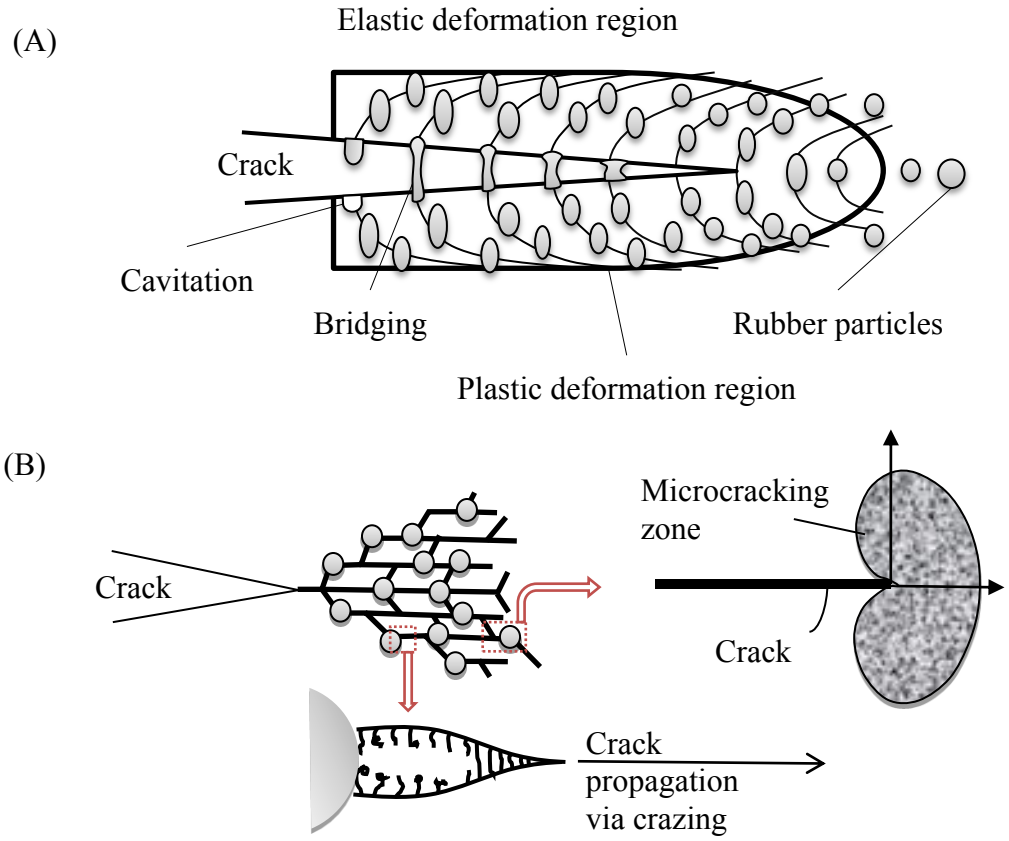

Figure 1.13 Energy dissipation mechanisms via shear band formation (A) versus crack path deflection, crazing, and microcraking (B). This figure was modified from the references.[68, 110]

The crack path deflection is caused by resistance of the secondary phase to the crack growth. This resistance is responsible for the generation of non-linear crack paths which distribute the internal stress when the stress exerted onto the front region of the crack is not high enough to break through the rigid phase.

Third, shear band formation (a type of plastic deformation) is a most efficient mechanism that enhances toughness. This irreversible deformation is a consequence of the shear yielding process of a local domain of the polymer matrix around the propagating crack. The degree of shear yielding depends on the stiffness of the polymer matrix that can vary with crystallinity and cross-linking density. Massive shear band formation has been often found in rubber-toughened epoxides or polycarbonate systems. Impact strength can be maximized when diffuse regions of the plastic deformation are introduced in the vicinity of elastically toughening agents.

Fourth, crazing is a type of the pseudo-crack propagation which involves tearing of polymer chains in the matrix. Crazing can be initiated in the vicinity of the crack tips and bring forth the fibrillar chain extension that bridges two surfaces undergoing crazing propagation. In a particle toughened polymer matrix, toughening particles can control the degree of the crazing growth as shown in Figure 1.13B. In general, in a high impact tensile test, crazing tends to begin at nearly the equator of the particles where stress is highly concentrated. This concentrated stress results in the crack growth being perpendicular to the tension direction by the breakdown of extended fibrillar chains of the polymer matrix when the concentrated stress is high enough. Crazing has been known to show stress whitening caused by an X-ray light scattering measurement such as SAXS due to the formation of (micro) voids.

Finally, microcracking of toughening particles is also an efficient way of energy absorption and dissipation that may be combined with crack blunting mechanism. In general, the shear band formation is a more efficient mechanism in enhancing toughness,

followed by crazing, crack bridging, microcracking, crack-deflection, and crack-pinning mechanisms.

Toughening Methods for Epoxide Thermosets

Many efforts at toughening or plasticizing brittle materials have been reported for a century. In the first attempt, camphor as a plasticizer was used to make a cellulose nitrate based macromolecule tractable. A toughened polyester resin was found in the late of 1920s by incorporating unsaturated vegetable oils into brittle Glyptal polyester resin to produce alkyd resins. These early attempts led to the development of plasticizing methods for different kinds of brittle polymers such as polyvinyl chloride (PVC), polystyrene (PS), polymethyl methacrylate (PMMA), and epoxide thermosets.

However, the use of plasticizers, e.g. diphenyl (diethyl or dibutyl) phthalate, or reactive compounds bearing long alky chains often compromised other important properties such as heat resistance, durability, tensile strength and so forth. Meanwhile, the introduction of a secondary phase into a brittle polymer matrix such as epoxides successfully improved the toughness of the resulting polymers. In general, a secondary phase or domain is introduced in a form of blends or particles as a toughening agent (Figure 1.13). The introduction of a secondary phase to a brittle network structure can be achieved by several approaches using various toughening agents. Some of toughening agents are listed in Figure 1.14.

The first approach is to use reactive rubbers (RR) that are oligomers or (co)polymers in a solid or liquid form. Solid reactive rubbers (SRRs), such as acrylonitrile-butadiene rubbers, are added at low volume fractions due to their high viscosity caused by their high molecular weight (200,000-30,000). Liquid reactive rubbers (LRRs) usually have much lower molecular weight oligomers (3,000-4,000) compared to SRRs. One of the most common LRRs is an acrylonitrile-butadiene copolymer terminated with various functional end groups such as epoxy, amine, vinyl,

carboxyl groups, called ETBN, ATBN, VTBN, and CTBN. Of these LRRs, CTBN and ATBN are most commonly used with DGEBA and DGEBF type epoxides. In addition to the use of LRRs, liquid reactive polymers such as amine-terminated polyether with a molecular weight of about 10,000 are also commonly used as a toughening agent. Both SRRs and LRRs should be pre-reacted with a base epoxide prior to use to produce epoxy-RR adducts, because epoxy-RR adducts prevent the chance of early phase separation and gives better miscibility with base liquid epoxides. The solubility of RRs generally depends on the acrylonitrile content in the RR backbone: the solubility increases but the particle sizes formed during cure decrease as AN content increases. Interestingly, it was also reported that mixture of two different LRRs or a LRR-SRR mixture may have a synergistic effect on the toughening of epoxides due to multimodal distribution of the precipitated secondary phase.

The second approach is to introduce thermoplastic modifiers (TP) such as polyether sulfone, polyether imide, polyaryl ether ketone, and polyphenylene oxide. They are typically useful for high temperature performance, because their relatively high glass transition temperatures and high modulus do not compromise the thermal and mechanical properties of modified epoxides. However, some critical issues might avoid employing this approach, because there are processibility issues related to their poor miscibility with epoxides. Furthermore, a less pronounced phase separation during cure (especially with low molecular ones) and non-reactivity results in poor interfacial strength with the epoxide matrix. As a result, TP might be not as effective of a toughening agent as RRs. For example, Kishi et al. observed induction of phase separation by tentative micro-segregation of polyether sulfone (PES) in DGEBA epoxide matrix using small-angle X-ray scattering [111]. However, they found that no increase of fracture toughness with increasing PES content up to 15 wt.%. In the same report, enhancement in the toughness of the PES-modified epoxide system observed in the presence of rubber particles, which was attributed to combined effects associated with the cavitation mechanism of rubber

particles and enhanced ductility due to PES.[111]. Some other thermoplastic modifiers were also developed for better miscibility, processibility and enhanced thermal property as well as increased fracture toughness.[66]

Another type of phase separation that may occur in micron or submicron (or nano) sizes can be achieved to toughen epoxides during cure by the formation of interpenetrating polymer networks (IPNs) via hybrid polymerizations. This approach will be dealt separately in a discrete section.

The final approach is to incorporate solid particles that are already prepared prior to cure into base epoxides. In general, the pre-formed solid particles (PSPs) can be divided into inorganic and organic particles with respect to their material origin. Depending on the surface treatment of PSPs, they become either non-reactive or reactive toughening agents. Basically, most of PSPs are not soluble in base epoxide resin solutions at room temperature. For this reason, the dispersion of PSPs in base epoxides is very important to obtain final products with homogeneous properties over all geometric positions.

Some of solid organic PSPs made of linear polymers with a low melting point are incorporated into a relatively high viscous epoxide at an elevated temperature using a melt dispersion technique (Figure 1.15). In this approach, the whole blend system should be stable in a certain temperature range until dispersion of discrete PSPs is completed. For example, ethylene-vinyl acetate (EVA) copolymers can be dispersed with a particle size of 0.5 to 5.0 μm in liquid epoxides depending on binary composition and temperature. Similar to EVA copolymers, polyether–polyamide copolymers with AB block structures have been known to become soluble at elevated temperature. The polyether–polyamide copolymers form discrete particles (0.5 to 2.0 μm) in liquid epoxides when the temperature goes back below its UCST range for their binary mixture. In this manner, the copolymer particles can be locked in the liquid epoxide matrix prior to cure.

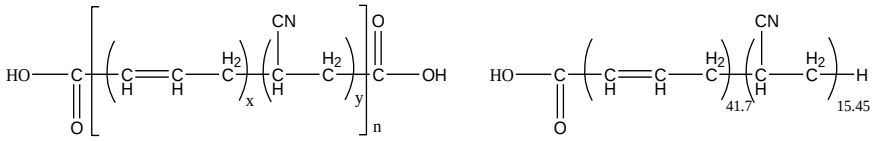

Hycar CTBN 1300X13

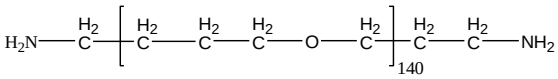

Dynamar HC-1101

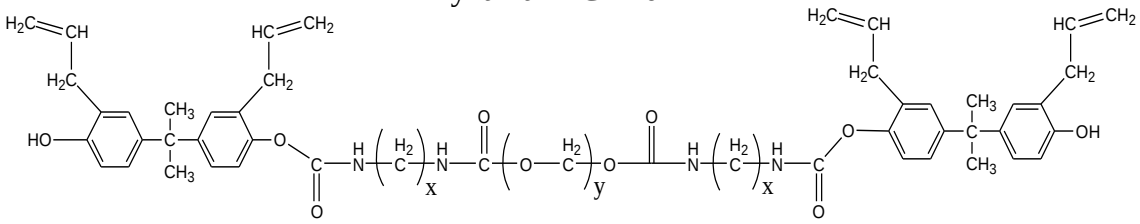

Phenolic end-capped polyurethane liquid rubber

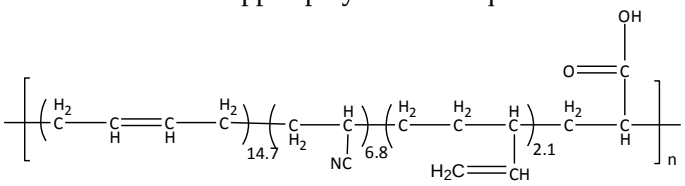

Carboxylated acrylonitrile-butadiene elastomer

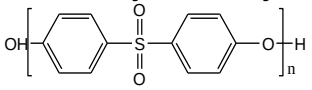

Polyethersulphone

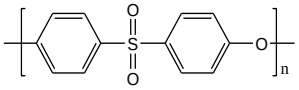

Polyphenylenesulphidesulphone

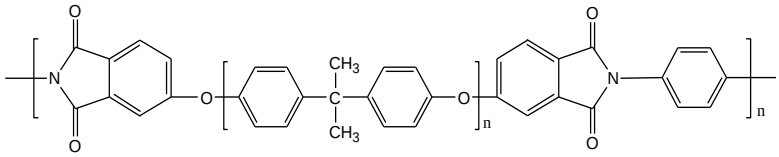

Polyetherimide

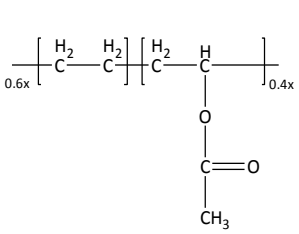

Ethylene-vinyl acetate copolymer

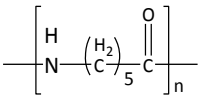

Nylon 6

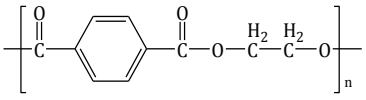

Polyethylene terephtahlate

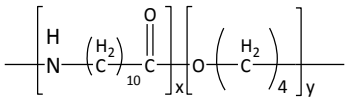

Nylon 11-tetrahydrafuran copolymer

Figure 1.14 Some conventional toughening agents grouped by liquid reactive rubbers, solid reactive rubbers, thermoplastic modifiers, and organic particles.

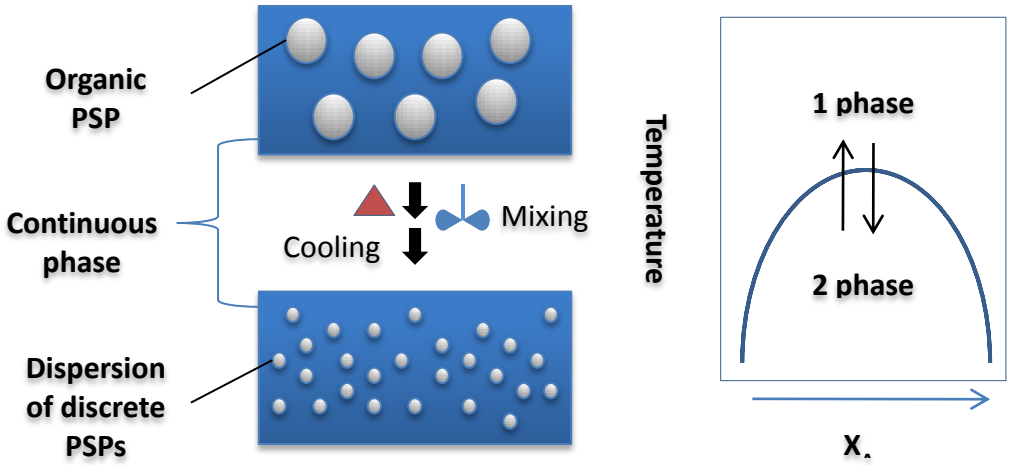

Figure 1.15 Schematic drawing of a melt dispersion technique and UCST characteristic for a binary mixture system containing epoxide solution and PSPs.

Hybrid Photopolymerizations

Conventional Hybrid Polymerization

Hybrid polymers are produced by polymerization of two organic monomers with different functional groups that are responsible for two separate polymerization mechanisms.[62, 112, 113] Typical hybrid polymerizations are based on a combination of monomers that undergo free-radical and ionic (anionic or cationic) polymerizations. The reaction of free-radical/anionic hybrid systems is often achieved by facilitating atom transfer/stabilizing free-radical polymerizations (ATRP or SFRP) of vinyl monomers and ring-opening polymerizations (ROP) of lactones or lactides using catalysts such as alkyl metal alkoxide.[114-116] The hybrid polymerizations can be carried out in a simultaneous or sequential manner. The resulting hybrid polymers form block, graft, and random copolymers.[117] In a similar way, (meth)acrylate/epoxide and (meth) acrylate/vinyl ether systems are polymerized by free-radical and cationic polymerization mechanisms. Depending on polymerization conditions, these two distinct polymerizations can be simultaneously or separately controlled. In theory, this controllable polymerization

kinetics allows two distinct polymers to grow without forming covalent bonds in between the two differently growing polymer chains since radical and cationic species are generally less reactive toward one another.[118-121] As a result, the two distinct polymer chains become interwoven and results in the formation of novel heterogeneous network structures, namely interpenetrating polymer networks (IPNs). [112, 113]

Interpenetrating Polymer Networks (IPNs)

The first developed IPN material was invented for phonograph records by crosslinking rubber in the presence of a crosslinked phenol-formaldehyde resin in 1914.[122] However, the first systematic research of an IPN material was delayed until 1960. In the late 1960, ion-exchange materials of IPNs were produced since IPNs exhibited lower degree of swelling than other crosslinked materials. Since then, the interest in IPN materials has been growing and a considerable number of studies have been conducted on IPN structure over the past few decades. It has been found that IPN structures and its physical properties of hybrid polymers are mainly affected by two distinct polymerization kinetic and processing order, and monomer functionality.[19-21, 112, 113, 119, 121, 123-125]

Different types of IPNs are obtained from various binary mixture systems. First, IPNs can be classified into two categories (SINs and SIPNs) by a synthetic process: simultaneous IPNs (SINs) are made by concurrence of two distinct polymerizations and sequential IPNs (SIPNs) by occurrence of two independent polymerizations at different time scales. Second, IPNs are also categorized into pseudo/semi-IPNs and full IPNs: pseudo and semi-IPNs are obtained when linear/branched polymers are growing in a crosslinked matrix. The former IPNs belong to SINs and the latter belongs to SIPNs. The full-IPNs are obtained when topological interlocking and entanglement of two cross-linked polymer matrix occur during hybrid polymerizations.

In general, two distinct polymerizations often inducing phase-separation during some stage of the polymerizations at the micro/nano-scale.[112, 113] Thus, kinetic approaches to the formation of these diverse IPNs described above have been correlated with phase separation and phase morphology.[112, 120, 121] Basically, phase separation, which is the degree of mixing, between two polymers depends on their thermodynamic equilibrium according to the Gibbs free energy and Flory-Huggins theory.[113, 126, 127] The thermodynamic equilibrium between two growing chains is more limited by kinetics, such as polymerization rate and kinetic sequence, and crosslink density, since crosslinking network of one polymer would restrict degree of freedom of the other polymer chains by preventing the diffusion and subsequent phase separation. This restriction would be more pronounced in full-IPNs than in semi-/pseudo IPNs.

Theoretically, the full-IPN polymers have been recognized in significantly enhancing mechanical performance of final cured hybrid polymer if each independent polymerization rapidly reached unity, because of the higher degree of mixing and the less phase separation. However, in reality the degree of phase separation can also vary with kinetic sequences and crosslink density of each polymer domain. It will be important to monitor phase development during hybrid polymerizations and understand phase behavior of the final cured polymers. In addition, monomer composition must be correlated with the polymer entities after the cure. Eventually, all of these factors influence the development of phase morphology in micro or nano scales, which has been extensively studied. It was found phase morphology have a strong correlation with mechanical properties of final cured hybrid polymers. [112, 113]

Hybrid Photopolymerization

The conventional hybrid systems have been investigated for thermal polymerizations. The traditional thermal curing is time-consuming and often requires high temperature and solvents. However, the traditional thermal methods have limitations

for some coating and adhesive applications for which heat sensitive substrates are used. In addition, evaporation of solvents from the thermal reaction systems may cause formation of pores on coatings or adhesives during process, which deteriorate physical and mechanical properties of final cured hybrid polymers. These issues can be addressed in photopolymerization systems.

Compared to the thermal hybrid systems, a major difference in hybrid photopolymerizations is photoinitiation. Rapid delivery of the required radiation energy throughout the samples can induce fast initiation of distinct polymerizations at room temperature [1, 2, 9] In addition, hybrid photopolymerizations are usually carried out in bulk mixture systems. Various binary mixtures have been studied for hybrid photopolymerizations containing a wide range of acrylates, epoxides, vinyl ethers or hybrid monomers bearing both vinyl and epoxide functional groups. [12, 19, 20, 118, 124, 125]. The majority of these hybrid mixtures are based on free-radical and cationic photopolymerizations. Since the photoinitiation is temporally and spatially controllable, the acrylate/epoxide hybrid systems opt for more diverse controls of two distinct polymerizations. [119, 127-129] This will be beneficial because it will provide faster and more accurate access to in situ applications such as stereolithography [29, 30, 101] when compared to the conventional thermal polymerization. In addition, combined features from photopolymerizations and IPN structure can be utilized for developing controllable physical properties including enhanced cracking energy, controllable phase separation for useful permeation or optical properties, and surface hardness. [12, 19-21, 119-121, 124].

Acrylate/epoxide Hybrid Photopolymerizations

In acrylate and epoxide photopolymerizations, atmospheric factors such as oxygen and water affect free-radical and cationic photopolymerizations, respectively. These atmospheric effects give rise to the change of the reaction environment, e.g. viscosity, concentrations of initiating species and propagating active centers, and so on,

during polymerization[16, 23, 32, 41] Specifically, interactions between oxygen and radicals and between water and cationic active centers directly affect polymerization rates and ultimate conversions, and ultimate properties, especially for coating applications.

Recent studies have shown that acrylate/epoxide hybrid systems are very promising to address issues with the atmospheric factors. [19-21, 123-125, 130] In general, the negative effects of oxygen and water are reduced by complementary natures of two distinct initiating species. However, it is not clear whether the interplay in between the two atmospheric factors affect flexibility in the onset of free-racial and cationic photopolymerization and final IPN structures similar to thermal systems. In addition, disparity in the polymerization kinetics between acrylates and epoxides monomers is generally observed regardless of monomer type and bulk viscosity. [12, 62, 131] This difference may limit the diversity of IPNs in acrylate/epoxide hybrid systems, because phase separation of two independent growing chains occurs at low conversion.[113]

To address these issues, various variables that affect the hybrid photopolymerization kinetics should be further understood. The variables include photoinitiator systems, light intensity, and temperature.[11-14, 123, 132] Those variables are basic components that impact the kinetics of both radical and cationic photopolymerizations. Among these variables, photoinitiator systems will play a great role in the kinetic sequence, the rate of polymerization, physical properties of final products. [12, 15, 29, 30, 101, 125, 133-135] In addition, little is known about how two different polymerizations affect one another in binary mixture systems as a function of monomer structures and composition. Furthermore, for the acrylate/hybrid systems, it is necessary to understand more clear correlation of two distinct polymerization kinetics with final network structure and phase development.

Photopolymerizations of Acrylates

Vinyl monomers can undergo polymerization by opening the carbon-carbon double bond via photogenerated radical, ionic, cationic species. Acrylate monomers,

known for their high reactivity, polymerize rapidly in the presence of free radicals (Figure 1.16). However, acrylates are not initiated by cationic species, because they have ester group that act as electron withdrawing groups and decrease the electron density on the double bond. This leads to a repulsive force between monomers and cationic species.[62]

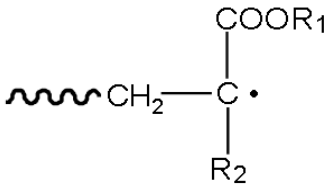

Figure 1. 16 Growing radical species of acrylates (R_2=H) and methacrylates (R_2=CH_3) during the free-radical polymerizations. R_1 is a secondary functionality that varies depending on monomer types. Examples of R_1 could be urethane, ether, or aliphatic alkyl chains.

For photoinitiated free-radical polymerizations, photoinitiators and their transient states play a key role in the photopolymerizations process by affecting monomer conversion and molecular weight of resulting polymers. There are two types of photoinitiators that contain usually benzoyl choromophore as a light absorbing moiety [1, 3, 136]. Type I is unimolecular cleavage initiators in which the unimolecular fragmentation occurs on α or β carbon (Fig. 1.17). The type I initiators are exited from ground (S0) states to singlet (S1) states by UV radiation. Through efficient intersystem crossing, singlet states of the initiators move on to triplet (T1) states that have a relatively longer lifetime than the S1 state [1, 2, 136]. Consequently most of the unimolecular cleavage reactions take place in triplet states of Type I PIs and, thus, proceed at high speeds.

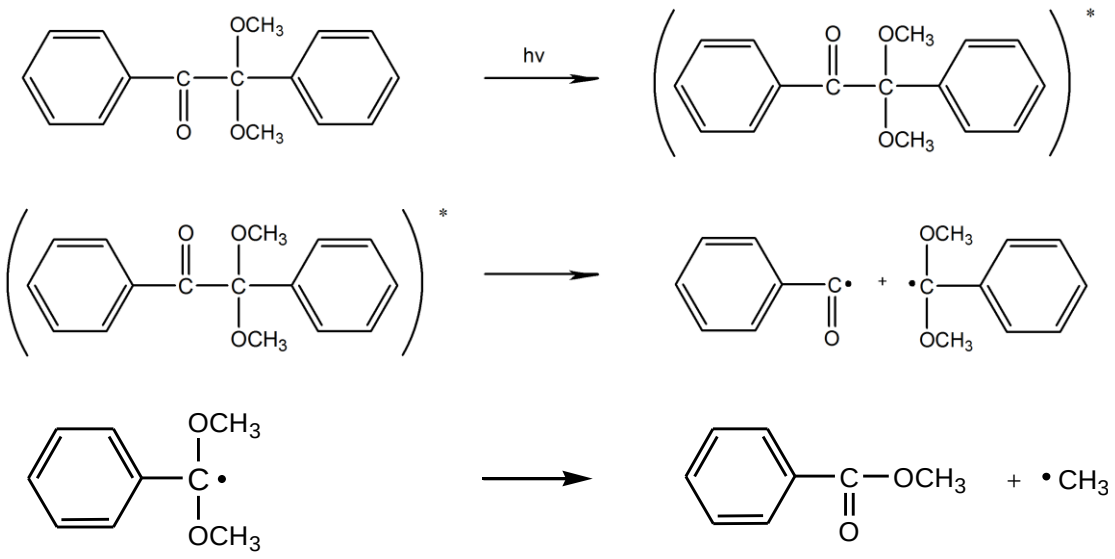

Figure 1.17 α-carbon bond cleavage of 2, 2-dimethoxy-2-pheylacetophenone (DMPA) upon illumination.

On the contrary, Type II radical photoinitiation requires hydrogen abstraction and electron transfer reactions in the presence of both photosensitizers (diaryl ketone) and coinitiators [1, 2, 17, 136]. After illumination, a photosensitizer (PS) in the first (T1) or the second (T2) triplet state begins to interact with a coinitiator that is a hydrogen donor, e.g. alcohols and thiols, or an electron donor such as an amine. The main radicals that initiate polymerization form on those coinitiator molecules. The combination of PS and a hydrogen donor is less effective than PS-amine systems in which the electron transfer is followed by a proton transfer (Figure 1.18)

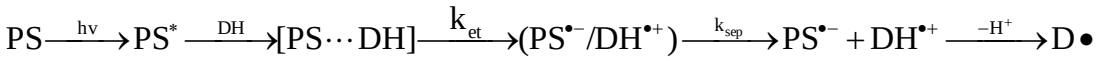

Figure 1.18 Type II photoinitiation in the presence of a photosensitizer (PS) and an electron donor (DH). Free-radical (D•) is generated from the interaction between photosensitizer (PS) and electron donor (DH): k_{et}, electron transfer rate constant; k_{sep}, separation rate constant.

The Effect of Oxygen

The inhibitory effect of oxygen on radical species, such as primary radicals and growing chain radicals, is attributed to its biradical structure. In the biradical structure one pair of electrons in the antibonding π orbitals form a covalent bond with radical species[16, 18]. Another unique feature of oxygen lies in its energy state at ambient condition. Ground-state oxygen is equivalent to triplet energy states in that oxygen is subjected to energy transfer to the other triplet state molecules[16, 18]. Through the former step, radical species are scavenged by forming peroxy radicals. The resulting peroxy radicals are more stable than other radical species due to their resonance effect. In the latter step, triplet state oxygen molecules collide with other triplet state PSs or PIs and allow energy transfer to quench them (Figure 1.19).

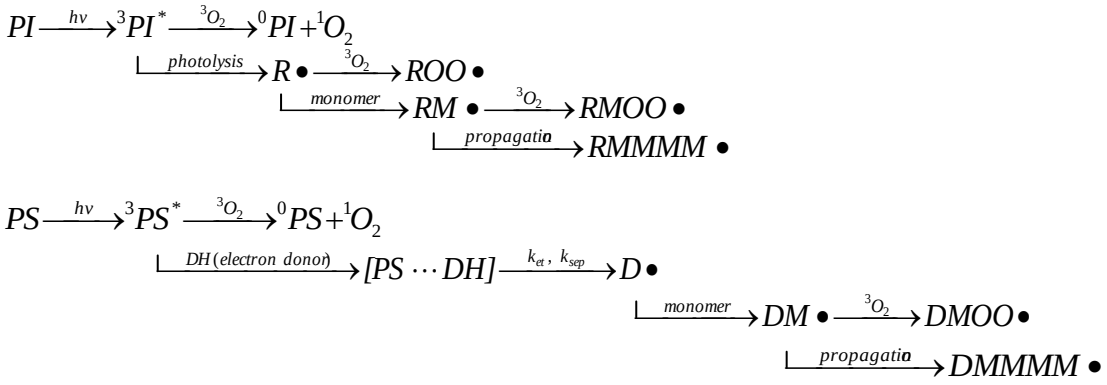

Figure 1.19 Inhibitory effects of oxygen molecules on free-radical polymerization using type I (upper) and type II initiator systems (down).

Dual & Three-Component Photoinitiators

Dual-type PI systems are distinguished from Type II photoinitiators. The dual-type mean radical and cationic photoinitiators initiate free radical and cationic photopolymerizations, respectively.[101, 135, 137] Thus, the dual PI can be utilized for hybrid photopolymerizations.[12, 123, 130] The onset time of two independent radical

and cationic polymerizations can be alternated by radiating at different wavelength ranges that can absorbed by the corresponding PIs. In addition, cationic photopolymerizations can be promoted by radicals in dark condition. For example, a free radical initiator, benzoin, is decomposed to hydroxyl benzyl (strong electron donor) and benzoyl (electron withdrawer) radicals upon illumination at wavelength between 350-360nm. At these wavelengths cationic photoinitiators do not absorb the photon energy. While benzoyl radicals undergo free-radical polymerization, hydroxyl benzyl radicals undergo electron transfer reactions through cationic photoinitiators (electron acceptor), e.g. onium salts and alkoxy pyridinium salts. Accordingly, the hydroxyl benzyl radicals are oxidized to form corresponding carbocations that react with cationic monomers via cationic polymerization. The reduced cationic photoinitiators are decomposed to relatively stable aryl radicals and neutral iodobenzene compounds.

On the other hand, the three-component system consists of an electron acceptor (dye), an electron donor (amine), and a second electron acceptor (cationic photoinitiator).[29, 30] Those components are selected by the thermodynamic feasibility for the electron transfer mechanism, which is governed by the Rehm-Weller equation. Above all, amines should be very carefully selected based on their oxidation potentials and pK_b values, because the oxidation potential affects electron transfer to dye. Also, pK_b values more than 8.37 significantly inhibit the cationic initiation and propagation by competing with epoxides and by scavenging protons.

Notes

1. Fouassier, J.P., *Photoinitiations, Photopolymerization, and Photocuring: Fundamentals and Applications*. 1st ed. 1995, Cincinati: Hanser/Gardner Publications, Inc.

2. Norman S. Allen, M.E., Ignazio Renato Bellobono, Elena Selli, *Currents Trends in Polymer Photochemistry*. 1st ed. 1995: Ellis Horwood.

3. Endruweit, A., Johnson, M.S., and Long, A.C., *Curing of Composite Components by Ultraviolet Radiation: A Review*. Polymer Composite, 2006. 27(2): p. 119.

4. Shu Yang, J.F., Chada Ruengruglikit, Qingrong Huang, and Joanna Aizenberg, *Synthesis of Photoacid crosslinkable hydrogels for the fabrication of soft, biomimetic microlens arrays.* . Journal of Materials Chemistry, 2005. 15: p. 4200-4202.

5. Fisher, J.P., Dean, D., Engel, P. S., Mikos, A. G., *Photoinitiated polymerization of biomaterials.* Annual Review of Materials Science, 2001. 31: p. 171-181.

6. Anseth, K.S.a.B., Jason A., *New Directions in Photopolymerizable Biomaterials.* MRS Bulleten, 2002: p. 130-136.

7. Baroli, B., *Photopolymerization of biomaterials: Issues and potentialities in drug delivery, tissue engineering, and cell encapsulation applications.* Journal of Chemical Technology and Biotechnology, 2006. 81(4): p. 491-499.

8. Richard Vendamme, S.-Y.O., Aiko Nakao, and Toyoki Kunitake, *Robust free-standing nanomembranes of orgainic/inorganic interpenetrating networks.* Nature materials, 2006. 5: p. 494-501.

9. Roffey, C.G., *Photopolymerization of Surface Coatings*. 1982, New York: John Wiley & Sons, Inc.

10. Z. Czech, a.R.M., *Solvent-Free Radiation-Curable Polyacrylate Pressure Sensitive Adhesive Systems.* Journal of Applied Polymer Science, 2003. 87: p. 182-191.

11. Decker, C., *Kinetics Study and New Applicatioins of UV Radiation Curing.* Macromolecular Chemistry and Physics, 2002. 23(18): p. 1067-1093.

12. Ying Cai, a.J.L.P.J., *Decreased oxygen inhibtion in photopolymerized acrylate/epoxide hybrid polymer coatings as demonstrated by Raman Spectroscopy.* Polymer, 2006. 47: p. 6560-6566.

13. Vishal Sipani, A.K., and Alec B. Scranton, *Dark Cure Studies of Cationic Photopolymerizations of Epoxides: Characterization of Kinetic Rate Constants at High Conversions.* Journal of Polymer Science: Part A: Polymer Chemistry, 2004. 42: p. 4409-4416.

14. Sipani, V. and Scranton, A.B., *Kinetic studies of cationic photopolymerizations of Phenyl glycidyl ether: termination/trapping rate constants for iodonium photoinitiators.* Journal of Photochemistry and Photobiology A: Chemistry 2003. 159: p. 189-195.

15. Vishal Sipani, a.A.B.S., *Dark-Cure Studies of Cationic Photopolymerizations of Epoxides: Chracterization of the Active Center Lifetime and Kinetic Rate Constants.* Journal of Polymer Science: Part A: Polymer Chemistry, 2003. 41: p. 2064-2072.

16. Gou, L., Opheim, B., and Scranton, A.B., *The effect of oxygen in free radical photopolymerization.* Recent Research Developments in Polymer Science 2004. 8: p. 125-141.

17. Smith, G.J., *Enhanced Intersystem Crossing in the Oxygen Quenching of Aromatic Hydrocarbon Triplet States with High Energies.* Journal of the Chemical Society, Faraday Transactions, 1982. 2(78): p. 769-773.

18. Christophersen, A.G., Jun, H., Jørgensen, K., and Skibsted, L. H., *Photobleaching of astaxanthin and canthaxanthin: quantum-yields dependence of solvent, temperature, and wavelength of irradiation in relation to packageing and storage of carotenoid pigmented salmonoids.* Z Lebensm Unters Forsch, 1991. 192: p. 443-439.

19. Decker C, N.T.V.T., Decker D, and Weber-Koehl E, *UV-radiation curing of acrylate/epoxide systems.* Polymer, 2001. 42(13): p. 5531-5541.

20. Decker C, a.B.T., *Interpenetrating polymer networks. II. Sunlight-induced polymerization of multifunctional acrylates.* Journal of Applied Polymer Science 1998. 70(11): p. 2269-2282.

21. Kaczmarek, H.a.D., C., *Interpenetrating polymer networks. I. Photopolymerization of multiacrylate systems.* Journal of Applied Polymer Science, 1994. 54(13): p. 2147-56.

22. O'Brien, A.K.a.B., Bowman N., *Impact of Oxygen on Photopolymerization Kinetics and Polymer Structure.* Macromolecules, 2006. 39: p. 2501-2506.

23. H. Cao, E.C., M. Tilley, and Y.C. Jean, *Oxygen inhibition effect on surface properties of UV-curable acrylate coatings.* ACS Symposium Series 847, 2003: p. 165-175.

24. Bolon, D.A.a.W.K.K., *Barrier coats versus inert atmosperes. The elimination of oxygen in free-radical polymerizations.* . Journal of Applied Polymer Science, 1978 (22): p. 2543-2551.

25. Christopher G. Williams, A.N.M., Tae Kyun Kima, Paul N. Mansonb and Jennifer H. Elisseeff, *Variable cytocompatibility of six cell lines with photoinitiators used for polymerizing hydrogels and cell encapsulation* Biomaterials, 2005. 26(11): p. 1211-1218.

26. James V. Crivello, R.A.O., *Benzyl Alcohols as Accelerators in the Photoinitiated Cationic Polymerization of Epoxide Monomers.* Journal of Polymer Science: Part A: Polymer Chemistry, 2002. 40: p. 2298-2309.

27. R. Tokar, P.K., and S. Penczek, *Cationic Polymerization of Glycidol: Coexistence of the Activated Monomer and Active Chain End Mechanism.* Macromolecules, 1994. 27: p. 320-322.

28. M. Sangermano, G.M., F. Morel, C. Decker, A. Priola, *Cationic Photopolymerization of Vinyl ether systems: influence of the presence of hydrogen donor additives.* European Polymer Journal, 1999. 35: p. 639-645.

29. Joe D. Oxman, D.W.J., Matthew C. Trom, Vishal Sipani, Beth Ficek, and Alec B. Scranton, *Evaluation of Initiator systems for controlled and sequentially curable Free-Radical/Cationic Hybrid Photopolymerizations.* Journal of Polymer Science: Part A: Polymer Chemistry, 2004. 43: p. 1747-1756.

30. Dongkwan Kim, a.A.S., *The role of diphenyl iodonium salt (DPI) in Three-componetn photointiator systems containing methylene blue (MB) and an electron donor.* Journal of Polymer Science: Part A: Polymer Chemistry, 2004. 42: p. 5863-5871.

31. Hartwig, A., *Influence of Moisture present during polymerisation on the properties of a photocured epoxy resin.* International Journal of Adhesion & Adhesives 2002. 22: p. 409-414.

32. A. Hartwig, B.S., and A. Luhring, *Influence of moisture on the photochemically induced polymerisation of epoxy groups in different chemical environment.* Polymer, 2002. 43: p. 4243-4250.

33. James V. Crivello, a.S.L., *Photoinitiated Catioinc Polymerization of Epoxy Alcohol Monomers.* Journal of Polymer Science: Part A: Polymer Chemistry, 2000. 38: p. 389-401.

34. Hartwig, A., Harder, A., Lühring, A., and Schröder, H., *(9-Oxo-9H-fluoren-2-yl)-phenyl-iodonium hexafluoroantimonate(V)-a photoinitiator for the cationic*

polymerisation of epoxides. European Polymer Journal, 2001. 37(7): p. 1449-1455.

35. Ricardo Acosta Ortiz, D.P.L., Mara de Lourdes Guillen Cisneros, Julio Cesar Rico Valverde, James V. Crivello, *A kinetic study of the acceleration effect of substituted benzyl alcohol on the cationic photopolymerization rate of epoxidized natural oils.* Polymer, 2005. 46: p. 1535-1541.

36. Crivello, J.V. and Ortiz, R.A., *Benzyl alcohols as accelerators in the photoinitiated cationic polymerization of epoxide monomers.* Journal of Polymer Science Part A: Polymer Chemistry, 2002. 40(14): p. 2298-2309.

37. R. T. Olsson, H.E.B., V. Kuck, and A. Hale, *Acceleration of the cationic polymerization of an Epoxy with hexandiol.* Journal of Thermal Analysis and Calorimetry, 2004. 76: p. 367-377.

38. Kim, D. and Jessop, J.L.P., *The role of water in photoinitiated cationic ring-opening photopolymerization of cyclehexane epoxides.* 2006 UV & EB Technology Conference & Exhibition, 2006.

39. Dongkwan Kim, a.J.L.P.J., *The role of water in photoinitiated cationic ring-opening photopolymerization of cyclehexane epoxides.* 2006 UV & EB Technology Conference & Exhibition, 2006.

40. Lin, Y. and Stansbury, J.W., *Near-Infrared Spectroscopy Investigation of Water Effects on the Cationic Photopolymerization of Vinyl Ether System.* Journal of Polymer Science: Part A: Polymer Chemistry, 2004. 42: p. 1985-1998.

41. Yan Lin, J.W.S., *Near-Infrared Spectroscopy Investigation of Water Effects on the Cationic Photopolymerization of Vinyl Ether System.* Journal of Polymer Science: Part A: Polymer Chemistry, 2004. 42: p. 1985-1998.

42. Hartwig, A., Schneider, B., and Luhring, A., *Influence of moisture on the photochemically induced polymerisation of epoxy groups in different chemical environment.* Polymer, 2002. 43: p. 4243-4250.

43. James, V.C., *The discovery and development of onium salt cationic photoinitiators.* Journal of Polymer Science Part A: Polymer Chemistry, 1999. 37(23): p. 4241-4254.

44. Crivello, J.V., *Photoinitiated Cationic Polymerization.* Annual Review of Materials Science, 1983. 13: p. 173-190.

45. Wolfram, S., *Cationic photopolymerization with the aid of pyridinium-type salts.* Macromolecular Rapid Communications, 2000. 21(10): p. 628-642.

46. Crivello, J.V., *Advances in the design of photoinitiators, photosensitizers and monomers for photoinitiated cationic polymerization* Designed monomers and polymers 2002. 5(2-3): p. 141-154.

47. Crivello, J.V., *The discovery and development of onium salt cationic photoinitiators.* Journal of Polymer Science Part A: Polymer Chemistry, 1999. 37(23): p. 4241-4254.

48. Fouassier, J.P., *Photoinitiation, Photopolymerization, and Photocuring*. 1st ed. 1995, Munich, New York: Hanser Publishers.

49. J. V. Crivello, K.D.J., *Propenyl ethers. III. Study of the photoinitiated cationic polymerization of propenyl ether monomers.* Journal of Polymer Science Part A: Polymer Chemistry, 1993. 31(8): p. 2143-2152.

50. Eric J. Goethals and Preza, F.D., *Carbocationic polymerizations* Progress in Polymer Science, 2007. 32(2): p. 220-246.

51. Pierre Sigwalt and Moreau, M., *Carbocationic polymerization: Mechanisms and kinetics of propagation reactions* Progress in Polymer Science, 2006. 31(1): p. 44-120.

52. Penczek, S., Cypryka, M., Duda, A., Kubisaa, P., and Słomkowskia, S., *Living ring-opening polymerizations of heterocyclic monomers* Progress in Polymer Science 2007. 32(2): p. 247-282

53. Nelson, E.W., Carter, T.P., and Scranton, A.B., *Fluorescence Monitoring of Cationic Photopolymerizations: Divinyl Ether Polymerizations Photosensitized by Anthracene Derivatives.* Macromolecules 1994, 1994. 27: p. 1013-1019.

54. Cho, J.-D. and Hong, J.-W., *Photo-curing kinetics for the UV-initiated cationic polymerization of a cycloaliphatic diepoxide system photosensitized by thioxanthone.* European Polymer Journal 2005 41 p. 367–374.

55. Yujing Hua, J.V.C., *Synergistic interaction of epoxides and N-vinylcarbazole during photoinitiated cationic polymerization.* Journal of Polymer Science Part A: Polymer Chemistry, 2000. 38(19): p. 3697-3709.

56. Hua, Y. and Crivello, J.V., *Development of Polymeric Photosensitizers for Photoinitiated Cationic Polymerization* Macromolecules 1994, 2001. 34 (8): p. 2488 -2494.

57. Nelson, E.W., Jacobs, J.L., Scranton, A.B., Anseth, K.S., and Bowman, C.N., *Photo-differential scanning calorimetry studies of cationic polymerizations of divinyl ethers* Polymer, 1995. 36(24): p. 4651-4656.

58. Nelson, E.W. and Scranton, A.B., *Kinetics of cationic photopolymerizations of divinyl ethers characterized using in situ Raman spectroscopy.* Journal of Polymer Science Part A: Polymer Chemistry, 1996. 34(3): p. 403-411.

59. Cho, J.D. and Hong, J.W., *Photo-curing kinetics for the UV-initiated cationic polymerization of a cycloaliphatic diepoxide system photosensitized.* European Polymer Journal, 2005. 41(2): p. 367-374.

60. Hua, Y. and Crivello, J.V., *Synergistic interaction of epoxides and N-vinylcarbazole during photoinitiated cationic polymerization.* Journal of Polymer Science Part A: Polymer Chemistry, 2000. 38(19): p. 3697-3709.

61. Geacintov, N.E., Shafirovich, V.Y., Li, B., Mao, B., and Ya, N., *Photoinduced Electron Transfer, Fluorescence, and Intrastrand Migration of Reactive Intermediates in Pyrenyl Sensitizer -Modified DNA Duplexes.* The Spectrum, 1997. 10(2): p. 1-16.

62. Odian, G., *Principles of Polymerization*. 4th ed. 2004, New York: John Wiley & Sons, Inc. .

63. Batog, A.E., Pet'ko, I. P., Penczek, P., *Aliphatic-Cycloaliphatic Epoxy Compounds and Polymers.* Advances in Polymer Science, 1999. 144.

64. Crivello, J.V., *Cationic Photopolymerizationi of Alkyl Glycidyl Ethers.* Journal of Polymer Science: Part A: Polymer Chemistry, 2006. 44: p. 3036-3052.

65. Bulut, U., and Crivello, J. V. , *Investigation of the Reactivity of Epoxide Monomers in Photoinitiated Cationic Polymerization* Macromolecules, 2005. 38(9): p. 3584 -3595.

66. Petrie, E.M., *Epoxy Adhesive Formulations*. First ed. 2006, New York: McGrow-Hill.

67. J.V. Crivello, a.W.-G.K., *Synthesis and Photopolymerization of 1-Propenyl Glycidyl Ether.* Journal of Polymer Science: Part A: Polymer Chemistry, 1994. 32: p. 1639-1648.

68. Packham, D.E., *Handbook of Adhesion*. Second ed. 2005, Chichester, England: John Wiley & Sons Ltd.

69. Goethals, E.J. and Du Prez, F., *Carbocationic polymerizations.* Progress in Polymer Science, 2007. 32(2): p. 220-246.

70. P. Sigwalt and Moreau, M., *Carbocationic polymerization: Mechanisms and kinetics of propagation reactions.* Progress in Polymer Science, 2006. 31(1): p. 44-120.

71. Szwarc, M., *The kinetics and mechanism of N-carboxy-α-amino-acid anhydride (NCA) polymerisation to poly-amino acids*, in *Fortschritte der Hochpolymeren-Forschung*. 1965. p. 1-65.

72. Allen, N.S., Edge, M., Bellobono, I.R., and Selli, E., *Currents Trends in Polymer Photochemistry*. 1st ed. 1995, Munich, New York: Ellis Horwood publisher.

73. Biedron, T., Brzezinska, K., Kubisa, P., and StanislawPenczek, *Macromonomers by activated polymerization of oxiranes. Synthesis and polymerization.* Polymer International, 1995. 36(1): p. 73-80.

74. Evans A.G., H., D., Plesch, P. H., Polanyi M., Skinner, H.A., and Weinberger, M.A. , *Fridel-Crafts Catalysts and polymerization.* Nature, 1946. 157: p. 102.

75. Polanyi, E.a., *Polymerisation of Discussion on " Some Aspects of the Chemistry of Macromolecules.' '*. Journal of the Chemical Society 1947: p. 252 - 306.

76. G. Sauvet, J.P.V.P.S., *The cationic dimerization of 1,1-diphenylethylene. II. Cation formation with titanium tetrachloride in dichloromethane solution.* Journal of Polymer Science: Polymer Chemistry Edition, 1978. 16(12): p. 3047-3064.

77. M. Masure, G.S.P.S., *The cationic dimerization of 1,1-diphenylethylene. III. Kinetics of initiation by aluminum chloride.* Journal of Polymer Science: Polymer Chemistry Edition, 1978. 16(12): p. 3065-3076.

78. Grattan, D.W. and Plesch, P.H., *The Initiation of Polymerisations by Aluminium Halides.* Makromolekulare Chemie, 1980. 181(4): p. 751-775.

79. Crivello, J.V. and Varlemann, U., *Structure and reactivity relationship in the photoinitiated cationic polymerization of 3,4-epoxycyclohexylmethyl-3'-4'-epoxycyclohexane carboxylate.* ACS symposium series, 1997. 673: p. 82-94.

80. Crivello, J.V., Ortiz, R. A. , *Design and synthesis of highly reactive photopolymerizable epoxy monomers.* Journal of Polymer Science Part A: Polymer Chemistry, 2001. 39(14): p. 2385-2395.

81. Crivello, J.V. and Kim, W.-G., *Synthesis and Photopolymerization of 1-Propenyl Glycidyl Ether.* Journal of Polymer Science: Part A: Polymer Chemistry, 1994. 32: p. 1639-1648.

82. Rajaraman, S.K., Mowers, W. A., Crivello, J.V., *Novel Hybrid Monomers Bearing Cycloaliphatic Epoxy and 1-Propenyl Ether Groups* Macromolecules, 1999. 32(1): p. 36 -47.

83. J. V. Crivello, S.S.L., *Synthesis and cationic photopolymerization of 1-butenyl glycidyl ether.* Journal of Polymer Science Part A: Polymer Chemistry, 1998. 36(7): p. 1179-1187.

84. Crivello, J.V. and Ortiz, R.A., *Design and synthesis of highly reactive photopolymerizable epoxy monomers.* Journal of Polymer Science Part A: Polymer Chemistry, 2001. 39(14): p. 2385-2395.

85. James V. Crivello, R.A.O., *Synthesis of epoxy monomers that undergo synergistic photopolymerization by a radical-induced cationic mechanism.* Journal of Polymer Science Part A: Polymer Chemistry, 2001. 39(20): p. 3578-3592.

86. Tokar, R., Kubisa, P., Penczek, S., and Dworak, A., *Cationic polymerization of glycidol: coexistence of the activated monomer and active chain end mechanism.* Macromolecules, 1994. 27(2): p. 320-322.

87. Krystyna, B., nacute, ska, R.S., ski, P., lstrok, aw Kubisa, S., and aw, P., *Activated monomer mechanism in cationic polymerization, 1. Ethylene oxide, formulation of mechanism.* Die Makromolekulare Chemie, Rapid Communications, 1986. 7(1): p. 1-4.

88. Tadeusz Biedron, K.B.P.K.S., *Macromonomers by activated polymerization of oxiranes. Synthesis and polymerization.* Polymer International, 1995. 36(1): p. 73-80.

89. Kubisa, P. and Penczek, S., *Cationic activated monomer polymerization of heterocyclic monomers.* Progress in Polymer Science, 1999. 24: p. 1409-1437.

90. Bednarek, M., Kubisa, P., and Penczek, S., *Coexistence of Activated Monomer and Active Chain End Mechanisms in Cationic Copolymerization of Tetrahydrofuran with Ethylene Oxide.* Macromolecules, 1999. 32: p. 5257-5263.

91. Bednarek, M., Biedron, T., Kaluzynski, K., Kubisa, P., Pretula, J., and Penczek, S., *Ring Opening Polymerization Processes Involving Activated Monomer Mechanism. Cationic Polymerization of Cyclic Ethers Containing Hydroxyl Groups.* Macromolecular Symposia, 2000. 157: p. 1-11.

92. Kubisa, P., *Hyperbranched Polyethers by Ring-Opening Polymerization: Contribution of Activated Monomer Mechanism.* Journal of Polymer Science: Part A: Polymer Chemistry, 2003. 41: p. 457-468.

93. Crivello, J.V. and Liu, S., *Photoinitiated cationic polymerization of epoxy alcohol monomers.* Journal of Polymer Science Part A: Polymer Chemistry, 2000. 38(3): p. 389-401.

94. Surésh K. Rajaraman, W.A.M.J.V.C., *Interaction of epoxy and vinyl ethers during photoinitiated cationic polymerization.* Journal of Polymer Science Part A: Polymer Chemistry, 1999. 37(21): p. 4007-4018.

95. Tom Scherzer, M.R.B., *Photoinitiated Cationic Polymerization of Cycloaliphatic Epoxide/Vinyl Ether Systems Studied by Near-Infrared Reflection Spectroscopy*. Macromolecular Chemistry and Physics, 2007. 208(9): p. 946-954.

96. Kim, Y.-M.K., L.; MacGregor, J.; Hamielec, A., *Thermal and real-time FTIR spectroscopic analysis of the photopolymerization of diepoxide-vinyl ether mixtures.* Journal of Thermal Analysis and Calorimetry, 2004. 78 (1): p. 153-164.

97. Decker, C., Bianchi, C., Decker, D., Morel, F., *Photoinitiated polymerization of vinyl ether-based systems.* Progress in Organic Coatings, 2001. 42(3-4): p. 253-266.

98. Hiroshi Sasaki, J.M.R., nacute, and ski, T.K., *Photoinitiated cationic polymerization of oxetane formulated with oxirane.* Journal of Polymer Science Part A: Polymer Chemistry, 1995. 33(11): p. 1807-1816.

99. Biedron, T., Szymanski, R., Kubisa, P., and Penczek, S., Makromol. Chem., Macromol. Symp., 1990. 32: p. 155.

100. Biedron, T., Kubisa, P., and Penczek, S., Journal of polymer science., 1991. 29: p. 619.

101. Hai-Qing Guo, A.K., Yotaro Morishima, and Mikiharu Kamachi, *Radical/Cation Transformation Polymerization and Its Applications to the Preparation of Block Copolymers.* Polymers for Advanced Technologies, 1997. 8: p. 196-202.

102. Tadatomi Nishikubo, T.I.E.T.A.U., *Syntheses of polymers with pendant photosensitive and photosensitizing groups by cationic copolymerizations of photosensitive and photosensitizing monomers.* Die Makromolekulare Chemie, Rapid Communications, 1984. 5(3): p. 131-135.

103. Sadahito Hashidate, Y.N.M.K.H.M.H.N., *Photocrosslinkable second-order nonlinear optical polymers synthesized by cationic copolymerization.* Polymers for Advanced Technologies, 1995. 6(9): p. 626-631.

104. Percec, V. and Tomazos, D., *Liquid crystalline copoly(vinylether)s containing 4(4')-methoxy-4' (4)-hydroxy-α-methylstilbene constitutional isomers as side groups.* Polymer Bulletin, 1987. 18(3): p. 239-246.

105. Park, J.B. and Lakes, R.S., *Biomaterials: an introduction*. Second ed. 1992, NY: Plenum.

106. Riew, C.K. and Gillham, J.K., *Rubber-modified Thermoset Resins*. Advances in Chemistry. Vol. 208. 1984, Washington DC: American Chemical Society.

107. Riew, C.K., *Rubber-Toughened Plastics*. Advances in Chemistry Series Vol. 222. 1989, Washington, DC: American Chemical Society.

108. Riew, C.K. and Kinloch, A.J., *Toughened Plastics I*. Advances in Chemistry. Vol. 233. 1993, Washington DC: American Chemical Society.

109. Riew, C.K. and Kinloch, A.J., *Toughened Plastics II*. Advances in Chemistry. Vol. 252. 1996, Washington DC: American Chemical Society.

110. Pearson, R.A., *Introduction of the toughening of polymers*, in *ACS Symposium series: Toughening of Plastics*, R.A. Pearson, H.-J. Sue, and A.F. Yee, Editors. 2000, American Chemical Society: Washington DC. p. 1-12.

111. Kishi, H., Shi, Y.-B., Huang, J., and Yee, A.F., *Shear ductility and toughenability study of highly cross-linked epoxy/polyethersulphone.* Journal of Materials Science, 1997. 32, (3): p. 761-771.

112. Sperling, L.H. and Mishra, V., *The Current Status of Interpenetrating Polymer Networks.* Polymers for Advanced Technologies, 1996. 7: p. 197-208.

113. B. Suthar, H.X.X., D. Klempner and K. C. Frisch, *A Review of Kinetic Studies of the Formation of Interpenetrating Polymer Networks.* Polymer for Advanced Technologies, 1996. 7: p. 221-233.

114. David Mecerreyes, J.A.P., M. Bengoetxea, and H. Grande, *Novel Pyrrole End-Functional Macromonomers Prepared by Ring-Opening and Atom-Transfer Radical Polymerizations.* Macromolecules, 2000. 33: p. 5486-5849.

115. D. Mecerreyes, J.H., R. D. Miller, J. L. Hedrick, C. Detrembleur, P. Lecomte, R. Jerome, J. San Roman, *First example of an unsymmetrical difunctional monomer polymerizable by two living/controlled methods.* Maromolecular Rapid Communications, 2000. 21: p. 779-784.

116. David Mecerreyes, M.T., and James L. Hedrick, *ABC BCD Polymerization: A Self-condensing Vinyl and Cyclic Ester Polymerization by Combination Free-Radical and Ring-Opening Techniques.* Macromolecules, 1999. 32: p. 8753-8759.

117. David Mecerreyes, G.M., Philippe Dubois, Robert Jerome, James L. Hendrick, Craig J. Hawker, Eva E. Malmstrom, and Mikael Trollsas. , *Simultanneous Dual Living Polymerization: A Novel One-step Approach to Block and Graft Copolymers.* Angewandte Chemie International Edition, 1998. 37(9): p. 1274-1276.

118. A. A. Baidak, J.M.L., L.H. Sperling, *Simultaneous Interpenetrating Polymer Networks Based on Epoxy-Acrylate Combinations.* Journal of Polymer Science: Part A: Polymer Chemistry, 1997. 35: p. 1973-1984.

119. Joseph R. Nowers, a.B.N., *The effect of interpenetrating polymer network formation on polymerization kinetics in an epoxy-acrylate system.* Polymer, 2006. 47: p. 1108-1118.

120. Roberio Marcos Alcantara, A.T.N.P., Glaucione Gomes de Barros, and Lurence A. Belfiore, *Pseudo-interpenetrating Polymer Networks Based on Tetrafuntional Epoxy Resins and Poly(methyl methacrylate).* Journal of Applied Polymer Science, 2003. 89: p. 1858-1868.

121. Mu-shih Lin, a.S.-T.L., *Mechanical behaviors of fully and semi-interpenetrating polymer networks based on epoxy and acrylics.* Polymer, 1997. 38(1): p. 53-58.

122. Alysworth, J.W., *US Patent.* 1916. 1(111): p. 284.

123. Yan Lin, J.W.S., *Kinetics studies of hybrid structure formation by controlled photpolymerization.* Polymer, 2003. 44: p. 4781-4789.

124. Decker, C., *Light-induced crosslinking polymerization.* Polymer International, 2002. 51(11): p. 1141-1150.

125. K. Moussa, a.C.D., *Semi-interpentrating polymer networks synthesis by Photocrosslinking of Acrylic Monomers in a polymer Matrix.* Journal of Polymer Science: Part A: Polymer Chemistry, 1993. 31: p. 2633-2542.

126. Rosen, S.L., *Fundamental Principles of Polymeric Materials*. 2nd ed. 1993, New York: John Wiley & Sons, Inc.

127. Filip E. Du Prez, P.T., and Eric J. Goethals, *Poly(ethrylene oxide)/Poly(methyl methacrylate) (Semi-)interpentrating Polymer Networks: Synthesis and Phase Diagrams.* Polymer for Advanced Technologies, 1996. 7: p. 257-264.

128. Heung Soo Shin, S.Y.K., Young Moo Lee, Kwang Hyun Lee, Seon Jeong Kim, Charles E. Rogers, *Permeation of solutes through interpenetrating polymer network hydrogels composed of poly(vinyl alcohol) and poly(acrylic acid).* Journal of Applied Polymer Science, 1998. 69(3): p. 479-486.

129. Jie Lu, Q.N., Jiqing Zhou, and Zheng-Hua Ping, *Poly(vinyl alcohol)/Poly(vinyl pyrrolidone) Interpenetrating Polymer Network: Synthesis and Pervaporation Properties.* Journal of Applied Polymer Science, 2003. 89: p. 2808-2814.

130. Lin, Y. and Stansbury, J.W., *The impact of water on photopolymerization kinetics of methacrylate/vinyl ether hybrid systems.* Polymers for Advanced Technologies, 2005. 16: p. 195-199.

131. Oxman, J.D., Jacobs, D.W., Trom, M.C., Sipani, V., Ficek, B., and Scranton, A.B., *Evaluation of Initiator systems for controlled and sequentially curable Free-Radical/Cationic Hybrid Photopolymerizations.* Journal of Polymer Science: Part A: Polymer Chemistry, 2004. 43: p. 1747-1756.

132. E. W. Nelson, J.L.J., A. B. Scranton, and K. S. Anseth and C. N. Bowman, *Photo-differential scanning calorimetry studies of cationic polymerizations of divinyl ethers.* Polymer, 1995. 36(24): p. 4651-4656.

133. E. W. Nelson, T.P.C., and A. B. Scranton, *Fluorescence Monitoring of Cationic Photopolymerizations: Divinyl Ether Polymerizations Photosensitized by Anthracene Derivatives.* Maromolecules, 1994. 27: p. 1013-1019.

134. Schnabel, W., *Cationic photopolymerization with the aid of pyridinium-type salts.* Macromolecular Chemistry and Physics, 2000. 21(10): p. 628-642.

135. M. Degirmenci, Y.H., Y. Yagci, *One-step, one-pot Photoinitiation of Free Radical and Free Radical Promoted Cationic Polymerizations.* Journal of Applied Polymer Science, 2002. 85: p. 2389-2395.

136. Miguel G. Neumann, C.C.S., Giovana C. Ferreira, Correa, Ivo C., *The initiating radical yields and the efficiency of polymerization for various dental photoinitiators excited by different light curing units.* Dental materials : official publication of the Academy of Dental Materials, 2006. 22(6): p. 576-584.

137. Harald Braun, Y.Y., Oskar Nuyken, *Copolymerization of butyl vinyl ether and methyl methacrylate by combination fo radical and radical promoted cationic mechanisms.* European Polymer Journal, 2002. 38: p. 151-156.

CHAPTER 2
RESEARCH OBJECTIVES

The background provided in the previous chapter illustrates that cationic photopolymerization of multifunctional epoxides is very promising for efficient cure at room temperature; however, problems associated with sluggish polymerizations (relative to acrylates) and the brittleness of the resulting polymers must be addressed. To address these issues, two reaction systems were studied in this research: photoinitiated cationic copolymerizations of a cycloaliphatic diepoxide with epoxidized elastomers and acrylate/epoxide hybrid photopolymerizations. Oligomer/monomer structures, viscosity, compositions, and photoinitiator system were hypothesized to play important roles in controlling photopolymerizations of the epoxide-based mixtures. Therefore, it is necessary to understand interplay among the variables for the chosen systems. The first approach builds upon recent literature in which copolymerizations of cycloaliphatic epoxides with oligomers have been reported. In this research, complex photoinitiated cationic copolymerizations of binary mixtures containing terminal hydroxyl groups and two different types of epoxide rings were investigated. A more direct link between the observed polymer kinetics and the resulting polymer properties was achieved. Similarly, hybrid acrylate/epoxide photopolymerizations have been investigated in recent years. Suitable photoinitiator systems and hybrid monomers have been reported due to the promise of this approach for providing control of the polymerization process and tunability of polymer properties, as well as for mitigating atmospheric sensitivity of the photopolymerizations. In this research, a more in-depth investigation of interactive effects of monomer structures and dual photoinitiator system on polymer kinetics and the resulting polymer properties was performed.

The goal of this thesis is to provide fundamental knowledge regarding the polymerization kinetics and physical properties of the resulting polymers for these two

promising photopolymerization systems. Systematic studies were performed by varying independent variables to control the photopolymerization kinetics and ultimate conversion of each monomer and oligomer in the system. The kinetic behavior of each monomer and oligomer controlled by the variables were correlated with data for the physical properties of resulting polymers. Consequently, a comprehensive understanding of the relationship between reaction formulations and ultimate properties of photopolymerized polymers was attained. Ultimately, this research can provide a fundamental guideline for industrial applications that use systems comparable to the photoinitiated cationic copolymerizations and acrylate/epoxide hybrid photopolymerization systems studied here. This overall goal was attained by accomplishing the specific objectives for the corresponding photopolymerization systems.

Photoinitiated Cationic Copolymerization Systems

Two different sets of binary mixtures containing a cycloaliphatic diepoxide and epoxidized, hydroxyl terminated elastomeric oligomers were characterized. For the kinetic studies, the oligomer structure (internal epoxide content), viscosity, and various binary mixture compositions are independent research variables. Specially, due to the presence of hydroxyl groups and two different types of epoxides, it is important to elucidate the contribution of two distinct propagation reactions: active chain end and activated monomer mechanisms. Finally, physical and mechanical properties of the two different sets of copolymers were characterized, compared, and interpreted with the results from the kinetic studies. The specific objectives of this study are to:

- Characterize the polymerization kinetics and ultimate conversion of the two distinct epoxides in cycloaliphatic diepoxide and epoxidized oligomers containing terminal hydroxyl groups as a function of oligomer structure (internal epoxide content), viscosity, and monomer composition (Chapter 3). To meet this objective, real-time monomer consumption of each type of epoxide was successfully obtained using

Raman spectroscopy. An important aspect of this objective is to clearly illustrate the contribution of the activated monomer mechanism associated with the terminal hydroxyl groups on the epoxidized oligomers.

- Determine the effects of the oligomer structure (internal epoxide content) and monomer composition on physical and mechanical properties of photopolymerized copolymer films or coatings, compared to homopolymers (Chapter 4). To meet this objective, themo-mechanical properties (storage modulus and tangent factor) were characterized using dynamic mechanical analysis, isothermal stress-strain behavior (ultimate strength and fracture toughness), and impact resistance.

Hybrid Photopolymerization Systems

In this research, binary mixtures for the hybrid photopolymerization systems contained acrylates and cycloaliphatic epoxides. Photoinitiated free-radical and cationic ring-opening polymerizations were simultaneously facilitated using a dual photoinitiator containing both free-radical and cationic photoinitiators. The photopolymerizations of several acrylate/epoxide mixtures were characterized: urethane diacrylate oligomer/cycloaliphatic (di)epoxide and monovinyl acrylates/cycloaliphatic diepoxide. For these hybrid systems, there is lack of a fundamental understanding of the mutual effects of acrylates and epoxides on hybrid photopolymerizations. Thus, in the presence of two distinct polymerizations, local chemical environments provided by bulk monomer entities and propagating polymer chains were hypothesized to affect the reactivity of each acrylate and epoxide monomer. In this condition, monomer composition effects could have a different impact on the polymerization kinetics of both monomers. Finally, the complexity of acrylate/epoxide hybrid systems was further untangled by elucidating the roles of the dual photoinitiator system. The specific objectives of this study are to:

- Determine the relative importance of the viscosity of bulk binary mixtures and the dual photoinitiator system for polymerization rates and degree of conversion of the

acrylates and epoxides in urethane diacrylate oligomer/cycloaliphatic epoxide hybrid systems (Chapter 5). This initial study led to an extended hypothesis for the effects of monomer structures on photopolymerization kinetics of each monomer component. It was necessary to exclude high viscosity of the hybrid mixtures due to the urethane diacrylate oligomers to clearly understand suppression of epoxide cationic photopolymerizations by the urethane diacrylates.

- Determine the effects of acrylate secondary functionalities on epoxide reactivity with varying monomer composition (Chapter 6). For this purpose, three model monovinyl acrylates, containing aliphatic alkyls, ether, and urethane secondary groups, were examined with a cycloaliphatic diepoxide. The polarity/solvation and basicity/nucleophilicity associated with the secondary functional groups were correlated to explain enhanced or inhibited kinetic behavior of the cycloaliphatic epoxide. Viscosity effect was also more clearly correlated with the role of a dual photoinitiator.
- Determine the effect of cycloaliphatic diepoxide on monovinyl acrylate reactivity as a function of monomer composition (Chapter 7). To understand the acrylate kinetic behavior during the hybrid photopolymerizations, hydrogen-abstraction and hydrogen-bonding capability associated with the acrylate secondary functional groups were correlated with polarity and dilution effects of the diepoxide. In addition, the impact of the dual photoinitiator system on the acrylate reactivity was examined to understand its role for the free-radical photopolymerization of the monovinyl acrylates.
- Illustrate the effects of acrylate secondary functionalities and monomer composition on the physical and mechanical properties of photopolymerized hybrid films or coatings (Appendix).

CHAPTER 3
PHOTOINITIATED CATIONIC COPOLYMERIZATIONS CONTAINING CYCLOALIPHATIC DIEPOXIDE AND ELASTOMERIC OLIGOMERS: EFFECTS OF THE OLIGOMER STRUCTURE AND COMPOSITION

Introduction

Multifunctional epoxide monomers containing two or more cyclic ether rings are very useful and versatile materials that have been widely used in coatings and adhesives. The crosslinked network structure of the final cured polymer provides excellent physical properties such as strength, durability, adhesion, corrosion resistance and chemical resistance[1]. In addition, the development of photoinitiators such as diaryliodonium and triarlysulfonium salts for the cationic ring-opening polymerization allows for efficient photoinitiated curing at low temperatures with a considerable reduction of curing time and energy consumption compared to thermal curing.[2, 3] These advantages are especially useful for aerospace and automotive repair and fabrication since conventional high performance rubber-modified epoxide systems cannot tolerate high temperature cure.

The cationic photopolymerization of epoxides exhibits unique advantages over the free-radical photopolymerization, including insensitivity to oxygen inhibition due to lack of radical coupling with oxygen[3], low shrinkage/residual stresses due to ring-opening reactions, and relatively low rate of termination, which allows the reaction to continue after illumination is ceased (dark polymerization[4-7]). Above all, highly crosslinked epoxide thermosets produced by the cationic photopolymerization exhibit the same excellent physical and mechanical properties as obtained in thermal curing systems. Despite these merits, the cationic photopolymerization is not free of shortcomings. For instance, the relatively low reactivities of some epoxides (*e.g.* alkyl glycidyl ethers) must be enhanced for certain applications requiring rapid formation of highly crosslinked structures.[8, 9] In addition, the cationic photopolymerization can be significantly

affected by high humidity since water can retard, inhibit, or accelerate the cationic propagation depending on epoxide monomer structures.[10, 11] Moreover, the highly crosslinked, rigid structure of photopolymerized epoxides can impart a high glass transition temperature, which may lead to undesirable brittleness at room temperature. This brittleness can result in catastrophic fracture failure and poor impact resistance. In addition, the low degree of elongation (resulting in low peel strength) of unmodified epoxide thermosets limit their utility in applications such as joint adhesive. This research will investigate a new method for overcoming these limitations.

In this study, the photoinitiated cationic copolymerization between cyclocaliphatic epoxide and epoxide-functionalized elatomeric oligomers were characterized. The cycloaliphatic epoxide is well known as a highly reactive compound due to its highly strained ring structure introduced by the oxidation of cycloolefins with unsaturated substituents.[12] For instance, the cationic photopolymerization of mono-functional cyclohexene oxide shows no induction period and a high rate of polymerization over common glycidyl ethers.[8, 9] In spite of the high reactivity of the mono-functional cycloaliphatic epoxides, cycloaliphatic diepoxides (CDEs) have received considerably more attention due to their low vapor pressure and better physical/mechanical properties for a wide range of photocuring applications.[12] However, many CDEs possess a nucleophilic group (such as an ester carbonyl) that may intramolecularly attack either of the alkylated active centers to form dioxacarbenium ions. This leads to a relatively sluggish propagation of cationic active center.[12, 13] In the presence of atmospheric water, the cationic photopolymerization of CDE-type monomers are not retarded, but are accelerated due to steric effects and the ease of proton release from an intermediate complex of the active center with a water molecule.[10]

In the presence of alcohol moieties (typically attached to the monomer), the rate of cationic ring-opening polymerization can be significantly enhanced due to the higher nucleophilicity of the hydroxyl groups (compared to the cycloaliphatic ether) toward

protonated epoxide monomers.[14] As a result, the propagation of cationic active centers in the presence of alcohol proceeds by two different propagation mechanisms: active chain end (ACE) mechanisms and activated monomer mechanisms (AM).[14] In addition, the elastomeric modifier with high viscosity provides several advantages such as no need of pre-reactions due to excellent miscibility, possible prevention of atmospheric water diffusion, no need of additional heat or solvent to melt, and toughening effect on final polymers.

While photo-induced cationic homopolymerizations of a single monomer have received significant attention, the more complex photoinitiated cationic copolymerization of binary mixtures containing terminal hydroxyl groups and two different types of epoxide rings are not well understood. If two monomers containing both cycloaliphatic epoxides and a normal aliphatic epoxide are mixed prior to polymerization, each of the two cationic active centers will have a distinct reactivity with each type of epoxide group and with any hydroxyl groups present in the system.[15] Therefore, the cycloaliphaticoaliphatic epoxide groups of the cycloaliphatic diepoxide should exhibit different selectivity toward the internal epoxides and terminal hydroxyl groups in EPOHs during photoinitiated cationic copolymerization. Eventually, the selectivity may control the reactivity of the internal epoxide and cycloaliphatic epoxide groups in the coexistence of two different propagation mechanisms described as ACE and AM. To validate this hypothesis, kinetic studies of copolymerizations containing two different epoxides were conducted at room temperature while systematically varying the EPOH internal epoxide content and compositions of the binary monomer mixtures.

Experimental

Materials

The cationically polymerizable monomer 3,4-epoxycyclohexylmethanyl 3,4-epoxycyclohexanecarboxylate (a cycloaliphatic diepoxide monomer, EEC, shown in

Table 1) was used in these experiments. This monomer (ERl-4221, Sigma Aldrich) was selected for its high reactivity and low shrinkage. Two different grades of epoxidized polybutadiene oligomers containing two hydroxyl terminal groups (EPOHs) were kindly donated from Cray Valley. The EPOHs have different internal epoxide equivalent weight (EEW) and two hydroxyl groups at the ends of their chains. The photoinitiators (PIs) used in this study were [4-2-hydroxyl-1-tetradecyloxy)-phenyl] phenyl iodonium (IHA, Polymer Science). Structures and relevant properties of all materials used are listed in Table 3.1.

Table 3.1 Selected properties and structure and of monomers, elastomeric oligomers, and photoinitiators used for this study.

Materials	EEW [g/eq]	Hydroxyl value [meq/g]	Viscosity @ 30℃ [mPa]	Structure
EPOH20	446	1.7	5,500	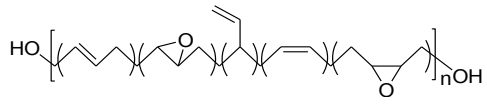
EPOH30	320	1.74	16,430	
EEC	132	N/A	280	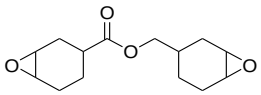
PI	N/A	N/A	N/A	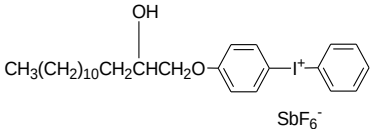

Characterization of Elastomeric Oligomers

Determination of Molecular Weight and Polydispersity

Gel permeation chromatography (GPC) was performed using a Shimadzu HPLC/GPC that consists of a differential refractomeric detector (RID-10A), solvent delivery pump (LC-10ATVP), and a system controller (SCL-10AVP). Tetrahydrofuran

(THF) eluent was pumped at a flow rate of 1.0 mL/min through PLgel Mixed D column (Polymer Labs). The average molecular weight and polydispersity index (PDI) of the oligomers was determined from the calibration curve based on a narrow range of polystyrene standards.

Determination of Epoxidation Degree in EPOHs

^{1}H- NMR spectra of the epoxidized polybutadiene oligomers were obtained using a Bruker DRX-400 nuclear magnetic resonance (NMR) spectrometer with $CDCl_3$ as the solvent and tetramethysilane (TMS) as an internal reference. The 10-20 mg oligomer samples were dissolved in 600 µl of the solvent $CDCl_3$. Chemical shifts were recorded in ppm relative to TMS. Molecular epoxidation degree of each EPOH was calculated by the relative peak areas of the epoxide and olefin hydrogen atoms (eq. 3.1):

$$\text{Epoxidation degree (mol\%)} = \frac{A_{H\ \text{epoxide}}}{A_{H_{1,4+1,2}} + A_{H_{1,2}} + A_{H\ \text{epoxide}}}(100) \qquad (eq.\ 3.1)$$

where $A_{H\ \text{epoxide}}$ corresponds to the summation of the integrated areas of the peaks at δ = 2.93 and δ = 2.68 divided by the number of protons on the respective 1,4-cis/trans expoxide carbons. $A_{H\ 1,4+1,2}$ is the integrated area of the multiplet centered at δ = 5.4 divided by the number of protons on the carbons of the 1,4-cis/trans and 1,2-vinyl double bonds. $A_{H\ 1,2}$ is the integrated area of the multiplet centered at δ = 4.96 divided by the number of protons on the carbons of the 1,2-vinyl double bonds. Here epoxidation degree indicates mole percentage.

Photoinitiator Photon Absorption Rate

The photoinitiator absorbance spectra were recorded in one nanometer increments using a 8453 UV-Visible Spectrophotometer (Agilent Technologies). The baseline of UV-Vis absorption spectra was obtained from the monomer, oligomer, or the mixture of the two at room temperature. The spectra of IHA were obtained for dilute solutions

(8mM) of the photoinitiator-monomer/oligomer mixtures at room temperature. All absorbance spectra were obtained in an air-tight, quartz cuvette cell with 1 mm path length to prevent any changes in concentration during measurements. The photon absorption rate constant, $k_{abs,}$ for the IHA photoinitiator was determined by integrating the overlap between the photon absorption at each specific wavelength and the emission spectrum of the light source [4-6]. The emission spectrum of the photoinitiation light source (Acticure Ultraviolet/Visible Spot Cure System, EXFO Photonic Solutions, Inc.) was measured using a calibrated miniature fiber optic spectrometer (USB4000, Ocean Optics).

In-Situ Kinetic Study Using Real-time Measurements

For the kinetic study, real-time Raman spectra were collected using the Mark II holographic fiber-coupled stretch probehead (Kaiser Optical Systems, Inc) attached to a HoloLab 5000R modular research Raman spectrograph. A 10× non-contact sampling objective with 0.8 cm working distance was used to deliver ~ 200-mW 785-nm near-infrared laser intensity to the sample and induce the Raman scattering effect. The exposure time for each spectrum was 100 msec and the time interval between each collected spectra was 7 seconds. A custom-made, thermostated sample holder was used to illuminate a capillary tube containing ~15 µl of the monomer mixture sealed 1-mm ID quartz capillary tubes. The sample was maintained at 25°C for all real-time experiments, and the monomer was illuminated using an Acticure® Ultraviolet/Visible Spot cure system (EXPO Photonic Solutions, Inc). This system is equipped with a high pressure 100-Watt mercury vapor short arc lamp and had the effective irradiance set to 100 mW/cm^2 measured by EFOS UV/Visible Radiometer R5000 for the filtered spectral range between 250 nm and 450 nm. The samples containing monomer, oligomer, or the combination of the two were thoroughly mixed with the photoinitiator using a mechanical mixer equipped with a Micro Surface Stirrer Shaft (BOLA, Germany).

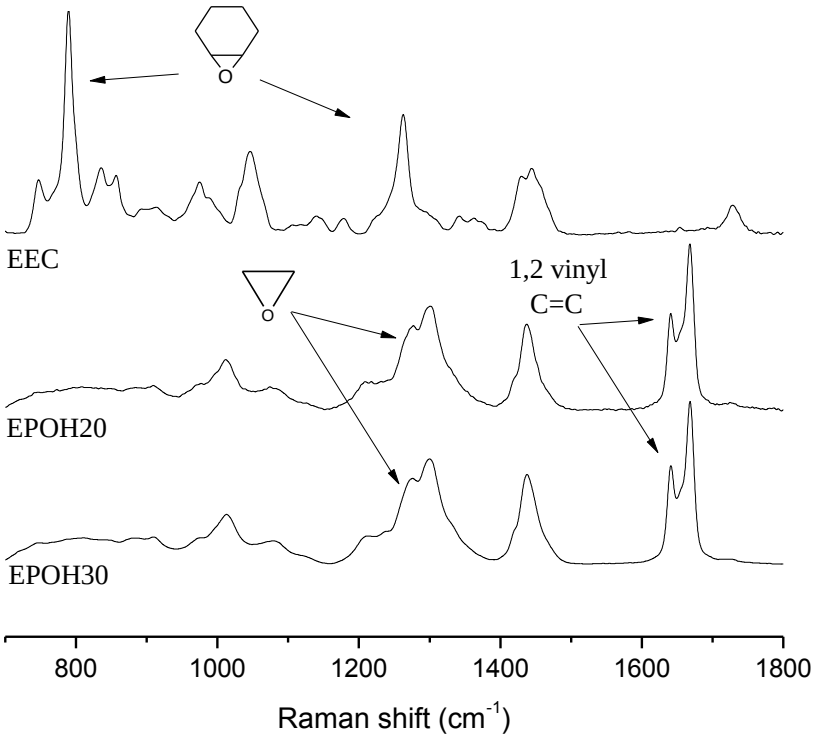

Figure 3.1 Raman spectra of neat cycloaliphatic diepoxide and epoxidized, hydroxyl terminated polybutadiene oligomers.

The Raman spectra of the cycloaliphatic diepoxide (EEC) and the epoxidized polybutadiene oligomers (EPOHs) were acquired (Figure 3.1). Reactive and reference bands were carefully selected using the secondary derivative method. Three EEC reactive bands representing the cycloaliphatic epoxide ring were located at 745 cm^{-1}, 789 cm^{-1}, and 1263 cm^{-1}. An internal reference band was chosen at 1727cm^{-1} representing the skeletal bending of the non-reactive CC=O group. Among the EEC reactive bands, 789 cm^{-1} peak associated with asymmetric cycloaliphatic epoxide ring deformation was used to calculate monomer conversion. For EPOHs, the reactive band at 1268 cm^{-1} is associated with in-phase breathing vibrations of the oxirane ring and a band at 1640 cm^{-1} associated with the 1,2-vinyl C=C stretching vibrations was selected as the reference.

Hence, the conversion of epoxide functional groups was calculated by eq. 3.2 after collecting Raman spectra from real-time measurements under full illumination conditions.

$$\text{Conversion, } \alpha = 1 - \frac{A_{rxn}(t)/A_{ref}(t)}{A_{rxn}(0)/A_{ref}(0)} \quad \text{or} \quad 1 - \frac{A_{rxn}(t)}{A_{rxn}(0)} \qquad (eq.3.2)$$

where A_{rxn} (t) and A_{ref} (t) represent the peak areas of the reactive and reference bands at a certain time, and A_{rxn} (0) and A_{ref} (0) are the peak areas of reactive and reference bands before reaction. In general, the spectral baselines and the reference band intensity remained constant during the real-time measurements.

Results and Discussion

Characterization of Elastomeric Oligomers

Two different grades of epoxidized, hydroxyl-terminated polybutadiene oligomers (EPOH20 and EPOH30) were examined by various spectroscopic methods to determine the molecular weights, molecular weight distribution (polydispersity), epoxidation degree, and polybutadiene structures. Epoxidation of natural or synthesized rubbers using organic oxidants or phase transfer catalysts has been extensively studied. It was reported that the epoxidation process of precursors possibly causes a side reaction through ether linkage formation between oxirane groups formed or chain scission. This could result in variation in the molecular weight and polydispersity of the precursors.[15-17] Thus, it was necessary to determine average molecular weights and polydispersity indexes for each oligomer used.

As shown in Table 3.2, GPC analysis revealed that the average molecular weights of EPOH20 and EPOH30 were approximately 2300 g/mole and 2800 g/mole, respectively. In addition, the molecular weight distributions of EPOH20 and EPOH30 were found to be similar with PDI values of 2.1 and 2.3 respectively. These values are close to the reported value (PDI = 2.0) for the hydroxyl terminated polybutadiene precursor.

Table 3.2 Properties and microstructures of epoxidized polybutadiene oligomers used.

	M_n (g/mole)/ polydispersity	^{1}H NMR			
		Internal Epoxides (mol%)	Carbon double bonds (mol%)		Total (mol%)
		1,4-trans/cis	1,4-trans/cis	1,2-vinyl	
EPOH20	2274/ 2.1	20 (60/40) [a]	48 (60)[b]	32 (40)[b]	100
EPOH30	2753/ 2.3	30 (58/42)[a]	39 (56)[b]	31 (44)[b]	100

[a] Relative percentage of each of the 1,4-trans and 1,4-cis epoxide groups over the total epoxide groups in the epoxidized polybutadiene oligomers

[b] Relative percentages of 1,4 trans/cis and 1,2-vinyl carbon double bond units over the total carbon double bonds in the epoxidized polybutadiene oligomers.

The epoxidized rubbers are important because the polar groups generally offer enhanced miscibility with the conventional epoxides[18] and better resistance to hydrocarbon oils and solvents[19]. In this study, the epoxidation degree and microstructures of EPOH20 and EPOH30 were evaluated by 1H NMR spectroscopy. The respresentative NMR spectrum and peak assignments are illustrated in Figure 3.2. The internal epoxide groups of the EPOH20 and EPOH30 were identified by two characteristic signals at $\delta = 2.68$ and $\delta = 2.93$ which are associated with the protons on the 1,4-trans/cis epoxide carbons, respectively [15, 16, 20]. A complex peak associated with three distinct protons (the 1,4-trans/cis protons and 1,2-vinyl protons bonded to unsaturated carbons) appears at a chemical shift of $\delta = 5.4$, and a resolved peak associated with 1,2-vinyl protons appears at $\delta = 4.96$.

Analysis of the NMR spectra reveals that the two oligomers have different distributions of epoxide and carbon double bond configurations (Table 3.2). For example, the EPOH30 exhibits a lower percentage of 1,4-trans/cis carbon double bond protons.

This indicates that, for this oligomer, a higher degree of epoxidation occurs on 1,4-trans/cis units of carbon double bonds relative to the vinyl units. This is not surprising due to the much higher reactivities of the 1,4-trans and 1,4-cis carbon double bonds compared to 1,2-vinyl units [16, 20] due to the substituent effect. This conclusion was corroborated with FT-IR spectroscopy (data not shown) in which no IR frequency band was observed around 780-880 cm^{-1} (associated with the monosubstituted epoxide groups[21]) for either oligomer. This is consistent with the analysis of Bussi et al. who systematically studied this effect by comparing model epoxide compounds and the epoxidized polybutadiene oligomers [15]. Therefore for both epoxidized elastomeric oligomers in this study, it is safe to assume that the amount of 1,2-epoxide groups is negligible.

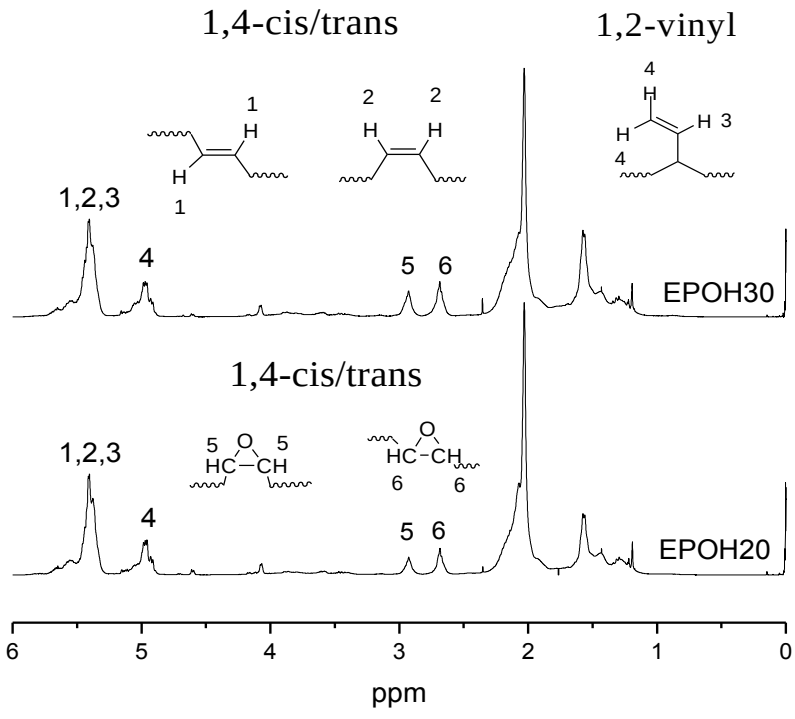

Figure 3.2 ^{1}H NMR spectra of neat epoxidized polybutadiene oligomer (EPOH20 and EPOH30).

Photoinitiator Photon Absorption Rate

UV-Vis spectroscopic studies were conducted to determine whether the epoxidized polybutadiene oligomers have an effect on the photon absorption rate (k_{abs}) of the cationic photoinitiator (IHA) in the neat binary EPOH-EEC mixtures with various compositions. The results shown in Figure 3.3 illustrate that the observed k_{abs} of the IHA photoinitiator is essentially independent of composition. Therefore, the elastomeric oligomer has little effect on the photon absorption rate.

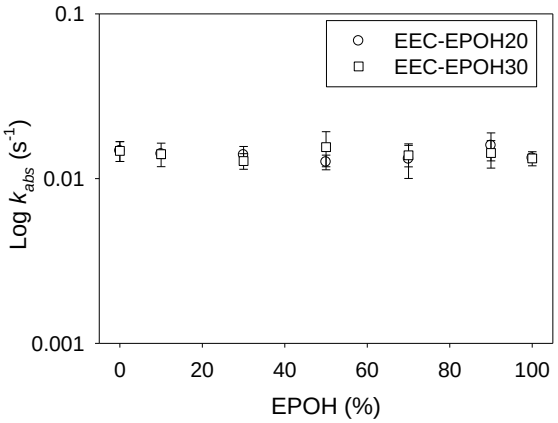

Figure 3.3 Effect of neat monomer/oligomers and binary monomer mixtures on the photon absorption rate of IHA photoinitiator.

Cationic Photopolymerization of Neat Monomer and Oligomers

Photoinitiated cationic ring-opening homopolymerizations of neat cycloaliphatic diepoxide monomer (EEC) and epoxidized, hydroxyl terminated polybutadiene oligomers were conducted at room temperature. Consumption of epoxide functional groups was monitored using real-time Raman spectroscopy. Figure 3.4 shows the conversion profiles of the corresponding neat systems. The figure illustrates that the cationic photopolymerization of the neat EEC monomer proceeded at a high rate until the conversion of ~20%, then underwent a transition to a sluggish propagation with

correspondingly low polymerization rate. The initial high reactivity of EEC may be attributed to the highly-strained ring structure, while the sudden change in polymerization rate may be attributed to the nucleophilic ester carbonyl in the EEC monomer [13]. In extensive studies of this effect, Crivello *et al*. [13] proposed that the cationic active centers interact with the nucleophilic esters to form dialkoxycarbenium ions of low reactivity.

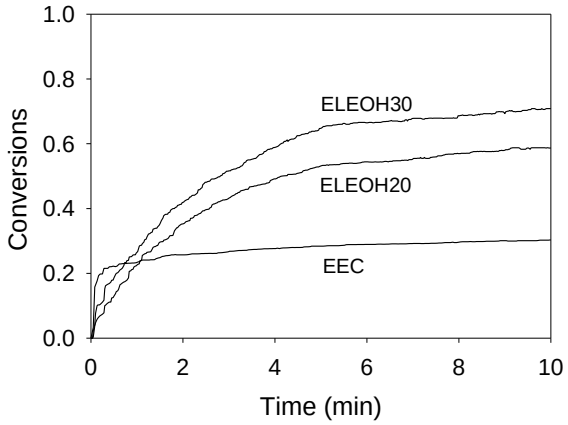

Figure 3.4 Conversion profiles of neat cycloaliphatic diepoxide (EEC) and neat epoxidized polybutadiene oligomers (EPOH20 and EPOH30). [IHA]= 8mM.

Figure 3.4 illustrates that the cationic photopolymerizations of the EPOH oligomers exhibits lower initial rates than the neat EEC monomer, but the polymerization rate does not exhibit the characteristic decline due to the absence of nucleophilic groups (such as ester carbonyls) in the polybutadiene backbone. Consequently, the observed final conversions are higher for the EPOH oligomers than for the neat EEC. Figure 3.4 also illustrates the difference in reactivity and degree of conversion between EPOH20 and EPOH30 oligomers. Higher rates of polymerization are observed with EPOH30, which contains a higher epoxide content. This is consistent with previously reported results by Boyang *et al*. who reported a higher rate of cationic photopolymerization for epoxidized elastomers which possessed higher internal epoxide contents [16]. These

authors also reported that the reactivity of internal epoxide groups follow the trend: 1,2-pendant epoxide > 1,4-*trans* epoxide > 1,4-c*is* epoxide [16, 20]. The relative concentrations of 1,4-cis and 1,4-trans internal epoxide groups in both EPOH20 and EPOH30 oligomers were almost the same (Table 3.2). In addition, hydroxyl values of the two oligomers are essentially the same at 1.7 meq/g and 1.74 meq/g for EPOH20 and EPOH30, respectively. Given that there are no 1,2-pendant epoxide groups originating from the 1,2-vinyl groups as already discussed, the higher reactivity of the EPOH30 is primarily attributed to the higher internal epoxide content.

Photoinitiated Cationic Copolymerization of EEC-EPOH Mixtures

Cationic photopolymerizations of binary monomer mixtures of EEC and EPOHs are considerably more complex than either homopolymerization. For example, a number of chemically different cationic active centers be present, and each type of active center will exhibit a distinct reactivity toward the hydroxyl groups (in the activated monomer mechanism) and toward each type of epoxide (EEC or EPOH) [15]. To investigate these effects, the photopolymerization kinetics of binary mixtures of EEC and EPOH were characterized using Raman spectroscopy as a function of the binary composition.

Effect of EPOH content on the Kinetics of Cycloalipatic Diepoxide

Figure 3.5 contains plots of the EEC epoxide conversion as a function of time for EEC-EPOH copolymerizations with the epoxidized oligomer content ranging from 0 to 90%. Figure 3.5A corresponds to EEC-EPOH20 polymerizations while 3.5B corresponds to EEC-EPOH30 systems. Here the conversion was determined using the integral of the Raman peak at 789 cm^{-1}, which is well resolved from all other peaks. The most prominent result illustrated in Figure 3.5 is that the ultimate limiting conversion of the EEC (the final plateau conversion) increases monotonically as the EPOH content is increased. This result is illustrated clearly by the ultimate limiting conversion (after 30

minutes of illumination) data shown in Table 3.3. This effect likely arises from the activated monomer propagation mechanism associated with the terminal hydroxyl groups on the epoxidized oligomers.

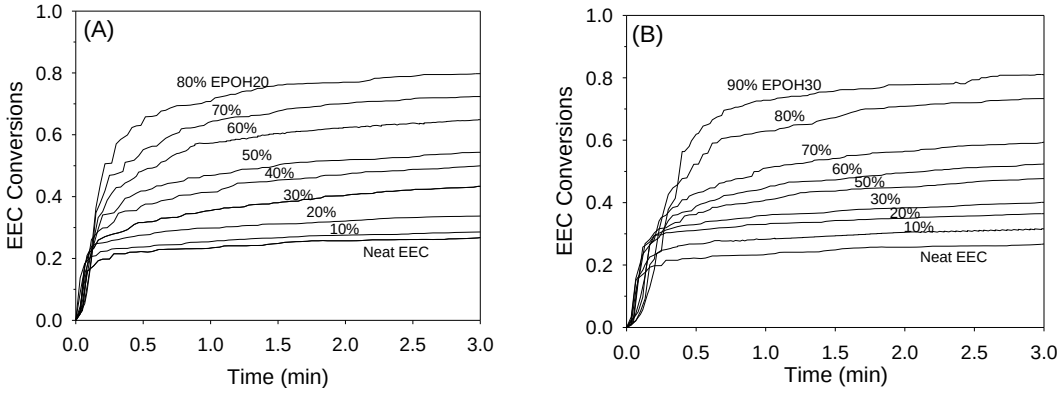

Figure 3.5 Effect of EPOH content on the kinetics of the cycloaliphatic diepoxide during photoinitiated cationic copolymerizations with EPOH20 (A) and EPOH30 (B). [IHA]=8mM for the total volume of the binary monomer mixtures.

Table 3.3 Effect of EPOH content on the ultimate limiting conversions of cycloaliphatic epoxides in EEC during homo and copolymerizations.

Systems	Ultimate limiting conversions of EEC (%)									
	EPOH Content (wt.%)									
	0	10	20	30	40	50	60	70	80	90
EEC-EPOH20	35±2	39±2	45±3	53±3	62±5	69±2	73±2	79±3	84±2	n/a
EEC-EPOH30	35±2	40±3	45±2	52±2	n/a	60±3	67±2	73±3	78±2	83±3

It is also interesting to examine the effect of the EPOH content on the initial polymerization rate, which corresponds to the slope of the conversion profiles immediately after illumination. To characterize this effect, Table 3.4 contains data for the

average normalized polymerization rate for conversions between 0 and 15%. For the EEC-EPOH20 systems, the data indicate that the initial EEC polymerization rate significantly increases as the EPOH content is increased from 0 to 10%. Again this trend can be attributed to the impact of the EPOH hydroxyl groups which allow monomer to be polymerized by the activated monomer mechanism. As the EPOH content is increased further, the initial EEC polymerization rate decreases gradually, but remains enhanced relative to pure EEC for EPOH contents up to ~40%. For EPOH20 contents higher than 50%, the initial EEC polymerization rate is lower than that in pure EEC. In contrast, for the EEC-EPOH30 systems, Table 3.4 shows that for EPOH30 contents of 10 to 30% the initial polymerization rate of EEC remains the same as the neat EEC, and for EPOH30 contents higher than 60%, the initial EEC polymerization rate is lower than that in pure EEC.

Table 3.4 Effect of EPOH content on the average polymerization rate of EEC for conversions between 0 and 15% during homo and copolymerizations.

Systems	Average normalized polymerization rate of EEC ($\times 10^{-2}$ s^{-1})									
	EPOH Content (wt.%)									
	0	10	20	30	40	50	60	70	80	90
EEC-EPOH20	3.5	5.9	4.4	4.1	3.4	3.5	2.8	2.6	2.6	n/a
EEC-EPOH30	3.5	3.8	3.6	3.8	n/a	3.0	2.2	2.1	1.7	1.4

The trends shown in Table 3.4 may be attributed to the effect of viscosity on the cationic photopolymerization kinetics.[21, 22] To investigate this effect more thoroughly, the viscosities of the EEC-EPOH mixtures were predicted using the Refutas equation (eq. 3.3),[23] and the results are shown in Figure 3.6. The Figure illustrates that the EEC-

EPOH30 mixtures exhibit a higher viscosity than the EEC-EPOH20 mixtures for the whole composition range, and that the viscosity increases exponentially with increasing EPOH content, as described by the following equation (eq. 3.3):

$$\upsilon_{mixture} = exp^{exp\left(\frac{VBI_{mixture}-10.975}{14.534}\right)} - 0.8 \qquad (eq.\ 3.3)$$

Where:

$$VBI_{mixture} = [w_{EEC} \times VBI_{EEC}] + [w_{EPOH} \times VBI_{EPOH}] \qquad (eq.\ 3.4)$$

and

$$VBI_{comp} = 14.534 \times \ln[\ln(\upsilon_{comp} + 0.8)] + 10.975 \qquad (eq.\ 3.5)$$

Here the symbol "VBI" stands for the viscosity blending index, while w_{EEC} and w_{EPOH} are the weight fraction of each component of the binary mixture, and υ_{comp} and $\upsilon_{mixture}$ represent the viscosity in centistokes of the components and the mixture, respectively.

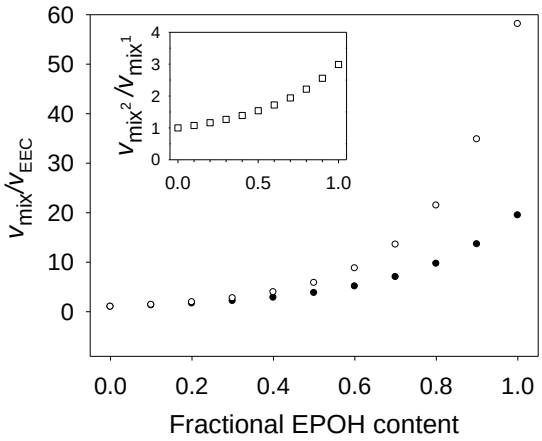

Figure 3.6 Effect of EPOH content on the viscosities of the EEC-EPOH mixtures. The ratios of predicted kinematic viscosity of each EEC-EPOH mixture to neat EEC were displayed as a function of EPOH content. In the subfigure, the predicted kinematic viscosity ratios of EEC-EPOH30 to EEC-EPOH20 mixtures were shown as a function of EPOH content. V_{mix} and V_{EEC} represent the kinematic viscosity of the respective EEC-EPOH mixtures and neat EEC. V_{mix}^1 and V_{mix}^2 represent the kinematic viscosity of EEC-EPOH20 and EEC-EPOH30, respectively.

Comparison of Figure 3.6 and Table 3.4 reveals that the significant reduction of the initial polymerization rate of EEC occurs at an epoxidized oligomer content at which the EEC binary mixtures exhibit an approximately 5-fold viscosity increase over the neat EEC (this occurs at an EPOH20 content of 60%, and an EPOH30 content of 50%). This effect may be attributed to the effect of viscosity on cationic polymerizations. At these relatively high viscosities, the propagation reaction may become diffusion controlled even at an early polymerization stage, and active centers may become trapped more easily.[4, 5] This effect may be more pronounced for EPOH30 due to its higher internal epoxide content.

Determination of Conversion of Internal Epoxide Rings of EPOH Oligomers

As seen in Figure 3.1, the reactive band at 789 cm^{-1} is very distinct for the cycloaliphatic epoxide rings of EEC, but the reactive band for the internal aliphatic epoxide rings of the epoxidized oligomers (near 1263 cm^{-1}) is not distinct from the band associated with the cycloaliphatic epoxide rings of the EEC monomer. These peaks are shown in Figure 3.7 for binary compositions ranging from 0 to 100% EEC.

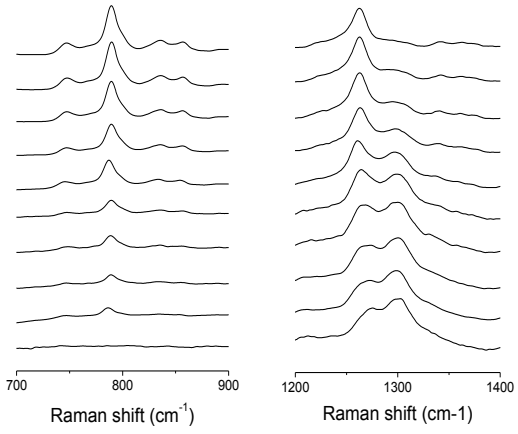

Figure 3.7 Evolution of Raman reactive peaks representing cycloaliphatic epoxide rings and internal epoxide rings of the respective EEC (left and right) and EPOH20 (right) as a function of monomer compositions.

The Raman spectra were used to determine the conversion of the EPOH epoxide groups using an adaptation of the methods recently reported by Samran *et al*. and Yuan *et al*. [24-26] First, the Raman peaks for the two different shift regions were redrawn by a secondary derivative method and the Raman intensities were determined by integrating peak area. The ratio of the two Raman peak intensities was then correlated with the concentration of the corresponding cycloaliphatic epoxides and internal aliphatic epoxide rings that are present in the EEC-EPOH mixtures (eq. 3.6).

$$\frac{A_{1263}/A_{1640}}{A_{785}/A_{1640}} = \frac{k_2[CE]_{0,EEC}+k_3[IE]_{0,EPOH}}{k_1[CE]_{0,EEC}} \qquad (eq.3.6)$$

where A_{785} and A_{1263} represent the peak intensities of the reactive bands at 785 cm^{-1} and 1263 cm^{-1} before the illumination. A_{1640} represents the peak intensities of 1,2-vinyl carbon double bond at 1640 cm^{-1} as an internal reference for the mixtures. For the neat EEC system, the Raman peak at 1727cm^{-1} representing the skeletal bending of the non-reactive CC=O group was used as an internal reference band. $[CE]_{0,EEC}$ and $[IE]_{0,EPOH}$ represent the initial concentrations of cycloaliphatic epoxide rings and internal epoxide rings in EEC and EPOHs, respectively. k_1, k_2, and k_3 are proportional constants for the corresponding epoxide rings. Rearrangement of eq. 3.6 resulted in a linear relationship between the peak intensity ratio of the two Raman reactive bands at 785 cm^{-1} and 1263 cm^{-1} and the concentration ratio of the two different epoxide groups (eq. 3.7).

$$\frac{A_{1263}/A_{1640}}{A_{785}/A_{1640}} = K_1+K_2\frac{[IE]_{0,EPOH}}{[CE]_{0,EEC}} \qquad (eq.\ 3.7)$$

where $K_1=k_2/k_1$ and $K_2 = k_3/k_1$. For the binary monomer mixtures, the Raman peak at 1263 cm^{-1} includes both cycloaliphatic epoxide rings and internal aliphatic epoxide rings. The change of this peak intensity indicates consumption of either or both of the two different epoxide rings during the photoinitiated cationic copolymerizations of the EEC-

EPOH systems occured. Therefore, the conversion compromising the combined consumption of the two different epoxide rings can be expressed in eq. 3.8.

$$\text{Conversion (\%)},\ \alpha_{1263} = \frac{A_{1263}(0)-A_{1263}(t)}{A_{1263}(0)}(100) \qquad (eq.\ 3.8)$$

The eq. 3.8 can be redrawn from eq. 3.6 using the assumption of the linear relationship between the Raman intensity at 1263 cm^{-1} and the concentration of each epoxide in EEC and EPOHs.

$$\frac{A_{1263}(0)-A_{1263}(t)}{A_{1263}(0)}(100)=$$

$$\frac{k_2[CE]_{0,EEC}+k_3[IE]_{0,EPOH}-(k_2[CE]_{t,EEC}-k_3[IE]_{t,EPOH})}{k_2[CE]_{0,EEC}+k_3[IE]_{0,EPOH}}(100) \qquad (eq.3.9)$$

where A1263(0) is the initial peak intensity of 1263 cm^{-1} before the illumination and A1263(t) is the instantaneous peak intensity after the illumination. Applying eq. 3.2 and eq. 3.7 to eq. 3.9, rearrangement further reduces eq. 3.9 to eq. 3.10.

$$\alpha_{1263}=\frac{K_1\alpha_{785}+K_2\left(\frac{[IE]_{0,\,EPOH}-[IE]_{t,EPOH}}{[CE]_{0,EEC}}\right)}{K_1+K_2\left(\frac{[IE]_{0,\,EPOH}}{[CE]_{0,EEC}}\right)}(100) \qquad (eq.3.10)$$

where α_{785} is the conversion of the cycloaliphatic epoxide rings of EEC at time, t, calculated using the Raman reactive band at 789 cm^{-1} for EEC. $[CE]_{t,EEC}$ and $[IE]_{t,EPOH}$ represent the instantaneous concentrations of the respective cycloaliphatic epoxide rings and internal epoxide rings in EEC and EPOHs after illumination. Given that all the parameters are known except for the instantaneous concentration of the internal epoxide rings at time, t, eq. 3.10 can be solved for $[IE]_{t,EPOH}$. Finally, the conversion of the internal epoxide rings of EPOHs was obtained by applying the $[IE]_{t,EPOH}$ to eq.3.2 with known initial concentrations of EEC and EPOHs. Based on eq. 3.7, a linear relationship

was obtained between the peak intensity ratio of the two Raman reactive bands and the concentration ratio of the two different epoxide groups as shown in Figure 3.8. The proportionality constants, K_1 and K_2 were determined to be 1.171 and 1.252, respectively.

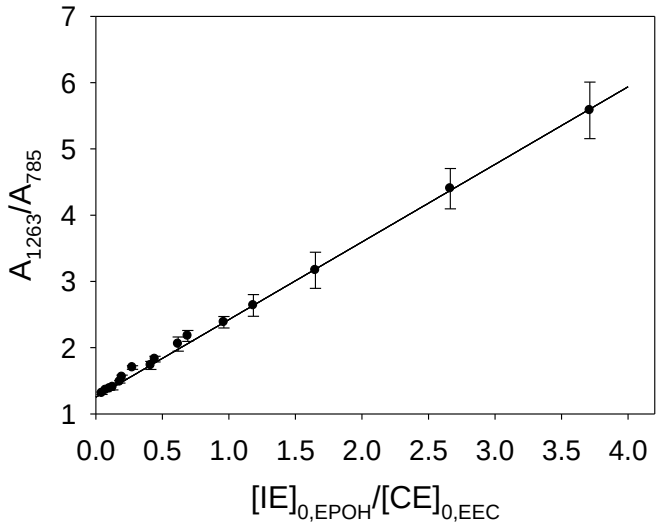

Figure 3.8 The linear relationship was obtained between the peak area ratio of the two Raman reactive bands and the concentration ratio of the two different epoxide groups for the binary monomer mixtures including EEC-EPOH20 and EEC-EPOH30 (R^2=0.98).

Effect of EEC content on the Kinetics of EPOH Oligomers

Figure 3.9 shows the conversion profiles of the EPOH internal epoxides as a function of time for EEC contents ranging from 0 to 40 wt.%. The figure illustrates that the polymerization rate and the ultimate limiting conversion of the internal epoxide rings decrease monotonically as the EEC content is increased for both of the epoxidized oligomers. This effect is more pronounced for EPOH20, which contains a lower epoxide content. In addition, the EPOH20 exhibits an induction period that increases with increasing EEC concentration.

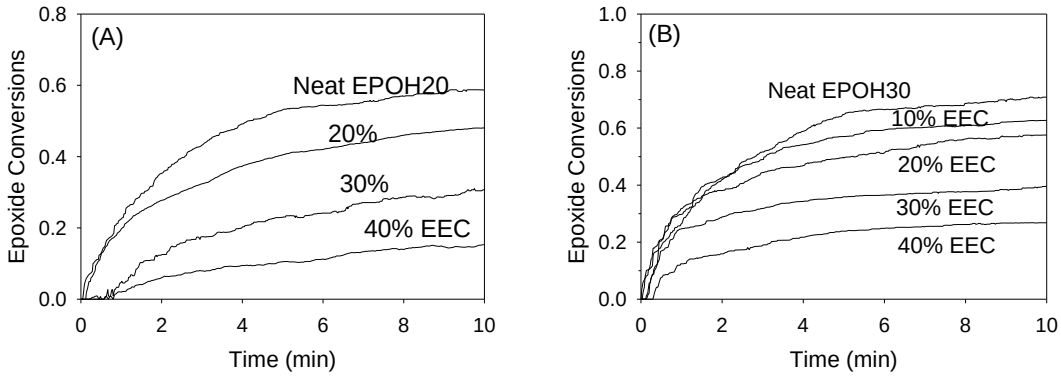

Figure 3.9 Effect of EEC content on the kinetics of epoxidized, hydroxyl terminated polybutadiene oligomers in the binary monomer mixtures including EEC-EPOH20 (A) and EEC -EPOH30 (B) during photoinitiated cationic copolymerizations. [IHA]=8mM for the total volume of the binary monomer mixtures.

It is also interesting to examine the effect of the EEC content on the initial polymerization rate of the EPOH epoxide groups. To characterize this effect, Table 3.5 contains data for the average normalized polymerization rate for conversions between 0 and 15%. The data illustrate that, for both epoxidized oligomers, the initial polymerization rate of the EPOH epoxide groups decreases monotonically as the EEC content is increased, and that this effect is more pronounced for EPOH20.

Table 3.5 Effect of EEC content on the average polymerization rate of EPOH20 and EPOH30 for conversions between 0 and 15% during homo and copolymerizations.

Systems	Average normalized polymerization rates of EPOH20 and EPOH30 ($\times 10^{-2}$ s^{-1})				
	EEC Content (wt.%)				
	0	10	20	30	40
EEC-EPOH20	0.40	n/a	0.29	0.08	0.04
EEC-EPOH30	0.88	0.87	0.86	0.62	0.16

Finally, it is interesting to compare the effect of the composition of the reaction system on the polymerization rates of each type of epoxide group in the system: the EEC cycloaliphatic epoxide and the internal epoxide of the epoxidized oligomer. Figure 3.10 provides this comparison by showing the initial polymerization rate for both the EEC epoxide and the EPOH30 internal epoxide. The figure illustrates that the polymerization rate of the EEC cycloaliphatic epoxide is higher than that of the epoxidized oligomer for the whole composition range, and that the difference increases as the EEC content is increased. In the case of higher amounts of EEC from 50% to 90%, the initial reactivities of the internal epoxides in EPOHs are essentially zero. For the EEC content lower than 50%, the initial polymerization rate of EPOHs monotonically increases as the EEC content decreases until the initial polymerization rate becomes similar to the level of the neat EPOHs.

This trend may be surprising since it may be expected that the addition of EEC could facilitate the cationic photopolymerization of the EPOH internal epoxides by reducing the viscosity of the bulk mixture system and increasing the mobility of the cationic active centers.

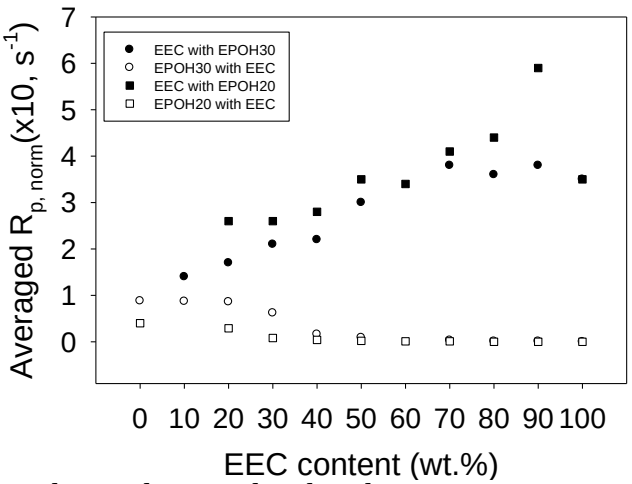

Figure 3.10 Averaged initial normalized polymerization rates of EEC and EPOH during cationic photopolymerizations of EEC-EPOH30 mixtures.

All of the kinetic results are consistent with the reaction mechanism shown in Figure 3.11. In the high EEC content regime, the increase in the polymerization rate with increasing EPOH content may be attributed to the activated monomer mechanism in which cationic active centers of cycloaliphatic epoxides in EEC selectively react with terminal hydroxyl groups rather than with the internal epoxides in the EPOH. Indeed, investigators have found that the propagation rate constant for the activated monomer mechanism is typically ~5 times higher than the propagation rate constant for the activated chain end mechanism [27]. This enhanced reactivity overcomes any negative effect from increasing viscosity for EPOH contents above ~50 wt.%. These conclusions are consistent with physical and mechanical property results that will be presented in the following chapter.

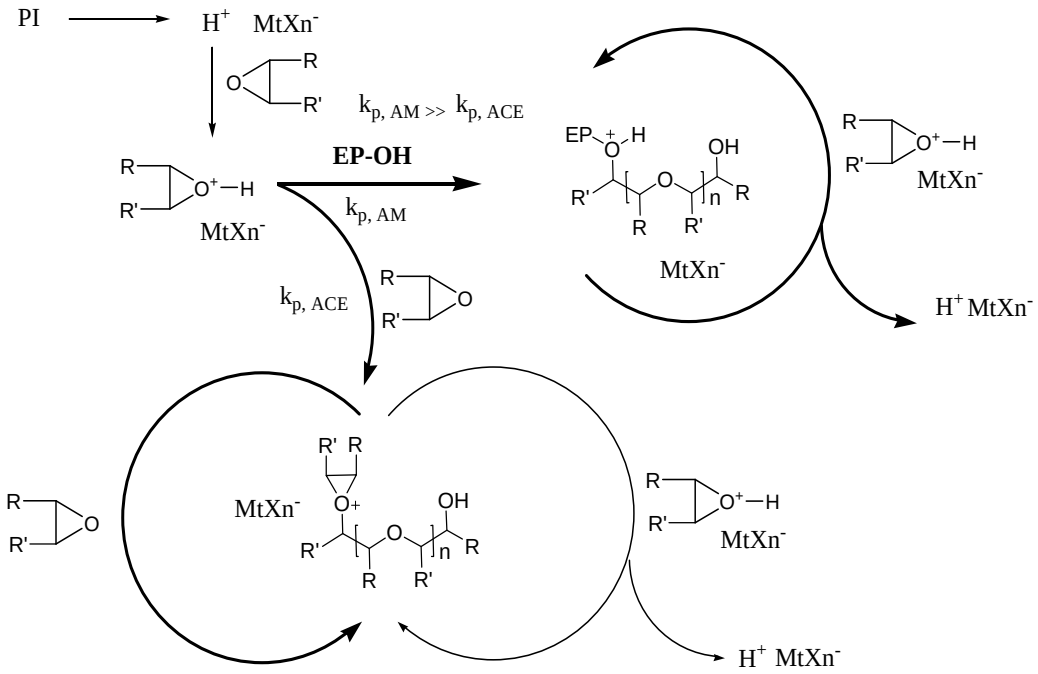

Figure 3.11 Coexistence of active chain end mechanism and activated monomer mechanism during photoinitiated cationic copolymerization of EEC-EPOH mixtures. $k_{p,ACE}$ and $k_{p,AM}$ are propagation rate constants in the respective active chain end and activated monomer mechanisms.

Conclusions

In this study, the photoinitiated cationic copolymerization of cycloaliphatic epoxide and epoxide-functionalized elastomeric oligomers were characterized. In these reaction systems, the cationic propagation reaction may occur by either the active chain end or the activated monomer mechanism. Several factors such as oligomer structures (epoxide content), viscosity, and monomer composition were carefully considered to understand the kinetic behavior of the two distinct epoxides in EEC and EPOHs. Independent, real-time monomer consumption of each type of epoxide was successfully obtained using Raman spectroscopy for EEC-EPOH mixtures as a function of monomer compositions.

The kinetic studies reveal a number of interesting results. The ultimate limiting conversion of EEC was monotonically enhanced with increasing EPOH content for both the EEC-EPOH20 and EEC-EPOH30 systems. In addition, the initial polymerization rate results suggest that the reactivity of the terminal hydroxyl groups in EPOHs is higher toward cationic active centers of cycloaliphatic epoxides in EEC than those of internal epoxides in EPOHs. Therefore, in the presence of EPOHs, the increase in the polymerization rate and the degree of conversion for EEC may be attributed to the contribution of the activated monomer mechanism associated with the hydroxyl group on the epoxidized oligomer. At high EPOH levels, the kinetic studies revealed that the cationic photopolymerization of EEC may be affected by the viscosity of the bulk mixture systems as a function of EPOH content. When the internal epoxide of the epoxidized elastomeric oligomer was monitored, the addition of EEC reduced the rate of polymerization and degree of conversion for EPOHs. The reduction in the kinetics was more pronounced for EPOH20 containing the low epoxide content when compared to EPOH30.

Notes

1. Petrie, E.M., *Epoxy Adhesive Formulations*. First ed. 2006, New York: McGrow-Hill.

2. Crivello, J.V., *The Discovery and Development of Onium Salt Cationic Photoinitiators.* Journal of Polymer Science: Part A: Polymer Chemistry, 1999. 37: p. 4241-4254.

3. Fouassier, J.P., *Photoinitiation, Photopolymerization, and Photocuring: Fundamentals and Applications* 1st ed. 1995, New York: Hanser.

4. Sipani, V. and Scranton, A.B., *Dark-Cure Studies of Cationic Photopolymerizations of Epoxides: Chracterization of the Active Center Lifetime and Kinetic Rate Constants.* Journal of Polymer Science: Part A: Polymer Chemistry, 2003. 41: p. 2064-2072.

5. Sipani, V. and Scranton, A.B., *Kinetic studies of cationic photopolymerizations of Phenyl glycidyl ether: termination/trapping rate constants for iodonium photoinitiators.* Journal of Photochemistry and Photobiology A: Chemistry 2003. 159: p. 189-195.

6. Sipani, V., Kirsch, Ann, Scranton, Alec B. , *Dark Cure Studies of Cationic Photopolymerizations of Epoxides: Characterization of Kinetic Rate Constants at High Conversions.* Journal of Polymer Science: Part A: Polymer Chemistry, 2004. 42: p. 4409-4416.

7. Ficek, B.A., Thiesen, A. M., and Scranton, A. B., *Cationic photopolymerizations of thick polymer systems: Active center lifetime and mobility.* European Polymer Journal, 2008. 44(1): p. 98-105.

8. Bulut, U., and Crivello, J. V. , *Investigation of the Reactivity of Epoxide Monomers in Photoinitiated Cationic Polymerization* Macromolecules, 2005. 38(9): p. 3584 -3595.

9. Crivello, J.V., *Cationic Photopolymerizationi of Alkyl Glycidyl Ethers.* Journal of Polymer Science: Part A: Polymer Chemistry, 2006. 44: p. 3036-3052.

10. Hartwig, A., Schneider, B., and Luhring, A., *Influence of moisture on the photochemically induced polymerisation of epoxy groups in different chemical environment.* Polymer, 2002. 43: p. 4243-4250.

11. Lin, Y. and Stansbury, J.W., *Near-Infrared Spectroscopy Investigation of Water Effects on the Cationic Photopolymerization of Vinyl Ether System.* Journal of Polymer Science: Part A: Polymer Chemistry, 2004. 42: p. 1985-1998.

12. Batog, A.E., Pet'ko, I. P., Penczek, P., *Aliphatic-Cycloaliphatic Epoxy Compounds and Polymers.* Advances in Polymer Science, 1999. 144.

13. Crivello, J.V. and Varlemann, U., *Structure and reactivity relationship in the photoinitiated cationic polymerization of 3,4-epoxycyclohexylmethyl-3'-4'-epoxycyclohexane carboxylate.* ACS symposium series, 1997. 673: p. 82-94.

14. Tokar, R., Kubisa, P., Penczek, S., and Dworak, A., *Cationic polymerization of glycidol: coexistence of the activated monomer and active chain end mechanism.* Macromolecules, 1994. 27(2): p. 320-322.

15. Bussi, P. and Ishida, H., *Partially miscible blends of epoxy resin and epoxidized rubber: Structural characterization of the epoxidized rubber and mechanical properties of the blends.* Journal of Applied Polymer Science, 1994. 53(4): p. 441-454.

16. Crivello, J.V. and Yang, B., *Synthesis and Photoinitiated Cationic Polymerization of Epoxidized Elastomers.* Journal of Macromolecular Science, Part A: Pure and Applied Chemistry, 1994. 31(5): p. 517 - 533.

17. Gregório, J.R., Engel Gerbase, A., Martinelli, M., Maldaner Jacobi, M.A., de Luca Freitas, L., Ambros von Holleben, M.L., and Dutra Marcico, P., *Very efficient epoxidation of 1,4-polybutadiene with the biphasic system methyltrioxorhenium (MTO)-CH2Cl2/H2O2.* Macromolecular Rapid Communications, 2000. 21(7): p. 401-403.

18. Riew, C.K., *Rubber-Toughened Plastics*. Advances in Chemistry Series Vol. 222. 1989, Washington, DC: American Chemical Society.

19. Udipi, K., *Epoxidation of styrene–butadiene block polymers. I.* Journal of Applied Polymer Science, 1979. 23(11): p. 3301-3309.

20. Choi, J., Lee, J., and Park, W., *Epoxidized polybutadiene as a thermal stabilizer for poly(3-hydroxybutyrate). I. Effect of epoxidation on the thermal properties of polybutadiene.* Fibers and Polymers, 2002. 3(3): p. 109-112.

21. Zhengang, Z., Mark, D.S., Yubiao, L., and Jun, H., *Cationic photopolymerization of epoxynorbornane linseed oils: The effect of diluents.* Journal of Polymer Science Part A: Polymer Chemistry, 2003. 41(21): p. 3440-3456.

22. Decker, C., Bianchi, C., Decker, D., and Morel, F., *Photoinitiated polymerization of vinyl ether-based systems.* Progress in Organic Coatings, 2001. 42(3-4): p. 253-266.

23. Al-Besharah, J.M., Salman, Omar A., and Akashah, Saed A., *Viscosity of crude oil blends.* Industrial & Engineering Chemistry Research, 1987. 26(12): p. 2445-2449.

24. Samran, J., Phinyocheep, P., Daniel, P., Derouet, D., and Buzaré, J.-Y., *Raman spectroscopic study of non-catalytic hydrogenation of unsaturated rubbers.* Journal of Raman Spectroscopy, 2004. 35(12): p. 1073-1080.

25. Zou, Y., Armstrong, S.R., and Jessop, J.L.P., *Apparent conversion of adhesive resin in the hybrid layer, Part 1: Identification of an internal reference for Raman spectroscopy and the effects of water storage.* Journal of Biomedical Materials Research Part A, 2008. 86A(4): p. 883-891.

26. Zou, Y., Armstrong, S.R., and Jessop, J.L.P., *Quantitative analysis of adhesive resin in the hybrid layer using Raman spectroscopy.* Journal of Biomedical Materials Research Part A. 94A(1): p. 288-297.

27. Biedron, T., Szymanski, R., Kubisa, P., and Penczek, S., Makromol. Chem., Macromol. Symp., 1990. 32: p. 155.

CHAPTER 4
CHARACTERIZATION OF PHYSICAL AND MECHANICAL PROPERTIES OF COPOLYMERS PRODUCED BY PHOTOINITIATED CATIONIC POLYMERIZATIONS: STRUCTURE AND PROPERTY RELATIONS

Introduction

The cationic photopolymerization of epoxides exhibits unique advantages over the free-radical photopolymerization including insensitivity to oxygen inhibition due to lack of radical coupling with oxygen[1]; low shrinkage/residual stresses; and relatively low rate of termination allowing cationic active centers to continuously proceeds even after illumination is ceased (dark polymerization[2-5]). In addition, efficient photoinitiated curing processes at low temperatures is especially useful for aerospace and automotive repair and fabrication since conventional high performance rubber-modified epoxide systems cannot tolerate high temperature cure. Above all, highly crosslinked epoxide thermosets produced by the cationic photopolymerization exhibit the same excellent physical and mechanical properties as those obtained in thermal curing systems.

Despite these merits, the highly crosslinked, rigid structure of photopolymerized epoxides can impart high glass transition temperatures and Young's modulus which may lead to undesirable brittleness. This brittleness can result in catastrophic fracture failure and poor impact resistance under high-rate loading conditions, high speed impact, *etc*. In addition, the low degree of elongation and shear displacement of unmodified epoxide thermosets limit their utility in certain applications such as joint adhesive due to low peel strength. To overcome these issues, enhanced flexibility and/or toughness are necessarily imparted to brittle network structures. The flexibility is a degree of elongation. Enhancement in the flexibility of a brittle epoxide matrix generally causes a reduction in tensile strength and modulus and lowers the glass transition temperature by decreasing the crosslink density of the epoxide network structure[6, 7]. The toughness is defined as

how efficiently a polymer matrix absorbs and dissipates internal stress concentrated near crack tip under an external force before reaching mechanical failure[7, 8]. Thus, the enhancement in toughness results in high elongation and moderate to high tensile strength. Consequently, toughness is considered important for to avoiding structural frailty and improving performance adaptability in various conditions.

Many efforts have been made to improve toughness of conventional epoxide systems using solid/liquid acrylonitrile butadiene rubbers with various reactive, terminal groups[9-11], epoxidized natural/synthetic rubbers[12-15] or oils[16-19], thermoplastic modifiers such as polyether sulfone[20], core-shell particles[21, 22], and so forth. The underlying strategy of using these modifiers is to introduce a secondary polymer domain into a continuous brittle epoxide matrix to induce bimodal distribution of two polymer phases When an external force is applied to a local region of the toughened epoxide matrix, the distinct secondary phase serves as a distributor or modulator of internal stress exerted by the external force. The internal stress distribution delays failure point by stopping or delaying crack propagation. Thus, under load-bearing conditions the toughened epoxide systems experience one or a combination of the following toughening mechanisms:[7, 23, 24] shear band formation, crazing, crack bridging, micro-cracking, crack path deflection, crack pinning and broadening (crack blunting). These mechanisms are listed in order of their efficiency in stress distribution. However, not all of those modifiers can be used for cationic photopolymerization systems. Some modifiers containing nucleophilic or basic groups can cause a delay or inhibition in cationic photopolymerizations, because protons generated from photolysis of cationic photoinitiator can be fixed or scavenged by some secondary moieties such as 1,2-position ether, nitrile, ester carbonyl, carbamate, amine groups.[25-28] In addition, a pre-reaction procedure or additional solvent needs to be involved in the curing process due to poor miscibility or dispersibility of some solid modifiers.

To avoid these limits, in this experiment epoxidized liquid polybutadiene oligomers containing hydroxyl terminal groups were used to modify the brittle properties of a cycloaliphatic diepoxide. While photo-induced cationic homopolymerizations of a single epoxidized elastomeric oligomer have received significant attention, the more complex photoinitiated cationic copolymerization of binary mixtures containing terminal hydroxyl groups and two different types of epoxide rings are not well understood in terms of structure-kinetics and structure-property relationships. Previously, higher selectivity of terminal hydroxyl groups in the elastomeric oligomers toward cationic active centers of the cycloaliphatic epoxides led to the enhancement in the polymerization kinetics and ultimate conversions for the cycloaliphatic epoxide. Thus, the kinetic studies revealed that activated monomer mechanisms associated with the hydroxyl groups in the elastomeric oligomers is primarily responsible for the propagation reactions of the cycloaliphatic epoxides, depending on binary mixture composition.

Therefore, this study focused on the structure-property relationship of final photopolymerized copolymers produced by the underlying kinetics of photoinitiated cationic copolymerizations of the binary monomer mixtures containing cycloaliphatic diepoxide and epoxidized, hydroxyl terminated polybutadiene oligomers.

Experimental

Materials

The cationically polymerizable monomer 3, 4-epoxycyclohexylmethanyl 3, 4-epoxycyclohexanecarboxylate (a cycloaliphatic diepoxide monomer, EEC, shown in Table 1) was used in these experiments. This monomer was a mixture of 91–97% CDE and cycloaliphatic mono-epoxide (ERl-4221, Sigma Aldrich) and was selected for its high reactivity and low shrinkage. Two different grades of epoxidized polybutadiene oligomers containing two hydroxyl terminal groups (EPOHs) were kindly donated from Cray Valley. The EPOHs have different internal epoxide equivalent weight (EEW) and

two hydroxyl groups at the ends of their chains. The photoinitiators (PIs) used in this study were [4-2-hydroxyl-1-tetradecyloxy)-phenyl] phenyl Iodonium (IHA, Polymer Science). Structures and relevant properties of all materials used are same as in the previous chapter.

Preparation of Thin Film Strips and Coatings

Samples containing monomer, oligomer, or their mixtures were thoroughly mixed with the photoinitiator using a mechanical mixer equipped with a Micro Surface Stirrer Shaft (BOLA, Germany). The mixed samples were placed in the vacuum oven at 35°C until the liquid mixture samples were completely degassed. To make film strips, the degassed, liquid samples were immediately poured between two quartz glass slides with a 100μm Teflon spacer to control sample thickness. For coatings, the same degassed, liquid samples were applied onto 3 in. × 6 in. × 0.025 in. aluminum panels (Type A alloy 3003 H14, Q-LAB) using a multi-film applicator. The aluminum panels were cleaned by the method modified from the literature[29] to avoid any organic contamination prior to the coating procedure. The sandwiched or coated samples were illuminated for 30 minutes using the Acticure® Ultraviolet/Visible Spot cure system (EXPO Photonic Solutions, Inc.). This lamp system is equipped with a high pressure 100-Watt mercury vapor short arc lamp and had the effective irradiance set to 100 mW/cm^2 measured by EFOS UV/Visible Radiometer R5000 for the filtered spectral range between 250 nm and 450 nm. All of the photopolymerized samples were stored in the dark condition at room temperature for a week in order to allow epoxide conversion to a final degree of conversion before they were subject to successive experiments.

The photopolymerized films sandwiched between the quartz glass slides were peeled off very carefully to avoid creating any scratches or notches on the surface and edges. No residues were observed on the surfaces of both quartz slides during the peel-off procedure. The thickness of the final film strips were 100 (± 10) μm. The width and

length of the film strip samples were 5 mm × 2.5 mm, respectively. To minimize the error that may arise from this slight variation in the thickness of the film strips, the widths of each film strip were corrected by applying a dimension factor of 0.25 when cutting the film to the specific dimension. The thin film samples produced by this procedure were subject to rheological analysis, thin film tension test, and gel content study.

The thickness of the photopolymerized coatings varied from 30 μm to 150 μm depending on research purpose. Finally, the coatings on the aluminum substrate were subject to several tests for impact resistance, surface hardness, and optical properties.

Characterization of Rheological Behavior for Photopolymerized Thin Films

Q800 Dynamic Mechanical Analysis (DMA, instruments) was used to determine and obtain the glass transition temperature and loss/storage modulus of resulting homo and copolymer films. The thin film clamp on rectangular specimens were used to apply direct tension on the thin film sample, because the tensile deformation mode is suitable for a dynamic modulus higher than 0.01 GPa.[30] Using a liquid nitrogen cooling element the temperature for rheological studies was cooled to -150°C and heated to 250°C at a ramping rate of 3°C/min, a frequency of 1 Hz, and an amplitude of 15 microns.

Characterization of Stress-Strain Behavior of Photopolymerized Thin Films

For uniaxial tension tests, Q800 Dynamic Mechanical Analysis, DMA (TA instruments) equipped with a thin film clamp was used to obtain stress-strain curves for the thin film strips. Temperature was isothermally maintained during the tension test at 25°C. The film tension test was performed repetitively, more than five times on average, for the reproducibility of individual film samples. For the film tension test, static force was applied to the film strip samples at 1N/min from 1N to 18N. The preload force and

the force track functions were used to precisely monitor the instantaneous change in the stress and strain during the tension test.

Characterization of Photopolymerized Coatings

Photopolymerized coatings were produced on 3 in. × 6 in. × 0.025 in. aluminum panels (Type A alloy 3003 H14, Q-LAB) as previously described. The photopolymerized coating of each formulation including neat EEC, neat EPOHs, and their mixtures was then tested to obtain gloss and hardness properties as well as impact resistance. For the physical property testing, the thickness of the finished coatings was about 45 μm (± 10). Gloss measurements were made by using a BYK Gardner micro-tri-gloss meter which measures gloss readings at the 20°, 60°, and 85° geometries within seconds for the respective high gloss, semi-gloss, and matt finishes. Each sample was measured a total of six times; three times perpendicularly to the length of the coated panel and three times parallel to its length. The quality of coating surface hardness was determined by the pencil test based on ASTM D3363-00. A minimum of five measurements in three different locations on the surface of each coating was performed for at least three replicated samples. The resistance of the coatings to the impact force from a 4-lb falling weight was determined using a Gardner Impact Tester (PF-1120, BYK) based on ASTM D2794. A minimum of five replicates was measured for each coating sample. Impact strength was determined when the coatings were damaged and confirmed under a digital microscope.

Characterization of Cross-section Morphology

Hitachi S-3400N Variable Pressure Scanning Electron Microscope (VP-SEM) was used at 10kV accelerating voltage to obtain electron micrographs for a cross-sectional area of photopolymerized films. The films (with rectangular dimensions of 25 mm long × 3 mm wide × 0.5 mm thick) were casted from a home-made silicon mold after photopolymerization with the same illumination setting as for DMA samples. The finished films were stored in a dark condition for a week prior to the cross-sectional

characterization. Finally, the finished films were taken out of the mold and cryogenically-fractured in liquid nitrogen. Fragments were then stained overnight using aqueous vapor containing 2% osmium tetraoxide in well-sealed glass petri dishes, followed by VP-SEM studies.

Results and Discussion

Thermo-mechanical Properties of Photopolymerized Copolymers

Dynamic mechanical analysis was performed for thin films of neat EEC/EPOH homopolymers and EEC-EPOH20/30 copolymers. Physical response of the corresponding polymer films to oscillatory deformation as a function of temperature was determined by storage modulus (elastic response to deformation), loss modulus (plastic response to deformation), and tan δ (ratio of the loss modulus to storage modulus, an indicator of occurrence of molecular mobility transitions).

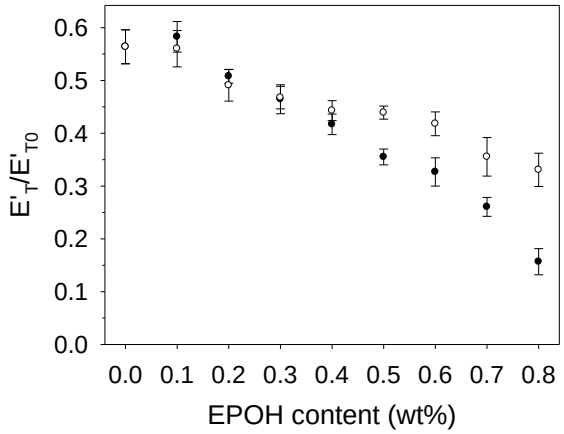

Figure 4.1 Effect of EPOH content on the storage modulus of EEC-EPOH20 and EEC-EPOH30 copolymers at room temperature.

The EEC-EPOH copolymers contain different amount of each EPOH20 and EPOH30 oligomer, and the internal epoxide content of the two elastomeric oligomers are

different. Hence, it was expected that the stiffness of the copolymers in the glassy state can be altered by EEC-EPOH composition and internal epoxide content of the two elastomeric oligomers. The stiffness of EEC-EPOH20 and EEC-EPOH30 copolymers under oscillatory deformation was compared by normalized storage modulus of each copolymer at room temperature as shown in Figure 4.1.The storage modulus (E'_{RT}) of the copolymers depended on the EPOH content and monotonically decreased with increasing epoxidized oligomer content. This trend is true for both EEC-EPOH20 and EEC-EPOH30 copolymers. The figure illustrates that there is no significant difference in the storage modulus in-between the two copolymers in the glassy state for the EPOH content ranging from 0 to 40 wt.%. As the EPOH content is increased further, the storage modulus of the two copolymers noticeably deviated from one another. The copolymers containing EPOH30 showed higher storage modulus than the copolymers containing EPOH20 when the EPOHs were added more than 40wt.%.

In the glass state (below T_g), the stiffness is related to changes in the stored elastic energy upon small deformation as molecular segments resist motion. The decreasing of the storage modulus with the increase of EPOH content illustrates that under oscillatory deformation at 1 Hz the crosslinked networks modified by the epoxidized elastomeric oligomers are less resistant to motion; in other words, less energy is stored. This contribution of the EPOH20 and EPOH30 oligomers are almost indistinguishable for the corresponding copolymers with the EPOH content between 0 and 40%. Above the EPOH content of 40%, the two different copolymers begin to exhibit different stiffness in the glassy state as the EPOH content is increased further.

It was also interesting to confirm the effects of the EPOH content and the oligomer structure on the network behavior of the copolymers at higher temperature. Figure 4.2 illustrates temperature dependence of storage modulus of EEC-EPOH copolymers. In the figure, the dynamic storage modulus curve of each EEC-EPOH20 and EEC-EPIH30 copolymer shows an infliction point near glass transition temperature

region at which the dynamic storage modulus rapidly reduced. The rapid reduction in the dynamic storage modulus occurred at different onset temperature as a function of the composition of EEC and EPOH. In addition, the dynamic storage modulus curves in Figure 4.2A and B reveals that all of the EEC-EPOH copolymers behave as characteristic thermosets, as indicated by the presence of rubbery plateaus. The pleteaue modulus monotonically decreased with increasing EPOH content in both EEC-EPOH20 and EEC-EPOH30 copolymers.

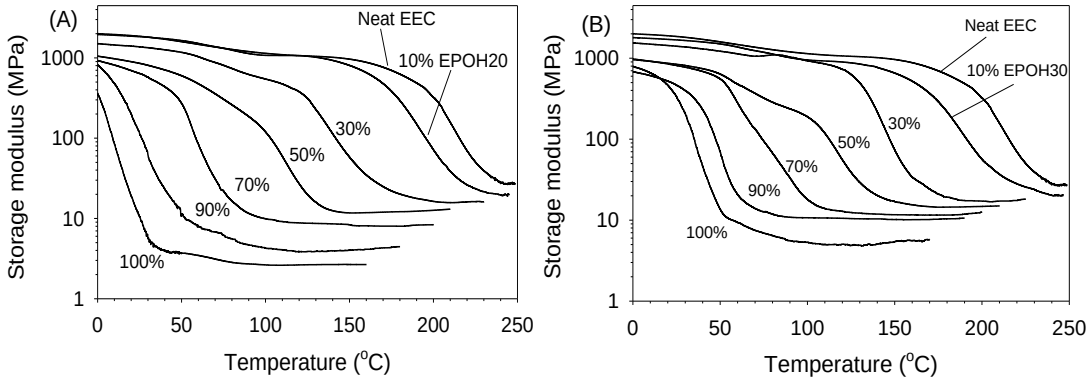

Figure 4.2 Profiles of dynamic storage modulus of EEC-EPOH20 (A) and EEC-EPOH30 (B) copolymers.

Crosslink density of Photopolymerized Polymers

Accroding to the statistical theory of rubber elasticity, the decrease in the storage modulus in the rubber plateau is related to crosslink density in the copolymer networks. Thus, the crosslink density (v_e) of each EEC-EPOH20 and EEC-EPOH30 copolymer was estimated using the following equation [16, 17, 31]:

$$v_e = \frac{E'}{3RT} \qquad (eq.\ 4.1)$$

Where E' represents the storage modulus of the crosslinked copolymer in the rubbery plateau region above the glass transition temperature (T_g), R is the gas constant,

and T is the absolute temperature. The rubber pletau modulus were taken approximately at 50ºC above the glass tranistion tempearture, based on tan δ_{max}. Although stress relaxation experiments may give more strictly valid results on the moecular weight between crosslinks[32], the estimated values based on q.4.1 gives qualitatively insight into the netwok structures of the copolymers for comparison purpose.

Table 4.1 Effect of EPOH content on the crosslink density values of the photopolymerized EEC-EPOH20 and EEC-EPOH30 copolymers.

	EPOH content						
	0	10	30	50	70	90	100
Copolymers	Crosslink Density (mol/m3)						
EEC-EPOH20	2065	1547	1314	1113	957	633	321
EEC-EPOH30	2065	1541	1376	1291	1215	1115	616

Table 4.1 illustrates the estimated crosslink density values of each homo and copolymer. The crosslik density values of the homopolymers shows the following order: EEC >> EPOH30 > EPOH20. The crosslink density of the EEC-EPOH copolymers decreased with increasing the EPOH content. The estimated crosslink denstiy vaules for the EEC-EPOH20 and EEC-EPOH30 oligomers were very similar for the EPOH conent between 0 and 50 wt.%, and noticeabley deviated from one another when the EPOH content was increased further. The higher crosslink density was observed for the copolymers with the EPOH30 content from 50 to 90 wt.%.

The highest crosslink density of the EEC homopolymer indicates a tight network structure wherease the EPOH20 and EPOH30 homopolymers have relatively looser

network structures. The two-fold high crosslink density of the EPOH30 homopolymer indicates more tight network structure than that of the EPOH20 homopolymer, which is attributed to the high internal epoxide content of the EPOH30 relative to the EPOH20. The monotonical decrease in the crosslink density of the copolymers with increasing the EPOHs illustrates that the crosslinked networks of the EEC are loosen by the epoxidized elastomeric oligomer during the photoinitiated cationic copolymerization. For the EPOH content lower than 50wt.%, the results shown in Table 4.1 indicate that the different internal epoxide content between the two EPOH20 and EPOH30 oligomers has a marginal effect on the crosslink density of the corresponding copolymers, and the crosslinked network structures modified by the EPOH20 and EPOH30 oligomers may have no significant difference. In constrat, with the EPOH content from 50 to 90%, the EEC-EPOH30 copolymers exhibited more tight network properties (higher plaetaue modulus and crosslink density) relatve to the EEC-EPOH20 copolymers due to relatively high internal epoxide content of the EPOH30 (Figure 4.2 and Table 4.1). This trend in the two composition regimes was consistenct with the stiffness data of these copolymers in the glassy state (Table 4.1 vs. Figure 4.2).

In general, as crosslink density of the copolymer decreases, the molecular motion of the network chains in the copolymer is less restricted and the glass transition temperature should decrease. Thus, the glass transition temperature of each copolymer film was determined from α-relaxation peak location of the loss factor (tan δ_{max}). Figure 4.3 illustrates the dependence of T_g on the composition of the miscible EEC and EPOH mixtures for a series of photopolymerized copolymers. The glass transition temperature of each homopolymer shows the following oder: EEC (210 ºC) >> EPOH30 (40 ºC) > EPOH20 (12 ºC). This order is the same as their crosslink density values. Figure 4.3 also illustrates that the glass transition temperature monotonically decreased with increasing the EPOH content for EEC-EPOH20 and EPOH30 copolymers. The variation of the glass

transition temperature of both EEC-EPOH20 and EEC-EPOH30 copolymers mirrors the same trend observed from stiffness data and crosslink density values.

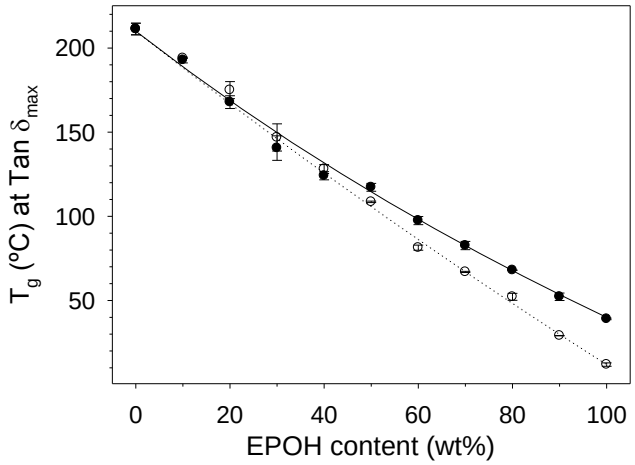

Figure 4.3 Effect of EPOH content on the glass transition temperatures of EEC-EPOH20 and EEC-EPOH30 copolymers.

In Figure 4.3, each set of T_g data corresponding to two different sets of copolymers were well predicted on basis of the Gordon-Taylor/Kelly-Bueche equation [14, 33].

$$T_g = \frac{\phi_1 T_{g1} + K'\phi_2 T_{g2}}{\phi_1 + K'\phi_2} \qquad (eq.\ 4.2)$$

Where T_{g1} and T_{g2} are the glass transition temperatures of the pure components, ϕ_1 and ϕ_2 are the volume fractions of the components in the copolymers, and the value of K′ can be employed as a fitting parameter. Here K' was determined to be 0.9 and 0.78 for EEC-EPOH20 and EEC-EPOH30 copolymers respectively. In this empirical equation, K' values provide a qualitative measure of the strength of the polymer interaction. The lower K' value of the EEC-EPOH30 copolymers indicates that the elastomeric domains of the EPOH30 have relatively weaker interaction with EEC networks compared to the

EPOH20 with lower internal epoxide content. The predicted curves based on Eq. 4.2 also illustrate a slightly negative deviation from linear mixing for both copolymers. The negative deviation was relatively more pronounced for the EEC-EPOH30 copolymers than the EEC-EPOH20, especially for the EPOH content from 50 to 100wt.%. This phenomenon was further elucidated by Lu and Weiss theory, in which negative deviation from linear mixing relationship is indicative of weak specific intermolecular interactions between miscible binary polymer blends [34]. According to their work, K′ further reflects the effect of relatively weak interaction between polymer components.

$$K' = k + \frac{A}{T_{g2} - 1} \qquad (eq.\ 4.3)$$

Where A has a proportional relationship with the Flory-Huggins interaction parameter and k is related to the change in specific heat of polymer components at their glass transition temperature. For this case, k and A were adjusted and found to be 0.5×10^{-3} and 190 for the EEC-EPOH20 copolymers and 1×10^{-3} and 163 for the EEC-EPOH30 copolymers. The more dominance of A for the EEC-EPOH20 copolymers indicates that the elastomeric domain of the EPOH20 is more compatibilized with the EEC for the EPOH content between 50 and 90wt%. This result is quite interesting because it was anticipated that the EEC-EPOH30 copolymers would have more compatibilized network structures due to their high internal epoxide content of the EPOH30 than that of the EPOH20.

One plausible explanation can be obtained from the different kinetic behavior of the two epoxidized oligomers during the photoinitiated cationic copolymerizations with the EEC (Chapter 3). In Chapter 3, the initial polymerization rates and ultimate conversions of the internal epoxides in both oligomers were essentially zero with the EEC content from 50% to 90%. As the EEC content was reduced further below 50%, the EPO30 oligomer exhibited higher polymerization rates and ultimate conversions than the

EPOH20. In this composition range, the weaker network interaction between the EEC and EPOH30 polymer may be attributed to more facilitated polymerizations between the internal epoxides in the EPOH30 elastomeric phases than in the EPOH20 phases during copolymerization. Again, overall results support the conclusion for the kinetic study: in the presence of EPOHs, the increase in the polymerization rate and the degree of conversion for EEC is attributed to the contribution of the activated monomer mechanism associated with the hydroxyl group on the epoxidized oligomer. In addition, the results showing the difference in T_g behavior (Figure 4.3) between the two copolymers support why the EEC-EPOH30 copolymers exhibited the higher storage modulus behavior the glassy state and higher crosslink density than the EEC-EPOH20 for the high EPOH content.

Furthermore, for the EPOH content below 50wt.%, consumption of internal epoxides of the epoxidized oligomers could be negligible, but the EEC monomer is consumed via both active chain end and activated monomer mechanisms. In this situation, the presence of the different propagation reactions may affect homogeneity of the copolymer network structures during photoinitiated cationic copolymerizations. Therefore, it is interesting to see phase behavior of the copolymers as a function of composition

Phase Behavior of Photopolymerized Copolymers

Figure 4.4 illustrates tan δ profiles for a series of each EEC-EPOH20 and EEC-EPOH30 copolymer. Compatibility between the polymer components is indicated by the number of δ peaks. Phase homogeneity of the copolymers can be qulitatively examined by considering the broadness of a maximum δ peak (δ_{max}). In Figure 4.4, the phase behavior of the EEC-EPOH copolymers are different for two composition regimes. For the low EPOH content regime, the tan δ profiles illustriate that a bimodal distribution of tan δ peaks are observed and that the δ_{max} peak is progressively broaden from 0 to 50

wt%. In addition, the maximum tan δ peak, representing continous network matrix, is proportionally shifted inward to reflect the decrease in the T_g due to the incorporation of the elastomeric constituent into the network matrix. For the high EPOH content above 50 wt%, each EEC-EPOH copolymer exhibits a single, uniform δ_{max} peak and their δ_{max} peaks are narrow compared to the EEC-EPOH copolymer in the low EPOH content regime. The δ_{max} peaks representing continous network matrix is proportionally shifted inward to reflect the decrease in the T_g as the EPOH content increases further.

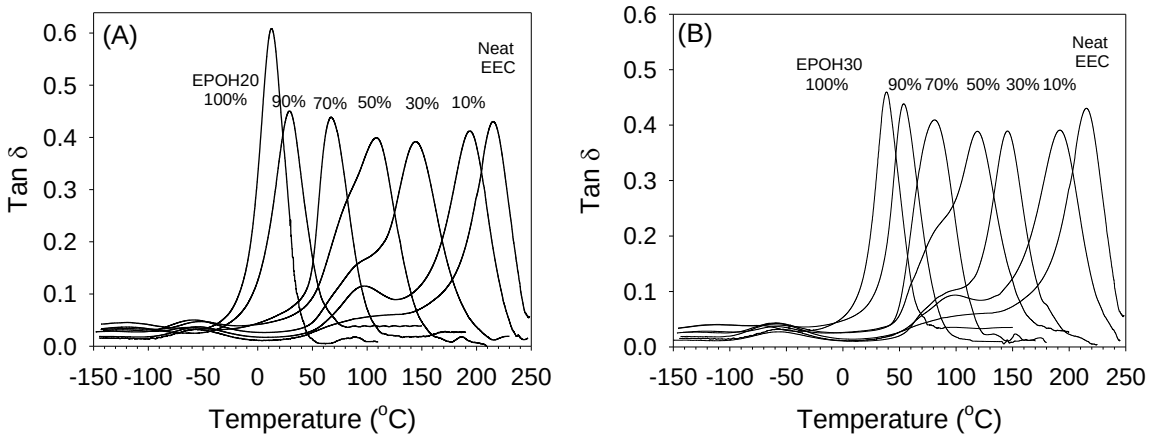

Figure 4.4 Tan δ profiles of EEC-EPOH20 (A) and EEC-EPOH30 (B) copolymers.

As discussed above, the two different propagation reactions via ACE and AM mechanisms are present in the photoinitiated cationic copolymerizations of the EEC with the EPOHs. Accoring to the kinetic study in Chapter 3, in the low EPOH content regime the contribution of AM mechanism to the increase in the EEC conversion is limited due to the low concentration ratio of the hydroxyl groups to the cycloaliphatic epoxides [35], although the propagation rate is much higher for the AM mechanism.[36] In this situation, the EEC monomers are consumbed by both ACE and AM mechanisms during the photoinitiated cationic copolymerization. At the same time, the internal epoxides

conversion in both EPOH20 and EPOH30 oligomers are negligible. The elasotmerinc oligomers are incorporated into the EEC network by the AM mechanism associated with their hydroxyl terminal groups. Consequently, this complexity in the propagation reactions in the EEC-EPOH copolymerizations possibly caused an increased microheterogenity in the network structure with the broad δ_{max} peaks and resulted in the biomodal phase behavior for the EEC-EPOH20 and EEC-EPOH30 copolymers.

As illustrated in Figures 4.4, the bimodal phase behavior of the EEC-EPOH copolymers appeared to fade out as the more elastomeric oligomers was incoportated above 50wt.%. In this composition regime, the progation of the EEC cationic active centers is more faciliated via the AM mechanism due to a high concentration ratio of the hydroxyl terminal groups to cyclicloaliphatic epoxides, which results in a greatly increased EEC converison as seen in the kinetic study (Chapter 3). In addition, the volume fractions of the EPOHs becomes greater than that of the EEC. For the high EPOH content regime, the EEC polymer constituent may be dissolved and incoporated into the elatomeric polymer phase via the AM mechanism. These combined reasons may explain the disapperance of the bimodal phase behavior and the narrow δ_{max} peaks for the EEC-EPOH copolymers. Both indicate well-compatibilized polymer phases. Furthermore, in the assumption of the well distribution of EEC monomes throghout the elastomeric phase, the cationic copolymerization of cyclicloaliaphatic epoxides with the terminal hydroxyl groups may preceed in a well-controlled manner like end-linking process.[35] This also possibly led to the narrower δ_{max} peaks. It seemed that the δ_{max} peaks of the EEC-EPOH30 copolymers was slightly borader than those of the EEC-EPOH20 copolymers for the high EPOH content regime between 50 and 90wt.%. This may be attributed to higher conversion of the internal epoxides in the EPOH30 elastomeric phases than those of the EPOH20 in the EEC-EOH20 copolymers. Overall implications on the phase behavior of the EEC-EPOH copolymers as a funtion of composition were schematically illlustrated in Figure 4.5.

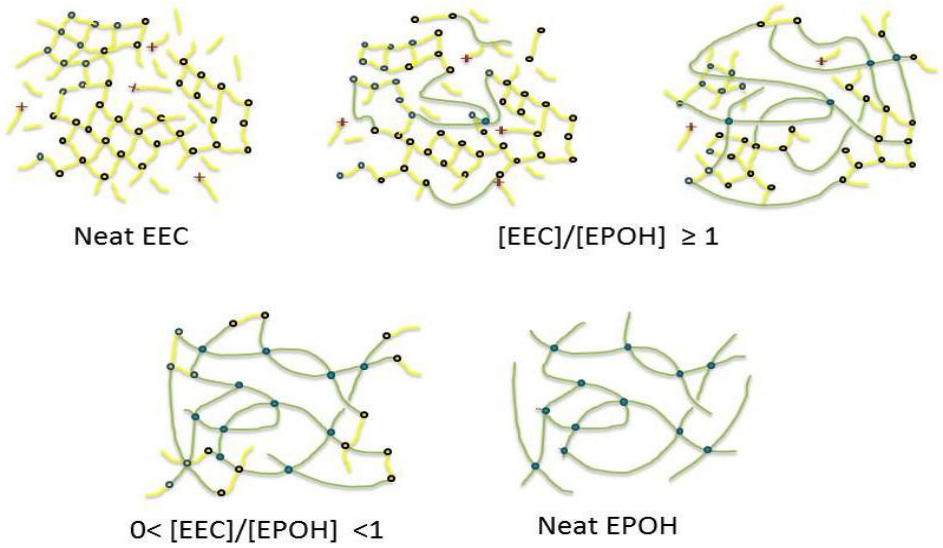

Figure 4.5 Phase behavior of EEC-EPOH copolymers as a function of compositions.

Tensile Strain-stress Behavior

It is necessary to correlate the different physical properties of the EEC-EPOH copolymers with their mechanical performance, because it also reflects the dependence of the mechanical properties of these copolymers on the composition and oligomer structure (internal epoxide content). Hence, all of the photopolymerized homo and copolymer films were applied to uniaxial tensile measurements to examine their stress-strain behavior.

Figures 4.6 and Table 4.2 illustrates tensile stress–strain behavior of the EEC-EPOH20 and EEC-EPOH30 copolymers as compared to pure EEC, EPOH20, and EPOH30 homopolymers. The stress-strain curves of all of the photopolymerized films show an increase in stress with strain until fracture occurs such that ultimate strength is observed at fracture. The EEC homopolymer exhibited a typical stress-strain curve of a hard, brittle thermoset with no yielding point and a steep initial slope (Young's modulus)

due to its highly crosslinked network. The ultimate strength (stress at fracture) and elongation-at-break were ~60MPa and ~6%. In contrast, the EPOH homopolymers exhibited a ductile behavior with a very low Young's modulus. The EPOH20 and EPOH30 homopolymers exhibited ultimate strengths of ~4MPa and ~16 MPa and elongation-at-break of ~49% and ~44%, respectively. The difference in these values of the two EPOHs is attributed to the higher internal epoxide content in the EPOH30 oligomer.

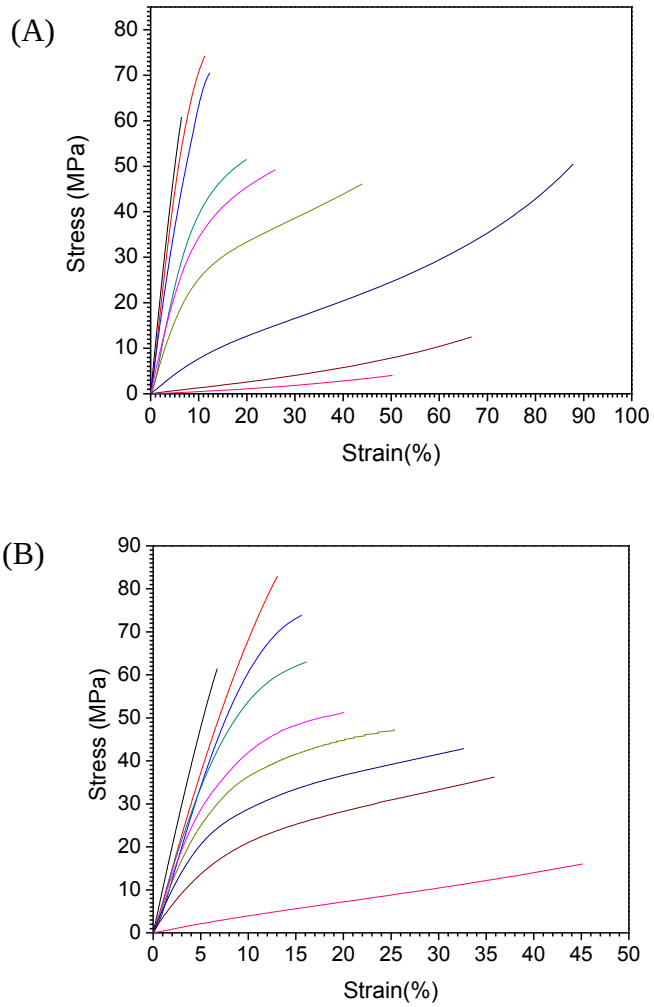

Figure 4.6 Tensile stress-strain behavior of photopolymerized EEC-EPOH20 (A) and EEC-EPOH30 copolymers (B).

Table 4.2 Properties of the EEC-EPOH20 and EEO-EPOH30 copolymers.

Copolymers	EPOH content	Young's Modulus (MPa)	Ultimate Strength (MPa)	Elongation at Break (%)	Fracture Toughness (MPa)
EEC-EPOH20 (EEC-EPOH30)	0%	1016±10	60±2	6±1	2.17
	10%	842±73 (822±98)	74±6 (80±7)	10±3 (13±3)	4.98 (5.92)
	30%	753±57 (801±29)	68±5 (71±3)	12±2 (14±2)	5.03 (6.48)
	50%	516±40 (748±79)	50±2 (59±3)	20±2 17±1	6.80 (6.75)
	60%	500±7 (695±52)	47±3 (50±3)	24±1 (20±2)	8.85 (7.39)
	70%	322±35 (651±22)	45±2 (45±6)	43±2 (25±3)	13.97 (8.83)
	80%	85±11 (619±67)	48±1 (40±5)	85±3 (34±2)	20.46 (10.20)
	90%	13±3 (326±19)	15±2 (35±3)	64±3 (37±2)	3.43 (8.89)
	100%	5±1 (45±3)	4±1 (16±2)	49±2 (44±1)	0.83 (3.63)

The stress–strain behaviors of all of the EEC-EPOH copolymers depend on the EPOH content and oligomer structure. For EEC-rich copolymers with the EPOH content from 0 to 30 wt.%, the ultimate strength and elongation-at-break are increased while Young's modulus decrease. As the EPOH content increases further from 10 to 90wt.%, the Young's modulus and ultimate strength tend to decrease while the low elongation at break and fracture toughness of the EEC homopolymer were greatly enhanced. For both EEC-EPOH20 and EEC-EPOH30 copolymers, maximum elongation at break was observed for the EPOH content of 80 to 90 wt.%. Maximum 5 to 10-fold enhanced

fracture toughness was observed when the EPOH content was 70 to 80 wt.% compared to the pure EEC homopolymer.

Young's modulus data of the EEC-EPOH20 and EEC-EPOH30 copolymers illustrated the same trend observed from their storage modulus behavior in the glassy state (Table 4.2 vs. Figure 4.1). The ultimate strength of both copolymers were almost similar for the EPOH content from 10 to 80 wt.%. With the EPOH content more than 50 wt.%, the EEC-EPOH20 copolymers exhibited higher elongation at break and up to 2-fold higher fracture toughness than the EEC–EPOH30. Therefore, the enhancement in the fracture toughness of the EEC-EPOH20 copolymers is attributed to the highly enhanced extensibility for this composition range. The relatively low toughness of the EPOH30 oligomers is attributed to the tighter network structure in the elastomeric phase for the corresponding copolymers due to higher conversion of internal epoxide content, and this results in the relatively lower extensibility. In general, with the EPOH content more than 50wt.%, both EEC-EPOH copolymers exhibited significantly enhanced extensibility and fracture toughness compared to the pure EEC homopolymer.

The significantly enhanced extensibility and fracture toughness of the EEC-EPOH copolymers with the EPOH content of 70 to 80% may be attributed to multimodal distribution of network chain length as shown in Figure 4.5. With such high EPOH contents, end-linking process between the EPOH hydroxyl groups and the EEC via the AM mechanism may be responsible for multimodal network structures. In the theory of the multimodal networks, crosslinked network segments consist of long and short chains and involve non-affine deformation of the network segments.[37, 38] At the beginning of the non-affine deformation mechanism, shorter chains reach their ultimate extensibilities as macroscopic deformation proceeds, these short chains remain at their almost fully stretched lengths, and the remaining chains of larger length continue to extend. Thus, the non-affine deformation mechanism requires the maximum extensibility of each type of chain to achieve enhanced ultimate properties such as elongation at break and fracture

toughness. A characteristic behavior of a crosslinked polymer containing multimodal network chain lengths is up-turn mode stress-strain behavior before fracture [38], which was observed from the EEC-EPOH20 copolymers. This characteristic was less pronounced with EEC-EPOH30 copolymers because the crosslink density of the EPOH30 elastomeric phase is higher than the EPOH20, which lead to less extensibility during the macroscopic deformation.

Impact Resistance of Photopolymerized Coatings

For the tensile measurements for all of the photopolymerized homo and copolymers shown in the previous section, a standard static force (1N/min) was applied. It is important to confirm whether the photopolymerized polymers behave similarly under high velocity-loading condition. For this purpose, falling weight impact resistance tests were performed for the photopolymerized coatings. Figure 4.7 illustrates the impact strength of the EEC-EPOH copolymer coatings of 45 (±5) μm thickness with different amounts of the EPOH as compared to the pure EEC and EPOH homopolymers.

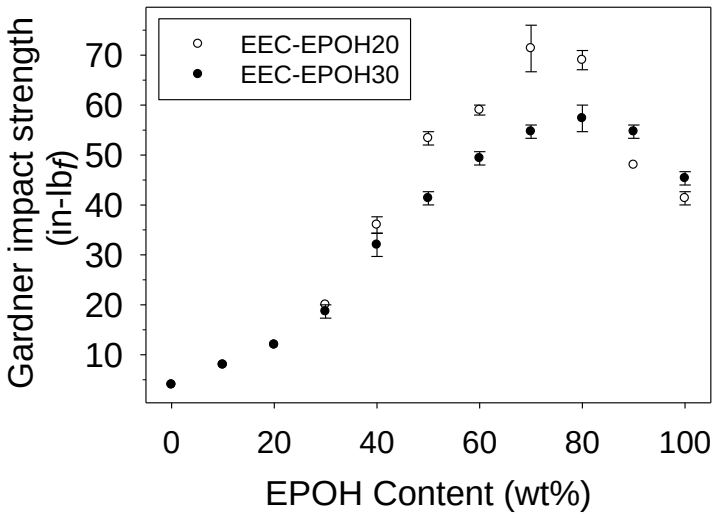

Figure 4.7 Impact strength of the photopolymerized EEC-EPOH20 and EEC-EPOH30 copolymer coatings.

In Figure 4.7, overall impact strength of all EEC-EPOH copolymers surpasses the pure EEC homopolymer. The impact strength of the copolymers monotonically increases with increasing the EPOH content. For both EEC-EPOH20 and EEC-EPOH30 copolymers, maximum impact strength was observed with ~80% EPOH, and this result in 14 to 18 fold increase in the impact resistance compared to the pure EEC homopolymer. The impact resistance of the two copolymers is not different with the EPOH content between 0 to 40wt.%. As the EPOH content increases further, the EEC-EPOH20 copolymers exhibit superior impact strength compared to the EEC-EPOH30 copolymers, except with 90 wt.% EPOH in that the EEC-EPOH30 exhibited higher impact strength. Again, this difference can be attributed to different extensibility associated with oligomer structure (internal epoxide content) between the EPOH20 and the EPOH30 oligomers. The overall impact resistant behavior of the two copolymers was consistent with the trend observed for other physical and mechanical properties presented in other sections.

The enhanced impact resistance of the EEC-EPOH20 copolymer with ~80wt.% is remarkable when considering that such thin coating on the standard aluminum substrate was used, of which failure occurred at ~80 in-lb_f,. This result emphasizes the importance of high extensibility and moderate ultimate strength for high impact resistance. In addition, damaged coatings remained on the standard aluminum substrate without peeling-off for both EEC-EPOH20 and EEC-EPOH30 copolymers when the EPOH content was more than 60 wt.%. The resistance to peel-off under impact force is important for coating applications to prevent possible corrosion of a metal substrate under the coatings. Further investigations on this issue are needed for different metal substrates.

Cross-section Morphology of Photopolymerized Copolymers

Scanning electron microscopic studies were performed to examine cryogenically-fractured surfaces of the EEC-EPOH20 and EEC-EPOH30 copolymer films for two different weight compositions. Figure 4.8 shows SEM photographs of EEC-EPOH20 (A,

and B) and EEC-EPOH30 (C and D) copolymers. The EEC-EPOH mixtures with EPOH content below and above the volume fraction inversion of the two components were selected for comparison.

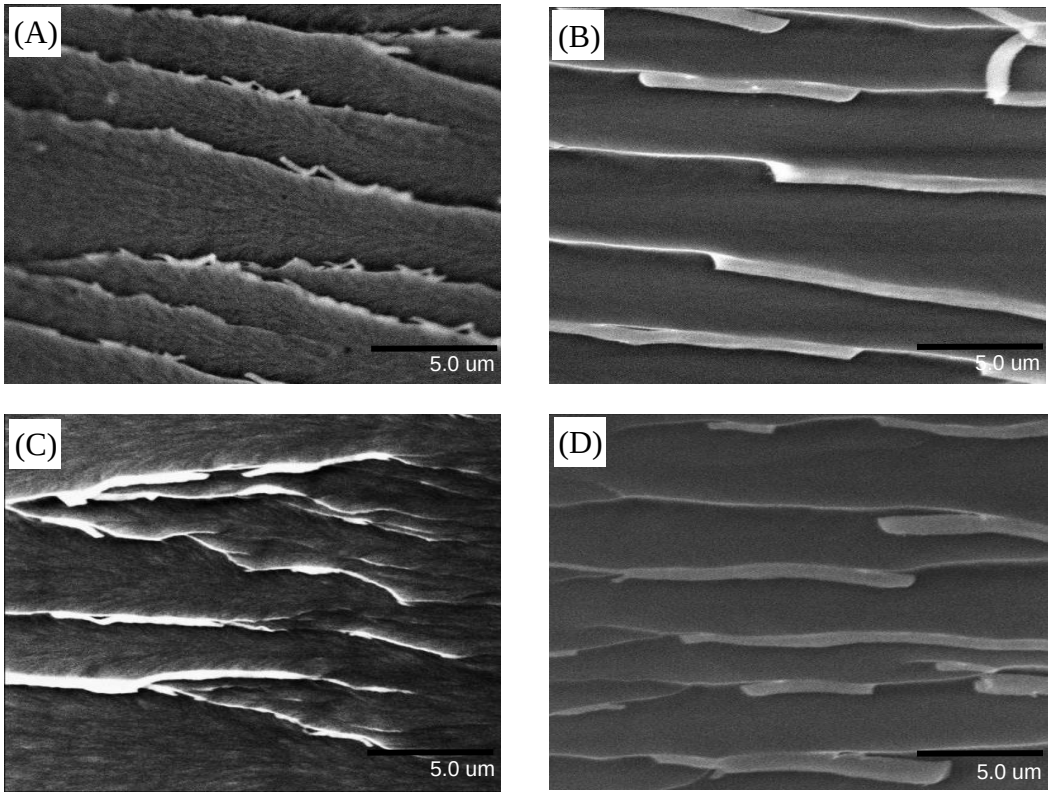

Figure 4.8 Surface morphology of freeze-fractured films of EEC-EPOH20 (A and B) and EEC-POH30 copolymers (C and D) with two different weight compositions: 70:30 (A and D) and 30:70 (C and F) weight ratios of EEC to EPOH.

In Figure 4.8, the fracture surface morphology varies with the binary composition for both EEC-EPOH20 and EEC-EPOH30 copolymers. Similar morphologies are observed between the two copolymers for the corresponding composition. In Figure 4.8A

and C, the topography of the fracture surfaces seems rough and heterogeneous for the 70:30 EEC-EPOH copolymers. The heterogeneous surface morphologies indicate that microphase separation occurs between the EEC matrix and EPOH polymer constituents. In addition, a sign of very weak plastic deformation along with crack path deflection was observed in the fracture surface. In addition, it seems that there is a slight difference in the phase behavior between the EEC-EPOH20 and EEC-EPOH30 as also illustrated from the tan δ profiles in Figure 4.4. On the other hand, Figure 4.8B and D shows smooth fractured surface in the matrix polymer. The homogenous morphology is indicative of no phase separation and implies that there is a phase inversion in which the EEC domains are well dissolved in the EPOH elastomeric matrix. Similarly, there is a sign of crack path deflection. In marked contrast to the 70:30 copolymers, extensive drawing of elastomeric domain on the deflected crack path is accompanied with significant plastic deformation.

The plastic deformation along with the deflected crack path was generally observed within 50 to 100 μm from the surface to the sample depth depending on binary mixture composition. Therefore, the comparison of the fractured surface morphologies for the two different compositions further elucidates why both EEC-EPOH20 and EEC-EPOH30 exhibit high fracture toughness (Table 4.2) and impact resistance (Figure 4.8) for the high EPOH content regime. However, higher resolution microscopic study is required to see the difference in the fracture surface morphology between the two copolymers for the 30:70 weight ratios.

Surface Hardness of Photopolymerized Coatings

Pencil hardness tests were performed to determine scratch hardness for the copolymer coatings as a function of composition. Table 4.3 illustrates that the scratch hardness of the pure EEC homopolymer slightly increases in the presence of the EPOH oligomers, but no significant dependence on EPOH content is observed. In addition, the

EEC-EPOH20 and EEC-EPOH30 copolymers exhibit similar scratch hardness for the corresponding compositions. Highest scratch hardness was observed with the EPOH content from 70 to 80 wt.% for both copolymers.

Table 4.3 Scratch hardness of the photopolymerized copolymer coatings.

	EPOH content (wt.%)										
	0	10	20	30	40	50	60	70	80	90	100
Copolymers	Scratch Hardness										
EEC-EPOH20	4H	4H	4H	5H	5H	5H	5H	5-6H	5-6H	5H	5H
EEC-EPOH30	4H	4H	4H	4H	4-5H	5H	5H	6H	6H	5-6H	5-6H

Gloss Property of Photopolymerized Coatings

One of the advantages related to the cycloaliphatic diepoxide is excellent exterior gloss property of final cured coatings which is desirable for automotive coatings and printing applications. In this study, all copolymerization systems including the EEC-EPOH20 and EEC-EPOH30 produced visually smooth and transparent surfaces. To more precisely confirm whether the binary mixture compositions and oligomer structure affect the glossiness, gloss measurements were performed for the photopolymerized EEC-EPOH copolymer coatings of 45 (±) um thickness as compared to the EEC and EPOH homopolymers. Gloss readings were recorded by measuring specular reflections of directly illuminated light at three different angle geometries (20º, 60º, and 85 º) from normal to each coating surface. Gloss measurements were performed parallel to the length of the coated panel first (Figure 4.9A) and then perpendicularly to its length (Figure 4.9B).

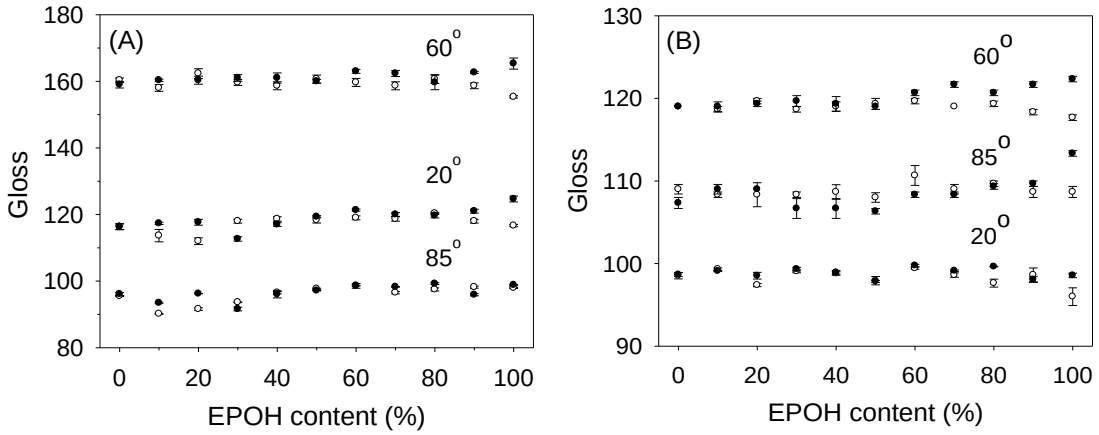

Figure 4.9 Optical properties of the photopolymerized coatings of EEC-EPOH20 (○) and EEC-EPOH30 (●) copolymers: gloss measurements were performed in a parallel direction (A) and perpendicular direction (B) to the length of the coated panel.

Figure 4.9 illustrates that gloss numbers depend on measurement angle geometry and measurement direction of the length of the coated panel. However, there was no signification deviation in the gloss numbers of all copolymer coatings from those of the pure EEC coating for three different angles and two different directions of the measurements. These results indicates that the binary mixture compositions and oligomer structure (internal epoxide content) have no direct impact on the glossiness of their final cured coatings for the given copolymer systems. In addition, further confirmation was performed by atomic force microscopy (data not shown). However, there was no significant difference in the surface topography and morphology of the final cured coatings regardless of binary mixture composition and oligomer structure.

Conclusions

The final cured cycloaliphatic diepoxide polymer exhibited brittle properties characterized by a high glass transition temperature and high Young's modulus. In addition, its fracture toughness and impact resistance were relatively low. This brittleness was modified by the photoinitiated cationic copolymerization with the epoxidized

elastomeric oligomers. The glass transition temperature (a location of δ_{max}) and Young's modulus of the final cured copolymers monotonically decreased with increasing the oligomer content. The ultimate tensile strength increased with increasing the oligomer content up to 30% and then decreased monotonically. The fracture toughness increased with increasing oligomer content from 10% to 90%. The highest fracture toughness and highest impact resistance were observed with the oligomer content of 70-80%. These enhanced properties were attributed to the multimodal network chain length distribution. The epoxidized oligomer containing relatively lower internal epoxide content exhibited much higher toughness and impact resistance.

Interestingly, the data trend obtained from the kinetic studies was consistent with physical properties when two sets of copolymers differed by oligomer structure (internal epoxide content) were compared (Chapters 3 vs. 4). In Chapter 3, results showed that in high amounts of the diepoxide above ~50wt.%, the initial polymerization rates of the epoxidized oligomers were essentially zero whereas the initial polymerization rates and ultimate conversion of the diepoxide were much higher than those of the oligomers. In this composition range, the ultimate conversions of the diepoxide were almost the same for the two separate copolymerization systems containing two respective oligomers that differed by the internal epoxide content. In the same way, Young's modulus, ultimate strength, elongation-at-break, fracture toughness, and impact resistance were also similar between the two copolymers in the similar composition range. With the diepoxide content lower than 50wt.%, the initial polymerization rates and ultimate conversion of the internal epoxides of the two different oligomers deviated from one another, and the ultimate conversions of the internal epoxides differed by 15% on average between the two oligomers. Similarly, noticeable differences between the two copolymers was observed in physical and mechanical properties, including glass transition temperature, storage/Young's modulus at room temperature, crosslink density, fracture toughness, impact resistance for the high EPOH content regime. The trends for the two different

composition regimes illustrated a clear link between the polymerization kinetic behavior and ultimate properties of the final cured copolymers.

Notes

1. Fouassier, J.P., *Photoinitiation, Photopolymerization, and Photocuring: Fundamentals and Applications* 1st ed. 1995, New York: Hanser.

2. Sipani, V. and Scranton, A.B., *Dark-Cure Studies of Cationic Photopolymerizations of Epoxides: Chracterization of the Active Center Lifetime and Kinetic Rate Constants.* Journal of Polymer Science: Part A: Polymer Chemistry, 2003. 41: p. 2064-2072.

3. Sipani, V. and Scranton, A.B., *Kinetic studies of cationic photopolymerizations of Phenyl glycidyl ether: termination/trapping rate constants for iodonium photoinitiators.* Journal of Photochemistry and Photobiology A: Chemistry 2003. 159: p. 189-195.

4. Vishal Sipani, A.K., and Alec B. Scranton, *Dark Cure Studies of Cationic Photopolymerizations of Epoxides: Characterization of Kinetic Rate Constants at High Conversions.* Journal of Polymer Science: Part A: Polymer Chemistry, 2004. 42: p. 4409-4416.

5. Ficek, B.A., Thiesen, A. M., and Scranton, A. B., *Cationic photopolymerizations of thick polymer systems: Active center lifetime and mobility*. European Polymer Journal, 2008. 44(1): p. 98-105.

6. Petrie, E.M., *Epoxy Adhesive Formulations*. First ed. 2006, New York: McGrow-Hill.

7. Packham, D.E., *Handbook of Adhesion*. Second ed. 2005, Chichester, England: John Wiley & Sons Ltd.

8. Park, J.B. and Lakes, R.S., *Biomaterials: an introduction*. Second ed. 1992, NY: Plenum.

9. McGarry, F.J. and Rosner, R.B., *Epoxy-Rubber Interactions,* in *Toughened Plastics I*. 1993, American Chemical Society. p. 305-315.

10. Mülhaupt, R. and Buchholz, U., *Compatibilized, Segmented Liquid Rubbers as Epoxy-Toughening Agents*, in *Toughened Plastics II*. 1996, American Chemical Society. p. 75-94.

11. Russell, B. and Chartoff, R., *The influence of cure conditions on the morphology and phase distribution in a rubber-modified epoxy resin using scanning electron microscopy and atomic force microscopy*. Polymer, 2005. 46(3): p. 785-798.

12. Hong, S.-G. and Chan, C.-K., *The curing behaviors of the epoxy/dicyanamide system modified with epoxidized natural rubber.* Thermochimica Acta, 2004. 417(1): p. 99-106.

13. Decker, C., Xuan, H.L., and Viet, T.N.T., *Photocrosslinking of functionalized rubber. III. Polymerization of multifunctional monomers in epoxidized liquid natural rubber.* Journal of Polymer Science Part A: Polymer Chemistry, 1996. 34(9): p. 1771-1781.

14. Bussi, P. and Ishida, H., *Partially miscible blends of epoxy resin and epoxidized rubber: Structural characterization of the epoxidized rubber and mechanical properties of the blends.* Journal of Applied Polymer Science, 1994. 53(4): p. 441-454.

15. Bussi, P. and Ishida, H., *Dynamic mechanical properties of epoxy resin/epoxidized rubber blends: Effect of phase separated rubber.* Journal of Polymer Science Part B: Polymer Physics, 1994. 32(4): p. 647-657.

16. Miyagawa, H., Mohanty, A.K., Misra, M., and Drzal, L.T., *Thermo-Physical and Impact Properties of Epoxy Containing Epoxidized Linseed Oil, 1.* Macromolecular Materials and Engineering, 2004. 289(7): p. 629-635.

17. Miyagawa, H., Mohanty, A.K., Misra, M., and Drzal, L.T., *Thermo-Physical and Impact Properties of Epoxy Containing Epoxidized Linseed Oil, 2.* Macromolecular Materials and Engineering, 2004. 289(7): p. 636-641.

18. Zhengang, Z., Mark, D. Soucek, Yubiao, Liu, Jun, Hu, *Cationic photopolymerization of epoxynorbornane linseed oils: The effect of diluents.* Journal of Polymer Science Part A: Polymer Chemistry, 2003. 41(21): p. 3440-3456.

19. Decker, D., Nguyen, T, Viet, T, and Thi, HP, *Photoinitiated cationic polymerization of epoxides.* Polymer International, 2001. 50: p. 986-997.

20. Kishi, H., Shi, Y.-B., Huang, J., and Yee, A.F., *Shear ductility and toughenability study of highly cross-linked epoxy/polyethersulphone.* Journal of Materials Science, 1997. 32, (3): p. 761-771.

21. Hazot, P., Pichot, C., and Maazouz, A., *Synthesis of hairy acrylic core-shell particles as toughening agents for epoxy networks.* Macromolecular Chemistry and Physics, 2000. 201(6): p. 632-641.

22. Blaiszik, B.J., Sottos, N.R., and White, S.R., *Nanocapsules for self-healing materials.* Composites Science and Technology, 2008. 68(3-4): p. 978-986.

23. Riew, C.K. and Kinloch, A.J., *Toughened Plastics I*. Advances in Chemistry. Vol. 233. 1993, Washington DC: American Chemical Society.

24. Riew, C.K. and Kinloch, A.J., *Toughened Plastics II*. Advances in Chemistry. Vol. 252. 1996, Washington DC: American Chemical Society.

25. Hartwig, A., Koschek, K., Lühring, A., and Schorsch, O., *Cationic polymerization of a cycloaliphatic diepoxide with latent initiators in the presence of structurally different diols.* Polymer, 2003. 44(10): p. 2853-2858.

26. Oxman, J.D., Jacobs, D.W., Trom, M.C., Sipani, V., Ficek, B., and Scranton, A.B., *Evaluation of Initiator systems for controlled and sequentially curable Free-Radical/Cationic Hybrid Photopolymerizations.* Journal of Polymer Science: Part A: Polymer Chemistry, 2004. 43: p. 1747-1756.

27. Sasaki, H., *Curing properties of cycloaliphatic epoxy derivatives.* Progress in Organic Coatings, 2007. 58(2-3): p. 227-230.

28. Crivello, J.V. and Varlemann, U., *Mechanistic study of the reactivity of 3,4-epoxycyclohexylmethyl 3′,4′-epoxycyclohexancarboxylate in photoinitiated cationic polymerizations.* Journal of Polymer Science Part A: Polymer Chemistry, 1995. 33(14): p. 2473-2486.

29. Kar, S. and Banthia, A.K., *Epoxy Resin Modified with Epoxidized Soybean Rubber.* Materials and Manufacturing Processes, 2004. 19(3): p. 459 - 474.

30. Nakayama, K., *Dynamic Mechanical Analysis*, in *Polymer Characterization Techniques and Their Application to Blends*, G.P. Simon, Editor. 2003, Oxford University Press: New York. p. 68-95.

31. Andjelkovic, D.D., Valverde, M., Henna, P., Li, F., and Larock, R.C., *Novel thermosets prepared by cationic copolymerization of various vegetable oils--synthesis and their structure-property relationships.* Polymer, 2005. 46(23): p. 9674-9685.

32. Ishida, H. and Allen, D.J., *Mechanical characterization of copolymers based on benzoxazine and epoxy.* Polymer, 1996. 37(20): p. 4487-4495.

33. Kelley, F.N. and Bueche, F., *Viscosity and glass temperature relations for polymer-diluent systems.* Journal of Polymer Science, 1961. 50(154): p. 549-556.

34. Lu, X. and Weiss, R.A., *Relationship between the glass transition temperature and the interaction parameter of miscible binary polymer blends.* Macromolecules, 1992. 25(12): p. 3242-3246.

35. Biedron, T., Kubisa, Przemyslaw, and Penczek, Stanislaw, *Polyepichlorohydrin diols free of cyclics: Synthesis and characterization.* Journal of Polymer Science Part A: Polymer Chemistry, 1991. 29(5): p. 619-628.

36. Biedron, T., Szymanski, R., Kubisa, P., and Penczek, S., Makromol. Chem., Macromol. Symp., 1990. 32: p. 155.

37. Erman, B. and Mark, J.E., *Calculations on Trimodal Elastomeric Networks. Effects of Chain Length and Composition on Ultimate Properties.* Macromolecules, 1998. 31(9): p. 3099-3103.

38. Mark, J.E. and Erman, B., *Rubberlike Elasticity: A Molecular Primer*. Second ed. 2007, New York: Cambridge University Press. 270.

CHAPTER 5
URETHANE ACRYLATE/EPOXIDE HYBRID PHOTOPOLYMERIZATIONS: UNDERSTANDING THE INTERPLAY BETWEEN VISCOSITY AND DUAL PHOTOINITIATOR SYSTEM

Introduction

The unique attributes of photopolymerizations have led to its adoption within the fields of coatings, optoelectronics, adhesives, stereolithography, composites, and biomaterials [1-4]. The innate advantages arise from the photoinitiation mechanism and the characteristics of initiating species, generated by photolysis. However, these reactive species are detrimentally affected by atmospheric conditions, such as oxygen and humidity. Molecular oxygen can quench the excited triplet state photoinitiator molecules and scavenge the initiator and polymer radicals due to the di-radical characteristics of the triplet state oxygen ($^3O_2$) and the activation to singlet state oxygen ($^1O_2$) by electron transfer with excited photoinitiators/sensitizers [5-7]. As a result, free-radical photopolymerization is inhibited and delayed until the concentration of dissolved oxygen in the polymerization system is reduced to a certain degree [8, 9]. In addition, continued diffusion of oxygen into curing systems stunts polymer chain growth at the air/coating interface, resulting in tacky coatings [10, 11]. Similarly, nucleophilic agents, such as water and alcohols, can negatively affect cationic photopolymerization since the basicity of those agents can inhibit, retard, or induce chain-transfer reactions with cationic active species [12-14]. Because water with its hydroxyl group has a high basicity, the participation of water in the propagation reactions of cationic photopolymerizations becomes problematic if the relative humidity is not controlled. Once the internal concentration of water increases over a certain threshold, the majority of propagating cationic active centers starts competing with water [15, 16], resulting in termination of growing polymer chains and the deterioration of the end-product performance.

Several approaches have been developed to address these problems with atmospheric factors. In the case of free-radical photopolymerization systems, expensive inerting equipment, waxes, or shielding films can be used to prevent oxygen from diffusing into the system. Higher concentration of initiator or high intensity irradiation sources can be used to produce a larger number of radicals to consume the dissolved oxygen faster and allow the polymer chains to grow. Other chemical species can be added to the photopolymerization system, such as amines to capture the oxygen, thiols to transform the normally inactive peroxy radical into a propagating active center, and a combination of singlet oxygen generator and trapper to consume dissolved oxygen[17]. For cationic photopolymerization systems, highly hydrophobic compounds, such as epoxide monomers containing silicon or long hydrocarbon chains, can prevent the diffusion of water from environments with high moisture content [18]. Another promising approach is the development of hybrid photopolymerization systems, which combine both free-radical and cationic mechanisms. In these hybrid systems, improved conversion and polymer properties can be realized since the radical species are not sensitive to nucleophilic agents and the cationic active species are not scavenged by triplet/singlet-state oxygen [19, 20].

Free-radical and cationic hybrid photopolymerization systems have been reported by mixing acrylate with epoxide or vinyl ether monomers and by synthesizing monomers with both epoxide and vinyl ether moieties [10, 14, 19]. The kinetic synergy has been demonstrated between these two distinguishable polymerization mechanisms for acrylate/epoxide hybrid systems using real-time infrared [19] and Raman [10] spectroscopies. In these systems, the formation of epoxide polymer domains at the coating surface prevented further diffusion of atmospheric oxygen into the sample. In addition, physical and mechanical properties of hybrid polymers can be tuned, not only by composition of acrylate and epoxide mixtures, but also by production of interpenetrating networks (IPNs) based on monomer functionality [21]. The development

of IPNs is significantly affected by the kinetics of the two independent reactions, such as the rate of polymerization, final conversion, and kinetic sequences. Thus, the degree of entanglement of two different polymer domains varies at micro/nano-scale during phase separation [21, 22], and the interaction of the two domains, (i.e., non-covalent bonding interaction) will have a direct effect on the ultimate performance of the polymer products.

Hybrid systems based on cycloaliphatic epoxides and urethane acrylate oligomers may further mitigate atmospheric sensitivity of the photopolymerizations and enable improved tunability of polymer properties. The high viscosity and hydrophobicity of selected urethane acrylate oligomers will hinder the diffusion of oxygen and water into the photopolymerization system, respectively. The introduction of low molecular weight epoxide monomers will improve the processibility of the formulations at room temperature. In addition, the elastic property of the urethane acrylate polymers will counteract the brittle nature of the epoxide polymers, improving fracture toughness and impact resistance of the final hybrid polymers. In this study, the conversion profiles of hybrid systems containing urethane acrylate oligomers and cycloaliphatic epoxides demonstrate the effects of viscosity and relative photoinitator concentration on the kinetics of the simultaneous free-radical and cationic reactions. A better understanding of these effects will ultimately facilitate optimization of formulations and reaction conditions for thin film and coating applications.

Experimental

Materials

High-viscosity (A-14-H, tradename CN964) and low-viscosity (A-25-L, tradename CN965) ester-type branched aliphatic urethane acrylate oligomers were supplied by Sartomer for the free-radical photopolymerization. Mono-functional (CHO) and di-functional (EEC) cycloaliphatic epoxides were donated from Sigma Aldrich for the cationic copolymerization. The α-cleavable free-radical photoinitiator 2,2-dimethoxy-

2-phenyl-acetophenone (DMPA, Aldrich) and the cationic photoinitiator diaryliodonium hexafluoroantimonate (IHA, Sartomer) were used to initiate the reaction of C=C double bonds and epoxide rings, respectively. All materials were used as received and are shown in Table 5.1.

Table 5.1 Structure and selected physical properties of monomers, oligomeric elastomers, and photoinitiators used for this study.

Materials	Acronyms (g/mole)	*f*	Viscosity [Poise]	Structure
Aliphatic urethane acrylate oligomers	A-14-H (1378)	2	17,675 @60℃	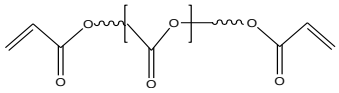
	A-25-L (2522)	2	9,975 @60℃	(branched ester)
Cyclo-aliphatic epoxides	CHO (98.14)	1	0.02 @ 25°C	
	EEC (252.31)	2	350 @ 25°C	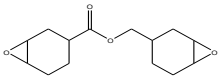
Photo-initiators	DMPA	NA	NA	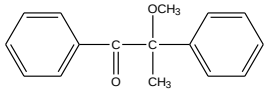
	IHA	NA	NA	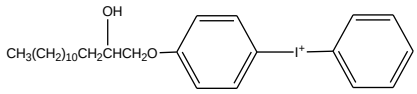 SbF_6^-

Epoxide/acrylate hybrid mixtures with the dual photoinitiator (PI) system were formulated as shown in Table 2. Epoxides and acrylates are mixed thoroughly by volume fraction. The concentration of each PI was maintained at 8 mM for the corresponding reaction systems. Hence, the relative concentration of individual PIs is inversely proportional to the fraction of the respective acrylates and epoxides (Table 2). The

photoinitiator powders were completely mixed with individual acrylates, epoxides, or their hybrid mixtures until the formulated liquids were transparent.

Table 5.2 Formulations of epoxide/acrylate hybrid mixtures with dual photoinitiator system.

Urethane acrylates (vol%)	Epoxides (vol%)	Initial viscosity	$[PI]_{each}$ = 8 mM for total volume	
			Relative concentration of each photoinitiator† (wt%)	
			DMPA	IHA
0	100	Lowest	0	0.50-0.61
25	75	Low	0.74	0.67-0.81
50	50	Intermediate	0.37	1.01-1.22
75	25	High	0.24	2.03-2.45
100	0	Highest	0.18	0

†Relative concentration of each PI was calculated by weight for the partial portion of the corresponding acrylate oligomers and epoxides.

Characterization of Kinetics of Hybrid Photopolymerizations

Real-time Raman spectra were collected using a holographic fiber-coupled stretch probehead (Mark II, Kaiser Optical Systems, Inc.) attached to a modular research Raman spectrograph (HoloLab 5000R, Kaiser Optical Systems, Inc.). A 10x non-contact sampling objective with 0.8-cm working distance was used to deliver ~200 mW 785 nm near-infrared laser intensity to the sample, thereby inducing the Raman scattering effect. The exposure time for each spectrum was 300 ms, and the time interval between data points was 4-5 s. Samples were illuminated for 30 min at 25°C in sealed 1 mm ID quartz capillary tubes using a 100 W high-pressure mercury lamp (Acticure® Ultraviolet/Visible

Spot Cure System, EXFO Photonic Solutions, Inc.). The full-spectrum light intensity of the system was set to 200 mW/cm^2 as measured by a radiometer having a wavelength range of 250-450 nm (R5000, EFOS).

The Raman spectrum of each acrylate and epoxide was acquired first to identify bands in the fingerprint region that could be used to calculate conversion (see Figure 5.1). The reactive band representing the acrylate C=C double bond is located at 1638 cm-1 and is associated with the C=C stretching vibrations; the reactive band representing the epoxide ring is located at 789 cm-1 and is associated with the asymmetric epoxide ring deformation. An internal reference band was selected at 605 cm-1, which represents the skeletal bending of the non-reactive acrylate carbonyl group.

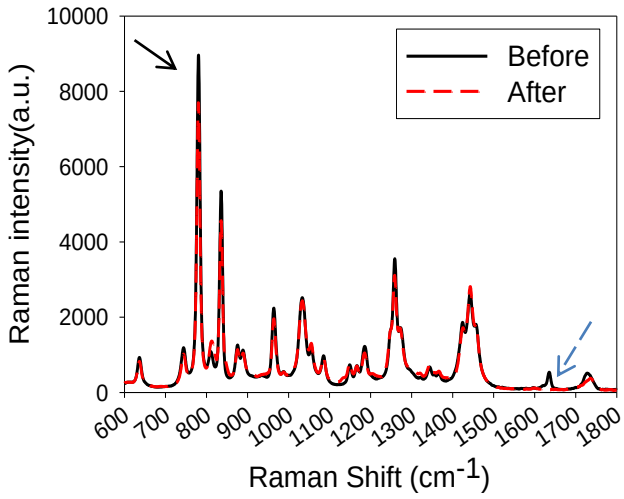

Figure 5.1 Comparison of the Raman spectra for an epoxide/acrylate hybrid mixture system before and after photopolymerization. The reactive band representing the acrylate C=C double bond is located at 1638 cm^{-1} (dot arrow); the reactive band representing the epoxide ring is located at 789 cm^{-1} (solid arrow).

The peak areas under each band were integrated and used to calculate the concentration of related functional groups. Since the spectral baselines and the reference

band intensity remained constant in these real-time reaction studies, the conversion of each functional group was calculated by ratioing the peak area of the reactive band at any given time [$A_{rxn}(t)$] to the peak area of the reactive band prior to illumination [$A_{rxn}(0)$]:

$$\text{Conversion, } \alpha = 1 - \frac{A_{rxn}(t)}{A_{rxn}(0)} \qquad (eq.\ 5.1)$$

The instantaneous rate of polymerization (R_p) was calculated by differentiating the degree of cure (α) with respect to time:

$$R_P = -\frac{d[M]_t}{dt} = -\frac{d}{dt}[M]_0(1-\alpha) = [M]_0\frac{d\alpha}{dt} \qquad (eq 5.2)$$

The normalized instantaneous rate of polymerization was determined by dividing R_p by the initial monomer concentration, $[M]_o$:

$$R_{p,norm} = R_P/[M]_0 = \frac{d\alpha}{dt} \qquad (eq\ 5.3)$$

Results and Discussion

Effect of Viscosity on Kinetics of Hybrid Photopolymerization

Free-radical Photopolymerizations of Urethane Acrylates

First, urethane acrylates, A-14-H and A-25-L, with only the free-radical photoinitiator DMPA present were studied using Raman spectroscopy to show the effect of viscosity on the free-radical photopolymerizations. The two urethane acrylate oligomers are similar in unit structure, but differ in molecular weight and viscosity. The molecular structure of A-14-H was assumed much less branched than A-25-L to have such high viscosity, since in general the viscosity of (pre)polymers rapidly increases beyond the critical molecular weight where the entanglement of the (pre)polymer chains begins to occur.

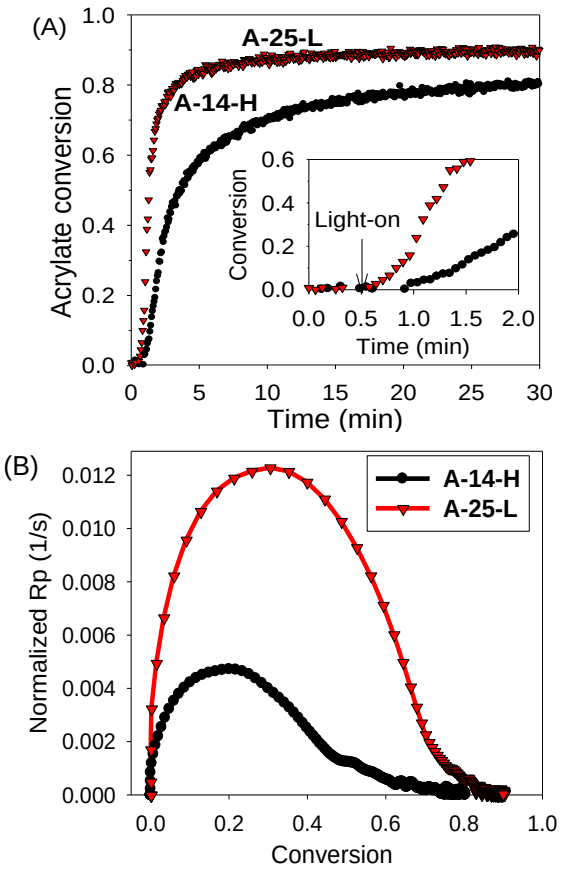

Figure 5.2 Effect of viscosity on the free-radical polymerization of urethane acrylates photopolymerized with 8 mM DMPA at room temperature. (A) real-time conversion profiles (with the induction period highlighted in the inset) and (B) normalized rate of polymerization as a function of conversion for the high-viscosity (A-14-H) and low-viscosity (A-25-L) oligomers.

In Figure 5.2, the final conversion and the normalized rate of polymerization ($R_{p,norm}$) are much lower for the high-viscosity acrylate (A-14-H). Since polymerization is more diffusion-controlled in highly viscous environments by slowing the diffusion of radical species and monomers toward each other during photopolymerization, the maximum $R_{p,norm}$ for A-14-H appeared at much lower conversions relative to the low-viscosity acrylate (A-25-L) system. In addition, the induction period of A-14-H was longer than that for A-25-L. (The diffusion of oxygen from the atmosphere was considered to be negligible during photopolymerization, since the acrylate samples were

cured in sealed tubes.) Since the induction time is proportional to the concentration of dissolved oxygen [23], A-14-H contained more dissolved oxygen than A-25-L (given that all experimental conditions, including concentration of DMPA, were kept constant). However, it was expected that the oxygen concentration would be greater in the low-viscosity acrylate, A-25-L. This difference may be explained by oxygen solubility considerations. Oxygen solubility tends to decrease with increasing number of carbon atoms of organic compounds due to the high energy required for the formation of cavities into which oxygen molecules are transferred when they are dissolved [24, 25]. Also, the additional presence of ether linkage tends to further decrease oxygen solubility in acrylate monomers [9]. Thus, the concentration of the dissolved oxygen may be lower for A-25-L because it has a longer hydrocarbon backbone and additional ether linkages, compared to A-14-H.

Cationic Photopolymerizations of Cycloaliphatic Epoxides

Secondly, cycloaliphatic epoxides, CHO and EEC, with only the cationic photoinitiator IHA present were studied using Raman spectroscopy to show the effect of epoxide structure on the cationic photopolymerizations. Although most cyclic ethers containing ester carbonyl exhibit relatively slow kinetic behaviors compared to free-radically polymerizable monomers [26, 27], the mono-functional cycloaliphatic epoxide (CHO) underwent a very fast cationic ring-opening photopolymerization (see Figure 5.3), exhibiting no induction period and reaching ~70% conversion in 30 s. The rate of polymerization for CHO, a Class-I cyclic ether monomer, is enhanced due to the extremely large distortion of the bond angle ascribed to the highly strained oxirane ring structure incorporated on an additional cyclic structure [28, 29]. However, the di-functional cycloaliphatic epoxide (EEC) underwent a very slow cationic ring-opening photopolymerization (see Figure 5.3), exhibiting a long induction period and reaching ~14% conversion after 30 min. The kinetic behavior of EEC is attributed to the

intramolecular interruption of growing active centers during propagation through nucleophilic attack by the ester groups in EEC [30].

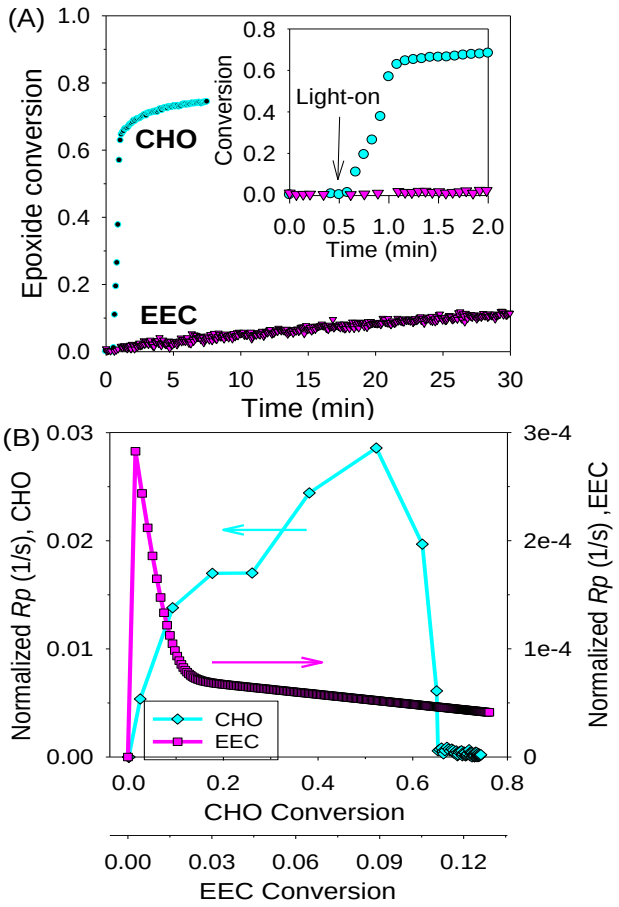

Figure 5.3 Effect of epoxide structure on the cationic polymerization of cycloaliphatic epoxides photopolymerizated with 8 mM IHA at room temperature. (A) Real-time conversion profiles (with the induction period highilighted in the inset) and (B) normalized rate of polymerization as a function of conversion for the mono-functional (CHO) and di-functional (EEC) epoxides.

Although the normalized rate of polymerization for EEC dropped due to the delay of propagation caused by the interruption of the EEC ester group (see Figure 5.3B), the propagating active centers of EEC continued to grow at long times, as by its non-zero $R_{p,norm}$ at 30 min.

Hybrid Photopolymerizations of Acrylate/CHO Mixture Systems

The simultaneous reactions of C=C double bonds and epoxide rings in hybrid systems were successfully monitored and discretely analyzed using real-time Raman spectroscopy. The viscosity of the hybrid mixtures was qualitatively increased by increasing the concentration of urethane acrylate oligomer relative to the concentration of epoxide. For the dual photoinitiator (PI) system, the absolute concentration of PI remained constant at 8 mM; however, the relative concentration of DMPA and IHA was varied according to the acrylate:epoxide (see Table 2).

Conversion profiles for the two acrylates (A-14-H and A-25-L) individually mixed with CHO by volume in various compositions are shown in Figure 5.4. In the presence of CHO, the rate of polymerization and the final conversion were greater for both acrylates, compared to the corresponding acrylate-only systems. Although there were some variations in the polymerization rate depending on the composition of epoxide/acrylate mixtures, both CHO/acrylate systems obtained ~90% conversion in 3 min and were almost completely polymerized by 30 min. The enhanced kinetic behaviors of A-14-H and A-25-L are most likely due to the diluent effect of CHO: as the initial viscosity of the polymerization systems is decreased, to a large extent, the acrylate kinetics becomes less diffusion-controlled in comparison with acrylate-only systems [31]. The free-radical polymerization rate considerably increased in A-14-H/CHO hybrid systems as the feed fraction of CHO increased (Figure 5.4A), although this trend was also true to a lesser extent for A-25-L/CHO systems (Figure 5.4B). However, free-radical photopolymerizations tended to proceed somewhat slower for the 25:75 acrylate:CHO ratio, although its final conversions at 30 min were similar to those of other ratios. In Similarly, the induction period decreased as the volume portion of CHO increased, except for the 25:75 acrylate:CHO ratio. These phenomena with the 25:75 acrylate:CHO ratio of may be due to solubility issues with PI and/or oxygen, although further study is needed to confirm a satisfactory explanation.

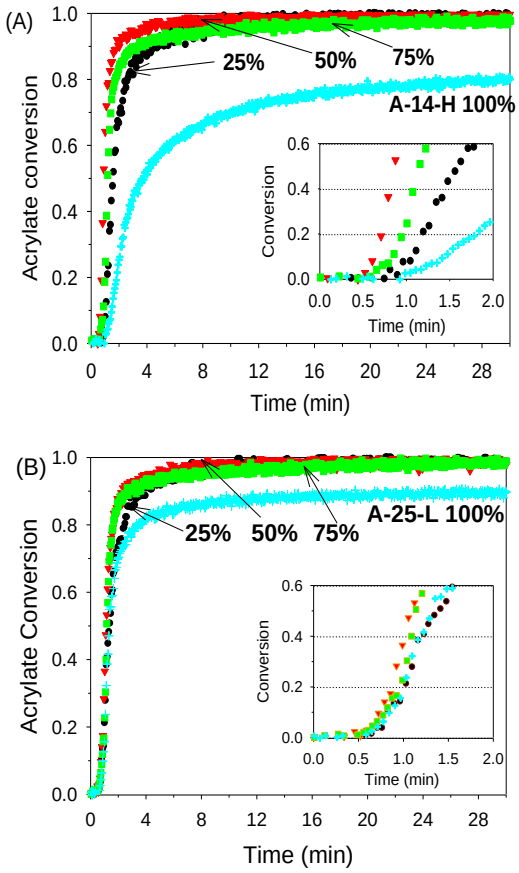

Figure 5.4 Effect of viscosity on the free-radical polymerization of CHO/urethane acrylate hybrid systems photopolymerized with 8 mM dual PI system at room temperature. Real-time C=C conversion profiles (with the induction period highlighted in the inset) of hybrid systems with varying amounts of A-14-H (A) and A-25-L (B): 25, 50, 75 and 100% urethane acrylate. Viscosity increases with increasing acrylate content.

In contrast to the enhanced kinetics of free-radical photopolymerizations in the presence of CHO, the epoxide cationic photopolymerizations were substantially suppressed by the presence of the urethane acrylate oligomers. Conversion profiles of the mono-functional CHO in the hybrid mixture systems are shown in Figure 5.5. Compared to the CHO-only system, the polymerization rate and the final conversion of CHO decreased during hybrid photopolymerization with increasing acrylate concentration in

the hybrid mixture system. This depressed kinetic behavior was more pronounced in the hybrid systems containing the high-viscosity A-14-H.

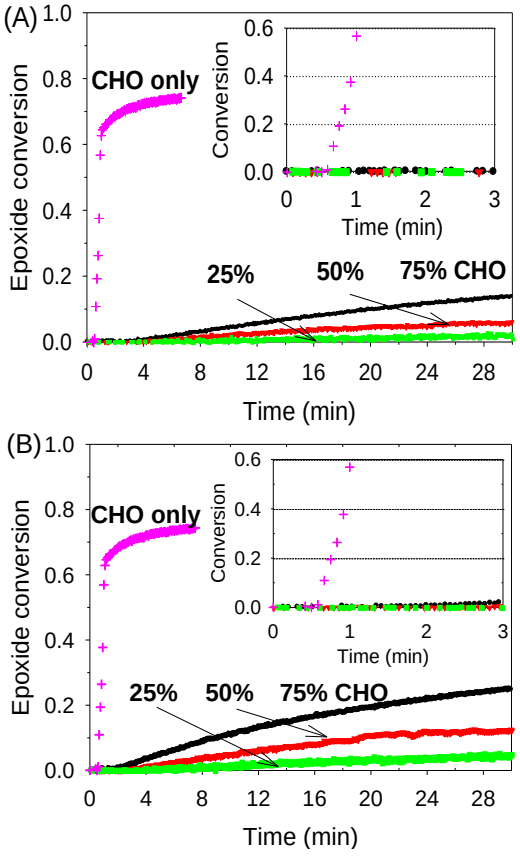

Figure 5.5 Effect of viscosity on the cationic polymerization of CHO/urethane acrylate hybrid systems photopolymerized with 8 mM dual PI system at room temperature. Real-time epoxide ring conversion profiles (with the induction period highlighted in the inset) of hybrid systems with varying amounts of A-14-H (A) and A-25-L (B): 25, 50, 75, and 100% CHO. Viscosity decreases with increasing epoxide content.

Furthermore, the duration of the induction period was proportional to the amount of acrylate, with longer periods observed for A-14-H systems. These pronounced induction periods and slow kinetic behaviors were a direct consequence of the initial viscosity of the formulation, as well as the gelation of the acrylate polymer network,

resulting in diffusion-controlled termination of cationic active centers [32, 33]. (The effect of water would be negligible since the relative humidity was below 30% for all experiments and the hydrophobicity of the urethane acrylate oligomers and sealed reaction tubes would prevent further diffusion of moisture from the atmosphere.), Since the viscosity of the hybrid systems was quickly further increased by the rapid formation of acrylate polymer networks due to the diluent effect of CHO, the diffusion of CHO monomers and cationic active species would be immensely limited by the acrylate gelation occurring in less than 2 min (corresponding to conversions > 60%).

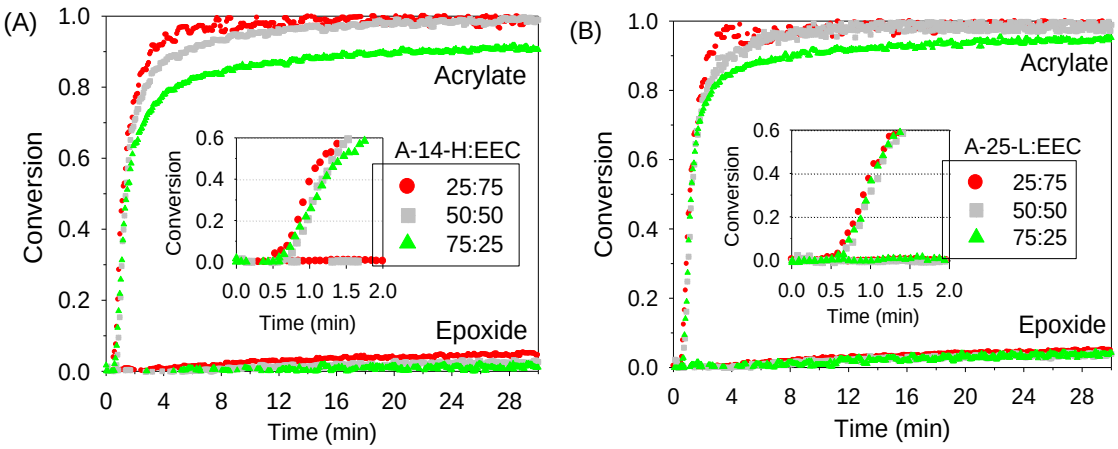

Figure 5.6 Effect of viscosity on the free-radical and cationic polymerizations of EEC/urethane acrylate hybrid systems photopolymerized with 8 mM dual PI system at room temperature. Real-time C=C (top) and epoxide ring (bottom) conversion profiles (with the induction period highlighted in the inset) of hybrid systems with varying amounts of A-14-H (A) and A-25-L (B): 25, 50, and 75%. Viscosity increases with increasing acrylate content.

Hybrid Photopolymerization of Acrylate/EEC Mixture Systems After Degassing

The hybrid photopolymerization of the di-functional EEC with the urethane acrylate oligomers behaved similarly to the CHO/acrylate hybrid systems. Again, the

EEC cationic photopolymerizations were suppressed by the increasing viscosity of the polymerization system due to the presence of highly viscous acrylates and the rapid formation of acrylate polymer domains during photopolymerization (see Figure 5.6).

However, when the hybrid mixture samples were degassed in a vacuum oven prior to photopolymerization, the onset of free-radical photopolymerizations for both A-14-H and A-25-L fell onto a similar time scale without the introduction of considerable induction periods (see Figure 5. 6 insets). For the 75:25 acrylate:EEC ratio, the final C=C conversions were lower than those for acrylate/CHO mixtures. Since the viscosity of EEC is 20 times higher than CHO at room temperature, the diluent effect of EEC was diminished at this low EEC concentration.

Effect of Photoinitiators on Hybrid Photopolymerizations

Cationic Photoinitiator (IHA)

In order to decouple the effect of the rapidly-forming acrylate network on the suppression of cationic ring-opening polymerization, only the cationic PI (IHA) was added to the acrylate/epoxide hybrid mixtures. Cationic ring-opening polymerizations of highly reactive CHO showed viscosity-dependent kinetic behaviors that were obviously suppressed by the presence of highly viscous urethane acrylate oligomers even in the absence of the free-radical PI (DMPA) as shown in Figure 5.7(A,B). The suppression of CHO polymerization was proportional to the increase of the initial viscosity with increasing acrylate content. The effect was more pronounced with the high-viscosity A-14-H.

Although no free-radical PI was present, acrylate polymerization did occur due to the production of propagating radicals as a by-product of the cationic PI photolysis (see Figure 5.7C,D). [14, 34] The free-radical polymerizations were delayed until the concentration of dissolved oxygen was sufficiently reduced through quenching reactions

with the excited triplet-state PI and scavenging radical species. The induction periods of the free-radical and cationic polymerizations both increased with increasing viscosity (i.e., increasing acrylate content). Even though the cationic polymerization was not hindered at early times by the free-radical polymerization, the diffusion-controlled propagation of the active centers was affected by the high viscosity due to greater acrylate concentration.

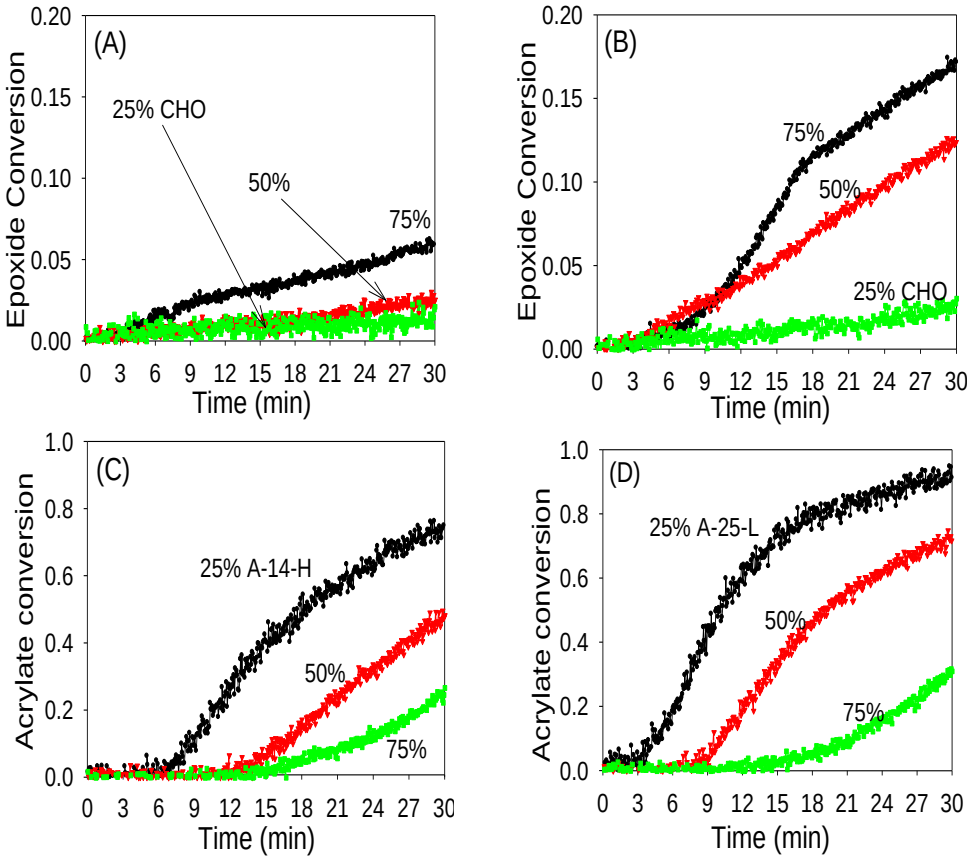

Figure 5.7 Effect of cationic photoinitiator concentration on the cationic and free-radical polymerizations of CHO/urethane acrylate hybrid systems photopolymerized with 8 mM IHA under full illumination at room temperature. Real-time conversion profiles of hybrid systems with varying epoxide:acrylate ratios: (A) CHO epoxide ring in A-14-H, (B) CHO epoxide ring in A-25-L, (C) A-14-H C=C in CHO, and (D) A-25-L C=C in CHO.CHO conversion profiles in the presence of A-14-H and A-25-L, respectively (A), (B) and acrylate conversion profiles of A-14-H (C) and A-25-L (D) in the presence of CHO in the hybrid systems with different compositions.

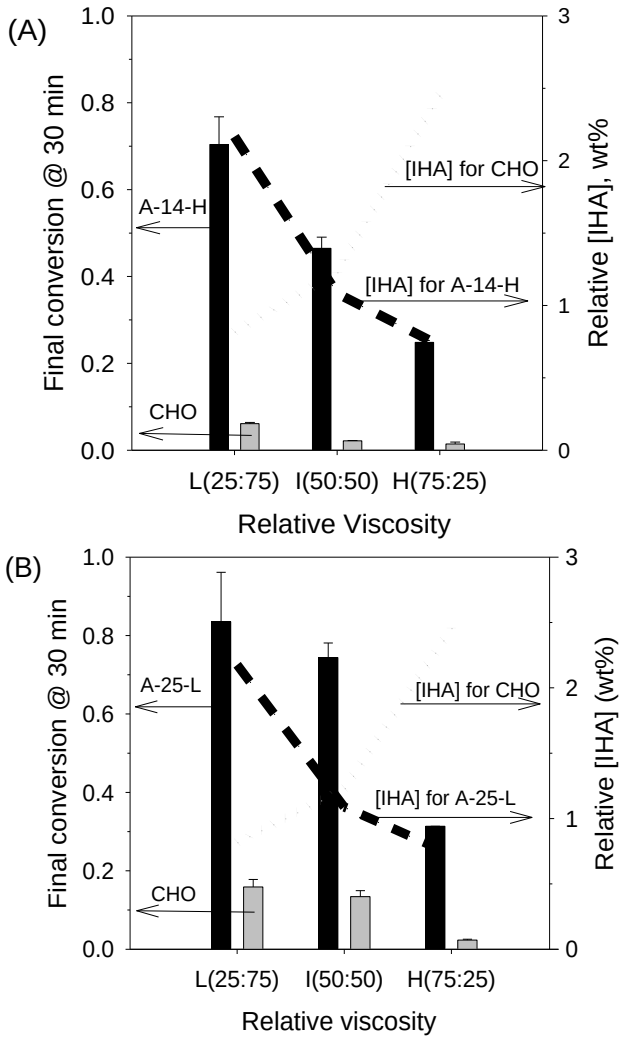

Figure 5.8 Effect of the relative cationic photoinitiator concentration on the final conversions of C=C and epoxide rings in CHO/urethane acrylate hybrid systems photopolymerized with 8 mM IHA at room temperature: (A) A-14-H:CHO and (B) A-25-L:CHO. Viscosity increases with increasing acrylate content (L (low), I (intermediate), and H (high)).

The concentration of IHA relative to the corresponding concentrations of acrylate and epoxide was calculated and plotted as a function of the compositions of the hybrid mixture systems, as well as the final conversion of epoxide and acrylates for the hybrid mixtures (see Figure 5.8). Increasing the concentration of IHA relative to the acrylate concentration resulted in increased final acrylate conversion. However, even though the

concentration of IHA relative to the epoxide concentration was low, the increased final CHO conversion further demonstrates the viscosity sensitivity of the cationic polymerization. In addition to the diluent effect of the acrylates, higher concentrations of IHA result in shorter free-radical induction periods since the dissolved oxygen is more rapidly consumed. Thus, high IHA concentrations are not effective in increasing epoxide conversions in hybrid systems, particularly those containing highly viscous acrylates. High IHA concentrations will enhance the free-radical photopolymerization, resulting in suppression of the viscosity-sensitive cationic ring-opening photopolymerization.

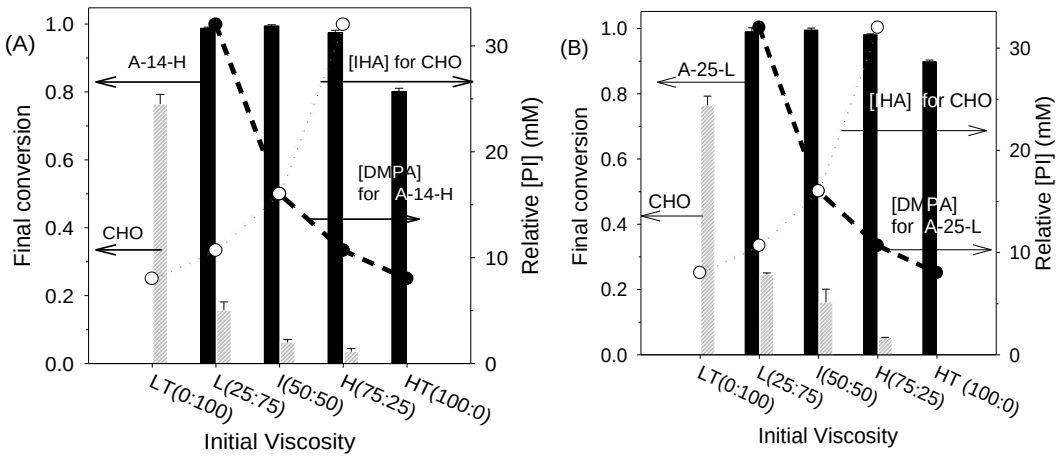

Figure 5.9 Effect of the relative photoinitiator concentrations on the final conversions of C=C and epoxide rings in CHO/urethane acrylate hybrid systems photopolymerized with 8 mM dual PI system at room temperature: (A) A-14-H:CHO and (B) A-25-L:CHO. Viscosity increases with increasing acrylate content (LT (lowest), L (low), I (intermediate), H (high), and HT (highest)).

Dual Photoinitiator System

In contrast to the hybrid systems containing only the cationic (IHA) photoinitiator, the acrylate conversion in hybrid systems containing the dual PI system (i.e., both both

DMPA and IHA), was consistently above 80% and was less dependent on the acrylate:epoxide ratio (comparison of Figures 4 and 7C, D). Although the dual PI system supports both free-radical and cationic photopolymerizations, the free-radical photopolymerization is more favored since, even with low concentrations of DMPA relative to the acrylate concentration, propagating radical species are generated through IHA photolysis (Figure 5.9). Thus, acrylate conversions are less dependent on the arylate:epoxide ratio. In addition, the diluent effect provided by CHO aids the diffusion of these propagating free radicals to promote high acrylate conversions (see 75:25 acrylate: epoxide cases in Figure 5.9).

In contrast, although the relative IHA concentration was three times greater for the 75:25 acrylate:epoxide hybrid mixture than the 25:75 mixture, the epoxide conversion remained low (< 10%). Thus, the cationic photopolymerizations were greatly affected by the free-radical photopolymerizations with high IHA concentration, which is in agreement with the previous arguments. Although the dual PI system advanced the free-radical photopolymerization, there is evidence that the epoxide conversion is boosted through the possibility of free-radically promoted cationic photopolymerizations [35, 36] when DMPA is present (comparison of Figures 5.8 and 5.9). The photolysis of DMPA produces hydroxyl benzyl (strong electron donor) radicals, which can undergo electron-transfer reactions with cationic photoinitiators (electron acceptor) such as IHA. Thus, carbocations that react then with epoxide monomers via cationic polymerization are produced without the direct photolysis of IHA. However, the hydroxyl benzyl radicals, as electron donors, may be more easily scavenged by electrophilic singlet oxygen activated from the dissolved oxygen in the triplet state. This scavenging would interrupt the redox reaction needed to form the carbocation, and thus, oxygen inhibition would be much more complicated in the dual PI system. In this regard, it necessary to carefully study the effect of dual photoinitiator system on the kinetics of epoxide using acrylates with low molecular weight to exclude high initial viscosity.

Conclusions

The kinetics of hybrid photopolymerizations containing cycloaliphatic epoxides and urethane acrylates was greatly affected by formulation viscosity and relative photoinitiator concentration. Increasing the epoxide concentration in the formulation promoted the free-radical polymerization of the acrylate by the diluent effect. However, increasing the acrylate concentration in the formulation suppressed the cationic polymerization of the epoxide in two ways: with the increased viscosity of hybrid formulations and with the formation of an acrylate polymer network early in the illumination period. These two diffusion-limiting factors led to substantial trapping of cationic active centers and epoxide monomers in the developing acrylate domains. With the dual photoinitiator system containing IHA and DMPA is used, the free-radical reaction is further enhanced, even with low concentrations of DMPA, by the generation of additional free-radical active centers through the photolysis of IHA. Thus, increasing the IHA concentration relative to the epoxide concentration does not result in higher epoxide conversion, but rather increased acrylate conversion. Although the cationic polymerization can also be promoted through a redox reaction between IHA onium ions and benzyl hydroxyl radicals from the photolysis of DMPA, any benefits may be diminished by oxygen inhibition and the rapidly increasing viscosity in the presence of highly viscous urethane acrylates. Therefore, careful optimization of system viscosity and the dual photoinitiator system concentration is needed to balance the simultaneous polymerizations of acrylate and epoxide for the development of hybrid polymers with desired physical properties.

Notes

1. Fouassier, J.P., *Photoinitiation, Photopolymerization, and Photocuring: Fundamentals and Applications* 1st ed. 1995, New York: Hanser.

2. Allen, N.S., et al., *Currents Trends in Polymer Photochemistry*. 1st ed. 1995: Ellis Horwood.

3. A. Endruweit, M.S.J., A.C. Long, *Curing of Composite Components by Ultraviolet Radiation: A Review.* Polymer Composite, 2006. 27(2): p. 119-128.

4. Fisher, J.P., Dean, D., Engel, P. S., Mikos, A. G., *Photoinitiated polymerization of biomaterials.* Annual Review of Materials Science, 2001. 31: p. 171-181.

5. Lijing Gou, B.O., and Alec B. Scranton, *The effect of oxygen in free radical photopolymerization.* Recent Research Developments in Polymer Science 2004. 8: p. 125-141.

6. Christophersen, A.G., et al., *Photobleaching of astaxanthin and canthaxanthin: quantum-yields dependence of solvent, temperature, and wavelength of irradiation in relation to packageing and storage of carotenoid pigmented salmonoids.* Z Lebensm Unters Forsch, 1991. 192: p. 443-439.

7. Smith, G.J., *Enhanced Intersystem Crossing in the Oxygen Quenching of Aromatic Hydrocarbon Triplet States with High Energies.* Journal of the Chemical Society, Faraday Transactions, 1982. 2(78): p. 769-773.

8. Decker, C. and A.D. Jenkins, *Kinetic approach of oxygen inhibition in ultraviolet- and laser-induced polymerizations.* Macromolecules, 1985. 18(6): p. 1241-1244.

9. Lijing Gou, C.N.C.A.B.S., *Measurement of the dissolved oxygen concentration in acrylate monomers with a novel photochemical method.* Journal of Polymer Science Part A: Polymer Chemistry, 2004. 42(5): p. 1285-1292.

10. Cai, Y. and J.L.P. Jessop, *Decreased oxygen inhibtion in photopolymerized acrylate/epoxide hybrid polymer coatings as demonstrated by Raman Spectroscopy.* Polymer, 2006. 47: p. 6560-6566.

11. H. Cao, E.C., M. Tilley, and Y.C. Jean, *Oxygen inhibition effect on surface properties of UV-curable acrylate coatings.* ACS Symposium Series 847, 2003: p. 165-175.

12. Lin, Y. and J.W. Stansbury, *Near-Infrared Spectroscopy Investigation of Water Effects on the Cationic Photopolymerization of Vinyl Ether System.* Journal of Polymer Science: Part A: Polymer Chemistry, 2004. 42: p. 1985-1998.

13. Hartwig, A., B. Schneider, and A. Luhring, *Influence of moisture on the photochemically induced polymerisation of epoxy groups in different chemical environment.* Polymer, 2002. 43: p. 4243-4250.

14. Yan Lin, J.W.S., *The impact of water on photopolymerization kinetics of methacrylate/vinyl ether hybrid systems.* Polymers for Advanced Technologies, 2005. 16: p. 195-199.

15. Hartwig, A., et al., *(9-Oxo-9H-fluoren-2-yl)-phenyl-iodonium hexafluoroantimonate(V) - a photoinitiator for the cationic polymerisation of epoxides.* European Polymer Journal, 2001. 37(7): p. 1449-1455.

16. Hartwig, A., *Influence of Moisture present during polymerisation on the properties of a photocured epoxy resin.* International Journal of Adhesion & Adhesives 2002. 22: p. 409-414.

17. Decker, C., *Kinetics Study and New Applicatioins of UV Radiation Curing.* Macromolecular Chemistry and Physics, 2002. 23(18): p. 1067-1093.

18. Zhigang Chen, Y.Z.B.J.C.D.C.W., *A humidity blocker approach to overcoming the humidity interference with cationic photopolymerization.* Journal of Polymer Science Part A: Polymer Chemistry, 2008. 46(13): p. 4344-4351.

19. Decker, C., Nguyen Thi Viet, T., Decker, D., Weber-Koehl, E. , *UV-radiation curing of acrylate/epoxide systems.* Polymer, 2001. 42(13): p. 5531-5541.

20. Decker, C., *Light-induced crosslinking polymerization.* Polymer International, 2002. 51(11): p. 1141-1150.

21. L.H. Sperling, a.V.M., *The Current Status of Interpenetrating Polymer Networks.* Polymers for Advanced Technologies, 1996. 7: p. 197-208.

22. Suthar, B., et al., *A Review of Kinetic Studies of the Formation of Interpenetrating Polymer Networks.* Polymer for Advanced Technologies, 1996. 7: p. 221-233.

23. Tom Scherzer, H.L., *Temperature Dependence of the Oxygen Solubility in Acrylates and its Effect on the Induction Period in UV Photopolymerization.* Macromolecular Chemistry and Physics, 2005. 206(2): p. 240-245.

24. Eley, D.D., *On the solubility of gases. Part I.—The inert gases in water.* Trans. Faraday Soc., 1939. 35.

25. Golovanov, I. and S. Zhenodarova, *Quantitative Structure-Property Relationship: XXIII. Solubility of Oxygen in Organic Solvents.* Russian Journal of General Chemistry, 2005. 75(11): p. 1795-1797.

26. Goethals, E.J. and F. Du Prez, *Carbocationic polymerizations.* Progress in Polymer Science, 2007. 32(2): p. 220-246.

27. P. Sigwalt and M. Moreau, *Carbocationic polymerization: Mechanisms and kinetics of propagation reactions.* Progress in Polymer Science, 2006. 31(1): p. 44-120.

28. Crivello, J.V., *Cationic Photopolymerizationi of Alkyl Glycidyl Ethers.* Journal of Polymer Science: Part A: Polymer Chemistry, 2006. 44: p. 3036-3052.

29. Bulut, U., and Crivello, J. V. , *Investigation of the Reactivity of Epoxide Monomers in Photoinitiated Cationic Polymerization* Macromolecules, 2005. 38(9): p. 3584 -3595.

30. Crivello, J.V. and U. Varlemann, *Structure and reactivity relationship in the photoinitiated cationic polymerization of 3,4-epoxycyclohexylmethyl-3'-4'-epoxycyclohexane carboxylate.* ACS symposium series, 1997. 673: p. 82-94.

31. Dusek, K. and M. Dusková-Smrcková, *Network structure formation during crosslinking of organic coating systems.* Progress in Polymer Science, 2000. 25(9): p. 1215-1260.

32. Sipani, V. and A.B. Scranton, *Kinetic studies of cationic photopolymerizations of Phenyl glycidyl ether: termination/trapping rate constants for iodonium photoinitiators.* Journal of Photochemistry and Photobiology A: Chemistry 2003. 159: p. 189-195.

33. Young-Min Kim, L.K.K., John F. MacGregor, *Kinetic Studies of Cationic Photopolymerizations of Cycloaliphatic Epoxide, Triethyleneglycol Methyl Vinyl Ether, and Cyclohexene Oxide.* POLYMER ENGINEERING AND SCIENCE, 2005. 45: p. 1546-1555

34. Crivello, J.V., Ortiz, R. A. , *Design and synthesis of highly reactive photopolymerizable epoxy monomers.* Journal of Polymer Science Part A: Polymer Chemistry, 2001. 39(14): p. 2385-2395.

35. M. Degirmenci, Y.H., Y. Yagci, *One-step, one-pot Photoinitiation of Free Radical and Free Radical Promoted Cationic Polymerizations.* Journal of Applied Polymer Science, 2002. 85: p. 2389-2395.

36. Umut Bulut, J.V.C., *Reactivity of oxetane monomers in photoinitiated cationic polymerization.* Journal of Polymer Science Part A: Polymer Chemistry, 2005. 43(15): p. 3205-3220.

CHAPTER 6
ACRYLATE/EPOXIDE HYBRID PHOTOPOLYMERIZATIONS: EFFECTS OF ACRYLATE SECONDARY FUNCTIONALITY ON REACTIVITY OF EPOXIDE

Introduction

Photopolymerization, which uses light energy to initiate a chemical reaction, is one of the most efficient ways to produce a variety of polymer structures. The major advantages of this technology are its energy savings, low production of volatile compounds, and ultra-fast curing process at ambient temperature, as well as ease of temporal and spatial control of reactions. These unique attributes have led to its adoption within the fields of coatings, optoelectronics, adhesives, membranes, stereolithography, composites, dental fillings, and biomaterials [1-3]. In industrial applications, ultraviolet (UV) light-curable systems are most prevalent and facilitate rapid free-radical or cationic polymerizations of a wide range of monomers such as (meth)acrylates, epoxides, and vinyl ethers [1]. The photopolymerizations of these monomers are primarily facilitated by free-radical or cationic species generated from photolysis of corresponding photoinitiators. The free-radical and cationic species are significantly affected by atmospheric conditions such as oxygen and humidity, respectively. The negative effects of continued diffusion of oxygen into curing systems on free-radical photopolymerizations have been intensively investigated [4-8]. Comparably, atmospheric moisture can have an adverse effect on cationic photopolymerization due to the basicity of water molecules. The addition of the basic water to the cationic active centers can cause acceleration, retardation, or inhibition of propagation, depending on monomer structures and water concentration in the reaction systems [9-11].

To overcome the problems with atmospheric factors, hybrid systems containing two different monomers, such as acrylates and epoxides, has been found a promising

approach. In conventional hybrid polymerizations, two distinct propagation mechanisms take place in a simultaneous or sequential step and are controlled by curing conditions, initiator systems, and the kinetics of the respective monomers [12-15]. These two distinct mechanisms allow two different polymer chains to form topologically interlocked and entangled polymer networks, known as interpenetrating polymer networks (IPN), without the formation of covalent bonds in between the respective polymers. Various types of UV-curable hybrid systems have been reported: acrylate/polymer matrix (where the polymer matrix is polymethylmethacrylate, polyvinyl chloride, polyurethane, polystyrene, or styrene-butadiene rubber) [16-19], acrylate/epoxidized polyisoprene [20], vinyl ether/unsaturated ester [21], vinyl ether/epoxide [20-24], (meth)acrylate/vinyl ether [25, 26], (meth)acrylate/epoxide [13, 25, 27-30], hybrid monomer or polymer systems [7, 27, 31], and thiol-ene/thiol-epoxy hybrid systems [32]. These photopolymerizable hybrid systems are mostly based on free-radical and cationic photopolymerizations and typically use a dual photoinitiator system containing a radical and cationic photoinitiator. Such hybrid systems can reduce the negative effects of oxygen and water because the radical species are not sensitive to water, while the positively charged cationic active centers are not scavenged by radical-coupling with oxygen in the propagation [1]. This complementary synergy plays a key role at the air/coating interface during hybrid photopolymerizations in order to produce a desired polymer product with a tack-free surface. In the case of acrylate/epoxide hybrid systems, epoxide polymer chains predominantly propagate at the interface without oxygen inhibition. This epoxide conversion at the surface leads to the reduction of oxygen diffusion from the atmosphere into the polymerizing system [7, 20, 27]. In addition, the reduced oxygen inhibition will provide more favorable conditions for free-radical polymerizations, thereby increasing the system viscosity with an increase of acrylate conversion at the near interface. As a result, moisture diffusion can be also reduced simultaneously.

Factors affecting the reactivity of acrylates and epoxides have been reported for various hybrid photopolymerization systems. For acrylates, functionality, photoinitiator type and concentration, viscosity of the hybrid mixtures, and polymer binder type that preexist such as availability of abstractable hydrogen, oxygen permeability, and miscibility are important considerations [16-19]. In addition, the degree of oxygen inhibition and curing conditions such as temperature affect the reactivity of acrylates [13, 20, 26-29]. For epoxides, viscosity, photoinitiator systems, atmospheric humidity, temperature, and acrylate kinetics have been shown to play important roles.

Although many of these factors have been examined for acrylate/epoxide hybrid systems, several fundamental questions have not clearly been addressed. For example, different chemical environments are locally created by bulk monomer/polymer entities, and propagating polymer chains certainly affect the kinetics and reactivity of both monomers. Thus, how the molecular structure of acrylate and epoxide monomers affect the kinetics of both photoinitiated free-radical and cationic polymerizations must be understood. In addition, monomer composition effects could have a different impact on the reactivity of both monomers in terms of their molecular structures. Furthermore, the complexity of acrylate/epoxide hybrid systems is further complicated by taking the effect of the dual photoinitiator system on the monomer reactivity into consideration. A complete understanding of the mechanisms that answer these questions will ultimately facilitate optimization of formulations and reaction conditions for thin film and coating applications using comparable hybrid photopolymerizations.

In this chapter, the effect of different acrylate secondary functionality on the reactivity of a cycloaliphatic diepoxide in a hybrid systems is studied during photopolymerization. Recently, acrylate secondary functionality has been shown to play a key role in affecting the reactivity of (meth)acrylates and degree of conversion [33-43]. The difference in the reactivity of various mono-(meth)acrylates has been primarily explained by several mechanistic theories, such as dipole moments, presence of

abstractable hydrogens, hydrogen bonding capability, and/or electronic and resonance effects. However, these factors have not been carefully evaluated in acrylate/epoxide hybrid photopolymerization systems. Thus, it was hypothesized that the acrylate secondary functionality may significantly affect the epoxide reactivity during the hybrid photopolymerization. In addition, it was hypothesized that the extent of its effects on the kinetics of the cationic photopolymerization will extensively vary with the concentration of that secondary functionality. Furthermore, the various ratios of a radical photoinitiator (PI) to a cationic PI concentration were examined by taking into consideration the extent of radical promoted cationic photopolymerizations [44-46].

Experimental

Materials

Three monovinyl acrylate monomers were selected as model compounds: hexyl acrylate (HA, 98%), 2-butylaminocarbonyloxyethyl acrylate (BCEA, >95%), and 2-(diethylamino) ethyl acrylate (DAEA, 98%) from Sigma-Aldrich and 2-butoxyethyl acrylate (BEA, >98%) from Scientific Polymer Products. Each acrylate contains a different secondary group in its backbone adjacent to the mono-functional acrylate group: aliphatic alkyl (HA), ether (BEA), and urethane (BCEA). The cationically polymerizable monomer 3,4-epoxycyclohexylmethanyl 3,4-epoxycyclohexanecarboxylate (a cycloaliphatic diepoxide monomer, EEC) was used in these experiments (ERl-4221, 91–97% EEC and the balance a cycloaliphatic mono-epoxide, Sigma Aldrich). This monomer was selected for its high reactivity and low shrinkage, as well as its broad miscibility with acrylic monomers. A non-reactive ethyl hexanoate was also purchased from Sigma-Aldrich. The α-cleavable free-radical photoinitiator 2,2-dimethoxy-2-phenyl-acetophenone (DMPA, Aldrich) and the cationic photoinitiator diaryliodonium hexafluoroantimonate (IHA, Sartomer) were used to initiate the reaction of C=C double

bonds and epoxide rings, respectively. All materials were used as received and are shown in Table 6.1.

Table 6.1 Structure and viscosity of monomers and photoinitiators studied.

Materials	Abbreviation (Viscosity [cP] @ 25°C)	Structure
Acrylates	HA (1.92)	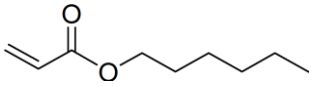
	BEA (1.97)	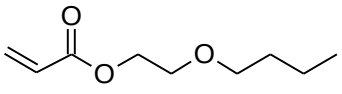
	BCEA (20)	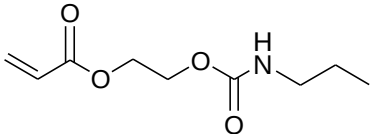
Cycloaliphatic diepoxide	EEC (350)	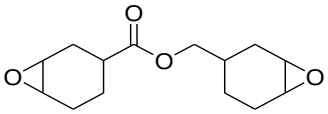
Ethyl hexanoate	EH (N/A)	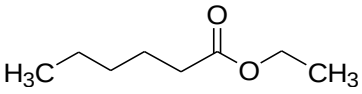
Photoinitiators	DMPA (N/A)	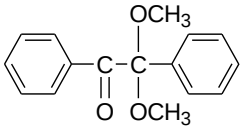
	IHA (N/A)	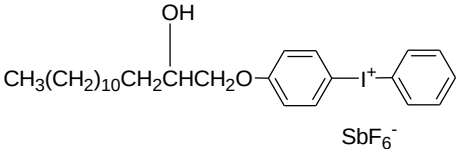

Molar ratios of epoxides and acrylates were mixed thoroughly. The concentration of each photoinitiator was calculated to be 32 mM for the corresponding monomer fraction. Accordingly, the relative concentration of the individual PIs was kept constant to the fraction of the respective acrylates and epoxides. The photoinitiator powders were

mixed with individual acrylates, epoxides, or their hybrid mixtures until the formulated liquids were transparent.

Photon Absorption Measurement of Photoinitiators

The absorbance spectra for photoinitiators were determined in one nanometer increments using an UV-Visible spectrophotometer (8453, Agilent Technologies). Photoinitiators were dissolved in neat monomers or mixtures of monomers. The absorbance measurements were performed via double-beam experiments in which reference spectra were obtained using the neat monomers or their mixtures. The same concentration (32 mM) of photoinitiators was adjusted for their respective monomers to simulate the experimental condition under which real-time kinetic studies were carried out. The absorbance spectra were obtained in an air-tight, quartz cell to prevent any changes in concentration during measurements. The photon absorption rate constant, $k_{abs,}$ for the IHA photoinitiator was determined by integrating the overlap between the photon absorption at each specific wavelength and the emission spectrum of the light source [47-49].The actual lamp emission spectrum was measured using a calibrated miniature fiber optic spectrometer (USB4000, Ocean Optics).

In-Situ Kinetic Study Using Real-time Measurement

Raman spectroscopy was used for real-time monitoring of acrylate and epoxide functional groups during hybrid photopolymerizations. Real-time Raman spectra were collected using a holographic fiber-coupled stretch probehead (Mark II, Kaiser Optical Systems, Inc.) attached to a modular research Raman spectrograph (HoloLab 5000R, Kaiser Optical Systems, Inc.). A 10x non-contact sampling objective with 0.8-cm working distance was used to deliver ~200 mW 785 nm near-infrared laser intensity to the sample, thereby inducing the Raman scattering effect. The exposure time for each spectrum was 100 ms, and the time interval between data points was 6 s. Samples were illuminated for 5 to 30 min at 25°C in sealed 1 mm ID quartz capillary tubes using a 100

W high-pressure mercury lamp (Acticure® Ultraviolet/Visible Spot Cure System, EXFO Photonic Solutions, Inc.). The spectrum-effective irradiance of the system was set to 100 mW/cm^2 for filter-passed wavelength band between 250nm and 450 nm as measured by a radiometer (R5000, EFOS). Raman samples were illuminated 30 seconds after real-time Raman measurements started.

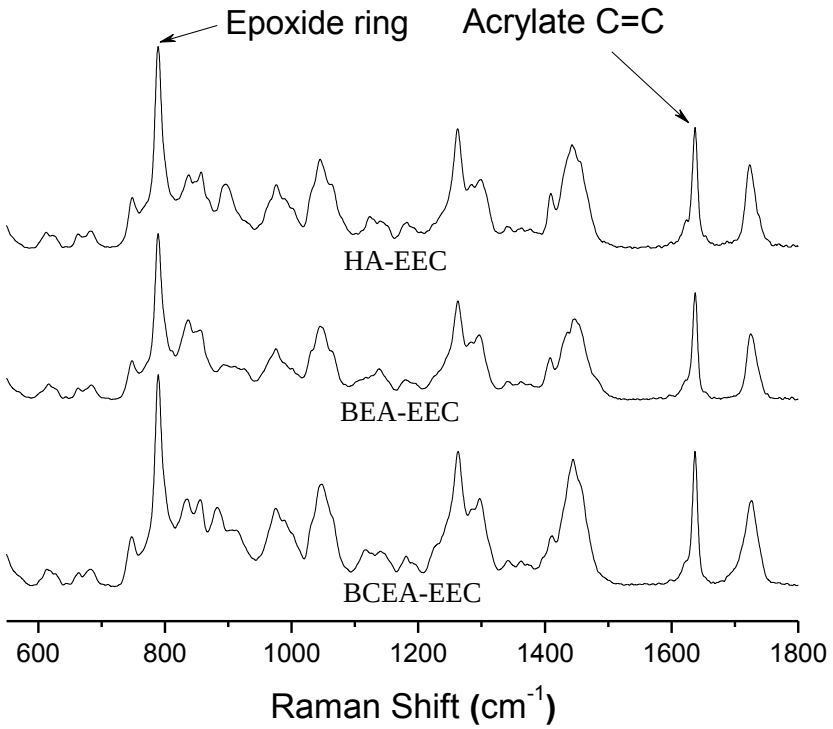

Figure 6.1 Raman spectra for acrylate/epoxide hybrid mixtures of 50:50 molar ratio systems before photopolymerization. The reactive band representing the acrylate C=C double bond is located at 1638 cm^{-1}; the reactive band representing the epoxide ring is located at 789 cm^{-1}.

The Raman spectrum of each acrylate and epoxide was acquired first to identify bands in the fingerprint region that could be used to calculate conversion (see Figure 6.1).

The reactive band representing the acrylate C=C double bond was located at 1638 cm^{-1} and is associated with the C=C stretching vibrations; the reactive band representing the epoxide ring was located at 789 cm^{-1} and is associated with the asymmetric epoxide ring deformation. An internal reference band was selected at 605 cm^{-1}, which represents the skeletal bending of the non-reactive acrylate carbonyl group. The peak areas under each band were integrated and used to calculate the concentration of the related functional groups. Since the spectral baselines and the reference band intensity remained constant in these real-time reaction studies, the conversion of each functional group was calculated by rationing the peak area of the reactive band at any given time, $A_{rxn}(t)$, to the peak area of the reactive band prior to illumination, $A_{rxn}(0)$:

$$\text{Conversion, } \alpha = 1 - \frac{A_{rxn}(t)}{A_{rxn}(0)} \qquad (eq.\ 6.1)$$

Results and Discussion

Photopolymerizations of Neat Monomer Systems

Cationic ring-opening polymerization of the neat diepoxide monomer (EEC) proceeded very slowly upon illumination. The polymerization rate and degree of conversion were significantly lower than those of the neat acrylate systems (Figure 6.2). Regarding the slow kinetic behavior of EEC, Crivello *et al.* mechanistically studied structure and reactivity relationship for photoinitiated cationic ring-opening polymerizations of various cycloaliphatic epoxides [50]. They proposed that propagation of cationic active centers possibly competes with several alternative pathways associated with ester carbonyl groups. In the alternative pathways, a growing oxonium ion is attacked by a nucleophilic ester carbonyl to form dialkoxycarbenium ions. When the propagating oxonium ions and dialkoxycarbenium ions are in equilibrium, the latter intermediates are energetically more stable than the former species. Thus, the intermediates are less reactive. In addition, the dialkoxycarbenium ions are more

sterically hindered and less likely to react with unprotonated monomers than the former species. As a result, the traditional propagation of cationic active centers is retarded, resulting in slow polymerization and low conversion as shown in Figure 6.2.

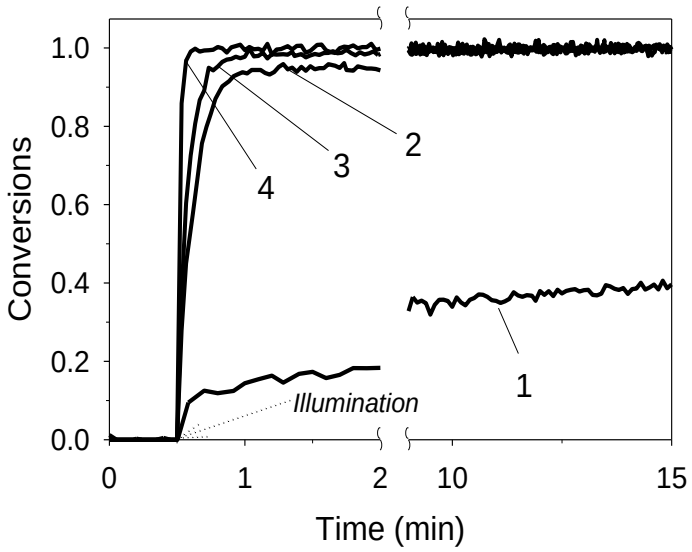

Figure 6.2 Real-time polymerization profiles of neat diepoxide with IHA and neat acrylates with DMPA: (1) EEC, (2) HA, (3) BEA, and (4) BCEA. [IHA] = [DMPA] = 32 mM for diepoxide and acrylates, respectively.

Effects of Acrylate Secondary Functionalities on Photoinitiated Cationic Ring-opening Polymerization

In-situ kinetic studies using real-time Raman spectroscopy were performed to simultaneously monitor the change in the reactive bands for acrylate carbon double bonds and cycloaliphatic epoxide rings of the respective acrylate and diepoxide monomers. Acrylate/epoxide hybrid systems with 1:1 molar ratios were compared to determine the effect of the secondary functional groups on the photoinitiated cationic ring-opening polymerizations of the diepoxide (Figure 6.3). The concentrations of DMPA and IHA were adjusted to be equal molarity for the volume fraction of acrylates and diepoxide in

their hybrid mixtures, respectively. As seen in Figure 6.3, the polymerization rate for the diepoxide was greatly enhanced in the presence of HA and BEA, compared to neat EEC system (Figure 6.2). Conversion of EEC monomer was also greatly increased in both equimolar hybrid systems. In contrast, the photoinitiated cationic ring-opening polymerization of EEC monomers was completely inhibited in the presence of BCEA containing a secondary urethane group (Figure 6.3). In general, the diepoxide cationic polymerization in the corresponding hybrid systems proceeded relatively slower than free-radical photopolymerizations of the monovinyl acrylates. This disparity in the rate of polymerization between acrylates and epoxide has been repeatedly observed in various (metha)acrylate/epoxide hybrid systems [20, 51]. Decker *et al*. showed the free-radical photopolymerization of hexanediol diacrylate proceeded at least twice as fast, despite the low viscosity of the diacrylate (~0.09 P at 25ºC), which served as a diluent to enhance the cationic polymerizations of high viscosity epoxides such as epoxidized polyisoprene (~10^3 poise at 170 ºC) [20]. This behavior was also true for highly viscous acrylate-containing hybrid systems: a bisphenol A derivative dimethacrylate (~14 P at 25ºC) or aliphatic urethane acrylates (100-180 P at 60 ºC) with a highly reactive cycloaliphatic diepoxide (~4 P at 25 ºC) under air or laminate conditions [28, 29]. Furthermore, the results in Figure 6.3 indicate that the disparity in the kinetics between the acrylates and diepoxide may significantly depend on the secondary functional groups of the monovinyl acrylates.

There are several plausible explanations to rationalize the enhanced or inhibited reactivity of EEC in coexistence of free-radical polymerization of the low viscosity acrylates. In this study, dilution effect, radical promoted cationic photopolymerization, and polarity/solvation effects were considered as main factors that affect the epoxide reactivity in the HA/EEC and BEA/EEC systems. For BCEA/EEC systems, nucleophilicity and bascisity were considered as a function of monomer composition to explain the complete inhibition of the EEC cationic photopolymerization.

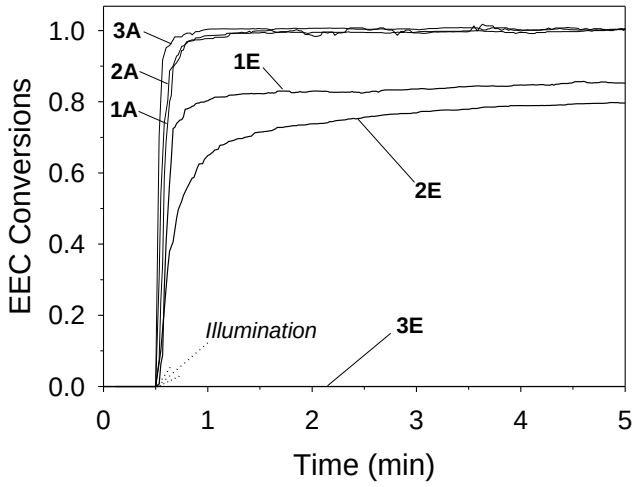

Figure 6.3 Real-time polymerization profiles of acrylate/diepoxide hybrid mixtures with 1:1 molar ratio: HA(1A)/EEC(1E), BEA(2A)/EEC(2E), BCEA(3A)/EEC(3E) hybrid systems. [DMPA] = 32 mM for acrylates, and [IHA] = 32 mM for diepoxide.

Dilution Effects of Acrylates on Diepoxide Reactivity

The dilution effect of low viscosity acrylates monomers is rationalized by a reduced initial viscosity in the polymerization system. In general, low viscosity acrylate monomers can be considered to be non-reactive diluents for the diepoxide. The reduced viscosity of the total reaction system offered by the non-reactive diluents, such as HA and BEA monomers, increased molecular mobility of the diepoxide monomers and growing cationic active species and thereby enhanced epoxide reactivity. Due to the lack of coupling termination between cationic species, the kinetics of cationic photopolymerization is viscosity-dependent such that the rate of polymerization and degree of conversion are greatly affected by the increased viscosity of the bulk polymerization system. In this regard, the viscosity dependence of the photoinitiated cationic ring-opening polymerization is somewhat opposite to the free-radical photopolymerization where the coupling termination between radical species is reduced by increased viscosity, resulting in a greatly enhanced rate of polymerization. Zong *et al*.

studied the effect of non-reactive diluents on cationic photopolymerization of epoxynorbornane linseed oils (ENLOs, 223 P at 25 ºC) [52]. They found that ENLO reactivity calculated by $R_{p,max}$ and final conversion proportionally increased with the amount of diluents. In addition, the introduction of reactive diluents enhanced the kinetics of cationic photopolymerization. Decker *et al.* studied the effect of initial viscosity on the photoinitiated cationic copolymerization of binary mixture systems containing two vinyl ether monomers with different viscosities and found approximately 10 times increased rate of polymerization as the initial viscosity of the binary mixture approximately 5000 times decreased [21]. In the HA/EEC and BEA/EEC hybrid systems, the viscosity of both HA and BEA monomers is 200 times lower than that of EEC. However, the dilution effect of the low-viscosity acrylate monomers was not solely responsible for the increased EEC reactivity. Another important factor will be discussed in the consecutive section.

The initial viscosity-dependent kinetic behaviors of epoxide have been also observed in different photopolymerization systems [21, 24, 28, 52]. Since the viscosity of the hybrid systems was quickly increased by the early formation of acrylate polymer networks, the diffusion mobility of epoxide monomers and cationic active species could be immensely limited by the acrylate gelation occurring at a low conversion of epoxides [20, 27, 29, 51]. In order to provide a more favorable environment for epoxides to grow before acrylates reach a gelation point, the molar concentration of a cationic PI was adjusted three times higher for epoxides than that used for the radical PI for acrylates [29]. However, the discrepancy in the rate of polymerization and final conversions between epoxides and acrylate remained the same [28, 29].

Radical Promoted Cationic Photopolymerization

Another plausible explanation for the enhanced reactivity of EEC in the presence of HA and BEA monomers may be found by taking into consideration photon absorption

rate (k_{abs}, number of photons absorbed by a photoinitiator molecule per unit time) of each photoinitiator (DMPA and IHA) in the dual photoinitiator system. The photon absorption rates for these systems were determined and are shown in the Table 6.2.

Table 6.2 Photon absorption rate of each free-radical and cationic photoinitiator in acrylate/epoxide mixture

	k_{abs}						
	EEC	HA	BEA	BCEA	HA/EEC (50:50)	BEA/EEC (50:50)	BCEA/EEC (50:50)
DMPA	0.30	0.33	0.38	0.32	0.19	0.16	0.17
IHA	0.39	0.78	0.72	0.73	0.44	0.46	0.46

Compared to the radical photoinitiator (DMPA), the cationic photoinitiator (IHA) exhibited greater photon absorption cross-section at a low spectral region below 320 nm wavelength as indicated by the higher $k_{abs,\ IHA}$ (Table 6.2). However, DMPA has photon absorption cross-section above the 320 nm in the region where there are strong lamp emission lines. In this spectral region, there is no photon absorption competition between DMPA and IHA. As a result, in the photopolymerization of actual acrylate/epoxide systems, the photolysis of DMPA takes place immediately in spite of the photon absorption competition in between the two photoinitiator at the spectral region below the 320 nm wavelength. The photolysis of DMPA rapidly generates two radical species, and a redox interaction between an electron-donating free radical and intact onium salt can results. Eventually, the redox process leads to radical-promoted cationic photopolymerizations based on the oxidation of a free radical by an onium salt [44, 45]. Yagci *et al*. also demonstrated that strong electron-donating radicals generated from free-radical photoinitiators, such as benzoin, reduce cationic photoinitiators with strong electron affinity (*e.g.*, diphenyl onium salts or alkoxy pyrdinium salts) to form primary

carbocations upon illumination around 350 nm, a wavelength at which the cationic photoinitiators do not absorb photons [53]. The free-radical photoinitiator (DMPA) used in this study generates an electron-withdrawing benzoyl radical and a strong electron-donating dimethoxy benzyl radical [1, 54]. The benzoyl radical is responsible for the conversion of carbon double bonds; whereas, the dimethoxy benzyl radical does not[55]. Instead, the latter species can undergo redox reaction by reducing IHA before the dimethoxy benzyl radical is further photodecomposed into a methyl radical. Thus, initial concentration of active cationic species can rapidly increase with the initial increase of the dimethoxy benzyl carbocations generated from the redox reaction. To confirm the dual photoinitiator effect on EEC reactivity, various DMPA/IHA ratios from 1:2 to 1:1 to 2:1 were examined (Figure 6.4).

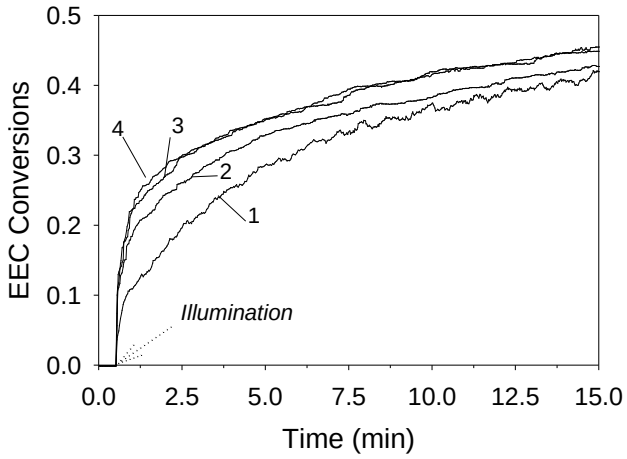

Figure 6.4 Effect of dual photoinitiator system on diepoxide reactivity with various ratios of [DMPA] to [IHA]. Neat EEC monomer with [IHA] = 32 mM (1), [DMPA] = 16 mM and [IHA] = 32 mM (2), [DMPA] = 32mM and [IHA] = 32 mM (3), and [DMPA] = 64 mM and [IHA] =32 mM (4).

The reactivity and conversions of EEC monomers were significantly enhanced at initial stages as the concentration of DMPA increased. This result indicates increased

cationic active centers via a redox mechanism as described above. However, the enhancement of the EEC reactivity by the dual photoinitiator system was somewhat lessened when the molar concentration of DMPA was higher than that of IHA (Figure 6.4). The lessening of this effect is because $[+]_{total} \approx [H^+]_{IHA}+[C^+]_{redox}$ becomes constant at [DMPA]/[IHA] ≥1. This result implies that, in the equimolar HA/EEC and BEA/EEC systems, the increased polymerization rates at conversions from 10% to 30% are mainly caused by the faster generation of cationic active centers via the radical promoted cationic polymerization.

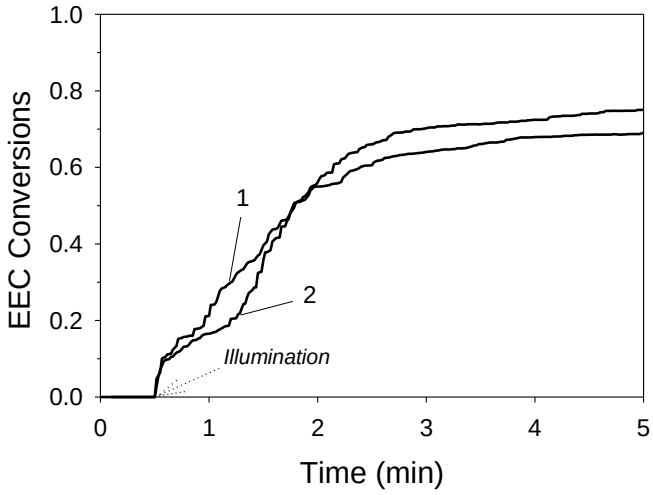

Figure 6.5 Conversion profiles of the diepoxide in equimolar mixtures of HA/EEC (1) and BEA/EEC (2) in the presence of the cationic photoinitiator (IHA) only. [IHA] = 32 mM for the diepoxide. Real-time Raman measurements were conducted at 25°C.

To correlate this result with the dilution effect of the acrylate monomers, EEC reactivity was also compared to the same molar ratio hybrid systems using the cationic photoinitiator only (Figure 6.5). The initial reactivity and overall rate of polymerization of epoxides were not as high as in the dual photoinitiator systems. Therefore, based on

the results in Figures 6.3, 6.4, and 6.5, propagation of the increased cationic active centers generated from the redox interaction becomes less diffusion-controlled with the reduction of the initial viscosity, which causes a significant increase in the rate of polymerization and degree of conversion. Another benefit of the dual photoinitiator system used in this study is that the spectral response of IHA can be further extended to increase the reactivity of epoxides in both neat epoxide systems and acrylate/epoxide hybrid systems [53, 54].

Polarity/solvation Effect of Acrylates

Solvent polarity has been found to have a pronounced effect on overall polymerization rate in cationic ring opening polymerization of heterocyclic monomers [56, 57], and the dependence of dissociation constants (K_D) of growing ion pairs on solvent polarity has been reported [56, 58]. In general, K_D increases as the polarity of cationic polymerization systems increases, which may shift equilibrium from ion pairs to loose/free ions, leading to an increasing polymerization rate due to a higher reactivity of the latter species. However, reactivities of loose/free ions and ions pairs were indistinguishable when examined in different solvent polarities where non-nucleophilic anions with a relatively large voluminous size (*e.g.*, SbF_6^- , PF_6^- , AsF_6^-) were used [56, 59]. Furthermore, the apparent propagation constant (compromising both ion species) decreased with increasing polarity of the polymerization system [56]. This indirect relationship was attributed to the preferential solvation of oxonium ions by both nucleophilic solvent and monomer molecules [58].

Similarly, the indirect relationship also held true for the acrylate/epoxide hybrid systems when polarity of each model acrylate was compared on the basis of Boltzmann-averaged dipole moments (μ_B) found in literature [34]: $\mu_{B,\,calc} \approx 1.83$ D for HA, 2.24 D for BEA, and 3.23 D for BCEA. When the BEA/EEC systems are compared to the HA/EEC systems (Figure 6.3), the difference in their polarities in affecting the reactivity

of growing ion pairs between cation and counter anion is negligible. It is more likely that the lower reactivity of EEC with BEA is caused by solvation of protons and/or carbocations by BEA monomers and polymer chains containing the secondary ether groups that possibly have an interaction with active cationic species, such as intermolecular hydrogen bonding. This argument is more generalized and reasonable by considering the disparity in the kinetics of the acrylates and diepoxide (Figure 6.3). Since acrylate polymer chains grow quickly before the diepoxide forms a highly crosslinked network structure, locally dense domains of acrylates polymer chains will be formed. The acrylate polymer chains rapidly developing may surround the active cationic species, including oxonium/oxiranium ions, protons and/or carbocations, and affect the concentration of available cationic active species for further propagation of diepoxide as a function of the types of acrylate secondary functional groups (Figure 6.6). In this situation, polarity associated with the secondary functionality begins to play an important role in controlling the kinetics of the cationic ring-opening polymerization of the diepoxide. Accordingly, solvating power, which affects the epoxide reactivity, should be correlated with nucleophilicity or basicity of acrylate secondary functional groups. The solvation of cationic species by heterocyclic monomers and their polymers has been also reported and attributed to nucleophilicity or basicity of heteroatoms in ring-opening polymerizations [56, 58, 60-65]. In the case of BCEA/EEC systems, neither the dilution effect nor the dual photoinitiator effect was observed, although the viscosity of the equimolar mixture of BCEA and EEC is still lower than the neat EEC system in the presence of both DMPA and IHA photoinitiators (Figure 6.3). The complete inhibition of the cationic photopolymerization suggested that available protons or carbocations for propagation may be severely depleted due to the secondary urethane groups. This hypothesis will be discussed in detail in correlation with monomer composition later in this chapter. Therefore, the intermolecular interaction of the acrylate secondary functional groups with cationic species plays a critical role in governing the epoxide reactivity

during the photopolymerization. Consequently, it is anticipated that the concentration of secondary functional groups becomes more important in controlling the kinetics and final polymer properties, especially when the composition of binary hybrid systems needs to be adjusted for practical applications. To further elucidate the role of the secondary functional groups as a function of their concentration, various acrylate/epoxide compositions were examined.

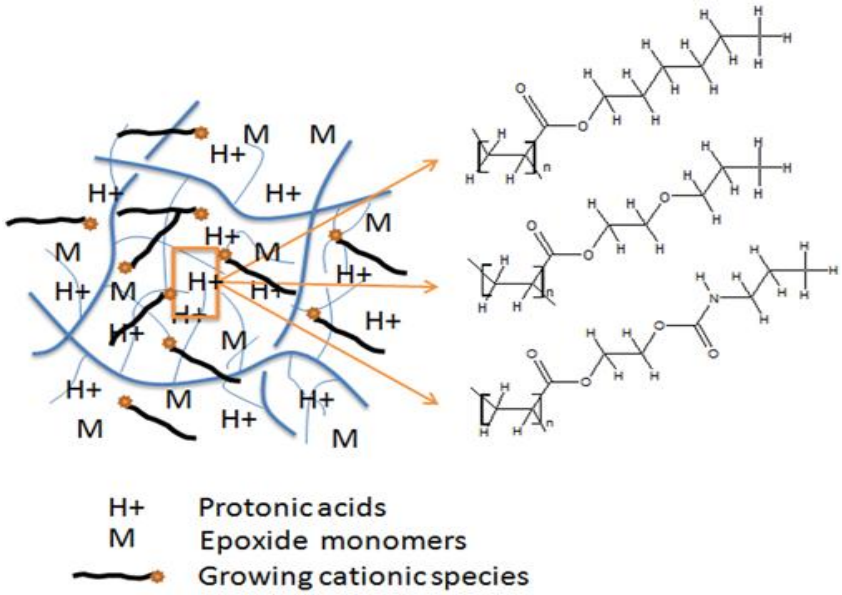

Figure 6.6 Possible intermolecular interaction between cationic active species and secondary functional groups in acrylate polymer chains formed early in the acrylates/epoxide hybrid photopolymerization.

Effects of Compositions on Epoxide Reactivity in HA/EEC and BEA/EEC Systems

It was postulated that acrylate secondary functional groups have a great influence on the cationic ring-opening polymerization as a function of their concentration in proximity of cationic species and affect the reactivity of EEC monomer. Hence, it was assumed that the intermolecular interaction between acrylate monomers/polymer chains

and cationic species are governed by the acrylate/epoxide compositions. Consequently, the cationic ring-opening polymerization of EEC was simultaneously monitored for the various acrylate/epoxide ratios using Raman spectroscopy.

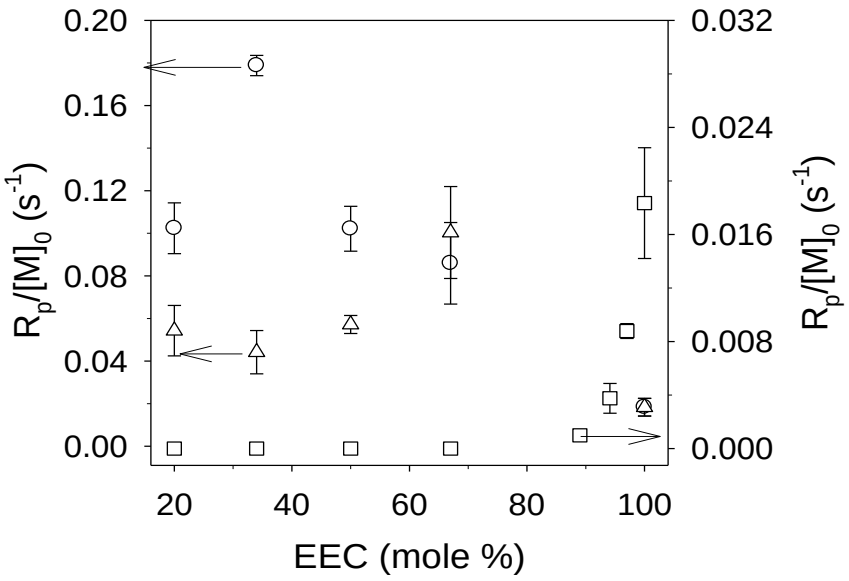

Figure 6.7 Effect of monomer compositions on the maximum rate of polymerization of the diepoxide during hybrid photopolymerizations: $R_{p,max}$'s of EEC with HA (○), EEC with BEA (△), and EEC with BCEA (□). [DMPA] = [IHA] = 32 mM for acrylates and diepoxide, respectively.

The reactivity of EEC in different hybrid systems was rationalized by maximum rate of polymerization ($R_{p,max}$) normalized by the monomer concentration. Figure 6.7 clearly shows the different effect of acrylate/epoxide compositions on the reactivity of EEC as a function of acrylate secondary functionality. In the presence of aliphatic carbons and ether groups, the overall reactivity of EEC was enhanced compared to EEC neat systems. In contrast, no enhancement in $R_{p,max}$ was found in the presence of urethane groups. In general, the results reveal that the extent of the enhancement of the EEC

kinetics was significantly affected by acrylate secondary functionality and its concentration.

In the presence of aliphatic alkyl groups, the overall rate of polymerization of EEC cationic photopolymerizations was immensely enhanced. There is an approximate 7-fold increase in $R_{p,max}$ in the presence of 33% HA, with a proportional increase in $R_{p,max}$ up to 13-fold as the concentration of HA increased to 67% (Figure 6.7). Similarly, the consumption of EEC monomers increased over 80% in proportional to the acrylate content. This enhancement is remarkable when compared to the neat EEC system (*i.e.*, only 20% of EEC monomers were consumed at 2 minute illumination (Figure 6.8A vs. 6.2). Again, this notable enhancement in the polymerization rate and the degree of conversion of EEC can be attributed to the dilution effect and the radical promoted cationic photopolymerization via redox process between electron-donating radical and the cationic photoinitiator. However, the reactivity of EEC began to decrease when the molar ratio of HA to EEC monomers was higher than 2 (Figure 6.7). With 80% HA, $R_{p,max}$ and conversion was somewhat reduced, although the reduced reactivity of EEC was still much higher than that of the neat system (Figures 6.7 and 6.8A vs. 6.2). In such a high volume fraction of the acrylate, the acrylate polymer chains rapidly form their large domains and surround epoxide monomers and the cationic species. This environment scattered throughout the reaction system may inflict diffusion-limited propagation on growing cationic active centers at a low conversions of EEC [47, 48, 66] . As a result, this constraint appears to decrease the $R_{p,max}$ and the degree of conversion for EEC. Therefore, the pure alkyl secondary functional groups of the HA monomers/polymer chains do not have a negative effect on the reactivity of EEC until the molecular diffusion of cationic species and monomers becomes restricted by the early formation of large acrylate polymer domains. This conclusion becomes clearer when comparing the BEA/EEC systems as a function of composition.

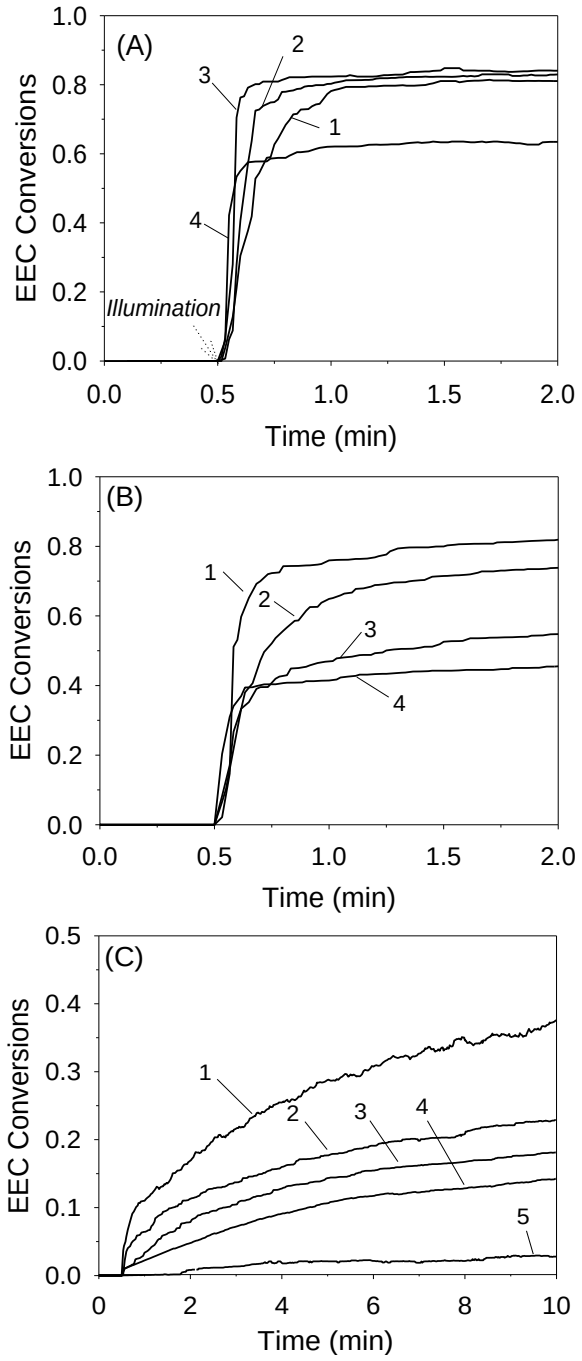

Figure 6.8 Conversion profiles of the diepoxide with HA (A), BEA (B), and BCEA (C) at various compositions. For the HA/EEC and BEA/EEC systems, the molar concentration of HA and BEA monomers ranges from 33% (1) to 50% (2) to 66% (3) to 80% (4). For the BCEA/EEC systems, the molar concentration of BCEA ranges from 0% (1) to 3% (2) to 6% (3) to 11% (4) to 34% (5). [DMPA] = [IHA] = 32 mM for acrylates and diepoxide, respectively.

In the case of BEA/EEC systems, the ether secondary groups differently affect the reactivity of EEC as a function of composition. In the presence of 33% BEA, the EEC cationic ring-opening polymerization showed an approximate 7-fold increase in $R_{p,max}$, as was observed in the HA/EEC system. In contrast to the HA/EEC system, the EEC reactivity began to decrease when the molar ratio of BEA to EEC was higher than 0.5 (Figure 6.7). In the Figures 6.7 and 6.8B, the overall rate of polymerization and $R_{p,max}$ of the EEC cationic photopolymerization began to decrease significantly as more ether secondary groups were introduced to the hybrid systems. In addition, the EEC conversion at the 2 minute illumination proportionally decreased roughly from 80% to 40% (Figure 6.8B). From the comparison of the BEA/EEC system with the HA/EEC system at various compositions, it was hypothesized that the secondary ether oxygen caused the slower cationic photopolymerization of EEC by intermolecular interaction of ether oxygen with cationic species (*e.g.*, hydrogen bonding) because solvation/stabilization of protons and/or secondary onium ions would result. This hypothesis is supported by previous reports. Hartwig *et al.* found that, in the presence of 12-crown-4 ether rings, protons can be fixed inside the rings and lead to retardation of EEC cationic photopolymerization [64]. In addition, complexation of protons by the crown ether-like structures of polyether oligomers based on 1,2–diols caused the retardation of epoxide consumption in the presence of the polyetherdiols. This result, however, was not observed when 1,4-butandiol was present [64]. Bulut *et al.* showed that propagation of growing cationic active centers can be significantly retarded by the stabilization of secondary oxonium ions via intramolecular hydrogen bonding with ether oxygen atoms, and this stabilization leads to an increase in activation energy [65]. In this study, the interaction between ether secondary groups of BEA and cationic species may differ to some degree because the ether oxygen is positioned in the side groups of the polymer chains and not in the backbone. Thus, the complexation may involve the fixation of protons and/or stabilization of secondary oxonium ions in pseudo-crown ether-like structures formed by

spatially coordinated side chains containing nucleophilic ester alkoxy oxygen and/or ether oxygen (Figure 6.9). Therefore, the lower reactivity of EEC in the BEA/EEC systems could be somewhat explained not only by a decrease in the diffusion of initiating protons, but also by the possible stabilization of secondary oxonium ions due to spatially coordinated solvation by ether secondary groups in acrylate polymer chains.

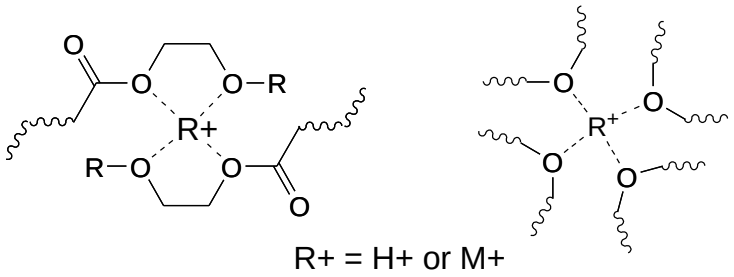

Figure 6.9 Possible conformation of cationic species in pseudo-crown ether-like structures formed by intermolecular hydrogen bonding between a proton and acrylate alkoxy oxygens and secondary ether oxygens (A) and between secondary ether oxygens and a proton (B).

Effects of Compositions on Epoxide Reactivity in BCEA/EEC Systems

No apparent cationic photopolymerization of EEC was observed until the concentration of BCEA was reduced to less than 11 mole % (10 wt.%), as shown in Figures 6.7 and 6.8C. To obtain a higher degree of conversion for the diepoxide, BCEA should be incorporated at less than 3 mole % (30.3 mM) for the given condition. In spite of the low BCEA concentration, the overall polymerization rate and $R_{p,max}$ were considerably lower than those of the neat EEC system (Figures 6.7 and 6.8C). The ester alkoxy oxygen of the urethane structure may act similarly as the ether oxgen in the BEA monomer, as rationalized for the 1:1 BEA/EEC system. On the other hand, the inhibition of the cationic photopolymerization becomes less effective as the concentration of BCEA

was lowered to the concentration of the cationic photoinitiator used (Figure 6.7). Thus, the factors considered for the EEC reactivity in the HA/EEC and BEA/EEC systems cannot favorably explain such a suppression of EEC monomer consumption in the presence of the urethane secondary groups. It is more likely that the fundamental structure of the secondary urethane structure caused this complete inhibition of EEC cationic photopolymerization.

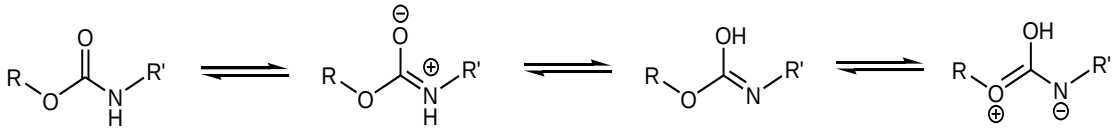

Figure 6.10 Possible negative charges in resonance structure of the urethane group.

The urethane structure is similar to an ester on one side and an amine on the other. By considering resonance structure, the polar urethane structure that resembles amides can have two possible negative charges, as shown in Figure 6.10. The partial negative charges on the oxygen and nitrogen atoms are expected to act as bases and cause scavenging of the cationic species. Nagarale *et al*. attributed the enhanced cation-exchange capacity of cation-exchange membranes coated with a thin urethane acrylate layer to the resonance stabilization of the urethane group, which resulted in a negatively charged urethane ion [67]. Consequently, propagation of oxonium ions at a very early stage may face interference from the strong nucleophilic ester carbonyl in the secondary urethane structure. In addition, the amine in the urethane structure may more negatively affect the cationic ring-opening polymerization of the diepoxide. Oxman *et al.* showed that some amine compounds can fully inhibit the cationic ring-opening polymerizations depending on their pK_b's and oxidation potential [30]. Accordingly, the urethane amine

of BCEA monomer may act as a proton scavenger under moderate or highly acidic conditions. The structural factors could be a great challenge in facilitating photoinitiated cationic photopolymerization by competing with the diepoxide monomers, which means that the control of the concentration of the secondary urethane becomes important. Thus, the complete inhibition of EEC consumption in the BCEA/EEC system may be related to the nucleophilicity and/or basicity of ester carbonyl and amine.

Based on this hypothesis, the effect of ester carbonyl on the reactivity of EEC was examined first by incorporating a non-reactive ester carbonyl compound, ethyl hexanoate (EH), into neat EEC system. The dual photoinitiator system was used in the 2:1 DMPA/IHA ratio for the neat EEC and EH/EEC systems. Figure 6.11 shows that, in the presence of EH, the cationic ring-opening polymerization of EEC was suppressed to a large degree. This result indicates that the dilution effect of EH and radical promoted cationic photopolymerizations were not as effective in the presence of EH ester carbonyl groups. The decreased EEC polymerization rate and the degree of conversion are most likely due to the high nucleophilicity of the ester carbonyl group of EH. The additional incorporation of the highly nucleophilic groups may similarly interfere with effective propagation, upon which the EEC ester carbonyl groups have considerable influence [68-70], as already discussed in the previous section. In addition, when comparing the 2:1 EH/EEC system to the 2:1 BEA/EEC system, the negative effect of EH ester carbonyl groups on EEC cationic photopolymerization is more severe than that of the ether group (Figure 6.11). Given that there is a low possibility of the complexation of cationic species within the ether crown-like structure of the non-reactive EH during the polymerization, the suppression of the EEC cationic photopolymerization appears to be predominantly affected by the ester carbonyl group rather than the ether groups in this case. Thus, the ester carbonyl in the secondary urethane group of BCEA monomer may be responsible for the inhibition of the EEC cationic photopolymerization in the BCEA/EEC systems. Nevertheless, this justification does not fully explain the complete inhibition of EEC

cationic photopolymerization in the 2:1 BCEA/EEC hybrid system (Figure 6.11), nor does it explain why the cationic photopolymerization was suppressed even with a low level of BCEA content.

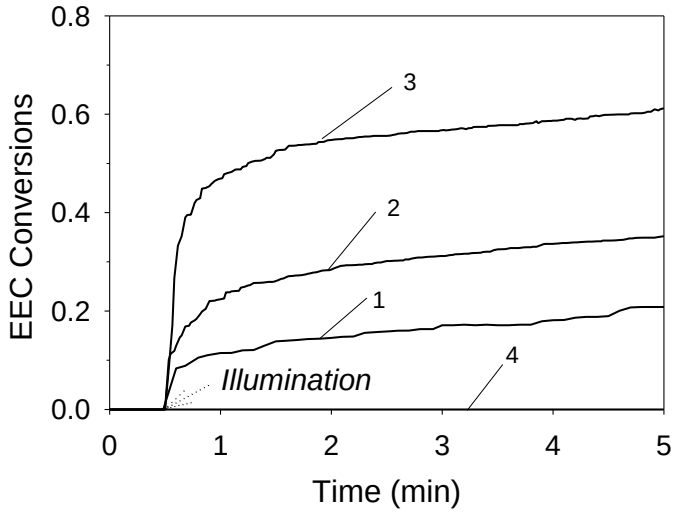

Figure 6.11 Effect of ester carbonyl groups on cationic photopolymerizations in the presence of ethyl hexanoate (1) in comparison with neat EEC (2), 2:1 BEA/EEC (3), and 2:1 BCEA/EEC (4). The molar ratio of EH to EEC was 2:1. The molar ratio of DMPA to IHA was adjusted to 2:1 for all samples.

Secondly, the basicity of ester carbonyl and urethane amine in the secondary urethane group of the BCEA monomer was also considered to be critical and was evaluated by comparing predicted pK_a values of conjugated acids for both moieties using SPARC On-line Calculator V4.5 (http://ibmlc2.chem.uga.edu/sparc). The SPARC On-line Calculator combines linear free energy calculations with perturbation theory and structure–activity relationships to predict ionizing pK_a values [71, 72]. Based on the predicted pK_a values, the urethane amine group is approximately 3-fold more basic than the ester carbonyl group in the urethane structure of the BCEA monomer (Table 6.3). The

basicity of the urethane amine was compared to that for the secondary amine in another acrylate, PABA. PABA monomer is similar to BCEA, but lacks the ester carbonyl, and was virtually created to validate how the presence of ester carbonyl group in the urethane affects the basicity of the urethane amine. Generally, the resonance stabilization of the urethane group should result in a pronounced decrease in basicity for the urethane amine. As expected, the urethane amine of BCEA was significantly less basic than the secondary amine according to the predicted pK_a values (Table 6.3).

Table 6.3 Comparison of predicted pK_a values of functional groups in various compounds.

Functional groups	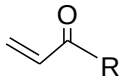			Secondary functional groups 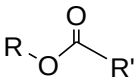		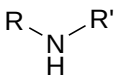		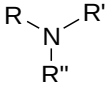
Materials	HA	BEA	BCEA	BCEA	EH	BCEA	PABA[a]	DAEA[b]
pK_a	-5.15	-5.28	-5.39	-4.13	-4.84	-1.58	10.65	8.53

[a] PABA, 4-(propylamino)butyl acrylate.

[b] DAEA, 2-(diethylamino)ethyl acrylate.

This approach was also extended to other acrylate monomers used, along with the non-reactive compound, EH (Table 6.3). The influence of acrylate ester carbonyl groups on the EEC reactivity was predicted to be the same in all cases. In other words, the net effect of the acrylate functional groups can be neglected. The predicted pK_a value of ester carbonyl in the secondary urethane structure is similar to that of EH; whereas, the urethane amine was determined to be more significantly basic by comparison. These results demonstrate how the cationic photopolymerization was suppressed by the presence of the urethane amine, which may detrimentally scavenge protons or

carbocations unless the concentration of BCEA is lower to the level of the cationic photoinitiator. Therefore, in the presence of the secondary urethane group, the combined properties of the ester carbonyl and urethane amine result in the detrimental inhibition of the cationic photopolymerizations.

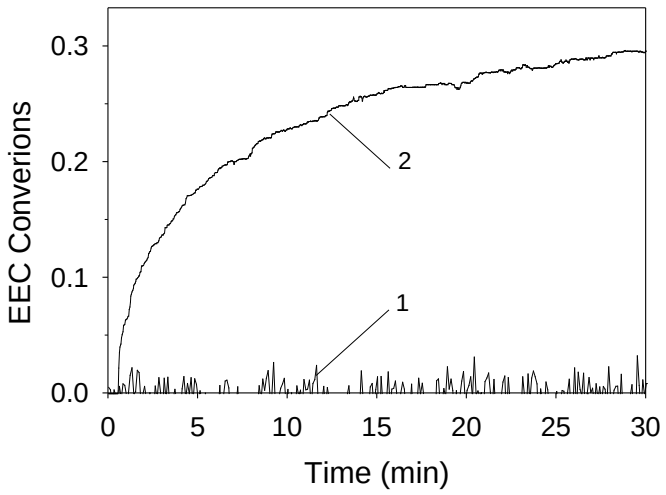

Figure 6.12 Comparison of diepoxide conversion profiles in the presence of tertiary amine of DAEA (1) and urethane amine of BCEA (2). [DAEA] = [BCEA] = 30.3 mM. [DMPA] = [IHA] = 32 mM for acrylates and diepoxide, respectively.

Furthermore, validation of this approach based on the predicted pK_a was performed using 2-(diethylamino) ethyl acrylate (DAEA). The predicted pK_a value of its tertiary amine is 8.53, making it significantly more basic than the urethane amine of BCEA (Table 6.3). Hence, the reactivity of EEC was evaluated using a small amount DAEA and BCEA in separate mixtures. As predicted, the cationic photopolymerization of EEC was completely inhibited in the presence of DAEA; while in the presence of BCEA, the cationic ring-opening polymerization of EEC sluggishly proceeded with time (Figure 6.12). Although the prediction of pK_a value has not been performed at the most

refined level, these results provide a reasonable explanation of the polymerization rate behavior observed in the presence of the various acrylates in this research.

Conclusions

This study systematically demonstrated that the effects of the molecular structure of acrylates on the kinetics of epoxide cationic photopolymerizations in coexistence of free-radical photopolymerizations. Specifically, it was hypothesized that non-vinyl secondary functional groups of acrylates have a great impact on the reactivity of epoxide monomers. The structural characteristics of the secondary functional groups are associated with viscosity, polarity/solvation, and nucleophilicity/basicity of acrylates. These key factors can influence the chemical environment of epoxide monomers undergoing cationic ring-opening polymerization. Because of the low viscosity of the model acrylates, the dilution effect seemed to predominate over other factors. However, significant enhancement in the polymerization rate and degree of conversion of the diepoxide was achieved when the dilution effect was synergistically coupled with the radical promoted cationic polymerization induced by the dual photoinitiator system. The synergetic effects depended greatly on the type of secondary functional group on the acrylate and their concentration in hybrid systems. In the presence of the secondary alkyl group, an over 7-fold increment in $R_{p,max}$ was found for a wide range of composition. However, in the presence of the secondary ether group, a 7-fold enhanced $R_{p,max}$ was obtained only when a low concentration of the secondary ether group was introduced; otherwise, the diepoxide reactivity tended to decrease with the increase in concentration of the secondary ether group. The different epoxide reactivities with subtle difference in the molecular structure of the acrylates were attributed to solvating power associated with the ether oxygen. The solvation of protons or carbocations may involve the formation of pseudo-crownether-like structures by intermolecular hydrogen bonding with spatially coordinated secondary ether groups of acrylate monomer and polymer chains. In contrast

to the alkyl and ether groups, the presence of the secondary urethane group completely suppressed the photoinitiated cationic ring-opening polymerization of the diepoxide. The detrimental effect of the secondary urethane was most likely due to its resonance stabilization and its basicity based on predicted pK_a values. The complete inhibition of the cationic photopolymerization is most likely dictated by the combined nucleophilicity and strong basicity associated with ester carbonyl and urethane amine in the urethane structure that interfere with propagating cationic active centers and scavenging protons or carbocations. Finally, the epoxide reactivity and its degree of conversion were very sensitive to the types and concentration of acrylate secondary functionality, such as heteroatoms and carbamate groups. Therefore, these findings provide fundamental guidelines that should be considered to optimize industrially relevant formulations and reaction conditions for thin-film and coating applications using acrylate/epoxide hybrid photopolymerizations for producing desirable strength of hybrid IPNs.

Notes

1. Fouassier, J.P., *Photoinitiation, Photopolymerization, and Photocuring: Fundamentals and Applications* 1st ed. 1995, New York: Hanser.

2. Fisher, J.P., Dean, D., Engel, P. S., Mikos, A. G., *Photoinitiated polymerization of biomaterials.* Annual Review of Materials Science, 2001. 31: p. 171-181.

3. Anseth, K.S. and Burdick, J.A., *New Directions in Photopolymerizable Biomaterials.* MRS Bulleten, 2002: p. 130-136.

4. Lijing Gou, B.O., and Alec B. Scranton, *The effect of oxygen in free radical photopolymerization.* Recent Research Developments in Polymer Science 2004. 8: p. 125-141.

5. Christophersen, A.G., Jun, H., Jørgensen, K., and Skibsted, L.H., *Photobleaching of astaxanthin and canthaxanthin: quantum-yields dependence of solvent, temperature, and wavelength of irradiation in relation to packageing and storage of carotenoid pigmented salmonoids.* Z Lebensm Unters Forsch, 1991. 192: p. 443-439.

6. O'Brien, A.K. and Bowman, B.N., *Impact of Oxygen on Photopolymerization Kinetics and Polymer Structure.* Macromolecules, 2006. 39: p. 2501-2506.

7. Cai, Y. and Jessop, J.L.P., *Decreased oxygen inhibtion in photopolymerized acrylate/epoxide hybrid polymer coatings as demonstrated by Raman Spectroscopy.* Polymer, 2006. 47: p. 6560-6566.

8. H. Cao, E.C., M. Tilley, and Y.C. Jean, *Oxygen inhibition effect on surface properties of UV-curable acrylate coatings.* ACS Symposium Series 847, 2003: p. 165-175.

9. Hartwig, A., Schneider, B., and Luhring, A., *Influence of moisture on the photochemically induced polymerisation of epoxy groups in different chemical environment.* Polymer, 2002. 43: p. 4243-4250.

10. Sangermano, M., Malucelli, G., Morel, F., Decker, C., and Priola, A., *Cationic Photopolymerization of Vinyl ether systems: influence of the presence of hydrogen donor additives.* European Polymer Journal, 1999. 35: p. 639-645.

11. Lin, Y. and Stansbury, J.W., *Near-Infrared Spectroscopy Investigation of Water Effects on the Cationic Photopolymerization of Vinyl Ether System.* Journal of Polymer Science: Part A: Polymer Chemistry, 2004. 42: p. 1985-1998.

12. Yoshinobu, N., Miho, Yamaguchi, Akiko, Kitayama, Kazuo, Iko, Masayoshi, Okubo, Tsunetaka, Matsumoto, *Internal stress of epoxy resin modified with*

acrylic polymers produced by in situ UV radiation polymerization. Journal of Applied Polymer Science, 1990. 39(5): p. 1045-1060.

13. Nowers, J.R. and Narasimhan, B., *The effect of interpenetrating polymer network formation on polymerization kinetics in an epoxy[hyphen (true graphic)]acrylate system.* Polymer, 2006. 47(4): p. 1108-1118.

14. L.H. Sperling, a.V.M., *The Current Status of Interpenetrating Polymer Networks.* Polymers for Advanced Technologies, 1996. 7: p. 197-208.

15. Suthar, B., Xiao, H.X., Klempner, D., and Frisch, K.C., *A Review of Kinetic Studies of the Formation of Interpenetrating Polymer Networks.* Polymer for Advanced Technologies, 1996. 7: p. 221-233.

16. Moussa, K. and C.Decker, *Semi-interpentrating polymer networks synthesis by Photocrosslinking of Acrylic Monomers in a polymer Matrix.* Journal of Polymer Science: Part A: Polymer Chemistry, 1993. 31: p. 2633-2542.

17. Kaczmarek, H. and Decker, C., *Interpenetrating polymer networks. I. Photopolymerization of multiacrylate systems.* Journal of Applied Polymer Science, 1994. 54(13): p. 2147-56.

18. Decker, C. and Bendaikha, T., *Interpenetrating polymer networks. II. Sunlight-induced polymerization of multifunctional acrylates.* Journal of Applied Polymer Science 1998. 70(11): p. 2269-2282.

19. Strehmel, B., Anwand, D., and Timpe, H.J., *The formation of semiinterpenetrating polymer networks by photoinduced polymerization*, in *Physics of Polymer Networks*. 1992. p. 70-77.

20. Decker, C., Xuan, H.L., and Viet, T.N.T., *Photocrosslinking of functionalized rubber. III. Polymerization of multifunctional monomers in epoxidized liquid natural rubber.* Journal of Polymer Science Part A: Polymer Chemistry, 1996. 34(9): p. 1771-1781.

21. Decker, C., Bianchi, C., Decker, D., and Morel, F., *Photoinitiated polymerization of vinyl ether-based systems.* Progress in Organic Coatings, 2001. 42(3-4): p. 253-266.

22. Rajaraman, S.K., Mowers, W. A., Crivello, J.V., *Interaction of epoxy and vinyl ethers during photoinitiated cationic polymerization.* Journal of Polymer Science Part A: Polymer Chemistry, 1999. 37(21): p. 4007-4018.

23. Tom Scherzer, M.R.B., *Photoinitiated Cationic Polymerization of Cycloaliphatic Epoxide/Vinyl Ether Systems Studied by Near-Infrared Reflection Spectroscopy.* Macromolecular Chemistry and Physics, 2007. 208(9): p. 946-954.

24. Kim, Y.-M., Kostanski, L.K., and MacGregor, J.F., *Photopolymerization of 3,4-epoxycyclohexylmethyl-3',4'-epoxycyclohexane carboxylate and tri (ethylene glycol) methyl vinyl ether*. Polymer, 2003. 44(18): p. 5103-5109.

25. Jung-Dae, C. and Jin-Who, H., *UV-initiated free radical and cationic photopolymerizations of acrylate/epoxide and acrylate/vinyl ether hybrid systems with and without photosensitizer*. Journal of Applied Polymer Science, 2004. 93(3): p. 1473-1483.

26. Yan Lin, J.W.S., *The impact of water on photopolymerization kinetics of methacrylate/vinyl ether hybrid systems.* Polymers for Advanced Technologies, 2005. 16: p. 195-199.

27. Decker, C., Nguyen Thi Viet, T., Decker, D., Weber-Koehl, E. , *UV-radiation curing of acrylate/epoxide systems.* Polymer, 2001. 42(13): p. 5531-5541.

28. Lecamp, L., Pavillon, C., Lebaudy, P., and Bunel, C., *Influence of temperature and nature of photoinitiator on the formation kinetics of an interpenetrating network photocured from an epoxide/methacrylate system.* European Polymer Journal, 2005. 41(1): p. 169-176.

29. Eom, H.S. and Jessop, J.L.P., *Epoxide/urethane acrylate hybrid photopolymerizations to minimize atmospheric sensitivity: Understanding the interplay between viscosity and dual photoinitiator system*, in *Basics and Applications of Photopolymerization Reactions*, J.P. Fouassier and X. Allonas, Editors. 2010. p. 39-52.

30. Oxman, J.D., Jacobs, D.W., Trom, M.C., Sipani, V., Ficek, B., and Scranton, A.B., *Evaluation of Initiator systems for controlled and sequentially curable Free-Radical/Cationic Hybrid Photopolymerizations.* Journal of Polymer Science: Part A: Polymer Chemistry, 2004. 43: p. 1747-1756.

31. Decker, C., Le Xuan, H, Nguyen, T, and Viet, T, *Photocrosslinking of functionalized rubber. II. Photoinitiated cationic polymerization of epoxidized liquid natural rubber*. Journal of Polymer Science Part A: Polymer Chemistry, 1995. 33(16): p. 2759-2772.

32. Carioscia, J.A., Stansbury, J.W., and Bowman, C.N., *Evaluation and control of thiol-ene/thiol-epoxy hybrid networks.* Polymer, 2007. 48(6): p. 1526-1532.

33. Jansen, J.F.G.A.D., Aylvin A. Dorschu, Marko and Coussens, B., *Effect of Preorganization Due to Hydrogen Bonding on the Rate of Photoinitiated Acrylate Polymerization*, in *Photoinitiated Polymerization*, K.D. Belfield and J.V. Crivello, Editors. 2003, American Chemical Society. p. 127-139.

34. Jansen, J.F.G.A., Dias, A.A., Dorschu, M., and Coussens, B., *Fast Monomers: Factors Affecting the Inherent Reactivity of Acrylate Monomers in Photoinitiated Acrylate Polymerization.* Macromolecules, 2003. 36(11): p. 3861-3873.

35. Jansen, J.F.G.A., Dias, A.A., Dorschu, M., and Coussens, B., *Effect of Preorganization Due to Hydrogen Bonding on the Rate of Photoinitiated Acrylate Polymerization*, in *Photoinitiated Polymerization*, K.D. Belfield and J.V. Crivello, Editors. 2003, American Chemical Society. p. 127-139.

36. Jansen, J.F.G.A., Dias, A.A., Dorschu, M., and Coussens, B., *Effect of Dipole Moment on the Maximum Rate of Photoinitiated Acrylate Polymerizations.* Macromolecules, 2002. 35(20): p. 7529-7531.

37. Lee, T.Y., Guymon, C.A., Jonsson, E.S., and Hoyle, C.E., *The effect of monomer structure on oxygen inhibition of (meth)acrylates photopolymerization.* Polymer, 2004. 45(18): p. 6155-6162.

38. Beckel, E.R., Stansbury, J.W., and Bowman, C.N., *Effect of Aliphatic Spacer Substitution on the Reactivity of Phenyl Carbamate Acrylate Monomers.* Macromolecules, 2005. 38(8): p. 3093-3098.

39. Berchtold, K.A., Nie, J., Stansbury, J.W., HacioÇ§lu, B., Beckel, E.R., and Bowman, C.N., *Novel Monovinyl Methacrylic Monomers Containing Secondary Functionality for Ultrarapid Polymerization: Steady-State Evaluation.* Macromolecules, 2004. 37(9): p. 3165-3179.

40. Beckel, E.R., Nie, J., Stansbury, J.W., and Bowman, C.N., *Effect of Aryl Substituents on the Reactivity of Phenyl Carbamate Acrylate Monomers.* Macromolecules, 2004. 37(11): p. 4062-4069.

41. Lee, T.Y., Roper, T.M., Jönsson, E.S., Guymon, C.A., and Hoyle, C.E., *Influence of Hydrogen Bonding on Photopolymerization Rate of Hydroxyalkyl Acrylates.* Macromolecules, 2004. 37(10): p. 3659-3665.

42. Kilambi, H., Reddy, S.K., Schneidewind, L., Lee, T.Y., Stansbury, J.W., and Bowman, C.N., *Design, Development, and Evaluation of Monovinyl Acrylates Characterized by Secondary Functionalities as Reactive Diluents to Diacrylates.* Macromolecules, 2007. 40(17): p. 6112-6118.

43. Berchtold, K.A., Nie, J., Stansbury, J.W., and Bowman, C.N., *Reactivity of Monovinyl (Meth)acrylates Containing Cyclic Carbonates.* Macromolecules, 2008. 41(23): p. 9035-9043.

44. Mustafa Degirmencl, O.I., and Yusuf Yagci, *Synthesis and Characterization of Cyclohexane Oxide Functional Poly(ε-caprolactone) Macromonomers and Their*

Use in Photoinitiated Cationic Homo- and Copolymerization. Journal of Polymer Science: Part A: Polymer Chemistry, 2004. 42: p. 3365-3372.

45. Wolfram, S., *Cationic photopolymerization with the aid of pyridinium-type salts.* Macromolecular Rapid Communications, 2000. 21(10): p. 628-642.

46. Dursun, C., Degirmenci, M., Yagci, Y., Jockusch, S., and Turro, N.J., *Free radical promoted cationic polymerization by using bisacylphosphine oxide photoinitiators: substituent effect on the reactivity of phosphinoyl radicals.* Polymer, 2003. 44(24): p. 7389-7396.

47. Sipani, V. and Scranton, A.B., *Dark-Cure Studies of Cationic Photopolymerizations of Epoxides: Chracterization of the Active Center Lifetime and Kinetic Rate Constants.* Journal of Polymer Science: Part A: Polymer Chemistry, 2003. 41: p. 2064-2072.

48. Sipani, V. and Scranton, A.B., *Kinetic studies of cationic photopolymerizations of Phenyl glycidyl ether: termination/trapping rate constants for iodonium photoinitiators.* Journal of Photochemistry and Photobiology A: Chemistry 2003. 159: p. 189-195.

49. Sipani, V., Kirsch, Ann, Scranton, Alec B. , *Dark Cure Studies of Cationic Photopolymerizations of Epoxides: Characterization of Kinetic Rate Constants at High Conversions.* Journal of Polymer Science: Part A: Polymer Chemistry, 2004. 42: p. 4409-4416.

50. Crivello, J.V. and Varlemann, U., *Mechanistic study of the reactivity of 3,4-epoxycyclohexylmethyl 3′,4′-epoxycyclohexancarboxylate in photoinitiated cationic polymerizations.* Journal of Polymer Science Part A: Polymer Chemistry, 1995. 33(14): p. 2473-2486.

51. Decker, D., Nguyen, T, Viet, T, and Thi, HP, *Photoinitiated cationic polymerization of epoxides.* Polymer International, 2001. 50: p. 986-997.

52. Zhengang, Z., Mark, D.S., Yubiao, L., and Jun, H., *Cationic photopolymerization of epoxynorbornane linseed oils: The effect of diluents.* Journal of Polymer Science Part A: Polymer Chemistry, 2003. 41(21): p. 3440-3456.

53. M. Degirmenci, Y.H., Y. Yagci, *One-step, one-pot Photoinitiation of Free Radical and Free Radical Promoted Cationic Polymerizations.* Journal of Applied Polymer Science, 2002. 85: p. 2389-2395.

54. Fouassier, J.-P. and Merlin, A., *Laser investigation of norrish type I photoscission in the photoinitiator irgacure (2,2-dimethoxy 2-phenyl-acetophenone).* Journal of Photochemistry, 1980. 12(1): p. 17-23.

55. Hageman, H.J., Van der Maeden, F.P.B., and Janssen, P.C.G.M., *Photoinitiators and photoinitiation, 1. Vinyl polymerization photoinitiated by benzoin methyl ether.* Die Makromolekulare Chemie, 1979. 180(10): p. 2531-2537.

56. Matyjaszewski, K., Słomkowski, S., and Penczek, S., *Kinetics and mechanism of the cationic polymerization of tetrahydrofuran in solution: THF-CH3NO2 system.* Journal of Polymer Science: Polymer Chemistry Edition, 1979. 17(1): p. 69-80.

57. Penczek, S., Cypryka, M., Duda, A., Kubisaa, P., and Słomkowskia, S., *Living ring-opening polymerizations of heterocyclic monomers* Progress in Polymer Science 2007. 32(2): p. 247-282

58. Matyjaszewski, K., *Solvation of onium ions in cationic ring-opening polymerization.* Macromolecules, 1988. 21(2): p. 519-520.

59. Odian, G., *Principles of Polymerization*. 4th ed. 2004, New York: John Wiley & Sons, Inc. .

60. Stanislaw Penczek, M.C., Andrzej Duda, Przemyslaw Kubisa, and Stanislaw Slomkowski, *Living ring-opening polymerizations of heterocyclic monomers.* Progress in Polymer Science, 2007. 32: p. 247-282.

61. Arkhipovich, G.N., Dubrovskii, S.A., Kazanskii, K.S., Ptitsina, N.V., and Shupik, A.N., *Study of solvation of alkali cations with poly(ethylene oxide).* European Polymer Journal, 1982. 18(7): p. 569-576.

62. Stanislaw Penczek, Przemyslaw Kubisa, Slomkowski, S., and Matyjaszewski, K., *Structure-Reactivity Relationships in Ring-Opening Polymerization*, in *Ring-Opening Polymerization*, J.E. McGrath, Editor. 1985, American Chemical Society. p. 117-135.

63. Crivello, J.V., *Cationic Photopolymerizationi of Alkyl Glycidyl Ethers.* Journal of Polymer Science: Part A: Polymer Chemistry, 2006. 44: p. 3036-3052.

64. Hartwig, A., Koschek, K., Lühring, A., and Schorsch, O., *Cationic polymerization of a cycloaliphatic diepoxide with latent initiators in the presence of structurally different diols.* Polymer, 2003. 44(10): p. 2853-2858.

65. Bulut, U., and Crivello, J. V. , *Investigation of the Reactivity of Epoxide Monomers in Photoinitiated Cationic Polymerization* Macromolecules, 2005. 38(9): p. 3584 -3595.

66. Vishal Sipani, A.K., and Alec B. Scranton, *Dark Cure Studies of Cationic Photopolymerizations of Epoxides: Characterization of Kinetic Rate Constants at High Conversions.* Journal of Polymer Science: Part A: Polymer Chemistry, 2004. 42: p. 4409-4416.

67. Nagarale, R.K., Shahi, V.K., Schubert, R., Rangarajan, R., and Mehnert, R., *Development of urethane acrylate composite ion-exchange membranes and their electrochemical characterization.* Journal of Colloid and Interface Science, 2004. 270(2): p. 446-454.

68. Crivello, J.V. and Varlemann, U., *The synthesis and study of the photoinitiated cationic polymerization of novel cycloaliphatic epoxides.* Journal of Polymer Science Part A: Polymer Chemistry, 1995. 33(14): p. 2463-2471.

69. James, V.C. and Ulrike, V., *Mechanistic study of the reactivity of 3,4-epoxycyclohexylmethyl 3',4'-epoxycyclohexancarboxylate in photoinitiated cationic polymerizations.* Journal of Polymer Science Part A: Polymer Chemistry, 1995. 33(14): p. 2473-2486.

70. Crivello, J.V. and Narayan, R., *Novel Epoxynorbornane Monomers. 2. Cationic Photopolymerization.* Macromolecules, 1996. 29(1): p. 439-445.

71. Hilal, S.H., Karickhoff, S.W., and Carreira, L.A., *A Rigorous Test for SPARC's Chemical Reactivity Models: Estimation of More Than 4300 Ionization pKa.* Quantitative Structure-Activity Relationships, 1995. 14(4): p. 348-355.

72. Sipil, J., Nurmi, H., Kaukonen, A.M., Hirvonen, J., Taskinen, J., and Yli-Kauhaluoma, J., *A modification of the Hammett equation for predicting ionisation constants of p-vinyl phenols.* European Journal of Pharmaceutical Sciences. 25(4-5): p. 417-425.

CHAPTER 7
ACRYLATE/EPOXIDE HYBRID PHOTOPOLYMERIZATIONS: EFFECTS OF DIEPOXIDE AND DUAL PHOTOINITIATOR SYSTEM ON REACTIVITY OF ACRYLATES

Introduction

In the previous chapter, fundamental questions that have received little attention in acrylate/epoxide hybrid photopolymerization systems were considered. Specifically, the effect of acrylate secondary functionalities upon the kinetics of cationic photopolymerization was determined using model monovinyl acrylate monomers and a dual photoinitiator system. Subtle differences in the acrylate molecular structure gave rise to differences in epoxide reactivity as a function of monomer composition. In addition, the dual photoinitiator system played an important role in altering epoxide reactivity.

Recently, acrylate secondary functionality has been shown to play a key role in affecting the reactivity of (meth)acrylates and degree of conversion [1-11]. The difference in the reactivity of various mono-(meth)acrylates has been primarily explained by several mechanistic theories, such as dipole moment theory, lability of abstractable hydrogen, and hydrogen-bonding capability. However, these factors have not been carefully evaluated in acrylate/epoxide hybrid photopolymerization systems. Therefore, in this chapter, the effects of diepoxide monomer on the reactivity of monovinyl acrylates with different secondary functional groups are studied as a function of monomer composition. It was hypothesized that free-radical photopolymerization of the monovinyl acrylates will exhibit different sensitivity to the presence of diepoxide monomers that undergo the cationic ring-opening polymerization. In addition, the effect of the dual photoinitiator system on acrylate reactivity was examined as a function of molar ratios of radical/cationic photoinitiators.

Experimental

Materials

Three monovinyl acrylate monomers were selected as model compounds: hexyl acrylate (HA, 98%), 2-butylaminocarbonyloxyethyl acrylate (BCEA, >95%), and 2-(diethylamino) ethyl acrylate (DAEA, 98%) from Sigma-Aldrich and 2-butoxyethyl acrylate (BEA, >98%) from Scientific Polymer Products. Each acrylate contains a different secondary group in its backbone adjacent to the mono-functional acrylate group: aliphatic alkyl (HA), ether (BEA), and urethane (BCEA). The cationically polymerizable monomer 3,4-epoxycyclohexylmethanyl 3,4-epoxycyclohexanecarboxylate (a cycloaliphatic diepoxide monomer, EEC) was used in these experiments (ERl-4221, a mixture of 91–97% EEC and cycloaliphatic mono-epoxide, Sigma Aldrich). This monomer was selected for its high reactivity and low shrinkage, as well as its broad miscibility with acrylic monomers. A non-reactive ethyl hexanoate was also purchased from Sigma-Aldrich. The α-cleavable free-radical photoinitiator 2,2-dimethoxy-2-phenyl-acetophenone (DMPA, Aldrich) and the cationic photoinitiator diaryliodonium hexafluoroantimonate (IHA, Sartomer) were used to initiate the reaction of C=C double bonds and epoxide rings, respectively. All materials were used as received and are shown in Table 6.1 of the previous chapter. Epoxides and acrylates were mixed by molar ratios. The concentration of each photoinitiator (PI) was calculated to be 32 mM for the corresponding monomer fraction. Accordingly, the relative concentration of the individual PIs was kept constant to the fraction of the respective acrylates and epoxides. The photoinitiator powders were mixed with individual acrylates, epoxides, or their hybrid mixtures until the formulated liquids were transparent.

In-Situ Kinetic study Using Real-time Measurement

Raman spectroscopy was used for real-time monitoring of acrylate and epoxide functional groups during hybrid photopolymerizations. Real-time Raman spectra were

collected using a holographic fiber-coupled stretch probehead (Mark II, Kaiser Optical Systems, Inc.) attached to a modular research Raman spectrograph (HoloLab 5000R, Kaiser Optical Systems, Inc.). A 10x non-contact sampling objective with 0.8-cm working distance was used to deliver ~200 mW 785 nm near-infrared laser intensity to the sample, thereby inducing the Raman scattering effect. The exposure time for each spectrum was 100 ms, and the time interval between data points was 6 s. Samples were illuminated for 5 to 30 min at 25°C in sealed 1 mm ID quartz capillary tubes using a 100 W high-pressure mercury lamp (Acticure® Ultraviolet/Visible Spot Cure System, EXFO Photonic Solutions, Inc.). The spectrum-effective irradiance of the system was set to 100 mW/cm^2 for filter-passed wavelength band between 250nm and 450 nm as measured by a radiometer (R5000, EFOS). Samples were illuminated with the mercury lamp 30 seconds after real-time Raman measurements started.

The Raman spectrum of each acrylate and epoxide was acquired to identify bands in the fingerprint region that could be used to calculate conversion (see Figure 6.1 in Chapter 6). The reactive band representing the acrylate C=C double bond was located at 1638 cm^{-1} and is associated with the C=C stretching vibrations; the reactive band representing the epoxide ring was located at 789 cm^{-1} and was associated with the asymmetric epoxide ring deformation [12]. An internal reference band was selected at 605 cm^{-1}, which represents the skeletal bending of the non-reactive acrylate carbonyl group. The peak areas under each band were integrated and used to calculate the concentration of the related functional groups. Since the spectral baselines and the reference band intensity remained constant in these real-time reaction studies, the conversion of each functional group was calculated by ratioing the peak area of the reactive band at any given time, $A_{rxn}(t)$, to the peak area of the reactive band prior to illumination, $A_{rxn}(0)$:

$$\text{Conversion, } \alpha = 1 - \frac{A_{rxn}(t)}{A_{rxn}(0)} \qquad (eq.\ 7.1)$$

Results and Discussion

Photopolymerizations of Neat Acrylate Monomers

Kinetic studies were performed using Raman spectroscopy for each neat acrylate system with the radical photoinitiator (DMPA). The acrylate reactivity increased in the following order: carbamate >> ether > pure alkyl groups (Figure 7.1).

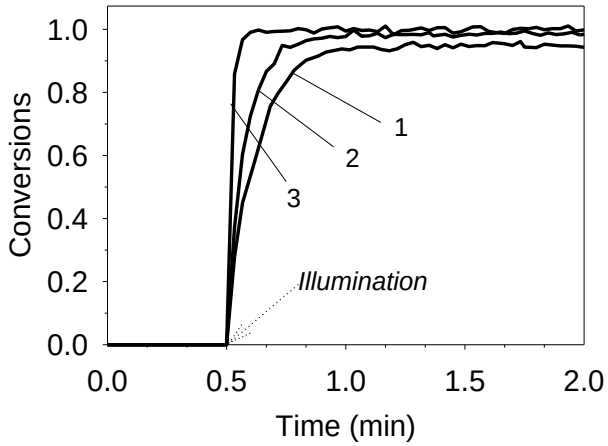

Figure 7.1 Real-time polymerization conversion profiles of neat acrylates: (1) HA, (2) BEA, and (3) BCEA with DMPA. [DMPA] = 32 mM.

Several factors associated with the secondary functional groups have been considered to understand these results for the monovinyl (meth)acrylates: (1) polarity/dipole moment, (2) hydrogen abstraction availability, and (3) hydrogen-bonding effect. Jansen *et al*. have proposed that the rate of polymerization (R_p) of monomers increases linearly with dipole moment of acrylates depending on secondary functionality [2, 4]. Boltzmann-averaged dipole moments ($\mu_{B,calc}$) of a large set of acrylates containing various secondary functionality and end groups were calculated and used as an index of polarity to compare those acrylates. The $\mu_{B,\ calc}$ values of HA analogues and BEA monomer were 1.83 D and 2.24 D, respectively. However, a direct correlation between

$R_{p,max}$ and $\mu_{B,\ calc}$ was found to be more valid when the dipole moments of neat acrylate monomers exceed 3.5 D [1]. Thus, the comparison of these $\mu_{B,\ calc}$ values was not sufficient to explain the higher reactivity of BEA.

The higher reactivity of BEA monomers could be more likely explained by hydrogen abstraction of labile hydrogens near the secondary ether functional groups [5, 13]. Stable peroxy radicals can be formed through hydrogen abstraction/oxidation on the ether linkage of growing BEA chains by accelerating the consumption of oxygen dissolved in and diffusing into the reaction system. The peroxy radicals would then able to abstract another labile hydrogen from adjacent ether groups of monomers or growing polymer chains, leading to reinitiation of radicals [5]. The diffusion of oxygen from the atmosphere was excluded due to the use of sealed capillary tubes; however, the recursive reaction would efficiently eliminate dissolved oxygen from the BEA polymerization system quicker, causing an increased polymerization rate. Since HA does not have abstractable hydrogens in its alkyl chains [14], the free-radical photopolymerization of HA would exhibit a lower polymerization rate and reach a final conversion slower.

Since DMPA is a Norrish Type I (α-cleavage) photoinitiator, intermolecular hydrogen abstraction is not needed to generate reactive radicals during the photodecomposition. Thus, the generation of initiating radicals from DMPA does not rely on the lability of abstractable hydrogen in the secondary functional groups. To elucidate hydrogen abstraction ability of the monovinyl acrylates associated with their secondary functional groups, the kinetics of neat acrylate systems were evaluated using the cationic photoinitiator (IHA) only (Figure 7.2). In the photolysis of IHA, one reactive radical is produced as a by-product in the presence of hydrogen donors via intermolecular hydrogen abstraction [15]. The free-radical photopolymerization of the BEA monomer was facilitated in the presence of IHA, which implies that the secondary ether oxygen could be involved in the generation of radical species via intermolecular hydrogen abstraction. However, the final conversion was relatively lower (~40%) than in the

presence of DMPA (~95%). No significant polymerization occurred in the neat HA system; thus, hydrogen abstraction was not prevalent, and the aryl radical was not reactive enough to initiate. These results support that hydrogen abstraction/oxidation associated with the secondary ether oxygen was responsible for the higher polymerization rate of BEA. The final theory based on hydrogen-bonding was not considered for HA and BEA because they are not capable of forming hydrogen bonds.

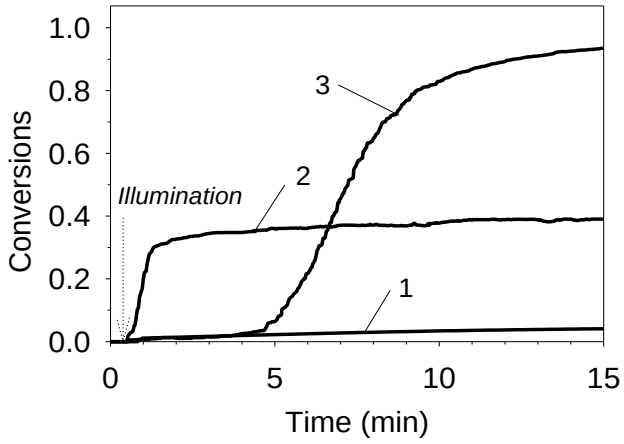

Figure 7.2 Real-time conversion profiles of neat acrylate systems with IHA only: (1)HA, (2) BEA, and (3) BCEA. [IHA] = 32 mM.

For the neat BCEA system, it is likely that the three factors work together to explain the faster polymerization rate and higher degree of conversion over other two acrylates (as shown in Figure 7.1). First, the $\mu_{B,calc}$ of a BCEA analogue is 3.23 D [2], which is higher than those of HA and BEA monomers and in the range of the linear relationship between $R_{p,max}$ and $\mu_{B,\,calc}$ [2, 4]. Second, there are obvious hydrogen-bonding effects associated with the urethane amide groups[1, 2]. Intermolecular hydrogen bonding between urethane groups could enhance the rate of polymerization through prealigned double bonds and increased formulation viscosity. Hence, radical propagation would

become more efficient, and radical termination could be reduced. Subsequently, an increase in radical concentration would result in early autoacceleration of the polymerization and enhanced polymerization rate. Finally, hydrogen abstraction could also take place from a two-carbon aliphatic spacer between the acrylic moiety and the secondary urethane group. Beckel *et al*. demonstrated the possibility of hydrogen abstraction using phenyl carbamate acrylates with a methyl-substituted aliphatic spacer at α and/or β positions [6]. They showed that hydrogen abstraction mostly occurs at the α carbon and results in a considerably increased rate of polymerization, while hydrogen abstraction from the β carbon minimally influences the rate of polymerization [6]. In Figure 7.2, polymerization of BCEA started slowly after 5-min illumination when the cationic photoinitiator IHA was used only. The overall polymerization of BCEA with IHA proceeded much slower than that of BEA, but reached higher conversions in the course of the polymerization time. This latent polymerization was also found in oligomeric urethane acrylates [16]. Thus, the hydrogen abstraction effect of the BCEA monomer seemed to be less pronounced in increasing the polymerization rate of BCEA, since BCEA was consumed very quickly within 5 sec in the presence of DMPA. Therefore, high polarity related to dipole moment and hydrogen-bonding capability together explain the high reactivity of BCEA over HA and BEA.

Effects of Monomer Compositions on Acrylate Reactivity

Various molar ratios of the acrylates to the diepoxide in the hybrid systems were examined using real-time Raman spectroscopy (Figures 7.3 and 7.4). Each acrylate was simultaneously photopolymerized with EEC using the dual photoinitiator system. To compare the reactivities, the maximum rate of polymerization, $R_{p,max}$, was calculated and normalized by the fractional concentration of the corresponding acrylates and diepoxide in their hybrid systems. In Figure 7.3, the $R_{p,max}$'s of the monovinyl acrylates showed different composition-dependent reactivity as a function of their secondary functional

groups. The reactivity of both HA and BEA showed a significant increase when 20% EEC was added by molar concentration as compared to their respective neat systems (Figure 7.3A).

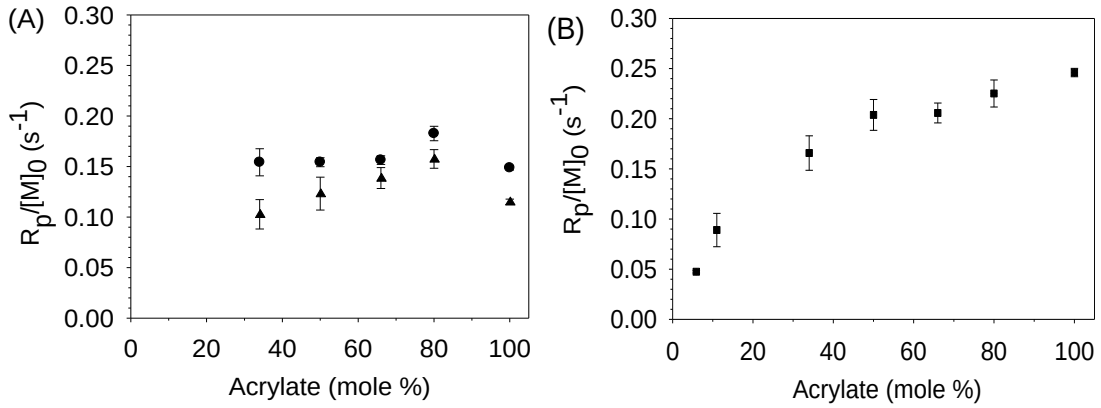

Figure 7.3 Effect of monomer compositions on the maximum rate of polymerization of the acrylate and diepoxide monomers during hybrid photopolymerizations: $R_{p,max}$ of HA (▲) and BEA (●) with EEC (A), and $R_{p,max}$ of BCEA (■) with EEC (B). [DMPA] = [IHA] = 32 mM for acrylates and diepoxide, respectively.

A plausible explanation of this enhancement might be attributed to the reduction of the coupling termination between active radicals due to increased viscosity of the polymerization systems by the addition of EEC to the formulation. However, no further enhancement in the reactivities of HA and BEA was observed as the EEC concentration exceeded 20%. The reactivity of HA tended to decrease as the concentration of EEC further increased in the HA/EEC systems. The reactivity of BEA seemed to be relatively less affected. Their overall polymerization rates indicated that the pure alkyl-containing HA monomer was more noticeably affected by the concentration of the diepoxide (EEC) than the ether-containing BEA monomer (Figures 7.3A and 7.4B). As a result, the reactivity and degree of conversion of BEA remained higher than that of HA over the given composition range of the respective hybrid systems (Figures 7.3A and 7.4A & B).

Although $R_{p,max}$ decreased with increasing EEC, the reactivities of both HA and BEA monomers in the presence of EEC were not diminished lower than that of their neat systems for the given composition range.

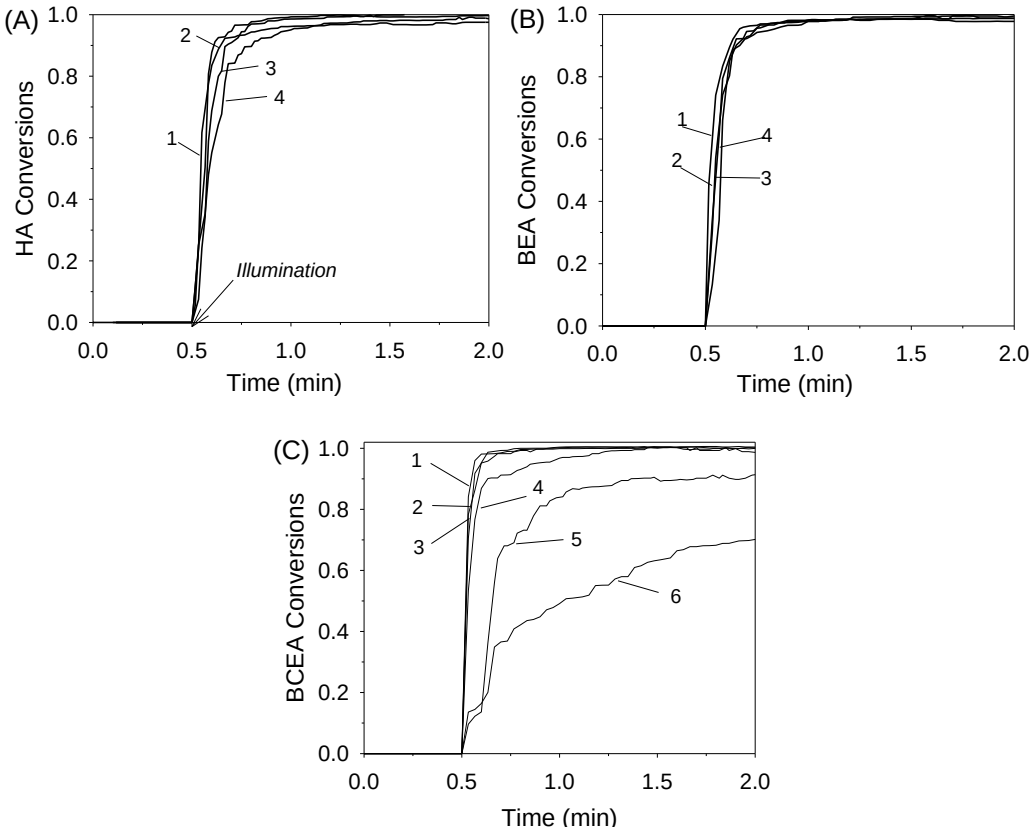

Figure 7.4 Effect of monomer composition on the free-radical photopolymerization of monovinyl acrylates during acrylate/epoxide hybrid photopolymerizations: HA (A), BEA (B), and BCEA (C) with EEC. For the HA/EEC and BEA/EEC systems, acrylate molar concentrations vary from 80% (1) to 66% (2) to 50% (3) to 33% (4). For the BCEA/EEC systems, acrylate molar concentrations vary from 80% (1) to 66% (2) to 50% (3) to 33% (4) to 11% (5) to 6% (6). [DMPA] =[IHA] = 32 mM for acrylates and diepoxide, respectively.

In contrast to the HA/EEC and BEA/EEC systems, the reactivity of BCEA continuously decreased with increasing EEC concentration (Figure 7.3B). In formulations

with 67% EEC, the $R_{p,max}$ of BCEA was 30% less than that of its neat system (Figure 7.3B), and its overall polymerization rate and degree of conversion began to decrease rapidly (Figure 7.4C) even though the viscosity of the hybrid systems increased upon the addition of the diepoxide monomer. In addition, the cationic photopolymerizations of the diepoxide (EEC) were significantly inhibited in the presence of BCEA (refer to results in Chapter 6).

These results indicate that the reactivity of the urethane-containing acrylate is affected by factors other than viscosity. Overall, these outcomes demonstrated that the subtle differences in secondary functional groups of the monovinyl acrylates mainly account for the difference in their composition-dependent reactivities during the acrylate/epoxide hybrid photopolymerization. However, it was not clear that the increased viscosity contributed solely to the abrupt increase in $R_{p,max}$'s of HA and BEA monomers in the presence of 20% EEC because the viscosity effect was negligible for BCEA/EEC systems with no polymerization of the EEC monomer. More insight is needed in order to understand why BEA maintained its reactivity regardless of the EEC content (except 20% EEC, when it increased) as compared to the HA monomer.

Thus, it was hypothesized that the polar nature of EEC might affect the acrylate reactivity in the small amount of the diepxoide. In addition, the role of the dual photoinitiator system was more carefully studied, since generation and consumption of radical species upon the photolysis of the radical photoinitiator (DMPA) is somewhat complex in the presence of the cationic photoinitiator (IHA), as discussed in the previous chapter.

Polarity Effect of Diepoxide

Polarity of the HA/EEC and BEA/EEC systems could increase if the EEC monomer containing one carbonyl ester and two ether groups acts as a highly polar solvent. Jansen *et al*. showed positive linear relationship between $\mu_{B,\,calc}$ and $R_{p,\,max}$ when

the $\mu_{B,\,calc}$ of the acrylate polymerization medium was adjusted from 2.05 D to 3.25 D by dilution with a highly polar inert solvent such as propylene carbonate (5.0 D); however, these results were found to be valid only up to 30 wt.% solvent [2, 4]. A strong solvent cage and a greater charge at the propagating radical accounted for the enhanced reactivity in a highly polar medium [2]. Thus, the free-radical photopolymerizations of the two acrylate monomers were evaluated for a tendency toward increasing $R_{p,max}$'s in the presence of small amounts of EEC.

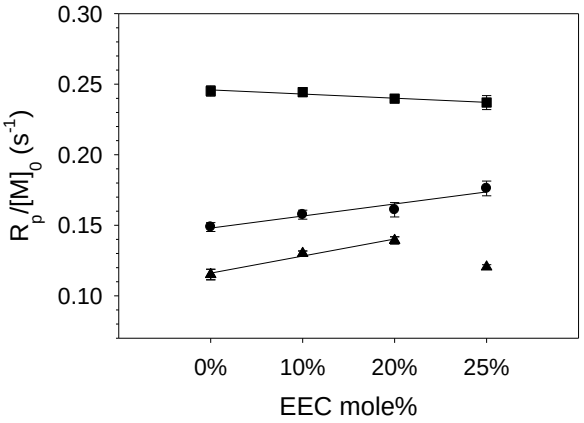

Figure 7.5 Effect of the presence of EEC on the maximum rate of polymerization of the acrylate free-radical photopolymerizations containing secondary functional groups: alkyl chains (HA, ▲), ether (BEA, ●), and urethane (■). [DMPA] = 32 mM for acrylates; no cationic photoinitiator (IHA) was used for the diepoxide (EEC).

Indeed, as shown in Figure 7.5, the reactivity of HA and BEA increased with increasing EEC concentration up to 20-25% molar concentration. This result agreed with the dipole moment theory described. In contrast, no polarity effect of the diepoxide was observed for BCEA (Figure 7.5). The decrease of $R_{p,max}$ of BCEA was proportional to the increase of EEC and resulted in low polymerization rates compared to the neat BCEA monomer for the given composition range.

Beckel *et al*. also reported similar results in which the theorized increase of $R_{p,max}$ was not observed for various phenyl carbamate acrylates ($\mu_{B,\ calc}$ = 1.8-3.7 D) with the addition of propylene carbonate ($\mu_{B,\ calc}$ = 5.0D), a highly polar solvent [8]. The reduced reactivity of those acrylates was attributed to simple dilution of monomer concentration. Similarly, that dilution effect could affect BCEA reactivity in the presence of the diepoxide. Moreover, the suppression of the EEC cationic photopolymerization by the secondary urethane group (as discussed in Chapter 6) may cause the reactivity of the BCEA monomer to be more controlled by the dilution effect of the uncured diepoxide than compared to the HA/EEC systems.

In summary, the abrupt increase and decrease of $R_{p,max}$ for the HA and BEA by 20% EEC, as shown in Figure 7.5 may be attributed to polarity and dilution effects of the diepoxide monomer; whereas, the dilution effect could be the primary reason for the continuous decrease of $R_{p,max}$ of BCEA, which contains a secondary urethane group .

Effect of the Dual Photoinitiator System on $R_{p,max}$

As shown in Figure 7.3, when both HA and BEA were further diluted with over 20% of the EEC monomer, the $R_{p,max}$ of BEA remained the same, while those of HA decreased with the same scale of the dilution. The proportional decrease in $R_{p,max}$ for the HA monomer can be attributed to the reduced monomer concentration, as discussed for the BCEA/EEC system in Figures 7.3B and 7.5. However, the dilution effect of the diepoxide was not pronounced in the BEA/EEC systems because the overall reactivities of BEA similar to that of its neat monomer system (Figures 7.3A and 7.4). It was not clear whether the constant reactivity of BEA in the hybrid systems was related to the presence of abstractable hydrogen. The cationic photoinitiator in the dual photoinitiator system might produce additional radical species via hydrogen abstraction from the hydrogen donors during the photolysis [15]. If additional radicals were generated on the growing BEA polymer chains, the recursive hydrogen abstraction/oxidation process

could effectively consume the dissolved oxygen and promote the reinitiation of radicals. In general, the relative concentration of IHA in the acrylate volume fraction increased with increasing diepoxide concentration in the hybrid systems. Consequently, the dilution effect of the diepoxide in the BEA/EEC systems might be offset to a large degree by the hydrogen abstraction/oxidation process.

In addition, it was not clear whether protonic acids generated by the photolysis of IHA would have an influence on the free-radical photopolymerizations of the monovinyl acrylates. According to the recent studies on the sensitivity to acid inhibition for highly reactive (meth)acrylate monomers [17, 18], strong protonic acids influence the reactivity of monovinyl acrylates by forming a radical-acid complex [18]. Beckel *et al*. proposed small amounts (~0.05wt%) of a strong acid would not influence the free-radical polymerizations of traditional acrylates, such as hexandiol diacrylate and tetrahydrofurfuryl acrylate, but would severely inhibit those of highly reactive acrylates containing a secondary cyclic carbonate and/or carbamate group [17]. However, further studies by Kilambi revealed that the free-radical photopolymerization rates of the traditional acrylates, such as hexyl acrylate (HA), are also greatly inhibited, depending on acid concentration (0.1-1 wt.%) and strength [18].

To elucidate the role of the dual photoinitiator system in this regard, the dilution effects of the diepoxide needed to be removed. To do so, the free-radical photopolymerization of each neat acrylate without the diepoxide was characterized using the dual photoinitiator system with varying DMPA/IHA ratios. In this regard, two hypotheses were established: (1) the reactivity of BEA will increase in proportion to the concentration of IHA and (2) the reactivity of the three acrylates will be negatively affected when the concentration of IHA is much greater than that of DMPA (*i.e.*, very low DMPA/IHA ratio).

In Figure 7.6, the reactivity of each acrylate was compared to $R_{p,max}$. The reactivity order of the three acrylates remained the same as in the neat systems containing

DMPA only. Contradictory to the first hypothesis, the $R_{p,max}$ of BEA was not enhanced as the IHA concentration increased up to four times greater than DMPA. On the other hand, the second hypothesis was partially validated: the $R_{p,max}$ of BCEA noticeably decreased from [DMPA]/[IHA] = 1, but the $R_{p,max}$, of HA and BEA was not influenced by the DMPA/IHA ratios.

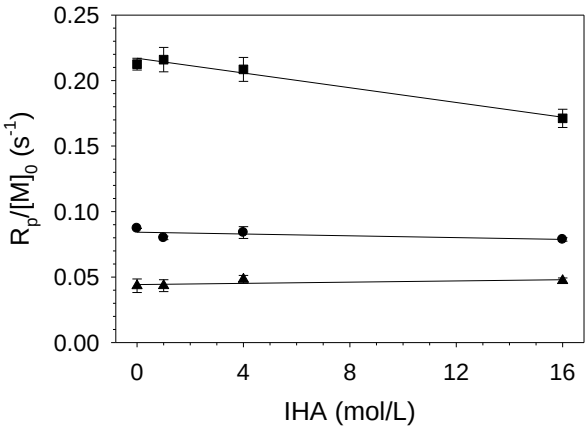

Figure 7.6 Effect of the dual photoinitiator system on the maximum rate of polymerization of the acrylates containing secondary functional groups: alkyl chains (HA, ▲), ether (BEA, ●), urethane (BCEA, ■). [DMPA] = 4 mM and [IHA] = 0 to 16 mM for acrylates. Photopolymerizations in real time were conducted at 25°C with effective irradiance =100 mW/cm^2 for the filtered wavelength regions.

These results can be understood by taking into consideration photon absorption competition between the two photoinitiators that absorb photons at unequal rates. Upon illumination, the radical photoinitiator begins to be decomposed quickly before the cationic photoiniator undergoes photolysis to generate the protonic acids because of the higher photon absorption of DMPA in the strong light emission region [19]. Once DMPA is photodecomposed, it generates benzoyl and dimethoxy benzyl radicals. The former radical is responsible for the conversion of carbon double bonds, whereas the latter is not

[20]. The electron-donating dimethoxy benzyl radical encounters undecomposed IHA and undergoes a redox reaction by which IHA is reduced to produce a carbocation before the dimethoxy benzyl radical is further decomposed to another reactive methyl radical. Thus, it is highly likely that a large fraction of the IHA molecules are initially decomposed by this redox process (cross-reference discussion in Chapter 6) [19, 21] in which the hydrogen abstraction associated with the secondary ether oxygen is not involved. As a result, the $R_{p,max}$ of BEA showed no independence on the DMPA/IHA ratios in the dual photoinitiator system.

Effect of the Dual Photoinitiator System on Degree of Conversion

Conversions of the monovinyl acrylates above their $R_{p,max}$ were also compared in Figure 7.7. Here, the degree of conversion of HA and BEA tended to rapidly decrease as a function of the DMPA/IHA ratio, especially between zero to one; however, the degree of conversion was much less variable at a low concentrations of IHA (Figures 7.6A and B). In contrast, the degree of conversion of BCEA was less dependent on the DMPA/IHA ratio at the given conditions (Figure 7.7C) [22, 23]. As discussed in the previous section, the photolysis of DMPA generates benzoyl and dimethoxy benzyl radicals. The latter electron-donating species can be further decomposed to a reactive methyl radical and initiate the free-radical polymerization if the electron-donating species is not consumed by the redox reaction with IHA. Thus, increasing the IHA concentration over DMPA could cause a proportional decrease in the concentration of total initiating radicals by interrupting the decomposition of the dimethoxy benzyl radicals via the redox process. Lower ultimate conversion would result, especially for neat HA and BEA systems (Figures 7.7A and B). However, the degree of conversion of BCEA could be less affected because BCEA had higher $R_{p,max}$ than the other two acrylates in the various DMPA/IHA ratios, even considering that the $R_{p,max}$ was reduced by the increase of the IHA concentration in the dual photoinitiator system. Accumulation of protonic acids seemed

to have a marginal effect on the degree of conversion at later stages of the polymerization for [DMPA]/[IHA] ≥ 1 (Figure 7.7).

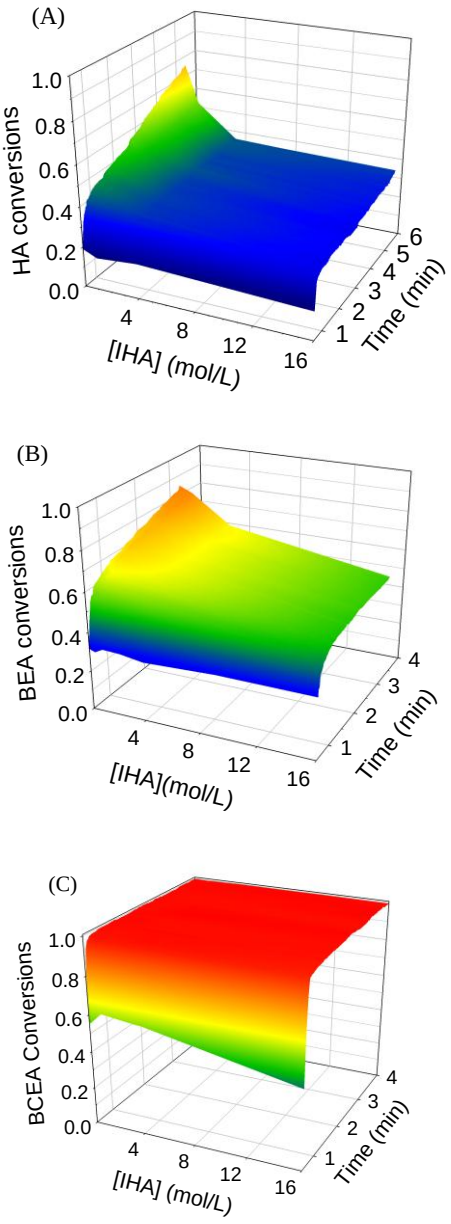

Figure 7.7 Effect of DMPA/IHA ratios on ultimate conversion of acrylates containing secondary functional groups: aliphatic carbon (HA, A), ether (BEA, B), and urethane (BCEA, C). [DMPA] = 4 mM and [IHA] = 0, 1, 4, and 16 mM.

The marginal effect of the acid inhibition on the degree of conversion is also expected in the hybrid systems because the protonic acids are simultaneously consumed by the cationic photopolymerization. Moreover, the ultimate conversion showed the same trend as the reactivity among the monovinyl acyrlates, which reiterates the importance of the acrylate secondary functionality on the degree of conversion. Therefore, the acid inhibition in the acrylate/hybrid systems studied here was a marginal factor for both reactivity and the degree of conversion when using the dual photoinitiator. Rather, the depletion of the initiating radical species via redox process proved a key factor. In addition, hybrid systems containing acrylates without labile hydrogen and/or hydrogen bonding capability, such as HA, may need a high initial concentration of DMPA in the presence of IHA, since the final conversions of neat HA were quite low with the DMPA/IHA ratio ≤ 1 (compare Figure 7.7A with Figure 4A).

Conclusions

This research has systematically demonstrated the effect of diepoxide and a dual photoinitiator system on kinetics and degree of conversion of three model monovinyl acrylates with different secondary functional groups including aliphatic carbon (HA), ether (BEA), urethane (BCEA) groups. The neat monovinyl acrylate systems exhibited different reactivities when comparing their normalized maximum rate of polymerization ($R_{p,max}$): BCEA >> BEA > HA. Comparison of the secondary functional groups implied that hydrogen-abstraction availability and hydrogen-bonding capability were responsible for the higher reactivities of BEA and BCEA, respectively. In the acrylate/epoxide hybrid systems, the monomer composition was considered a key factor affecting the reactivities of the acrylates. The polarity effect of the dipoxide was found to enhance $R_{p,max}$ of both HA and BEA when the more polar diepoxide was introduced up to the limiting concentration, at which the direct correlation between dipole moment and the rate of polymerization is valid. Above the limiting diepoxide concentration, the dilution effect of

the diepoxide began to play a role in affecting $R_{p,max}$, especially for HA; however, the reactivity of BEA was similar to that of its neat system. The difference in monomer composition-dependent kinetic behavior was attributed to the lability of abstractable hydrogens associated with the secondary ether group that may counterbalance the dilution effect by the reduced acrylate monomer concentration. On the other hand, the $R_{p,max}$ of BCEA, which is capable of hydrogen-bonding capable, was solely influenced by the dilution effect of the diepoxide and resulted in a continuous decrease of the reactivity with increasing diepoxide concentration in the corresponding hybrid systems.

The dual photoinitiator system used for the simultaneous initiation of the free-radical and cationic photopolymerizations was carefully evaluated for the monovinly acrylates without the diepoxide. To discern the role of each photoinitiator, various DMPA/IHA molar ratios were examined. The maximum polymerization rates of HA and BEA showed no dependence on the DMPA/IHA ratios, but BCEA exhibited decreased reactivity as the IHA proportion increased in the dual photoinitiator system. In contrast, the degree of conversion significantly affected for HA and BEA when the DMPA/IHA ratio $\leq$ 1. However, again, BCEA remained relatively constant. Photon absorption competition between the radical (DMPA) and cationic photoinitiators (IHA) was found to be critical in understanding this effect. Sensitivity of the acid inhibition and redox process were carefully assessed, and the reactivities of HA and BEA were not sensitive to the acid inhibition associated with the concentration of the protonic acids generated from IHA. This insensitivity stemmed from the photolysis of the cationic photoinitiator being initially delayed or proceeding slowly due to the redox process. Meanwhile, the redox process tended to lower the concentration of initiating radical species that further facilitate the free-radical photopolymerization. This reduced radical active center concentration resulted in decreased degree of conversion after the maximum rate of polymerization for HA and BEA. Thus, in the hybrid systems containing acrylates without labile hydrogens and/or hydrogen-bonding capability (*e.g.*, HA), a high initial

concentration of DMPA in the presence of IHA was needed. In contrast to HA and BEA, BCEA (with its higher susceptibility to acid inhibition) exhibited decreased reactivity with increasing IHA concentration in the dual photoinitiator system. However, the degree of conversion was most likely not affected by the redox process.

Therefore, designing formulations containing acrylates and epoxides requires accounting for polarity and dilution effect of epoxide monomers and selecting acrylates with appropriate secondary functionalities. Doing so enables tuning of the kinetics and degree of conversion for each monomer in hybrid photopolymerizations, which in turn produces desirable properties of final IPNs. Finally, these findings provide fundamental guidelines to optimize industrially relevant formulations and reaction conditions for thin-film and coating applications using these acrylate/epoxide hybrid photopolymerizations.

Notes

1. Jansen, J.F.G.A.D., Aylvin A. Dorschu, Marko and Coussens, B., *Effect of Preorganization Due to Hydrogen Bonding on the Rate of Photoinitiated Acrylate Polymerization*, in *Photoinitiated Polymerization*, K.D. Belfield and J.V. Crivello, Editors. 2003, American Chemical Society. p. 127-139.

2. Jansen, J.F.G.A., Dias, A.A., Dorschu, M., and Coussens, B., *Fast Monomers: Factors Affecting the Inherent Reactivity of Acrylate Monomers in Photoinitiated Acrylate Polymerization.* Macromolecules, 2003. 36(11): p. 3861-3873.

3. Jansen, J.F.G.A., Dias, A.A., Dorschu, M., and Coussens, B., *Effect of Preorganization Due to Hydrogen Bonding on the Rate of Photoinitiated Acrylate Polymerization*, in *Photoinitiated Polymerization*, K.D. Belfield and J.V. Crivello, Editors. 2003, American Chemical Society. p. 127-139.

4. Jansen, J.F.G.A., Dias, A.A., Dorschu, M., and Coussens, B., *Effect of Dipole Moment on the Maximum Rate of Photoinitiated Acrylate Polymerizations.* Macromolecules, 2002. 35(20): p. 7529-7531.

5. Lee, T.Y., Guymon, C.A., Jonsson, E.S., and Hoyle, C.E., *The effect of monomer structure on oxygen inhibition of (meth)acrylates photopolymerization.* Polymer, 2004. 45(18): p. 6155-6162.

6. Beckel, E.R., Stansbury, J.W., and Bowman, C.N., *Effect of Aliphatic Spacer Substitution on the Reactivity of Phenyl Carbamate Acrylate Monomers.* Macromolecules, 2005. 38(8): p. 3093-3098.

7. Berchtold, K.A., Nie, J., Stansbury, J.W., HacioÇ§lu, B., Beckel, E.R., and Bowman, C.N., *Novel Monovinyl Methacrylic Monomers Containing Secondary Functionality for Ultrarapid Polymerization: Steady-State Evaluation.* Macromolecules, 2004. 37(9): p. 3165-3179.

8. Beckel, E.R., Nie, J., Stansbury, J.W., and Bowman, C.N., *Effect of Aryl Substituents on the Reactivity of Phenyl Carbamate Acrylate Monomers.* Macromolecules, 2004. 37(11): p. 4062-4069.

9. Lee, T.Y., Roper, T.M., Jönsson, E.S., Guymon, C.A., and Hoyle, C.E., *Influence of Hydrogen Bonding on Photopolymerization Rate of Hydroxyalkyl Acrylates.* Macromolecules, 2004. 37(10): p. 3659-3665.

10. Kilambi, H., Reddy, S.K., Schneidewind, L., Lee, T.Y., Stansbury, J.W., and Bowman, C.N., *Design, Development, and Evaluation of Monovinyl Acrylates Characterized by Secondary Functionalities as Reactive Diluents to Diacrylates.* Macromolecules, 2007. 40(17): p. 6112-6118.

11. Berchtold, K.A., Nie, J., Stansbury, J.W., and Bowman, C.N., *Reactivity of Monovinyl (Meth)acrylates Containing Cyclic Carbonates.* Macromolecules, 2008. 41(23): p. 9035-9043.

12. Cai, Y. and Jessop, J.L.P., *Decreased oxygen inhibtion in photopolymerized acrylate/epoxide hybrid polymer coatings as demonstrated by Raman Spectroscopy.* Polymer, 2006. 47: p. 6560-6566.

13. Andrzejewska, E. and Andrzejewski, M., J. Polym. Sci., Part A: Polym. Chem., 1998. 36(null): p. 665.

14. Moussa, K. and Decker, C., *Light-induced polymerization of new highly reactive acrylic monomers.* Journal of Polymer Science Part A: Polymer Chemistry, 1993. 31(9): p. 2197-2203.

15. Crivello, J.V., *The Discovery and Development of Onium Salt Cationic Photoinitiators.* Journal of Polymer Science: Part A: Polymer Chemistry, 1999. 37: p. 4241-4254.

16. Eom, H.S. and Jessop, J.L.P., *Epoxide/urethane acrylate hybrid photopolymerizations to minimize atmospheric sensitivity: Understanding the interplay between viscosity and dual photoinitiator system*, in *Basics and Applications of Photopolymerization Reactions*, J.P. Fouassier and X. Allonas, Editors. 2010. p. 39-52.

17. Beckel, E.R., Stansbury, J.W., and Bowman, C.N., *Evaluation of a Potential Ionic Contribution to the Polymerization of Highly Reactive (Meth)acrylate Monomers.* Macromolecules, 2005. 38(23): p. 9474-9481.

18. Kilambi, H., Konopka, D., Stansbury, J.W., and Bowman, C.N., *Factors affecting the sensitivity to acid inhibition in novel acrylates characterized by secondary functionalities.* Journal of Polymer Science Part A: Polymer Chemistry, 2007. 45(7): p. 1287-1295.

19. M. Degirmenci, Y.H., Y. Yagci, *One-step, one-pot Photoinitiation of Free Radical and Free Radical Promoted Cationic Polymerizations.* Journal of Applied Polymer Science, 2002. 85: p. 2389-2395.

20. Hageman, H.J., Van der Maeden, F.P.B., and Janssen, P.C.G.M., *Photoinitiators and photoinitiation, 1. Vinyl polymerization photoinitiated by benzoin methyl ether.* Die Makromolekulare Chemie, 1979. 180(10): p. 2531-2537.

21. Dursun, C., Degirmenci, M., Yagci, Y., Jockusch, S., and Turro, N.J., *Free radical promoted cationic polymerization by using bisacylphosphine oxide photoinitiators: substituent effect on the reactivity of phosphinoyl radicals.* Polymer, 2003. 44(24): p. 7389-7396.

22. Fouassier, J.P., *Photoinitiation, Photopolymerization, and Photocuring*. 1st ed. 1995, Munich, New York: Hanser Publishers.

23. Fouassier, J.-P. and Merlin, A., *Laser investigation of norrish type I photoscission in the photoinitiator irgacure (2,2-dimethoxy 2-phenyl-acetophenone).* Journal of Photochemistry, 1980. 12(1): p. 17-23.

CHAPTER 8
CONCLUSIONS AND RECOMMENDTAIONS

In this contribution, slow polymerization of epoxides at room temperature and brittleness of the final cured polymers through photopolymerizations of multicomponent epoxides and acrylate/epoxide hybrid mixtures have been addressed. A cycloaliphatic diepoxide was used as a model compound that exhibits the aforementioned problems that needs to be enhanced as discussed in the background. Hence, this diepoxide was consistently used while other components were differed for each photopolymerization system.

The goal of this research was to provide fundamental knowledge regarding the polymerization kinetics and physical properties of the resulting polymers for these two promising photopolymerization systems. To achieve this goal, several variables including monomer/oligomer structures, viscosity, compositions, and photoinitiator system were hypothesized to play important roles in controlling photopolymerizations of the two epoxide-based mixtures. Results showed that these variables have combined effects on photopolymerizations kinetics and ultimate properties for these two distinct epoxide-based mixtures.

Through photoinitiated cationic copolymerization, photopolymerization rate and ultimate conversion of the diepoxide were enhanced in the presence of the epoxidized elastomers. Specifically, it was found that monomer/oligomer compositions and oligomer structure (internal epoxide content) are predominant factors to achieve significant enhancement in ultimate properties of the final cured copolymers. For acrylate/epoxide hybrid photopolymerization, acrylates structures were found to be the most important factor among the variables that affects polymerization rates and ultimate conversion of the cycloaliphatic (mono)diepoxide. Combined effects of viscosity and dual photoinitiators were important to significantly enhance the polymerization rate and

ultimate conversions of the diepoxide. Monomer composition and acrylate structures mainly controlled ultimate properties of the final cured hybrid polymers. For both photopolymerization systems, the presence of the cycloaliphatic epoxide also has a pronounced effect on photopolymerization kinetics and ultimate conversion of the other reactive oligomers and monomers. Ultimate properties of polymers produced from two reaction mixtures generally exhibited brittleness in the presence of a high amount of the cycloaliphatic epoxide over 50%.

Ultimately, this research can provide a fundamental guideline for industrial applications that use systems comparable to the photoinitiated cationic copolymerizations and acrylate/epoxide hybrid photopolymerization systems studied here. In addition, it is anticipated that photopolymerization systems of multifunctional cycloaliphatic epoxide-based mixtures receive more attention as an alternative for conventional, ubiquitous epoxide resins based on chemical derivatives of bisphenol A which is recently known for its ultralow dose hormone disruptor. In this chapter, the major conclusions of the research on the photopolymerizations of multicomponent epoxide-based mixtures will be overviewed for each chapter and recommendations for future research into these areas will be suggested.

Photoinitiated Cationic Copolymerizations of Cycloaliphatic Diepoxide with Elastomeric Oligomers

As illustrated in Chapter 3, the epoxide-based mixtures studied contain two distinct types of epoxides and hydroxyl groups that provide a complexity of photoinitiated cationic copolymerizations. With this condition, understanding of the cationic propagation reaction of the two types of epoxides was a key to elucidate the difference in the kinetic behavior of the cycloaliphatic diepoxide and the epoxidized oligomers. Results showed that the monotonic increase in the polymerization rate and ultimate conversion of the diepoxide with increasing oligomer content was mainly attributed to the contribution of the activated monomer mechanism associated with

hydroxyl terminal groups in the oligomers. At high epoxidized oligomer levels, the kinetic studies revealed that the cationic photopolymerization of the diepoxide may be affected by the viscosity of the bulk mixture systems as a function of the oligomer content. When the internal epoxide of the epoxidized elastomeric oligomer was monitored, the addition of the diepoxide reduced the rate of polymerization and degree of conversion for the epoxidized oligomers. The reduction in the kinetics was more pronounced for the oligomer containing the low internal epoxide content. In the case of higher amounts of the diepoxide from 50% to 90%, the initial reactivities of the internal epoxides in the oligomer are essentially zero. These results indicated the reactivity of the terminal hydroxyl groups is higher toward cationic active centers of the cycloaliphatic diepoxides than those of internal epoxides in the epoxidized oligomers. Considering binary compositions of the two reactive epoxides, another ordinary propagation reaction via the active chain end mechanism also coexists as illustrated in Chapter 2.

In consideration that a small amount (~0.5 wt.%) of the photoinitiator was used and high viscosity of the epoxidized oligomers, the observed enhancement of the polymerization rate and ultimate conversion of the cycloaliphatic epoxide is very promising for practical applications. The reason for using a small amount of the photoinitiator is that there is a solubility issue with the epoxidized oligomer at higher photoinitiator concentrations. The solubility of the photoinitiator in the epoxidized oligomers can be increased if it is dissolved in a solvent prior to mixing with the epoxide mixtures. However, several factors (e.g. polarity, basicity, miscibility, and viscosity) associated with a solvent should be addressed. In addition, validation of the long term stability of the photoinitiator in a solvent is recommended. For example, in this research a commercial sulfonium salt-type photoinitiator was initially tried because it comes in propylene carbonate. However, some diepoxide/oligomer mixtures often turned opaque after short term storage.

To further enhance polymerization rates and ultimate conversions of both diepoxide and oligomers at room temperature, the incorporation of additional alcohols with small molecular weight may be useful due to a combined contribution of the AM mechanism and this would reduce viscosity. For this ternary system, it will be necessary to carefully select the alcohols and finely optimize mixture composition.

To give a more comprehensive guideline for industrial applications, more diverse cycloaliphatic epoxides with different epoxide functionality will be interesting for this photopolymerization system. In addition, cycloaliphatic diepoxides without the nucleophilic ester carbonyl or with different space length between the epoxide rings may give enhanced versatility for industrially significant applications. Furthermore, dark or shadow photopolymerizations for cycloaliphatic epoxide-based multicomponent mixtures will also give a useful knowledge for applications for which full illumination is limited and enhanced flexibility or toughness is required. In this case, interplay between various variables that control cationic active center migration should be experimentally assessed.

Relationship between Kinetic Behavior and Ultimate Properties of Copolymers Produced By Photoinitiated Cationic Polymerization

As illustrated in Chapter 4, the cured cycloaliphatic diepoxide polymer exhibited brittle properties characterized by high glass transition temperature and high Young's modulus. In addition, its facture toughness and impact resistance were relatively low. This brittleness was modified by the photoinitiated cationic copolymerization with the epoxidized elastomeric oligomers. The fracture toughness increased with increasing the oligomer content from 10% to 90%. The highest fracture toughness and highest impact resistance were observed for the oligomer contents of 70 -80%. These enhanced properties were attributed to the multimodal network chain length distribution. The epoxidized oligomer containing relatively lower internal epoxide content exhibited much higher toughness and impact resistance. The glass transition temperature (a location of

δ_{max}) and Young's modulus of the final cured copolymers monotonically decreased with increasing oligomer content. The ultimate tensile strength increased with increasing the oligomer content up to 30%, and then decreased monotonically.

Interestingly, the data trend obtained from the kinetic studies was consistent with physical properties when two sets of copolymers that differed by oligomer structure (internal epoxide content) were compared (Chapters 3 vs. 4). In Chapter 3, results showed that in high amounts of the diepoxide above ~50wt.%, the initial polymerization rates of the epoxidized oligomers were essentially zero, but the initial polymerization rates and ultimate conversion of the diepoxide were much higher than those of the oligomers. In this composition range, the ultimate conversions of the diepoxide were almost same for the two separate copolymerization systems containing two respective oligomers that differed by internal epoxide content. In the same way, Young's modulus, ultimate strength, elongation-at-break, fracture toughness, and impact resistance were also similar between the two copolymers in the similar composition range. With the diepoxide content lower than 50wt.%, the initial polymerization rates and ultimate conversion of the internal epoxides of the two different oligomers deviated from one another, and the ultimate conversions of the internal epoxides differed by 15% on average between the two oligomers. Similarly, physical and mechanical properties including glass transition temperature, storage/Young's modulus at room temperature, crosslink density, fracture toughness, and impact resistance deviated from one another. The consistent, deviated results found from the similar composition regime illustrated a clear link between the kinetic behavior and ultimate properties of the two different copolymerization systems.

Although crosslink density and phase behavior of photopolymerized homo/copolymers were provided, there is still a lack of direct information about network structure. For example, an understanding of swelling behavior of the photopolymerized copolymers correlated with some network model theories may help to obtain a more improved relationship between polymer structure and ultimate properties.

In addition, it was assumed that our cationic copolymerization systems containing the cycloaliphatic diepoxide and the epoxidized oligomer would be less sensitivity to atmospheric water due to two reasons. First, it was reported that cationic photopolymerization of cycloaliphatic diepoxide are monotonically accelerated with increasing humidity. This acceleration that prevails at the air/interface coating will increase a surface viscosity, thereby decreasing further the diffusion of atmospheric water into the reaction system. Similarly, an increased viscosity of bulk mixtures due to the epoxidized oligomer may help to prevent continuous diffusion of atmospheric water in the initial stage of the photopolymerization. To confirm this promising assumption, surface property tests or morphological studies for the copolymers photopolymerized under different humidity will be useful because cationic propagation reaction of conventional epoxides is known to be sensitive to humidity.

Finally, for photoinitiated cationic shadow copolymerization systems performance of shadow cured polymers should be compared to fully illuminated polymers for validation purposes.

Urethane Acrylate/epoxide Hybrid Photopolymerizations

Photopolymerizations of urethane acrylate oligomer/cycloaliphatic epoxide hybrid mixtures were illustrated in Chapter 5. The kinetics of hybrid photopolymerizations containing cycloaliphatic epoxides and urethane acrylates was greatly affected by formulation viscosity and relative photoinitiator concentration. In this study, two urethane diacrylate oligomers were used. These diacrylate oligomers have similar structures but differ in viscosity. In general, increasing the diacrylate oligomers in the formulation suppresses the cationic polymerization of the cycloaliphatic mono/diepoxides. This trend was more pronounced with a higher viscosity diacrylate oligomer. In contrast, increasing the epoxide concentration in the formulation promoted the free-radical polymerization of the diacrylate oligomers via the diluent effect. The major reasons for the suppressed

kinetic behavior of the epoxides are the increased viscosity of hybrid mixtures and formation of an acrylate polymer network early in the illumination period. With the dual photoinitiator system containing a free radical and cationic photoinitiators, increasing the IHA concentration relative to the epoxide concentration does not result in higher epoxide conversion but rather increased diacrylate conversion.

The initial concept for the hybrid mixtures was to increase insensitivity of the free-radical and cationic photopolymerizations to atmospheric oxygen and water, respectively. It was assumed that the initial concept would be realized by increased viscosity at the air/coating interface caused by the high viscosity and high hydrophobicity of urethane diacrylate oligomers as well as epoxide conversion at the surface. However, it was difficult to distinguish various factors such as monomer structure from the viscosity effect, and it was necessary to more clearly understand the role of the dual photoinitiator system in the hybrid photopolymerization. Therefore, the surprising results that were not expected led to the initiative to explore the effects of monomer structures on photopolymerization kinetics of each monomer component.

In the presence of the urethane diacrylate oligomers, the kinetic behavior of the cycloaliphatic diepoxide was quite different from the previous results with the epoxidized oligomers (Chapter 3 vs. 5). These two opposite results also exemplify how important an oligomer structure is for the cationic photopolymerizations of the cycloaliphatic epoxide when considering the similar viscosity between the two distinct oligomers. Accordingly, when a high viscosity acrylate oligomer is introduced a hydroxyl-containing compound of a low viscosity will help to enhance the polymerization rate and ultimate conversion of the cycloaliphatic epoxide. In this approach, it will be necessary to thoroughly understand the effect of alcohol structure on both free-radical and cationic propagation reactions in a systematic way.

Acrylate/epoxide Hybrid Photopolymerizations: Effects of Acrylate Secondary Functionality of Reactivity of Diepoxide

In Chapter 6, the effects of the molecular structure of acrylates on the kinetics of epoxide cationic photopolymerizations during acrylate/epoxide hybrid photopolymerization were systematically demonstrated. Specifically, it was hypothesized that non-vinyl secondary functional groups of acrylates have a great impact on the reactivity of epoxide monomers. The structural characteristics of the secondary functional groups are associated with viscosity, polarity/solvation, and nucleophilicity/basicity of acrylates. These key factors can influence the chemical environment of epoxide monomers undergoing cationic ring-opening polymerization. Results showed that these factors associated with the acrylate secondary functional groups have interactive effects on the cationic photopolymerization of the cycloaliphatic diepoxide. For example, significant enhancement in the polymerization rate and degree of conversion of the diepoxide was achieved when the dilution effect was synergistically coupled with the radical-promoted cationic polymerization induced by the dual photoinitiator system. In addition, the synergetic effects depended greatly on the type of secondary functional group on the acrylate and their concentration in hybrid systems. In the presence of the secondary alkyl group, an over 7-fold increment in $R_{p,max}$ was found for a wide range of composition. However, in the presence of the secondary ether group, a 7-fold enhanced $R_{p,max}$ was obtained only when a low concentration of the secondary ether group was introduced; otherwise, the diepoxide reactivity tended to decrease with an increase in the concentration of the secondary ether group. The different epoxide reactivities, with subtle difference in the molecular structure of the acrylates, were attributed to solvating power associated with the ether oxygen. In contrast, the presence of the secondary urethane group completely suppressed the photoinitiated cationic ring-opening polymerization of the diepoxide. The complete inhibition of the cationic photopolymerization was attributed

to the combined nucleophilicity and strong basicity associated with ester carbonyl and urethane amine in the urethane structure.

In industry, it is a common practice to use low light intensity (< 50 mW/cm^2) and low photoinitiator concentration in order to reduce the manufacturing cost. From a general relationship between light intensity and polymerization kinetics, the low intensity light will further increase a disparity in polymerization rate and ultimate conversion between acrylates and epoxides, and the acrylate secondary functionality effects will be more pronounced. For acrylate/hybrid mixtures containing the dual photoinitiator system, spectral response of cationic photoinitiators can be further enhanced in the presence of the free-radical photoinitiator used in this research. This enhanced spectral response of cationic photoinitiators will allows one to reduce its concentration. Furthermore, the influence of the acrylate secondary functional groups on cationic photopolymerizations of different types of epoxides will show a similar trend for comparable hybrid systems. Therefore, the findings from this research can provide profound insights into reaction formulation for various acrylate/epoxide hybrid photopolymerizations.

For new hybrid systems, if multifunctional acrylates containing more than two C=C bonds are considered, it will be more beneficial to compare kinetic behavior of epoxides for two different acrylate concentration regimes. For example, at a low concentration regime, non-vinyl functionalities of the acrylates will be a dominant factor that affects the kinetics of the epoxides. On the other hand, at a high concentration regime, cationic ring-opening polymerizations will be rapidly diffusion-controlled early in the illumination period due to rapid formation of highly crosslinked acrylate networks. In this situation, the high number of carbon double bonds will dictate other factors affecting the kinetics of epoxides. In addition, other interesting options will be monovinyl acrylate oligomers or polybutadiene acrylate oligomers.

Acrylate/epoxide Hybrid Photopolymerizations: Effects of Diepoxide and Dual Photoiniator on Reactivity of Acrylates

In Chapter 7, the effects of the cycloaliphatic diepoxide and the dual photoinitiator systems on free-radical photopolymerizations of three monovinyl acrylates were demonstrated. The reactivity of the model acrylates (characterized by normalized maximum rate of polymerization) depended on their secondary functionalities which include alkyl carbon, ether, and urethane groups. The latter two secondary functional groups provided hydrogen abstraction and hydrogen bonding capability for the corresponding acrylates. Accordingly, the kinetic behavior of these monovinyl acrylates was differently affected by the diepoxide.

Polarity and dilution effects associated with the diepoxide were considered as a function of monomer composition. With low diepoxide contents, the $R_{p,max}$ of the acrylates containing aliphatic carbon and ether secondary groups increased monotonically with increasing the diepoxide content. Above the limit concentration, the reactivities of the two acrylates suddenly decreased to the levels of their neat acrylate system. The two acrylates showed different reactivity when the reaction mixtures were further diluted by the diepoxide: the alkyl carbon-containing acrylate showed continuous decrease in the $R_{p,max}$ whereas the reactivity of the ether acrylate remained same. Compared to the alkyl carbon acrylate, the different kinetic behavior of the ether acrylate was attributed to the secondary ether group, because dissolved oxygen can be more efficiently consumed through hydrogen abstraction/oxidation due to the presence of labile hydrogen in the ether group. Consequently, the dilution effect was counterbalanced by the contribution of the ether group. On the other hand, the $R_{p,max}$ of the hydrogen-bonding capable acrylate associated with the urethane group was significantly influenced by the sole dilution effect of the diepoxide and resulted in a continuous decrease of the reactivity with increasing concentration of the diepoxide in the corresponding hybrid systems.

The dual photoinitiator system utilized for the simultaneous initiation of the free-radical and cationic photopolymerizations were carefully evaluated for the monovinly acrylates without the diepoxide. To discern the role of the dual photoinitiator system, various molar ratios of a free radical photoinitiator to a cationic photoinitiator were examined for each neat acrylate system. The maximum polymerization rates of the alkyl carbon and ether containing acrylates showed no dependence on the two photoinitiator ratios, but the urethane containing monomer exhibited decreased reactivity as the cationic photoinitiator proportion increased in the dual photoinitiator system. In contrast, the ultimate conversions of the two alkyl carbon and ether acrylates were significantly affected when the two photoinitiator ratios varied from 0 to 1, whereas the urethane acrylate was relatively not influenced. In general, understanding the photon absorption competition between the radical and cationic photoinitiators was critical to untangle the complexity of the reactivity of the monovinyl acrylates during the hybrid photopolymerization. In this regard, sensitivity of the acid inhibition and redox process were carefully assessed, and careful adjustment of the concentration of the free-radical photoinitiator is required to avoid low ultimate conversions of the monovinyl acrylates.

Therefore, designing the reaction formulation containing acrylates and epoxides requires taking into account polarity and dilution effect of epoxide monomers and selection of radical and cationic photoinitiators. Specifically, these factors should be considered with acrylate secondary functionalities when tuning polymerization kinetics and ultimate conversions of monovinyl acrylates.

In industry, reversing the kinetic order for the two distinct polymerizations has attracted significant attention. In most cases, acrylates are usually polymerized faster than epoxides during hybrid photopolymerizations. This general polymerization order has proved to not only provide moldable properties for easy processing but also tailor ultimate properties of final processed polymers. However, to develop more diverse materials possessing novel properties, controlling the kinetic order of acrylates and

epoxides is very important for industrial applications. Furthermore, the profound insights into the relationship between the factors associated with the diepoxide and acrylate reactivity may help to tune the kinetic order of two distinct polymerizations. This tunable polymerization kinetics of acrylates through the acrylate/epoxide hybrid photopolymerizations can provide a new opportunity to produce novel materials that can be useful for various applications such as stereolithography, nanocomposites, dental materials, opto-electronics, and anti-reflecting coatings.

Ultimate Properties of Acrylate/epoxide Hybrid Polymers

Physical and mechanical properties of final cured hybrid polymers were correlated with ultimate conversions of each monovinyl acrylate and cycloaliphatic diepoxide. Since acrylate secondary functionalities (alkyl carbon, ether, and urethane) significantly affected ultimate conversion of epoxide, the ultimate properties of final cured hybrid polymers depended on the acrylate types and monomer composition. The ultimate conversion of the diepoxide was generally high with the alkyl carbon acrylate relative to the ether acrylate for the whole monomer composition, whereas the diepoxide conversion was essentially zero with the urethane acrylate unless the urethane acrylate content was reduced to the level of the cationic photoinitiator concentration. Therefore, physical and mechanical properties of the cured hybrid polymers were affected by the monovinyl acrylate type and monomer composition.

For the mixtures of cycloaliphatic epoxide and alkyl/ether acrylates, macrophase separation between the acrylate and the diepoxide polymers was confirmed by two distinct tan delta peaks that represent each polymer constituent. The phase separation seemed to be kinetically induced, because the two acrylate and diepoxide monomers were miscible and their mixtures were transparent. The occurrence of the macro-phase separation indicated that there were no covalent bonds between the two distinct polymers and no interpenetrating network structures (IPNs) in the cured hybrid polymers. The

distance between the two distinct tan delta peaks was not affected by monomer composition for the alkyl carbon acrylate hybrid mixture. However, the distance tended to decrease for the ether acrylate hybrid mixture. In the presence of the urethane acrylate, the tan delta peak representing the diepoxide polymer was not observed for the given monomer composition due to negligible fraction of the diepoxide polymer associated with zero conversion. Gel content data showed a trend similar to this phase behavior. Mechanical properties such as Young's modulus and tensile strength decreased as acrylate content increased for alkyl carbon and ether acrylate hybrid mixtures. This trend was opposite for the urethane hybrid system. Surface property of each hybrid polymer characterized by pencil hardness test also showed a similar trend as a function of monomer composition.

With respect to macrophase separation that occurred in the mixtures of cycloaliphatic epoxide and alkyl/ether acrylates, introduction of hybrid monomers bearing both vinyl and cycloaliphatic epoxide groups into these mixtures may control the degree of phase separation. For these ternary systems, the effects of hybrid monomer type and concentration on the polymerization kinetics of both acrylates and diepoxide should be studied. It would also be beneficial to observe their effect on the ultimate properties of final cured hybrid polymers.

The effect of the urethane acrylate on the ultimate conversion of the diepoxide and ultimate properties of the final cured polymers seemed to be too negative. However, this hybrid system can provide a true moldable property since the diepoxide is still liquid in the reaction system after illumination. The practical problem will be how to polymerize the diepoxide after/during molding processing. Here dynamic modulation methods were proposed to increase ultimate conversion of the diepoxide by controlling illumination time and temperature. A successful example was presented in Appendix for urethane (di)acrylate/diepoxide mixture of 2:1 molar ratio. Mechanical strength and toughness was significantly enhanced after the dynamic modulation process. It is

necessary to explore this dynamic modulation process for various urethane acrylate/epoxide hybrid systems. Specifically, kinetic chain length of the acrylate radicals may be significantly affected because radical coupling termination occurs after the illumination is ceased. In addition, after high temperature is applied, hybrid photopolymerization system is vitrified due to an increase in epoxide conversion. In this situation, radical propagation reaction becomes more diffusion-controlled when the illumination resumes. Therefore, with the dynamic modulation approach, molecular weight distribution (or crosslink density), phase separation, and network structure may be quite different from the hybrid polymers cured under a full illumination condition at room temperature.

APPENDIX A

CALIBRATION OF EFFECTIVE SPECTRAL IRRIDIANCE

In this research, a high pressure 100-Watt mercury vapor short arc lamp was used for the kinetic studies. The effective spectral irradiance was set to 100 mW/cm^2 measured by EFOS UV/Visible Radiometer R5000 for the filtered spectral range between 250 nm and 450 nm. However, the same radiometer could not be used to measure the light intensity due to the difficulty in a geometrical set up of the radiometer under a collimator lens (RLQ-1, Asahi Spectra) equipped with the mercury vapor lamp. To realize the same effective irradiance for film and coating samples, light intensity through a collimator lens (RLQ-1, Asahi Spectra) was calibrated using a radiometer specified at 365nm emission (9811, Cole-Parmer). Various effective spectral irradiances measured by EFOS UV/Visible Radiometer R5000 were compared to the corresponding light intensities measured by the 365nm radiometer. Thus, a calibration curve was established to match the effective irradiance measured by the 365nm radiometer to that measured by the EFOS UV/Visible Radiometer R5000 (Figure A.1).

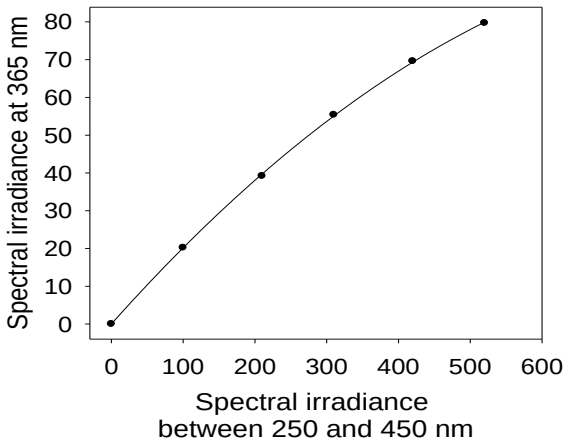

Figure A.1 Calibration of spectral irradiances for different spectral ranges measured by two different radiometers. The dots illustrate measured values fitted by a least square method (R^2=0.999).

APPENDIX B

ULTIMATE PROPERTIES OF ACRYLATE/EPOXIDE HYBRID POLYMERS

Ultimate properties of Acrylate/epoxide hybrid polymers produced by photopolymerizations were tested. First, gel contents of HA/EEC, BEA/EEC, BCEA/EEC hybrid polymer films with the thickness of 120 (±10) μm were compared in Figure B.1. The gel contents of HA/EEC and BEA/EEC films monotonically increased with increasing the portion of the EEC polymers. In contrast, the BCEA/EEC films showed the proportional decrease in the gel content as the EEC content increased in the hybrid polymers due no conversion of the EEC monomer during the hybrid photopolymerizations.

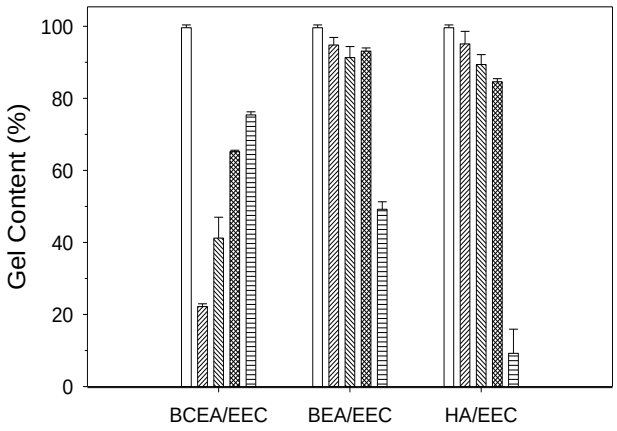

Figure B.1 Gel contents of HA/EEC, BEA/EEC, and BCEA/EEC hybrid polymer films after immersion in aceton solvent for 24 hours. Pure acrylate film (▤), hybrid films of 2:1 acrylate to EEC (▩), 1:1 acrylate to EEC (▧), 1:2 acrylate to EEC (▨), and pure EEC film (□).

Second, Young's modulus of the HA/EEC and BEA/EEC films containing three different acrylate/epoxide compositions were compared as a function of the ratios of δ_{EEC} height to $\delta_{HA \text{ or } BEA}$ height for the respective hybrid films. Figure B.2 illustrates that the

HA/EEC films exhibit higher Young's modulus than those of the BEA/EEC films for the whole composition range. The higher modulus of each HA/EEC film for the corresponding composition was attributed to higher conversion of the EEC monomer for the HA/EEC hybrid systems compared to the BEA/EEC. However, measurements of the Young's modulus for the BCEA/EEC films were difficult especially when the volume fraction of the EEC was higher than that of the BCEA because large volume portions of the BCEA/EEC hybrid films were liquid as indicated by the gel content result.

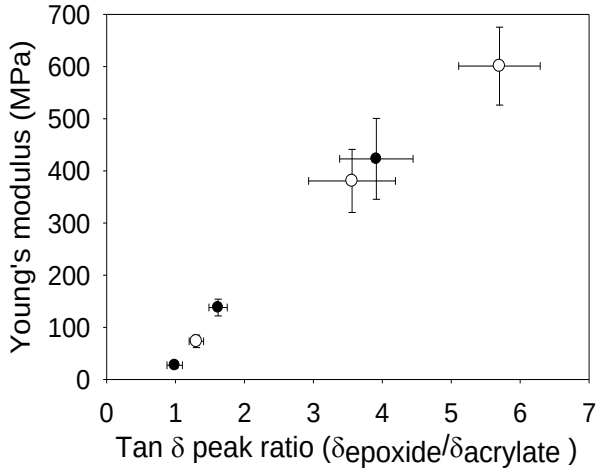

Figure B.2 Young's modulus of each HA/EEC (◯) and BEA/EEC (●) film as a function of the tan δ peak ratios of the epoxide to the acrylate polymers.

Finally, phase behavior of the HA/EEC and BEA/EEC hybrid polymer films was also compared as a function of composition. The tan delta profiles of both hybrid polymer films exhibited macro-phase separation as shown in Figure B.3. In addition, the heights of the δ_{EEC} were higher for the HA/EEC films compared to the BEA/EEC films, which was also attributed to the higher conversion of EEC for the HA/EEC hybrid polymers. In contrast, Figure B.4 illustrates that the 2:1 BEA/EEC film exhibits the δ_{BCEA} peak only, not $\delta_{EEC,}$ which is well consistent with the results of both kinetic study and gel

content measurements. In addition, the BEA/EEC film of 2:1 molar ratio exhibited more ductile and soft behavior of stress-strain curve as shown in Figure B.5. The mechanical property of the BEA/EEC film of 2:1 molar ratio was incredibly enhanced when a dynamic modulation method was applied. The dynamic modulation method will be discussed in Appendix C.

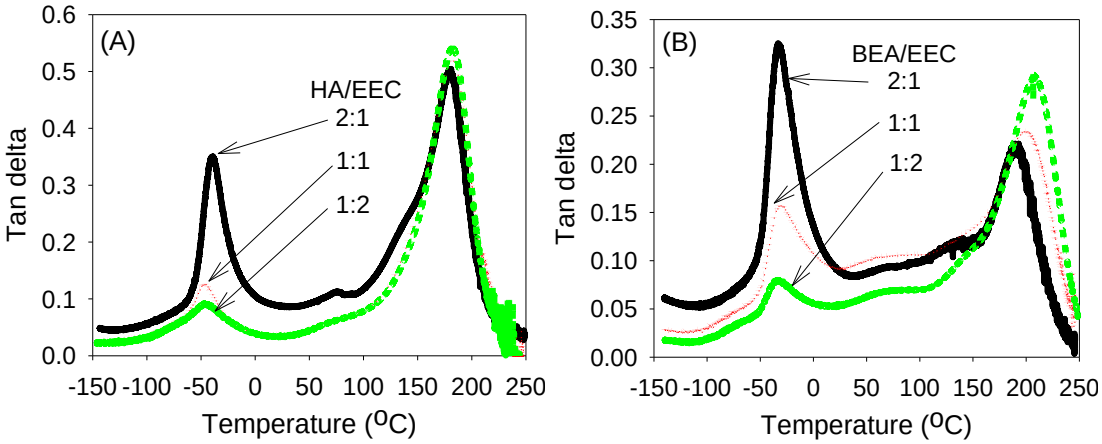

Figure B.3 Tan δ profiles of HA/EEC (A) and BEA/EEC (B) hybrid polymer films with the thickness of 120 μm. The left $\delta_{acrylate}$ indicates acrylate polymer phase while the right $\delta_{epoxide}$ epoxide polymer phase.

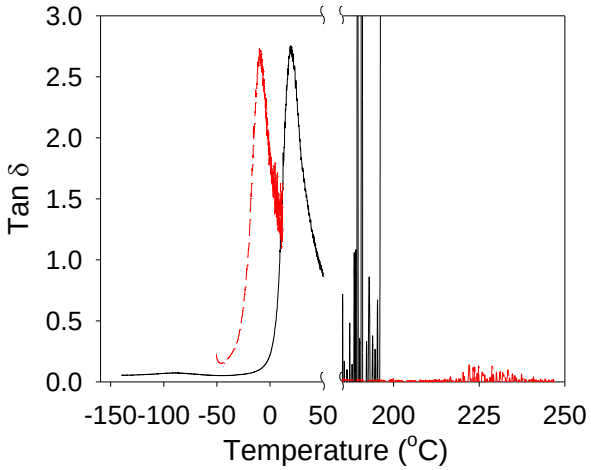

Figure B.4 Tan δ profiles of pure BCEA (black line) polymer and 2:1 BCEA/EEC hybrid polymer (red dotted line) films with the thickness of 120 μm.

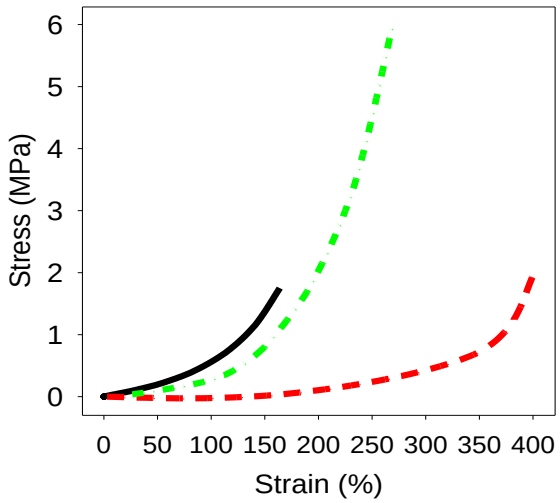

Figure B.5 Stress-strain behavior of pure BCEA (black line) polymer, 2:1 BCEA/EEC hybrid polymer (red dotted and dash-dot lines before and after the dynamic modulation treatment) films with the thickness of 120 µm.

APPENDIX C
DYNAMIC MODULATION OF PROCESSING VARIABLES FOR URETHANE ACRYLATE/EPOXIDE HYBRID PHOTOPOLYMERIZATIONS

Radical and cationic photopolymerizations are energy-efficient technologies providing a rapid curing for coatings and adhesives, compared to thermal polymerizations. However, their kinetics is often interrupted by atmospheric factors, namely oxygen and water that affect radical and cationic active species, respectively. The kinetic failure is closely related to the end-product performance. In order to address the problems with those factors, hybrid photopolymerization systems containing urethane acrylate oligomers and cycloaliphatic diepoxide were studied. It was assumed that these hybrid systems prevent diffusion of atmospheric oxygen and water to the photopolymerizaiton system due to hydrophobicity and high visocisty of the urethane acrylate oligomers. In addition, rapid consumption of the cycloaliphatic diepoxide rapidly at the coating surface due to interaction between cationic active center and atmospheric water can increase surface viscosity and prevent further diffusion of the oxygen to the reaction system. Furthemore, there is a great potential to tunable physical properties of the resulting polymers by forming various interpenetrating network structures via the combination of elastic urethane acrylate oligomers with brittle cycloaliphatic epoxide resins.

However, in Chpater 5, results showed that cationic photopolymerization of the cycloaliphatic diepoxide was inhibited in the presence of the urethane acrylate oligomers. To accelerate polymerizaiton rate and ultimate conversion of the diepoxide for the urehane acrylate/diepoxide hybrid systems, the effects of the elevated temperature and the dynamic modulation method on both acrylate and epoxide polymerization kinetics were studied. For this purpose, UV light illumination and heat energy were precisely controlled in a sequential/simultaneous manner. In conjuction with the control over the

process variables, Raman spectroscopic technique was used to obtain simultaneous kinetic information, such as the polymerization rates and ultimate conversions of acrylate and epoxide photopolymerizations in the hybrid systems.

The dynamic modulation method that controls light-illumination time and heat significantly enhanced polymerization rate and ultimate conversion of the diepoxides during hybrid photopolymerizations. The enhanced kinetics of the diepoxide in the presence of the urethane acrylate oligomers was attributed to effective diffusion of cationic active centers that promote cationic epoxide ring-opening polymerizations.

Figure C.1A illustrates that free-radical photopolymerizations of the urethane acrylate oligomers are not significantly affected by the variation in the isothermal temperature from 25 ºC to 50 ºC to 75 ºC. In contrast, Figure C.1B illustrates that polymerization rates and degree of conversion of the diepoxide in the presence of the urethane acrylate oligomer increase with increasing isothermal temperature in the reaction capillary tube.

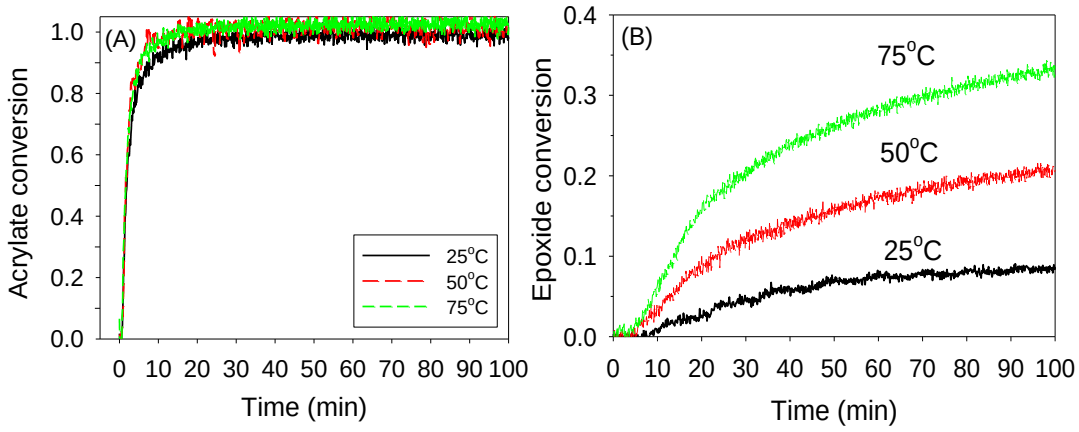

Figure C.1 Effect of isothermal temperatures on the kinetics of urethane acrylate oligomer (A) and cycloaliphatic diepoxide (B) of 25:75 volume ratio during hybrid photopolymerizations. [DMPA] = [IHA] = 8 mM for the corresponding acrylate and diepoxide. The spectral irradiance was set to 100 mW/cm^2 for the filtered spectral range between 250 and 450 nm.

Figure C.2A illustrates that free-radical photopolymerizations of the urethane acrylate oligomers are not significantly affected by elevated temperatures after 10 minute illumination from 25 ºC to 50 ºC or 75 ºC compared to isothermal temperature conditions. In contrast, Figure C.2B illustrates that polymerization rates and degree of conversion of the diepoxide in the presence of the urethane acrylate oligomer increase for the two different elevated temperatures. The figure also illustrates that the elevated temperatures result in higher ultimate conversions compared to the isothermal temperature conditions.

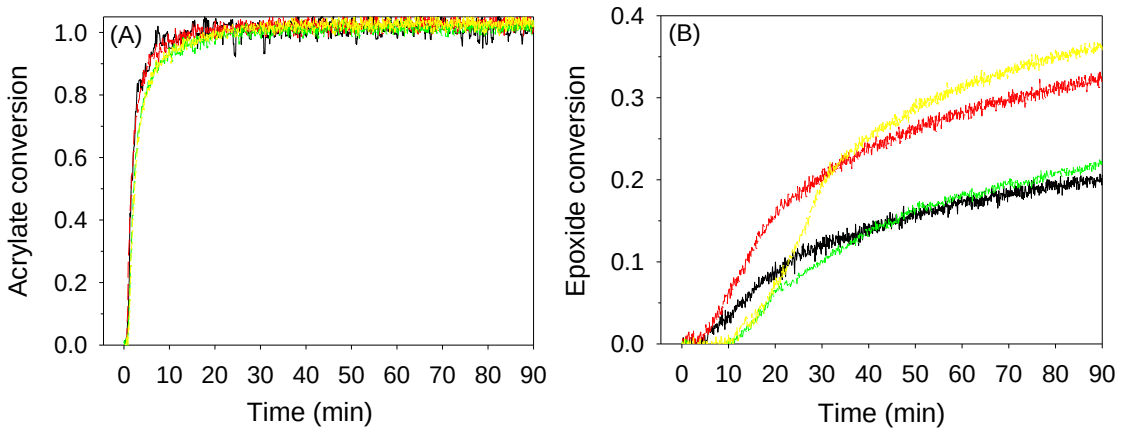

Figure C.2 Effect of elevated temperatures from 25 ºC to 50 ºC (green line) or 75 ºC (yellow line) on the kinetics of urethane acrylate oligomer (A) and cycloaliphatic diepoxide (B) of 25:75 volume ratio during hybrid photopolymerizations compared to isothermal temperature conditions at 50 ºC (black line) and 75 ºC (red line). The temperature was elevated after 10 minute illumination. [DMPA] = [IHA] = 8 mM for the corresponding acrylate and epoxide. The spectral irradiance was set to 100 mW/cm^2 for the filtered spectral range between 250 and 450 nm.

Figure C.3 shows the effect of illumination on the kinetics of both acrylate and diepoxide during the hybrid photopolymerization while temperature in the reaction capillary tube is being elevated. For one experimental condition, illumination was ceased after 10 minute illumination, followed by elevating temperature from 25 ºC to 75 ºC. For

the other experimental set-up, full illumination condition was applied during the whole course of the reaction (Figure C.3).

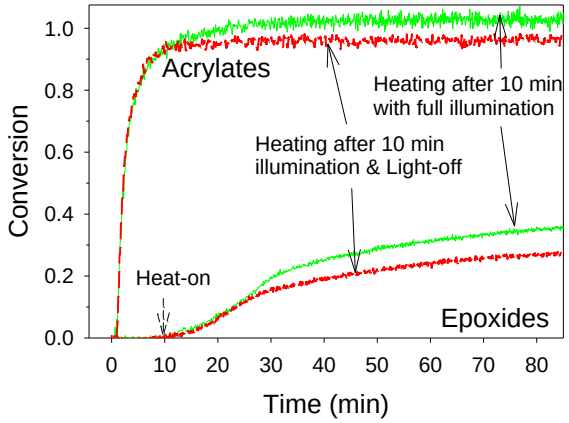

Figure C.3 Effect of combination of illumination and elevated temperature on the kinetics of urethane acrylate oligomer (upper curves) and cycloaliphatic diepoxide (bottom curves) of 25:75 volume ratio during hybrid photopolymerizations. The temperature was elevated from 25 ºC to 75 ºC after 10 minute illumination with light-on (green line) or light-off (red line).

Figure C.4 illustrates conversion profiles of the urethane acrylate oligomer and the diepoxide under dynamic modulation of illumination time and reaction temperature during the hybrid photopolymerization. During the dynamic modulation, consumption of the acrylate carbon-double bond is prevented after the illumination is ceased while conversion of epoxide functional groups increase as reaction temperature is elevated. Once the diepoxide conversion is maximized during the elevated temperature, the hybrid sample is reilluminated at the same light intensity. The reillumination resulted in high conversions of both diepoxide and urethane acrylate oligomer. This dynamic modulation is freely tunable and may generate novel properties of final hybrid polymers because this process can alter interpenetrating network structures. Finally, ultimate conversions of the

urethane acrylate oligomer and diepoxide were compared for various processing methods as shown in Figure C.5

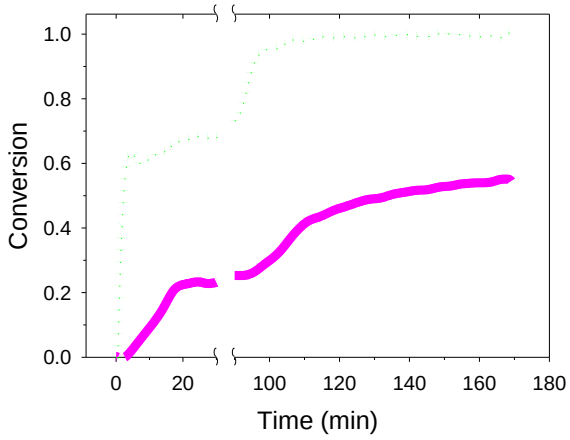

Figure C.4 Effect of dynamic modulation on the kinetics of urethane acrylate oligomer (green dotted line) and cycloaliphatic diepoxide (pink line) of 25:75 volume ratio during hybrid photopolymerizations. Dynamic modulation sequence: (1) initial illumination for 1.5 minute at room temperature; (2) light-off and heating from 25 ºC to 75 ºC (temperature inside the reaction capillary tube; (3) isothermally maintained at 75 ºC for approximately 60 minute; (4) reillumination at 75 ºC

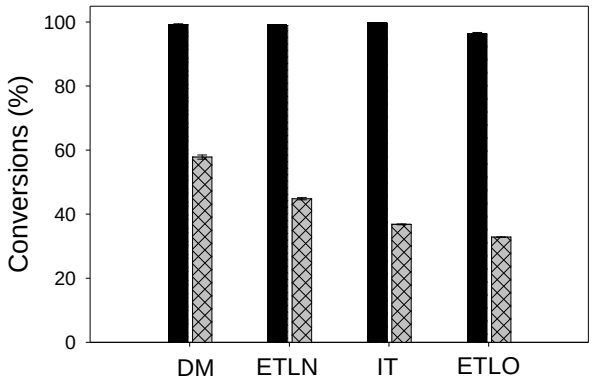

Figure C.5 Ultimate conversions of urethane acrylate oligomer (■) and cycloaliphatic diepoxide (⊠) during hybrid photopolymerizations via various processing methods. DM: dynamic modulation, ETLN: elevated temperature from 25 ºC to 75 ºC after 10 minute illumination followed by full illumination, IT: isothermal temperature at 75 ºC, and ETLO: elevated temperature from 25 ºC to 75 ºC after10 minute illumination followed by light-off.

APPENDIX D
ATOMIC FORCE MICROSCOPY FOR CATIONICALLY PHOTOPOLYMERIZED EPOXIDE COATINGS

Atomic force microscopy (AFM) was used to examine surfaces of pure EEC, EEC-EPOH20 and EEC-EPOH20 copolymer coatings. All coatings were stored in dark room for one week prior to AFM study. All AFM images are listed in Figures D.1, D.2, and D.3. Overall no signficant differences in surface roughness and morphology between the pure EEC and EEC-EPOH copolymer coatings.

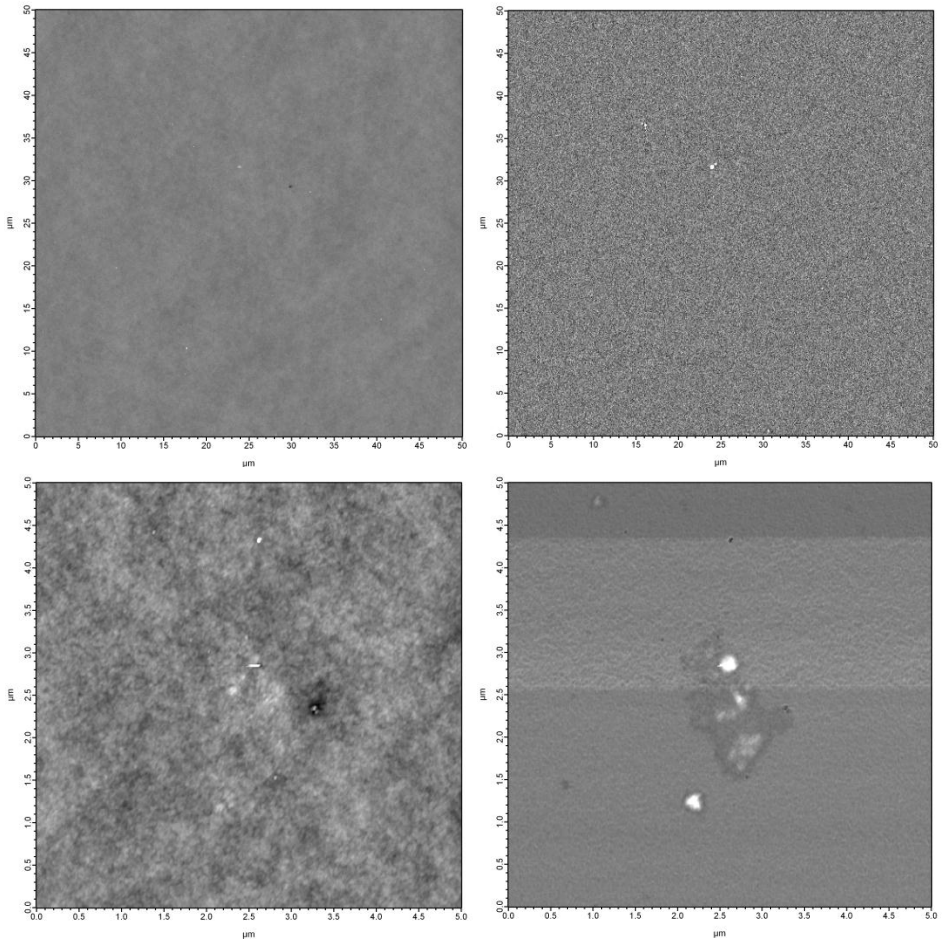

Figure D.1 Surface roughness (A and C) and phase morphology (B and D) of pure EEC coatings in different resolution scales.

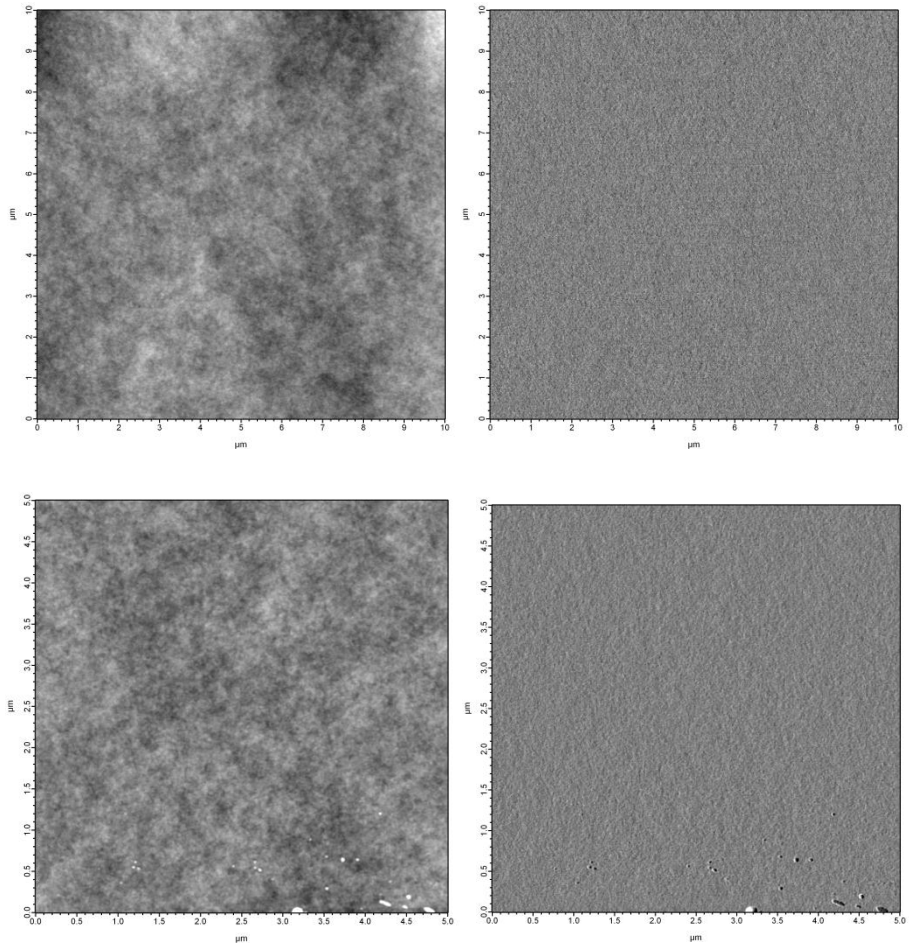

Figure D.2 Surface roughness (A and C) and phase morphology (B and D) of EEC-EPOH20 copolymer coatings containing the EPOH20 of 30 wt.% (A and B) and 80wt.% (C and D).

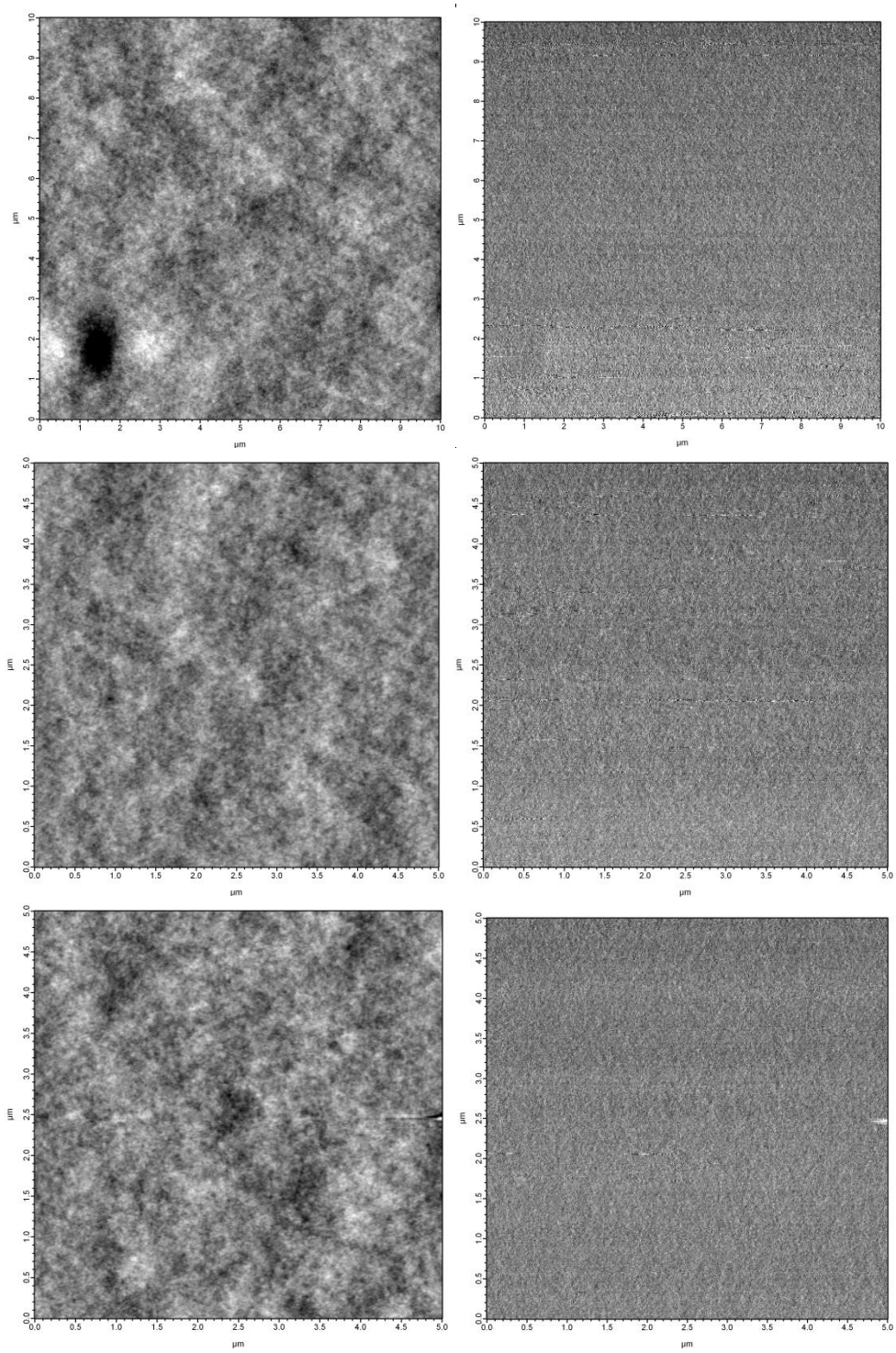

Figure D.3 Surface roughness (A, C, and E) and phase morphology (B, D, and F) of EEC-EPOH20 copolymer coatings containing the EPOH30 of 20 wt.% (A and B), 30wt.%(C and D), and 60wt.% (E and F).

REFERENCES

Al-Besharah, Jasem M., Salman, Omar A., and Akashah, Saed A. 1987. Viscosity of crude oil blends. *Industrial & Engineering Chemistry Research* 26 (12):2445-2449.

Allen, Norman S., Michele Edge, Ignazio Renato Bellobono, and Elena Selli. 1995. *Currents Trends in Polymer Photochemistry*. 1st ed: Ellis Horwood.

Alysworth, J.W. 1916. US Patent. 1 (111):284.

Andjelkovic, Dejan D., Marlen Valverde, Phillip Henna, Fengkui Li, and Richard C. Larock. 2005. Novel thermosets prepared by cationic copolymerization of various vegetable oils--synthesis and their structure-property relationships. *Polymer* 46 (23):9674-9685.

Andrzejewska, E., and M. Andrzejewski. 1998. *J. Polym. Sci., Part A: Polym. Chem.* 36 (null):665.

Anseth, Kristi S. and Burdick, Jason A. 2002. New Directions in Photopolymerizable Biomaterials. *MRS Bulleten*:130-136.

Arkhipovich, G. N., S. A. Dubrovskii, K. S. Kazanskii, N. V. Ptitsina, and A. N. Shupik. 1982. Study of solvation of alkali cations with poly(ethylene oxide). *European Polymer Journal* 18 (7):569-576.

Baidak, A. A., Liegeois, J.M., Sperling, L.H. 1997. Simultaneous Interpenetrating Polymer Networks Based on Epoxy-Acrylate Combinations. *Journal of Polymer Science: Part A: Polymer Chemistry* 35:1973-1984.

B. Suthar, H. X. Xiao, D. Klempner and K. C. Frisch. 1996. A Review of Kinetic Studies of the Formation of Interpenetrating Polymer Networks. *Polymer for Advanced Technologies* 7:221-233.

Baroli, B. 2006. Photopolymerization of biomaterials: Issues and potentialities in drug delivery, tissue engineering, and cell encapsulation applications. *Journal of Chemical Technology and Biotechnology* 81 (4):491-499.

Batog, A. E., Pet'ko, I. P., Penczek, P. 1999. Aliphatic-Cycloaliphatic Epoxy Compounds and Polymers. *Advances in Polymer Science* 144.

Beckel, Eric R., Jun Nie, Jeffrey W. Stansbury, and Christopher N. Bowman. 2004. Effect of Aryl Substituents on the Reactivity of Phenyl Carbamate Acrylate Monomers. *Macromolecules* 37 (11):4062-4069.

Beckel, Eric R., Jeffrey W. Stansbury, and Christopher N. Bowman. 2005. Effect of Aliphatic Spacer Substitution on the Reactivity of Phenyl Carbamate Acrylate Monomers. *Macromolecules* 38 (8):3093-3098.

Beckel, Eric R., Jeffrey W. Stansbury, and Christopher N. Bowman. 2005. Evaluation of a Potential Ionic Contribution to the Polymerization of Highly Reactive (Meth)acrylate Monomers. *Macromolecules* 38 (23):9474-9481.

Bednarek, M., T. Biedron, K. Kaluzynski, P. Kubisa, J. Pretula, and S. Penczek. 2000. Ring Opening Polymerization Processes Involving Activated Monomer Mechanism. Cationic Polymerization of Cyclic Ethers Containing Hydroxyl Groups. *Macromolecular Symposia* 157:1-11.

Bednarek, Melania, Przemyslaw Kubisa, and Stanislaw Penczek. 1999. Coexistence of Activated Monomer and Active Chain End Mechanisms in Cationic Copolymerization of Tetrahydrofuran with Ethylene Oxide. *Macromolecules* 32:5257-5263.

Berchtold, Kathryn A., Jun Nie, Jeffrey W. Stansbury, and Christopher N. Bowman. 2008. Reactivity of Monovinyl (Meth)acrylates Containing Cyclic Carbonates. *Macromolecules* 41 (23):9035-9043.

Berchtold, Kathryn A., Jun Nie, Jeffrey W. Stansbury, Bilge HacioÇ§lu, Eric R. Beckel, and Christopher N. Bowman. 2004. Novel Monovinyl Methacrylic Monomers Containing Secondary Functionality for Ultrarapid Polymerization: Steady-State Evaluation. *Macromolecules* 37 (9):3165-3179.

Biedron, T., R. Szymanski, P. Kubisa, and S. Penczek. 1990. *Makromol. Chem., Macromol. Symp.* 32:155.

Biedron, Tadeusz, Krystyna Brzezinska, Przemyslaw Kubisa, and StanislawPenczek. 1995. Macromonomers by activated polymerization of oxiranes. Synthesis and polymerization. *Polymer International* 36 (1):73-80.

Biedron, Tadeusz, Kubisa, Przemyslaw, and Penczek, Stanislaw. 1991. Polyepichlorohydrin diols free of cyclics: Synthesis and characterization. *Journal of Polymer Science Part A: Polymer Chemistry* 29 (5):619-628.

Blaiszik, B. J., N. R. Sottos, and S. R. White. 2008. Nanocapsules for self-healing materials. *Composites Science and Technology* 68 (3-4):978-986.

Bolon, D.A. and Webb K.K. 1978. Barrier coats versus inert atmosperes. The elimination of oxygen in free-radical polymerizations. *Journal of Applied Polymer Science* (22):2543-2551.

Bulut, Umut., and Crivello, J. V. 2005. Investigation of the Reactivity of Epoxide Monomers in Photoinitiated Cationic Polymerization *Macromolecules* 38 (9):3584 -3595.

Bussi, Philippe, and Hatsuo Ishida. 1994. Dynamic mechanical properties of epoxy resin/epoxidized rubber blends: Effect of phase separated rubber. *Journal of Polymer Science Part B: Polymer Physics* 32 (4):647-657.

Bussi, Philippe, and Hatsuo Ishida. 1994. Partially miscible blends of epoxy resin and epoxidized rubber: Structural characterization of the epoxidized rubber and mechanical properties of the blends. *Journal of Applied Polymer Science* 53 (4):441-454.

Cai, Ying , and Julie L.P. Jessop. 2006. Decreased oxygen inhibtion in photopolymerized acrylate/epoxide hybrid polymer coatings as demonstrated by Raman Spectroscopy. *Polymer* 47:6560-6566.

Carioscia, Jacquelyn A., Jeffrey W. Stansbury, and Christopher N. Bowman. 2007. Evaluation and control of thiol-ene/thiol-epoxy hybrid networks. *Polymer* 48 (6):1526-1532.

Chen, Zhigang, Ying Zhang, Bret J. Chisholm, and Dean C. Webster. 2008. A humidity blocker approach to overcoming the humidity interference with cationic photopolymerization. *Journal of Polymer Science Part A: Polymer Chemistry* 46 (13):4344-4351.

Cho, J. D., and J. W. Hong. 2005. Photo-curing kinetics for the UV-initiated cationic polymerization of a cycloaliphatic diepoxide system photosensitized. *European Polymer Journal* 41 (2):367-374.

Cho, Jung-Dae, and Jin-Who Hong. 2005 Photo-curing kinetics for the UV-initiated cationic polymerization of a cycloaliphatic diepoxide system photosensitized by thioxanthone. *European Polymer Journal* 41 367–374.

Choi, Ju, Jong Lee, and Won Park. 2002. Epoxidized polybutadiene as a thermal stabilizer for poly(3-hydroxybutyrate). I. Effect of epoxidation on the thermal properties of polybutadiene. *Fibers and Polymers* 3 (3):109-112.

Christopher G. Williams, Athar N. Malika, Tae Kyun Kima, Paul N. Mansonb and Jennifer H. Elisseeff. 2005. Variable cytocompatibility of six cell lines with photoinitiators used for polymerizing hydrogels and cell encapsulation *Biomaterials* 26 (11):1211-1218.

Christophersen, A. G., Jun, H., Jørgensen, K., and Skibsted, L. H. 1991. Photobleaching of astaxanthin and canthaxanthin: quantum-yields dependence of solvent, temperature, and wavelength of irradiation in relation to packageing and storage of carotenoid pigmented salmonoids. *Z Lebensm Unters Forsch* 192:443-439.

Crivello, J.V. 1983. Photoinitiated Cationic Polymerization. *Annual Review of Materials Science* 13:173-190.

Crivello, J.V. 1999. The discovery and development of onium salt cationic photoinitiators. *Journal of Polymer Science Part A: Polymer Chemistry* 37 (23):4241-4254.

Crivello, J.V., and R. Narayan. 1992. Epoxidized triglycerides as renewable monomers in photoinitiated cationic polymerization. *Chemistry of Materials* 4 (3):692-699.

Crivello, J. V., and U. Varlemann. 1995. The synthesis and study of the photoinitiated cationic polymerization of novel cycloaliphatic epoxides. *Journal of Polymer Science Part A: Polymer Chemistry* 33 (14):2463-2471.

Crivello, J.V., and Whan-Gi Kim. 1994. Synthesis and Photopolymerization of 1-Propenyl Glycidyl Ether. *Journal of Polymer Science: Part A: Polymer Chemistry* 32:1639-1648.

Crivello, James V. 2002. Advances in the design of photoinitiators, photosensitizers and monomers for photoinitiated cationic polymerization *Designed monomers and polymers* 5 (2-3):141-154.

Crivello, James V. 2006. Cationic Photopolymerizationi of Alkyl Glycidyl Ethers. *Journal of Polymer Science: Part A: Polymer Chemistry* 44:3036-3052.

Crivello, James V., and Saoshi Liu. 2000. Photoinitiated cationic polymerization of epoxy alcohol monomers. *Journal of Polymer Science Part A: Polymer Chemistry* 38 (3):389-401.

Crivello, James V., and Ramesh Narayan. 1996. Novel Epoxynorbornane Monomers. 2. Cationic Photopolymerization. *Macromolecules* 29 (1):439-445.

Crivello, James V., and Ricardo Acosta Ortiz. 2002. Benzyl alcohols as accelerators in the photoinitiated cationic polymerization of epoxide monomers. *Journal of Polymer Science Part A: Polymer Chemistry* 40 (14):2298-2309.

Crivello, James V., Ortiz, R. A. 2001. Design and synthesis of highly reactive photopolymerizable epoxy monomers. *Journal of Polymer Science Part A: Polymer Chemistry* 39 (14):2385-2395.

Crivello, James V., and Ulrike Varlemann. 1995. Mechanistic study of the reactivity of 3,4-epoxycyclohexylmethyl 3′,4′-epoxycyclohexancarboxylate in photoinitiated cationic polymerizations. *Journal of Polymer Science Part A: Polymer Chemistry* 33 (14):2473-2486.

Crivello, James V., and Bo Yang. 1994. Synthesis and Photoinitiated Cationic Polymerization of Epoxidized Elastomers. *Journal of Macromolecular Science, Part A: Pure and Applied Chemistry* 31 (5):517 - 533.

Crivello, James. V., and Ulrike Varlemann. 1997. Structure and reactivity relationship in the photoinitiated cationic polymerization of 3,4-epoxycyclohexylmethyl-3'-4'-epoxycyclohexane carboxylate. *ACS symposium series* 673:82-94.

Czech, Z. and Miler, R. 2003. Solvent-Free Radiation-Curable Polyacrylate Pressure Sensitive Adhesive Systems. *Journal of Applied Polymer Science* 87:182-191.

D. J. Hourston, and Y. Zia. 1983. Semi- and Fully Interpenetrating Polymer Netwoks Based on Polyurethane-Polyacrylate Sytems. I. The polyurethane Networks. *Journal of Applied Polymer Science* 28:2139-2149.

D. Mecerreyes, J. Humes, R. D. Miller, J. L. Hedrick, C. Detrembleur, P. Lecomte, R. Jerome, J. San Roman. 2000. First example of an unsymmetrical difunctional monomer polymerizable by two living/controlled methods. *Maromolecular Rapid Communications* 21:779-784.

David Mecerreyes, Geroges Moineau, Philippe Dubois, Robert Jerome, James L. Hendrick, Craig J. Hawker, Eva E. Malmstrom, and Mikael Trollsas. . 1998. Simultanneous Dual Living Polymerization: A Novel One-step Approach to Block and Graft Copolymers. *Angewandte Chemie International Edition* 37 (9):1274-1276.

David Mecerreyes, J. A. Pomposo, M. Bengoetxea, and H. Grande. 2000. Novel Pyrrole End-Functional Macromonomers Prepared by Ring-Opening and Atom-Transfer Radical Polymerizations. *Macromolecules* 33:5486-5849.

David Mecerreyes, Mikael Trollsas, and James L. Hedrick. 1999. ABC BCD Polymerization: A Self-condensing Vinyl and Cyclic Ester Polymerization by Combination Free-Radical and Ring-Opening Techniques. *Macromolecules* 32:8753-8759.

Decker C, and Bendaikha T. 1998. Interpenetrating polymer networks. II. Sunlight-induced polymerization of multifunctional acrylates. *Journal of Applied Polymer Science* 70 (11):2269-2282.

Decker, C, Le Xuan, H, Nguyen, T, and Viet, T. 1995. Photocrosslinking of functionalized rubber. II. Photoinitiated cationic polymerization of epoxidized liquid natural rubber. *Journal of Polymer Science Part A: Polymer Chemistry* 33 (16):2759-2772.

Decker, C., Bianchi, C., Decker, D., Morel, F. 2001. Photoinitiated polymerization of vinyl ether-based systems. *Progress in Organic Coatings* 42 (3-4):253-266.

Decker, C., Nguyen Thi Viet, T., Decker, D., Weber-Koehl, E. 2001. UV-radiation curing of acrylate/epoxide systems. *Polymer* 42 (13):5531-5541.

Decker, C., H. Le Xuan, and T. Nguyen Thi Viet. 1996. Photocrosslinking of functionalized rubber. III. Polymerization of multifunctional monomers in epoxidized liquid natural rubber. *Journal of Polymer Science Part A: Polymer Chemistry* 34 (9):1771-1781.

Decker, Christian. 2002. Kinetics Study and New Applicatioins of UV Radiation Curing. *Macromolecular Chemistry and Physics* 23 (18):1067-1093.

Decker, Christian. 2002. Light-induced crosslinking polymerization. *Polymer International* 51 (11):1141-1150.

Decker, Christian, and Aubrey D. Jenkins. 1985. Kinetic approach of oxygen inhibition in ultraviolet- and laser-induced polymerizations. *Macromolecules* 18 (6):1241-1244.

Decker, D, Nguyen, T, Viet, T, and Thi, HP. 2001. Photoinitiated cationic polymerization of epoxides. *Polymer International* 50:986-997.

Dongkwan Kim, and Alec Scranton. 2004. The role of diphenyl iodonium salt (DPI) in Three-componetn photointiator systems containing methylene blue (MB) and an electron donor. *Journal of Polymer Science: Part A: Polymer Chemistry* 42:5863-5871.

Dursun, Canan, Mustafa Degirmenci, Yusuf Yagci, Steffen Jockusch, and Nicholas J. Turro. 2003. Free radical promoted cationic polymerization by using bisacylphosphine oxide photoinitiators: substituent effect on the reactivity of phosphinoyl radicals. *Polymer* 44 (24):7389-7396.

Dusek, K., and M. Dusková-Smrcková. 2000. Network structure formation during crosslinking of organic coating systems. *Progress in Polymer Science* 25 (9):1215-1260.

E. W. Nelson, J. L. Jacobs, A. B. Scranton, and K. S. Anseth and C. N. Bowman. 1995. Photo-differential scanning calorimetry studies of cationic polymerizations of divinyl ethers. *Polymer* 36 (24):4651-4656.

E. W. Nelson, T. P. Carter, and A. B. Scranton. 1994. Fluorescence Monitoring of Cationic Photopolymerizations: Divinyl Ether Polymerizations Photosensitized by Anthracene Derivatives. *Maromolecules* 27:1013-1019.

Eley, D. D. 1939. On the solubility of gases. Part I.—The inert gases in water. *Trans. Faraday Soc.* 35.

Endruweit, M.S. Johnson, A.C. Long. 2006. Curing of Composite Components by Ultraviolet Radiation: A Review. *Polymer Composite* 27 (2):119-128.

Eom, Ho Seop, and Julie L.P. Jessop. 2010. Epoxide/urethane acrylate hybrid photopolymerizations to minimize atmospheric sensitivity: Understanding the interplay

between viscosity and dual photoinitiator system. In *Basics and Applications of Photopolymerization Reactions*, edited by J. P. Fouassier and X. Allonas.

Evans A.G., Holden, D., Plesch, P. H., Polanyi M., Skinner, H.A., and Weinberger, M.A. 1946. Fridel-Crafts Catalysts and polymerization. *Nature* 157:102.

Ficek, B. A., Thiesen, A. M., and Scranton, A. B. 2008. Cationic photopolymerizations of thick polymer systems: Active center lifetime and mobility. *European Polymer Journal* 44 (1):98-105.

Filip E. Du Prez, Peiwan Tan, and Eric J. Goethals. 1996. Poly(ethrylene oxide)/Poly(methyl methacrylate) (Semi-)interpentrating Polymer Networks: Synthesis and Phase Diagrams. *Polymer for Advanced Technologies* 7:257-264.

Fisher, J. P., Dean, D., Engel, P. S., Mikos, A. G. 2001. Photoinitiated polymerization of biomaterials. *Annual Review of Materials Science* 31:171-181.

Fouassier, Jean-Pierre, and Andre Merlin. 1980. Laser investigation of norrish type I photoscission in the photoinitiator irgacure (2,2-dimethoxy 2-phenyl-acetophenone). *Journal of Photochemistry* 12 (1):17-23.

Fouassier, Jean Pierre. 1995. *Photoinitiation, Photopolymerization, and Photocuring: Fundamentals and Applications* 1st ed. New York: Hanser.

G. Sauvet, J. P. Vairon P. Sigwalt. 1978. The cationic dimerization of 1,1-diphenylethylene. II. Cation formation with titanium tetrachloride in dichloromethane solution. *Journal of Polymer Science: Polymer Chemistry Edition* 16 (12):3047-3064.

Geacintov, N.E., Shafirovich, V.Y., Li, B., Mao, B., and Ya, N. 1997. Photoinduced Electron Transfer, Fluorescence, and Intrastrand Migration of Reactive Intermediates in Pyrenyl Sensitizer-Modified DNA Duplexes. *The Spectrum* 10 (2):1-16.

Goethals, E. J., Du Prez, F. 2007. Carbocationic polymerizations. *Progress in Polymer Science* 32 (2):220-246.

Golovanov, I., and S. Zhenodarova. 2005. Quantitative Structure-Property Relationship: XXIII. Solubility of Oxygen in Organic Solvents. *Russian Journal of General Chemistry* 75 (11):1795-1797.

Gou, Lijing, Chris N. Coretsopoulos, and Alec B. Scranton. 2004. Measurement of the dissolved oxygen concentration in acrylate monomers with a novel photochemical method. *Journal of Polymer Science Part A: Polymer Chemistry* 42 (5):1285-1292.

Grattan, David W., and Peter H. Plesch. 1980. The Initiation of Polymerisations by Aluminium Halides. *Makromolekulare Chemie* 181 (4):751-775.

Gregório, José Ribeiro, Annelise Engel Gerbase, Márcia Martinelli, Marly Antonia Maldaner Jacobi, Liane de Luca Freitas, Maria Luiza Ambros von Holleben, and Paulo Dutra Marcico. 2000. Very efficient epoxidation of 1,4-polybutadiene with the biphasic system methyltrioxorhenium. *Macromolecular Rapid Communications* 21 (7):401-403.

H. Cao, E. Currie, M. Tilley, and Y.C. Jean. 2003. Oxygen inhibition effect on surface properties of UV-curable acrylate coatings. *ACS Symposium Series 847*:165-175.

Hageman, H. J., F. P. B. Van der Maeden, and P. C. G. M. Janssen. 1979. Photoinitiators and photoinitiation, 1. Vinyl polymerization photoinitiated by benzoin methyl ether. *Die Makromolekulare Chemie* 180 (10):2531-2537.

Hai-Qing Guo, Atsushi Kajiwara, Yotaro Morishima, and Mikiharu Kamachi. 1997. Radical/Cation Transformation Polymerization and Its Applications to the Preparation of Block Copolymers. *Polymers for Advanced Technologies* 8:196-202.

Harald Braun, Yusuf Yagci, Oskar Nuyken. 2002. Copolymerization of butyl vinyl ether and methyl methacrylate by combination fo radical and radical promoted cationic mechanisms. *European Polymer Journal* 38:151-156.

Hartwig, A., A. Harder, A. Lühring, and H. Schröder. 2001. (9-Oxo-9H-fluoren-2-yl)-phenyl-iodonium hexafluoroantimonate(V)-a photoinitiator for the cationic polymerisation of epoxides. *European Polymer Journal* 37 (7):1449-1455.

Hartwig, A., K. Koschek, A. Lühring, and O. Schorsch. 2003. Cationic polymerization of a cycloaliphatic diepoxide with latent initiators in the presence of structurally different diols. *Polymer* 44 (10):2853-2858.

Hartwig, A., B. Schneider, and A. Luhring. 2002. Influence of moisture on the photochemically induced polymerisation of epoxy groups in different chemical environment. *Polymer* 43:4243-4250.

Hartwig, Andreas. 2002. Influence of moisture present during polymerisation on the properties of a photocured epoxy resin. *International Journal of Adhesion & Adhesives* 22:409-414.

Hazot, Pascale, Christian Pichot, and Abderrahim Maazouz. 2000. Synthesis of hairy acrylic core-shell particles as toughening agents for epoxy networks. *Macromolecular Chemistry and Physics* 201 (6):632-641.

Heung Soo Shin, So Yeon Kim, Young Moo Lee, Kwang Hyun Lee, Seon Jeong Kim, Charles E. Rogers. 1998. Permeation of solutes through interpenetrating polymer network hydrogels composed of poly(vinyl alcohol) and poly(acrylic acid). *Journal of Applied Polymer Science* 69 (3):479-486.

Hilal, S. H., S. W. Karickhoff, and L. A. Carreira. 1995. A Rigorous Test for SPARC's Chemical Reactivity Models: Estimation of More Than 4300 Ionization pKa. *Quantitative Structure-Activity Relationships* 14 (4):348-355.

Hiroshi Sasaki, Jerzy M. Rudzin, nacute, and Toyoji Kakuchi ski. 1995. Photoinitiated cationic polymerization of oxetane formulated with oxirane. *Journal of Polymer Science Part A: Polymer Chemistry* 33 (11):1807-1816.

Hong, Shinn-Gwo, and Chau-Kai Chan. 2004. The curing behaviors of the epoxy/dicyanamide system modified with epoxidized natural rubber. *Thermochimica Acta* 417 (1):99-106.

Hua, Yujing, and James V. Crivello. 2000. Synergistic interaction of epoxides and *N*-vinylcarbazole during photoinitiated cationic polymerization. *Journal of Polymer Science Part A: Polymer Chemistry* 38 (19):3697-3709.

Hua, Yujing, and James V. Crivello. 2001. Development of Polymeric Photosensitizers for Photoinitiated Cationic Polymerization *Macromolecules 1994* 34 (8):2488 -2494.

Ishida, Hatsuo, and Douglas J. Allen. 1996. Mechanical characterization of copolymers based on benzoxazine and epoxy. *Polymer* 37 (20):4487-4495.

J. V. Crivello, K. D. Jo. 1993. Propenyl ethers. III. Study of the photoinitiated cationic polymerization of propenyl ether monomers. *Journal of Polymer Science Part A: Polymer Chemistry* 31 (8):2143-2152.

J. V. Crivello, S. S. Liu. 1998. Synthesis and cationic photopolymerization of 1-butenyl glycidyl ether. *Journal of Polymer Science Part A: Polymer Chemistry* 36 (7):1179-1187.

J.V. Crivello, and Whan-Gi Kim. 1994. Synthesis and Photopolymerization of 1-Propenyl Glycidyl Ether. *Journal of Polymer Science: Part A: Polymer Chemistry* 32:1639-1648.

James, V. Crivello. 1999. The discovery and development of onium salt cationic photoinitiators. *Journal of Polymer Science Part A: Polymer Chemistry* 37 (23):4241-4254.

James V. Crivello, and Saoshi Liu. 2000. Photoinitiated Catioinc Polymerization of Epoxy Alcohol Monomers. *Journal of Polymer Science: Part A: Polymer Chemistry* 38:389-401.

James V. Crivello, Ricardo Acosta Oritz. 2002. Benzyl Alcohols as Accelerators in the Photoinitiated Cationic Polymerization of Epoxide Monomers. *Journal of Polymer Science: Part A: Polymer Chemistry* 40:2298-2309.

James V. Crivello, Ricardo Acosta Ortiz. 2001. Synthesis of epoxy monomers that undergo synergistic photopolymerization by a radical-induced cationic mechanism. *Journal of Polymer Science Part A: Polymer Chemistry* 39 (20):3578-3592.

James, V. Crivello, and Varlemann Ulrike. 1995. Mechanistic study of the reactivity of 3,4-epoxycyclohexylmethyl 3',4'-epoxycyclohexancarboxylate in photoinitiated cationic polymerizations. *Journal of Polymer Science Part A: Polymer Chemistry* 33 (14):2473-2486.

Jansen, Johan F. G. A. , Aylvin A. Dias, Marko Dorschu, and Betty Coussens. 2003. Effect of Preorganization Due to Hydrogen Bonding on the Rate of Photoinitiated Acrylate Polymerization. In *Photoinitiated Polymerization*, edited by K. D. Belfield and J. V. Crivello: American Chemical Society.

Jansen, Johan F. G. A., Aylvin A. Dias, Marko Dorschu, and Betty Coussens. 2002. Effect of Dipole Moment on the Maximum Rate of Photoinitiated Acrylate Polymerizations. *Macromolecules* 35 (20):7529-7531.

Jansen, Johan F.G.A, Aylvin A. Dias, Marko Dorschu, and Betty Coussens. 2003. Fast Monomers: Factors Affecting the Inherent Reactivity of Acrylate Monomers in Photoinitiated Acrylate Polymerization. *Macromolecules* 36 (11):3861-3873.

Jie Lu, Quangtrong Nguyen, Jiqing Zhou, and Zheng-Hua Ping. 2003. Poly(vinyl alcohol)/Poly(vinyl pyrrolidone) Interpenetrating Polymer Network: Synthesis and Pervaporation Properties. *Journal of Applied Polymer Science* 89:2808-2814.

Joe D. Oxman, Dwight W. Jacobs, Matthew C. Trom, Vishal Sipani, Beth Ficek, and Alec B. Scranton. 2004. Evaluation of Initiator systems for controlled and sequentially curable Free-Radical/Cationic Hybrid Photopolymerizations. *Journal of Polymer Science: Part A: Polymer Chemistry* 43:1747-1756.

Joseph R. Nowers, and Balaji Narasimhan. 2006. The effect of interpenetrating polymer network formation on polymerization kinetics in an epoxy-acrylate system. *Polymer* 47:1108-1118.

Jung-Dae, Cho, and Hong Jin-Who. 2004. UV-initiated free radical and cationic photopolymerizations of acrylate/epoxide and acrylate/vinyl ether hybrid systems with and without photosensitizer. *Journal of Applied Polymer Science* 93 (3):1473-1483.

K. Moussa, and C.Decker. 1993. Semi-interpentrating polymer networks synthesis by Photocrosslinking of Acrylic Monomers in a polymer Matrix. *Journal of Polymer Science: Part A: Polymer Chemistry* 31:2633-2542.

Kaczmarek, H. and Decker, C. 1994. Interpenetrating polymer networks. I. Photopolymerization of multiacrylate systems. *Journal of Applied Polymer Science* 54 (13):2147-56.

Kar, S., and A. K. Banthia. 2004. Epoxy Resin Modified with Epoxidized Soybean Rubber. *Materials and Manufacturing Processes* 19 (3):459 - 474.

Kilambi, H., D. Konopka, J. W. Stansbury, and C. N. Bowman. 2007. Factors affecting the sensitivity to acid inhibition in novel acrylates characterized by secondary functionalities. *Journal of Polymer Science Part A: Polymer Chemistry* 45 (7):1287-1295.

Kilambi, Harini, Sirish K. Reddy, Lauren Schneidewind, Tai Yeon Lee, Jeffrey W. Stansbury, and Christopher N. Bowman. 2007. Design, Development, and Evaluation of Monovinyl Acrylates Characterized by Secondary Functionalities as Reactive Diluents to Diacrylates. *Macromolecules* 40 (17):6112-6118.

Kim, Dongkwan and Jessop, Julie L.P. . 2006. The role of water in photoinitiated cationic ring-opening photopolymerization of cyclehexane epoxides. *2006 UV & EB Technology Conference & Exhibition*.

Kim, Y.-M.; Kostanski, L.; MacGregor, J.; Hamielec, A. 2004. Thermal and real-time FTIR spectroscopic analysis of the photopolymerization of diepoxide-vinyl ether mixtures. *Journal of Thermal Analysis and Calorimetry* 78 (1):153-164.

Kim, Young-Min, L. Kris Kostanski, and John F. MacGregor. 2003. Photopolymerization of 3,4-epoxycyclohexylmethyl-3',4'-epoxycyclohexane carboxylate and tri (ethylene glycol) methyl vinyl ether. *Polymer* 44 (18):5103-5109.

Kim, Young-Min, L. Kris Kostanski, and John F. MacGregor. 2005. Kinetic Studies of Cationic Photopolymerizations of Cycloaliphatic Epoxide, Triethyleneglycol Methyl Vinyl Ether, and Cyclohexene Oxide. *Polymer Engineering and Science* 45:1546-1555

Kishi, H., Y-B. Shi, J. Huang, and A.F. Yee. 1997. Shear ductility and toughenability study of highly cross-linked epoxy/polyethersulphone. *Journal of Materials Science* 32, (3):761-771.

Krystyna, Brzezi, nacute, Ryszard Szyma ska, Przemys ski, lstrok, Stanis aw Kubisa, and Penczek aw. 1986. Activated monomer mechanism in cationic polymerization, 1. Ethylene oxide, formulation of mechanism. *Die Makromolekulare Chemie, Rapid Communications* 7 (1):1-4.

Kubisa, P., and S. Penczek. 1999. Cationic activated monomer polymerization of heterocyclic monomers. *Progress in Polymer Science* 24:1409-1437.

Kubisa, Przemyslaw. 2003. Hyperbranched Polyethers by Ring-Opening Polymerization: Contribution of Activated Monomer Mechanism. *Journal of Polymer Science: Part A: Polymer Chemistry* 41:457-468.

Lecamp, L., C. Pavillon, P. Lebaudy, and C. Bunel. 2005. Influence of temperature and nature of photoinitiator on the formation kinetics of an interpenetrating network photocured from an epoxide/methacrylate system. *European Polymer Journal* 41 (1):169-176.

Lee, T. Y., C. A. Guymon, E. Sonny Jonsson, and C. E. Hoyle. 2004. The effect of monomer structure on oxygen inhibition of (meth)acrylates photopolymerization. *Polymer* 45 (18):6155-6162.

Lee, Tai Y., Todd M. Roper, E. Sonny Jönsson, C. A. Guymon, and C. E. Hoyle. 2004. Influence of Hydrogen Bonding on Photopolymerization Rate of Hydroxyalkyl Acrylates. *Macromolecules* 37 (10):3659-3665.

Lijing Gou, Blaine Opheim, and Alec B. Scranton. 2004. The effect of oxygen in free radical photopolymerization. *Recent Research Developments in Polymer Science* 8:125-141.

Lin, Yan, and Jeffrey W. Stansbury. 2004. Near-Infrared Spectroscopy Investigation of Water Effects on the Cationic Photopolymerization of Vinyl Ether System. *Journal of Polymer Science: Part A: Polymer Chemistry* 42:1985-1998.

Lin, Yan, and Jeffrey W. Stansbury. 2005. The impact of water on photopolymerization kinetics of methacrylate/vinyl ether hybrid systems. *Polymers for Advanced Technologies* 16:195-199.

M. Degirmenci, Y. Hepuzer, Y. Yagci. 2002. One-step, one-pot Photoinitiation of Free Radical and Free Radical Promoted Cationic Polymerizations. *Journal of Applied Polymer Science* 85:2389-2395.

M. Masure, G. Sauvet P. Sigwalt. 1978. The cationic dimerization of 1,1-diphenylethylene. III. Kinetics of initiation by aluminum chloride. *Journal of Polymer Science: Polymer Chemistry Edition* 16 (12):3065-3076.

M. Sangermano, G. Malucelli, F. Morel, C. Decker, A. Priola. 1999. Cationic Photopolymerization of Vinyl ether systems: influence of the presence of hydrogen donor additives. *European Polymer Journal* 35:639-645.

Matyjaszewski, K., S. Słomkowski, and S. Penczek. 1979. Kinetics and mechanism of the cationic polymerization of tetrahydrofuran in solution: THF-CH3NO2 system. *Journal of Polymer Science: Polymer Chemistry Edition* 17 (1):69-80.

Matyjaszewski, Krzysztof. 1988. Solvation of onium ions in cationic ring-opening polymerization. *Macromolecules* 21 (2):519-520.

McGarry, F. J., and R. B. Rosner. 1993. Epoxy-Rubber Interactions. In *Toughened Plastics I*: American Chemical Society.

Miguel G. Neumann, Carla C. Schmitt, Giovana C. Ferreira, Correa, Ivo C. 2006. The initiating radical yields and the efficiency of polymerization for various dental photoinitiators excited by different light curing units. *Dental materials : official publication of the Academy of Dental Materials* 22 (6):576-584.

Miyagawa, Hiroaki, Amar K Mohanty, Manjusri Misra, and Lawrence T Drzal. 2004. Thermo-Physical and Impact Properties of Epoxy Containing Epoxidized Linseed Oil, 1. *Macromolecular Materials and Engineering* 289 (7):629-635.

Miyagawa, Hiroaki, Amar K Mohanty, Manjusri Misra, and Lawrence T Drzal. 2004. Thermo-Physical and Impact Properties of Epoxy Containing Epoxidized Linseed Oil, 2. *Macromolecular Materials and Engineering* 289 (7):636-641.

Moussa, K., and C.Decker. 1993. Semi-interpentrating polymer networks synthesis by Photocrosslinking of Acrylic Monomers in a polymer Matrix. *Journal of Polymer Science: Part A: Polymer Chemistry* 31:2633-2542.

Moussa, K., and C. Decker. 1993. Light-induced polymerization of new highly reactive acrylic monomers. *Journal of Polymer Science Part A: Polymer Chemistry* 31 (9):2197-2203.

Mu-shih Lin, and Shin-Tien Lee. 1997. Mechanical behaviors of fully and semi-interpenetrating polymer networks based on epoxy and acrylics. *Polymer* 38 (1):53-58.

Mülhaupt, R., and U. Buchholz. 1996. Compatibilized, Segmented Liquid Rubbers as Epoxy-Toughening Agents. In *Toughened Plastics II*: American Chemical Society.

Mustafa Degirmencl, Oner Izgin, and Yusuf Yagci. 2004. Synthesis and Characterization of Cyclohexane Oxide Functional Poly(ε-caprolactone) Macromonomers and Their Use in Photoinitiated Cationic Homo- and Copolymerization. *Journal of Polymer Science: Part A: Polymer Chemistry* 42:3365-3372.

Nagarale, R. K., Vinod K. Shahi, Rolf Schubert, R. Rangarajan, and R. Mehnert. 2004. Development of urethane acrylate composite ion-exchange membranes and their electrochemical characterization. *Journal of Colloid and Interface Science* 270 (2):446-454.

Nakayama, Kazuo. 2003. Dynamic Mechanical Analysis. In *Polymer Characterization Techniques and Their Application to Blends*, edited by G. P. Simon. New York: Oxford University Press.

Nelson, E. W., T. P. Carter, and A. B. Scranton. 1994. Fluorescence Monitoring of Cationic Photopolymerizations: Divinyl Ether Polymerizations Photosensitized by Anthracene Derivatives. *Macromolecules 1994* 27:1013-1019.

Nelson, E. W., and A. B. Scranton. 1996. Kinetics of cationic photopolymerizations of divinyl ethers characterized using *in situ* Raman spectroscopy. *Journal of Polymer Science Part A: Polymer Chemistry* 34 (3):403-411.

Nelson, E.W., J.L. Jacobs, A.B. Scranton, K.S. Anseth, and C.N. Bowman. 1995. Photo-differential scanning calorimetry studies of cationic polymerizations of divinyl ethers *Polymer* 36 (24):4651-4656.

Norman S. Allen, Michele Edge, Ignazio Renato Bellobono, Elena Selli. 1995. *Currents Trends in Polymer Photochemistry*. 1st ed: Ellis Horwood.

Nowers, Joseph R., and Balaji Narasimhan. 2006. The effect of interpenetrating polymer network formation on polymerization kinetics in an epoxy[hyphen (true graphic)]acrylate system. *Polymer* 47 (4):1108-1118.

O'Brien, Allison K and Christopher, Bowman N. 2006. Impact of Oxygen on Photopolymerization Kinetics and Polymer Structure. *Macromolecules* 39:2501-2506.

Odian, George. 2004. *Principles of Polymerization*. 4th ed. New York: John Wiley & Sons, Inc.

Oxman, Joe D., Dwight W. Jacobs, Matthew C. Trom, Vishal Sipani, Beth Ficek, and Alec B. Scranton. 2004. Evaluation of Initiator systems for controlled and sequentially curable Free-Radical/Cationic Hybrid Photopolymerizations. *Journal of Polymer Science: Part A: Polymer Chemistry* 43:1747-1756.

P. Sigwalt, and M. Moreau. 2006. Carbocationic polymerization: Mechanisms and kinetics of propagation reactions. *Progress in Polymer Science* 31 (1):44-120.

Packham, D.E. 2005. *Handbook of Adhesion*. Second ed. Chichester, England: John Wiley & Sons Ltd.

Park, J.B., and R.S. Lakes. 1992. *Biomaterials: an introduction*. Second ed. NY: Plenum.

Pearson, Raymond A. 2000. Introduction of the toughening of polymers. In *ACS Symposium series: Toughening of Plastics*, edited by R. A. Pearson, H.-J. Sue and A. F. Yee. Washington DC: American Chemical Society.

Penczek, Stanislaw, Marek Cypryka, Andrzej Duda, Przemyslaw Kubisaa, and Stanisław Słomkowskia. 2007. Living ring-opening polymerizations of heterocyclic monomers *Progress in Polymer Science* 32 (2):247-282

Percec, Virgil, and Dimitris Tomazos. 1987. Liquid crystalline copoly(vinylether)s containing 4(4′)-methoxy-4′ (4)-hydroxy-α-methylstilbene constitutional isomers as side groups. *Polymer Bulletin* 18 (3):239-246.

Petrie, Edward M. 2006. *Epoxy Adhesive Formulations*. First ed. New York: McGrow-Hill.

Pierre Sigwalt, and Michel Moreau. 2006. Carbocationic polymerization: Mechanisms and kinetics of propagation reactions *Progress in Polymer Science* 31 (1):44-120.

Polanyi, Evans and. 1947. Polymerisation of Discussion on " Some Aspects of the Chemistry of Macromolecules.' '. *Journal of the Chemical Society* 252 - 306.

R. T. Olsson, H. E. Bair, V. Kuck, and A. Hale. 2004. Acceleration of the cationic polymerization of an Epoxy with hexandiol. *Journal of Thermal Analysis and Calorimetry* 76:367-377.

R. Tokar, P. Kubisa, and S. Penczek. 1994. Cationic Polymerization of Glycidol: Coexistence of the Activated Monomer and Active Chain End Mechanism. *Macromolecules* 27:320-322.

Rajaraman, S.K., Mowers, W. A., Crivello, J.V. 1999. Interaction of epoxy and vinyl ethers during photoinitiated cationic polymerization. *Journal of Polymer Science Part A: Polymer Chemistry* 37 (21):4007-4018.

Rajaraman, Surésh K., William A. Mowers, and James V. Crivello. 1999. Novel Hybrid Monomers Bearing Cycloaliphatic Epoxy and 1-Propenyl Ether Groups *Macromolecules* 32 (1):36 -47.

Ricardo Acosta Ortiz, Diana Prieto Lopez, Mara de Lourdes Guillen Cisneros, Julio Cesar Rico Valverde, James V. Crivello. 2005. A kinetic study of the acceleration effect of substituted benzyl alcohol on the cationic photopolymerization rate of epoxidized natural oils. *Polymer* 46:1535-1541.

Richard Vendamme, Shin-Ya Onoue, Aiko Nakao, and Toyoki Kunitake. 2006. Robust free-standing nanomembranes of orgainic/inorganic interpenetrating networks. *Nature materials* 5:494-501.

Riew, C. Keith. 1989. *Rubber-Toughened Plastics*. Vol. 222, *Advances in Chemistry Series* Washington, DC: American Chemical Society.

Riew, C. Keith, and John K. Gillham. 1984. *Rubber-modified Thermoset Resins*. Vol. 208, *Advances in Chemistry*. Washington DC: American Chemical Society.

Riew, C. Keith, and Anthony J. Kinloch. 1993. *Toughened Plastics I*. Vol. 233, *Advances in Chemistry*. Washington DC: American Chemical Society.

Riew, C. Keith, and Anthony J. Kinloch. 1996. *Toughened Plastics II*. Vol. 252, *Advances in Chemistry*. Washington DC: American Chemical Society.

Roberio Marcos Alcantara, Alfredo Tiburcio Nunes Pires, Glaucione Gomes de Barros, and Lurence A. Belfiore. 2003. Pseudo-interpenetrating Polymer Networks Based on Tetrafuntional Epoxy Resins and Poly(methyl methacrylate). *Journal of Applied Polymer Science* 89:1858-1868.

Roffey, C.G. 1982. *Photopolymerization of Surface Coatings*. New York: John Wiley & Sons, Inc.

Rosen, Stephen L. 1993. *Fundamental Principles of Polymeric Materials*. 2nd ed. New York: John Wiley & Sons, Inc.

Russell, Bobby, and Richard Chartoff. 2005. The influence of cure conditions on the morphology and phase distribution in a rubber-modified epoxy resin using scanning electron microscopy and atomic force microscopy. *Polymer* 46 (3):785-798.

Sadahito Hashidate, Yukio Nagasaki Masao Kato Hiro Matsuda Hachiro Nakanishi. 1995. Photocrosslinkable second-order nonlinear optical polymers synthesized by cationic copolymerization. *Polymers for Advanced Technologies* 6 (9):626-631.

Samran, Jareerat, Pranee Phinyocheep, Philippe Daniel, Daniel Derouet, and Jean-Yves Buzaré. 2004. Raman spectroscopic study of non-catalytic hydrogenation of unsaturated rubbers. *Journal of Raman Spectroscopy* 35 (12):1073-1080.

Sangermano, M., G. Malucelli, R. Bongiovanni, G. Gozzelino, F. Peditto, and A. Priola. 2002. Coatings obtained through cationic UV curing of epoxide systems in the presence of epoxy functionalized polybutadiene. *Journal of Materials Science* 37 (22):4753-4757.

Sangermano, M., G. Malucelli, F. Morel, C. Decker, and A. Priola. 1999. Cationic Photopolymerization of Vinyl ether systems: influence of the presence of hydrogen donor additives. *European Polymer Journal* 35:639-645.

Sasaki, Hiroshi. 2007. Curing properties of cycloaliphatic epoxy derivatives. *Progress in Organic Coatings* 58 (2-3):227-230.

Shu Yang, Jamie Ford, Chada Ruengruglikit, Qingrong Huang, and Joanna Aizenberg. 2005. Synthesis of Photoacid crosslinkable hydrogels for the fabrication of soft, biomimetic microlens arrays. . *Journal of Materials Chemistry* 15:4200-4202.

Sipani, Vishal, and Scranton, Alec B 2003. Dark-Cure Studies of Cationic Photopolymerizations of Epoxides: Chracterization of the Active Center Lifetime and Kinetic Rate Constants. *Journal of Polymer Science: Part A: Polymer Chemistry* 41:2064-2072.

Sipani, Vishal, and Scranton, Alec B 2003. Kinetic studies of cationic photopolymerizations of Phenyl glycidyl ether: termination/trapping rate constants for

iodonium photoinitiators. *Journal of Photochemistry and Photobiology A: Chemistry* 159:189-195.

Sipani, Vishal, Kirsch, Ann, Scranton, Alec B. . 2004. Dark Cure Studies of Cationic Photopolymerizations of Epoxides: Characterization of Kinetic Rate Constants at High Conversions. *Journal of Polymer Science: Part A: Polymer Chemistry* 42:4409-4416.

Sipil, Julius, Harri Nurmi, Ann Marie Kaukonen, Jouni Hirvonen, Jyrki Taskinen, and Jari Yli-Kauhaluoma. A modification of the Hammett equation for predicting ionisation constants of p-vinyl phenols. *European Journal of Pharmaceutical Sciences* 25 (4-5):417-425.

Smith, Gerald J. 1982. Enhanced Intersystem Crossing in the Oxygen Quenching of Aromatic Hydrocarbon Triplet States with High Energies. *Journal of the Chemical Society, Faraday Transactions* 2 (78):769-773.

Socrate, George. 2001. *Infrared and Raman characteristic group frequencies. Tables and charts*. 3rd ed. Vol. 35. Chichester: John Wiley & Sons, Ltd.

Sperling, L.H. and Mishra, V. 1996. The Current Status of Interpenetrating Polymer Networks. *Polymers for Advanced Technologies* 7:197-208.

Stanislaw Penczek, Przemyslaw Kubisa, Stainslaw Slomkowski, and Krzystof Matyjaszewski. 1985. Structure-Reactivity Relationships in Ring-Opening Polymerization. In *Ring-Opening Polymerization*, edited by J. E. McGrath: American Chemical Society.

Stanislaw Penczek, Marek Cypryk, Andrzej Duda, Przemyslaw Kubisa, and Stanislaw Slomkowski. 2007. Living ring-opening polymerizations of heterocyclic monomers. *Progress in Polymer Science* 32:247-282.

Strehmel, B., D. Anwand, and H. J. Timpe. 1992. The formation of semiinterpenetrating polymer networks by photoinduced polymerization. In *Physics of Polymer Networks*.

Surésh K. Rajaraman, William A. Mowers James V. Crivello. 1999. Interaction of epoxy and vinyl ethers during photoinitiated cationic polymerization. *Journal of Polymer Science Part A: Polymer Chemistry* 37 (21):4007-4018.

Suthar, B., H. X. Xiao, D. Klempner, and K. C. Frisch. 1996. A Review of Kinetic Studies of the Formation of Interpenetrating Polymer Networks. *Polymer for Advanced Technologies* 7:221-233.

Szwarc, M. 1965. The kinetics and mechanism of N-carboxy-α-amino-acid anhydride (NCA) polymerisation to poly-amino acids. In *Fortschritte der Hochpolymeren-Forschung*.

Tadatomi Nishikubo, Takashi Iizawa Eiji Takahashi Akira Udagawa. 1984. Syntheses of polymers with pendant photosensitive and photosensitizing groups by cationic copolymerizations of photosensitive and photosensitizing monomers. *Die Makromolekulare Chemie, Rapid Communications* 5 (3):131-135.

Tadeusz Biedron, Krystyna Brzezinska Przemyslaw Kubisa StanislawPenczek. 1995. Macromonomers by activated polymerization of oxiranes. Synthesis and polymerization. *Polymer International* 36 (1):73-80.

Tokar, R., P. Kubisa, S. Penczek, and A. Dworak. 1994. Cationic polymerization of glycidol: coexistence of the activated monomer and active chain end mechanism. *Macromolecules* 27 (2):320-322.

Tom Scherzer, Helmut Langguth. 2005. Temperature Dependence of the Oxygen Solubility in Acrylates and its Effect on the Induction Period in UV Photopolymerization. *Macromolecular Chemistry and Physics* 206 (2):240-245.

Tom Scherzer, Michael R. Buchmeiser. 2007. Photoinitiated Cationic Polymerization of Cycloaliphatic Epoxide/Vinyl Ether Systems Studied by Near-Infrared Reflection Spectroscopy. *Macromolecular Chemistry and Physics* 208 (9):946-954.

Udipi, K. 1979. Epoxidation of styrene–butadiene block polymers. I. *Journal of Applied Polymer Science* 23 (11):3301-3309.

Umut Bulut, James V. Crivello. 2005. Reactivity of oxetane monomers in photoinitiated cationic polymerization. *Journal of Polymer Science Part A: Polymer Chemistry* 43 (15):3205-3220.

Vanessa Z. -H. Chan, James Hoffman, Victor Y. Lee, Hermis latrou, Apostolos Avgeropoulos, Nikos Hadjichristidis, Robert D. Miller, Edwin L. Thomas. 1999. Ordered Bicontinuous Nanoporous and Nanorelief Ceramic Films from self Assembling Polymer Precursors. *Science* 286:1716-1718.

Wolfram, Schnabel. 2000. Cationic photopolymerization with the aid of pyridinium-type salts. *Macromolecular Rapid Communications* 21 (10):628-642.

Yan Lin, Jeffrey W. Stansbury. 2003. Kinetics studies of hybrid structure formation by controlled photpolymerization. *Polymer* 44:4781-4789.

Yoshinobu, Nakamura, Miho, Yamaguchi, Akiko, Kitayama, Kazuo, Iko, Masayoshi, Okubo, Tsunetaka, Matsumoto. 1990. Internal stress of epoxy resin modified with acrylic polymers produced by *in situ* UV radiation polymerization. *Journal of Applied Polymer Science* 39 (5):1045-1060.

Yujing Hua, James V. Crivello. 2000. Synergistic interaction of epoxides and N-vinylcarbazole during photoinitiated cationic polymerization. *Journal of Polymer Science Part A: Polymer Chemistry* 38 (19):3697-3709.

Zhengang, Zong, D. Soucek Mark, Liu Yubiao, and Hu Jun. 2003. Cationic photopolymerization of epoxynorbornane linseed oils: The effect of diluents. *Journal of Polymer Science Part A: Polymer Chemistry* 41 (21):3440-3456.

Zou, Yuan, Steven R. Armstrong, and Julie L. P. Jessop. Quantitative analysis of adhesive resin in the hybrid layer using Raman spectroscopy. *Journal of Biomedical Materials Research Part A* 94A (1):288-297.

Zou, Yuan, Steven R. Armstrong, and Julie L. P. Jessop. 2008. Apparent conversion of adhesive resin in the hybrid layer, Part 1: Identification of an internal reference for Raman spectroscopy and the effects of water storage. *Journal of Biomedical Materials Research Part A* 86A (4):883-891.